

**THE RELATIONSHIP BETWEEN ARTERIAL BLOOD PRESSURE  
AND CEREBRAL BLOOD FLOW:  
INSIGHTS INTO AGING, ALTITUDE AND EXERCISE**

by

JONATHAN DAVID SMIRL

M.Sc., The University of British Columbia, 2011  
B.Sc., The University of Victoria, 2004

A THESIS SUBMITTED IN PARTIAL FULFILLMENT OF  
THE REQUIREMENTS FOR THE DEGREE OF

DOCTOR OF PHILOSOPHY

in

College of Graduate Studies

(Interdisciplinary Studies)

THE UNIVERSITY OF BRITISH COLUMBIA

(Okanagan)

June 2015

© Jonathan David Smirl, 2015

## **Abstract**

The majority of previous research on the relationship between blood pressure and cerebral blood flow (CBF) through the application of transfer function analysis (TFA) has been performed under spontaneous conditions. Under these circumstances, there is little input signal power (blood pressure), which makes linear interpretation of the output (CBF) results tenuous. In five experimental studies, the general aim of this thesis was to provide new insights on the relationship(s) between blood pressure and CBF throughout the aging spectrum.

The first study determined the reproducibility of TFA metrics during spontaneous and driven blood pressure oscillations. The results revealed that squat-stand maneuvers were the most robust and reliable method to evaluate this relationship throughout aging. Consequently, this methodology was employed for the research studies.

The second study examined the pressure-flow response in younger adults with acutely elevated cerebrovascular resistance index (CVRI). Augmenting CVRI, even without changes in CO<sub>2</sub>, resulted in increased phase lead and reduced amplitude modulation; therefore, the impact of CVRI needs to be considered for the parsimonious interpretation of TFA metrics.

The third experiment examined the pressure-flow relationship in three adult populations: young and old healthy adults, and heart transplant recipients. Findings revealed comparable cerebral pressure-flow responses in all groups, despite elevated CVRI (older groups), and blunted cardiac baroreceptors (long-term heart transplant

recipients). Thus, it appears the acutely increased phase and decreased gain noted in the second study may not accurately reflect the chronic elevations in CVRi in older adults.

Through the unique approach of oscillating blood pressure during exercise, the fourth study demonstrated that the cerebrovasculature high-pass filter model is intact in both young and older populations.

The final study at high-altitude (5050m) explored the cerebral pressure-flow relationship prior to, during acclimatization, and return from high-altitude. Despite the marked oxygen desaturation, there were no changes to the pressure-flow response across the entire range of exposure acclimatization timelines.

In conclusion: 1) squat-stand maneuvers provide a meritorious way to examine cerebral-pressure flow responses; and 2) effective pressure-flow relationships are maintained during healthy aging and exercise, and persist despite blunting of cardiac baroreflexes and reductions in arterial oxygen saturation.

## **Preface**

The study presented in chapter three (*Comparison of squat-stand and oscillatory lower body negative pressure methodologies*) was approved by the clinical ethical committee of the University of British Columbia (H14-01951). A version this study was selected for an oral presentation at CARNet 2015 (annual scientific meeting of the cerebral autoregulation research network). Methodological comparison of active and passive driven oscillations in blood pressure; implications for the assessment of cerebral-pressure flow relationships. Jonathan D. Smirl, Keegan Hoffman, Yu-Chieh Tzeng, Alex Hansen and Philip N. Ainslie. (2015) I was responsible for the majority of the data collection, data analysis, writing, and formatting of the abstract. A version of this manuscript has been submitted to the *Journal of Applied Physiology* and has been accepted pending revisions. Methodological comparison of active and passive driven oscillations in blood pressure; implications for the assessment of cerebral-pressure flow relationships. Jonathan D. Smirl, Keegan Hoffman, Yu-Chieh Tzeng, Alex Hansen and Philip N. Ainslie. (2015) I was responsible for the data collection, data analysis, writing, and formatting of the manuscript.

The study presented in chapter four (*Influence of increased cerebrovascular resistance*) was approved by the clinical ethical committee of the University of British Columbia (H11-03287). A version this study was accepted as an oral presentation at CARNet 2012 (annual scientific meeting of the cerebral autoregulation research network). Jonathan D. Smirl, and Philip N. Ainslie. (2012) Influence of Cerebrovascular Resistance on Dynamic Cerebral Autoregulation in Humans. I was responsible for the majority of the data collection, data analysis, writing, and formatting

of the abstract. A version of this manuscript has been accepted and published in the *Journal of Applied Physiology* and has been reproduced with permission. <sup>1</sup> Influence of cerebrovascular resistance on dynamic pressure-flow relationships in humans. Jonathan D. Smirl, Yu-Chieh Tzeng, Brad Monteleone, and Philip N. Ainslie. I was responsible for majority of the data collection, data analysis, writing, and formatting of the manuscript.

The study presented in chapter five (*Influence of long-term heart transplantation*) was approved by the clinical ethical committee of the Universities of British Columbia (H11-02576) and the University of Alberta (Prooooo11560). A version this study was accepted as a poster presentation at CARNet 2014 (annual scientific meeting of the cerebral autoregulation research network). Jonathan D. Smirl, Mark J. Haykowsky, Michael D. Nelson, Yu-Chieh Tzeng, Katelyn R. Marsden, Helen Jones, and Philip N. Ainslie. (2014) The relationship between cerebral blood flow and blood pressure in long-term heart transplant recipients. I was responsible for majority of the data collection, data analysis, writing, and formatting of the abstract. A version of this manuscript has been accepted and published in *Hypertension* and has been reproduced with permission. <sup>2</sup> Relationship between cerebral blood flow and blood pressure in long-term heart transplant recipients. Jonathan D. Smirl, Mark J. Haykowsky, Michael D. Nelson, Yu-Chieh Tzeng, Katelyn R. Marsden, Helen Jones, and Philip N. Ainslie. I was responsible for the data collection, data analysis, writing, and formatting of the manuscript.

The study presented in chapter six (*Influence of aging during supine cycling exercise*) was approved by the clinical ethical committees of the University of British

Columbia (H14-01951). A version this study was selected for a poster presentation at UK Physiological Society 2015. The relationship between blood pressure and cerebral blood flow during supine cycling: Influence of aging. Jonathan D. Smirl, Keegan Hoffman, Yu-Chieh Tzeng, Alex Hansen and Philip N. Ainslie. I was responsible for the majority of the data collection, data analysis, writing, and formatting of the abstract. A version of this manuscript has been submitted to the *Journal of Physiology* and has been accepted pending revisions. The relationship between blood pressure and cerebral blood flow during supine cycling: Influence of aging. Jonathan D. Smirl, Keegan Hoffman, Yu-Chieh Tzeng, Alex Hansen and Philip N. Ainslie. I was responsible for the data collection, data analysis, writing, and formatting of the manuscript.

This study presented in chapter seven (*Influence of high altitude*) was approved by the clinical ethical committee of the University of British Columbia (H11-03287). A version this study was accepted as an oral presentation at CARNet 2013 (annual scientific meeting of the cerebral autoregulation research network). Jonathan D. Smirl, Nia C.S. Lewis, Samuel J.E. Lucas, Gregory R. duManoir, Kurt J. Smith, Nima Sherpa, Aperna S. Basnyat and Philip N. Ainslie. Cerebral Pressure-Flow Relationship in Lowlanders and Natives at High Altitude. I was responsible for majority of the data collection, data analysis, writing, and formatting of the abstract. A version of this manuscript has been accepted and published in the *Journal of Cerebral Blood Flow and Metabolism* and has been reproduced with permission. <sup>3</sup> Jonathan D. Smirl, Nia C.S. Lewis, Samuel J.E. Lucas, Gregory R. duManoir, Kurt J. Smith, Akke Bakker, Aperna S. Basnyat and Philip N. Ainslie. Cerebral Pressure-Flow Relationship in Lowlanders

and Natives at High Altitude. I was responsible for majority of the data collection, data analysis, writing, and formatting of the manuscript.

## Table of Contents

<b>Abstract.....</b>	<b>ii</b>
<b>Preface.....</b>	<b>iv</b>
<b>Table of Contents .....</b>	<b>viii</b>
<b>List of Tables .....</b>	<b>xii</b>
<b>List of Figures.....</b>	<b>xiv</b>
<b>List of Abbreviations .....</b>	<b>xix</b>
<b>Acknowledgements .....</b>	<b>xx</b>
<b>Dedication .....</b>	<b>xxi</b>
<b>Chapter One: Introduction .....</b>	<b>1</b>
1.1. Purpose of thesis .....	1
1.2. Literature Review.....	4
1.3. Anatomical aspects of cerebral circulation .....	4
1.4. Measurement of cerebral blood flow .....	5
1.4.1. Historical perspective.....	5
1.4.2. Modern technological advancements.....	8
1.5. Factors that influence cerebral blood flow.....	24
1.5.1. Arterial blood gases .....	24
1.5.2. Intracranial pressure.....	30
1.5.3. Cerebral perfusion pressure .....	31
1.5.4. Neurogenic factors .....	34
1.5.5. Neurovascular coupling .....	36
1.5.6. Local metabolic factors.....	42
1.5.7. Posture.....	47
1.3.8. Aging.....	48
1.5.9. Acute exercise.....	49
1.5.10. Chronic exercise.....	49
1.5.11. Selected pathology - heart transplantation.....	50

1.6. Underlying relationships between arterial blood pressure and cerebral blood flow regulation .....	52
1.6.2. Static vs. dynamic cerebral autoregulation .....	56
1.6.3. Key studies on dynamic relationship between blood pressure and cerebral blood flow .....	60
1.6.4. Comparison of commonly used methodologies to assess this relationship ....	78
1.6.5. Rationale for the use of transfer function analysis.....	82
<b>Chapter Two: Methodological Overview.....</b>	<b>84</b>
2.1. Instrumentation .....	84
2.1.1. Transcranial Doppler ultrasound.....	84
2.1.2. Finger photoplethysmography .....	91
2.1.3. Electrocardiography .....	93
2.1.4. Gas analysis .....	94
2.2. Signal Processing .....	95
2.2.1. Fourier transform .....	98
2.2.2. Transfer function analysis.....	103
2.2.3. Coherence .....	104
2.2.4. Phase .....	105
2.2.5. Gain.....	109
<b>Chapter Three: Comparison of squat-stand and oscillatory lower body negative pressure methodologies .....</b>	<b>110</b>
3.1. Aims and Hypotheses .....	111
3.2. Rationale .....	112
3.3. Methods.....	117
3.4. Results.....	122
3.5. Discussion .....	136
3.6. Key finding .....	151

<b>Chapter Four: Influence of increased cerebrovascular resistance.....</b>	<b>152</b>
4.1. Aims and Hypotheses .....	153
4.2. Rationale .....	154
4.3. Methods.....	155
4.4. Results.....	162
4.5. Discussion .....	168
4.6. Key finding .....	175
<b>Chapter Five: Influence of long-term heart transplantation.....</b>	<b>176</b>
5.1. Aims and Hypotheses .....	177
5.2. Rationale .....	178
5.3. Methods.....	179
5.4. Results.....	184
5.5. Discussion .....	192
5.6. Key finding .....	196
<b>Chapter Six: Influence of aging during supine cycling exercise.....</b>	<b>197</b>
6.1. Aims and Hypotheses .....	198
6.2. Rationale .....	199
6.3. Methods.....	204
6.4. Results.....	209
6.5. Discussion .....	221
6.6. Key finding .....	228
<b>Chapter Seven: Influence of high altitude.....</b>	<b>229</b>
7.1. Aims and Hypotheses .....	230
7.2. Rationale .....	231
7.3. Methods.....	233
7.4. Results.....	240
7.5. Discussion .....	250
7.6. Key finding .....	259

<b>Chapter Eight: Overall Conclusions .....</b>	<b>260</b>
8.1. Overall significance and contribution of the thesis research .....	260
8.2. Strengths and limitations of the thesis research .....	265
8.3. Potential applications of research findings .....	268
8.4. Future directions .....	269
<b>Bibliography .....</b>	<b>271</b>
<b>Appendices: .....</b>	<b>300</b>
<b>Appendix A: Supplementary information for high altitude study .....</b>	<b>300</b>
A.1. Time-domain analysis of squat-stand maneuvers .....	300
A.2. Transcranial colour-coded duplex analysis .....	303

## List of Tables

Table 3.1.	Hemodynamic and cerebrovascular responses during spontaneous baselines during upright and supine postures.....	123
Table 3.2.	Transfer function analysis of spontaneous data between MAP and MCAv under upright and supine conditions in younger adults measured on Day 1 and Day 2. Reproducibility is calculated for between-day within subject coefficient of variations.....	125
Table 3.3.	Transfer function analysis of spontaneous data between MAP and MCAv under upright and supine conditions in older adults measured on Day 1 and Day 2. Reproducibility is calculated for between-day within subject coefficient of variations.....	126
Table 3.4.	Transfer function analysis of driven data between MAP and MCAv under upright and supine conditions in younger adults measured on Day 1 and Day 2. Reproducibility is calculated for between-day within subject coefficient of variations .....	127
Table 3.5.	Transfer function analysis of driven data between MAP and MCAv under upright and supine conditions in older adults measured on Day 1 and Day 2. Reproducibility is calculated for between-day within subject coefficient of variations .....	128
Table 3.6.	Summary of previous literature assessing the reproducibility of the cerebral pressure-flow relationship .....	139
Table 4.1.	Absolute and normalized point estimates of the power spectrum densities of mean arterial pressure, middle cerebral artery velocity, and posterior cerebral artery velocity during the squat-stand maneuvers for the three interventions .....	160
Table 4.2.	Hemodynamic and cerebrovascular responses during squat-stand maneuvers.....	164
Table 5.1.	Participant characteristics of long-term heart transplant recipient study .....	181
Table 5.2.	Hemodynamic and Cerebrovascular Responses During Squat-Stand Maneuvers .....	186

Table 5.3.	Transfer function analysis for cardiac baroreceptor sensitivity.....	188
Table 5.4.	Transfer function analysis between blood pressure and middle cerebral artery velocity.....	189
Table 6.1.	Summary of previous literature assessing the cerebral pressure-flow relationship during moderate exercise (~50% of heart rate reserve).....	202
Table 6.2.	Hemodynamic and cerebrovascular responses in younger adults at rest and during exercise with spontaneous and driven blood pressure (0.05 and 0.10 Hz) oscillations .....	210
Table 6.3.	Hemodynamic and cerebrovascular responses in older adults at rest and during exercise with spontaneous and driven blood pressure (0.05 and 0.10 Hz) oscillations.....	211
Table 6.4.	Transfer function analysis metrics in younger adults for the relationship between mean arterial pressure and cerebral blood flow at rest and during moderate exercise .....	213
Table 6.5.	Transfer function analysis metrics in older adults for the relationship between mean arterial pressure and cerebral blood flow at rest and during moderate exercise .....	214
Table 7.1.	Participant characteristics of high altitude study .....	234
Table 7.2.	Transfer function analysis of spontaneous seated data between blood pressure middle cerebral artery velocity, and posterior cerebral artery velocity.....	241
Table 7.3.	Transfer function analysis of driven data between blood pressure middle cerebral artery velocity, and posterior cerebral artery velocity .....	242
Table 7.4.	Hemodynamic and cerebrovascular responses during spontaneous baseline.....	244

## List of Figures

Figure 1.1.	An image of the simple bubble flow meter used by Dumke and Schmidt in 1943 for the first true measurement of cerebral blood flow.....	10
Figure 1.2.	Sample of the experimental protocol used in 1948 by Kety and Schmidt for the first cerebral blood flow measurements in man .....	11
Figure 1.3.	Illustration of the typical sampling of nitrous oxide concentration (as measured by volume %) from the radial artery and jugular vein during the Kety-Schmidt method during a 10-minute sampling period while inhaling 15% nitrous oxide .....	13
Figure 1.4.	The first transcranial Doppler, the “UrDoppler” as first constructed by Rune Aaslid .....	17
Figure 1.5.	Example of the Doppler shift .....	18
Figure 1.6.	The previously reported middle cerebral artery diameter changes as they relate to over and under estimation of cerebral blood flow with respect to alterations in end tidal CO <sub>2</sub> .....	26
Figure 1.7.	The relationship between cerebral blood flow and arterial pH and arterial CO <sub>2</sub> .....	28
Figure 1.8.	The relationship between cerebral blood flow and steady-state changes in arterial O <sub>2</sub> .....	29
Figure 1.9.	The cerebral autoregulatory curve as first proposed by Dr. Niels Lassen in 1959.....	33
Figure 1.10.	A section of the capillary cell wall, that highlights the main cells (astrocytes, pericytes and endothelium) responsible for the relatively impermeable blood-brain barrier.....	38
Figure 1.11.	The relationship between cerebral perfusion pressure and cerebral blood flow and cerebral vascular resistance.....	55
Figure 1.12.	A modified representation of the classic cerebral autoregulation curve that was first presented by Lassen in 1959 and the current view on the cerebral autoregulation curve .....	56

Figure 1.13.	A schematic diagram illustrating two theoretical models that can influence the interpretation of cerebral autoregulation data.....	59
Figure 1.14.	The typical arterial blood pressure, cerebral blood flow and cerebrovascular resistance responses to the thigh cuff deflation during hypocapnia, normocapnia and hypercapnia.....	61
Figure 1.15.	Quantification of the cerebral blood flow response to a thigh cuff deflation on the autoregulatory index scale.....	63
Figure 1.16.	Typical waveforms from the 0.05 Hz squat-stand maneuvers for blood pressure and cerebral blood flow velocity during hypocapnia, normocapnia and hypercapnia.....	67
Figure 1.17.	Findings from the study assessing the frequency dependant nature of cerebral autoregulation in neonates .....	69
Figure 1.18.	Group averaged TFA data for gain, phase and coherence.....	71
Figure 1.19.	Trace from a typical subject performing repeated squat-stand maneuvers at 0.10 Hz for blood pressure cerebral blood flow and end tidal CO <sub>2</sub> .....	74
Figure 1.20.	Projection pursuit regression ridge functions for the cerebral pressure-flow relationship at 0.03 Hz and 0.08 Hz .....	77
Figure 1.21.	Between subject relationships for the transfer function analysis metrics and either RoR or ARI.....	80
Figure 2.1.	The relationship between the angle of insonation and the cosine of that angle .....	86
Figure 2.2.	Example of insonation angles and probe placement for the middle cerebral artery and the posterior cerebral artery.....	87
Figure 2.3.	Example the 2-dimensional waveform created by the spectral analysis of the Doppler shift from the red blood cell velocity and the surrounding envelope .....	88
Figure 2.4.	Example a typical experimental set up.....	92
Figure 2.5.	Example a typical electrocardiogram trace during a data collection.....	93

Figure 2.6.	Example of the relationship between the input and output signals at 1 cycle per second, represented in the time-domain waveform for a linear system.....	97
Figure 2.7.	Example a time-domain waveform and frequency components of two sinusoidal waveforms.....	100
Figure 2.8.	A Fourier transform is applied to the time-domain data to create the frequency-domain spectral analysis. A cross-spectral analysis is applied to the power spectrums of the mean arterial pressure and the cerebral blood flow velocity to create the transfer function. The transfer function is then utilized to calculate the coherence, phase and gain .....	101
Figure 2.9.	Example of aliasing in the data due to under sampling the signal .....	102
Figure 3.1.	Typical trace for blood pressure, middle cerebral artery velocity and end tidal CO <sub>2</sub> during spontaneous, 0.05 Hz and 0.10 Hz squat-stand maneuvers. The data are representative of the younger adults in the study .....	115
Figure 3.2.	Typical trace for blood pressure, middle cerebral artery velocity and end tidal CO <sub>2</sub> during spontaneous, 0.05 Hz and 0.10 Hz oscillatory lower body negative pressure maneuvers. The data are representative of the younger adults in the study .....	116
Figure 3.3.	Absolute values of the power spectrum densities for the mean arterial pressure and cerebral blood velocity in younger adults under spontaneous, 0.05 Hz and 0.10 Hz conditions .....	129
Figure 3.4.	Absolute values of the power spectrum densities for the mean arterial pressure and cerebral blood velocity in older adults under spontaneous, 0.05 Hz and 0.10 Hz conditions .....	130
Figure 3.5.	Bland-Altman plots of the significant differences between squat-stand and oscillatory lower body negative pressure in younger adults .....	131
Figure 3.6.	Bland-Altman plots of the significant differences between squat-stand and oscillatory lower body negative pressure in older adults .....	132

Figure 3.7.	Within-subject coefficient of variance expressed as percentages for coherence, phase, absolute gain and normalized gain during spontaneous supine, spontaneous upright, oscillatory lower body negative pressure and squat-stand maneuvers.....	134
Figure 4.1.	Absolute values of the power spectrum densities for the mean arterial pressure, middle cerebral artery velocity, and posterior cerebral artery velocity during the squat-stand maneuvers for the three interventions .....	158
Figure 4.2.	Normalized values of the power spectrum densities for the mean arterial pressure, middle cerebral artery velocity, and posterior cerebral artery velocity during the squat-stand maneuvers for the three interventions .....	159
Figure 4.3.	Representative individual data of the raw wave form highlighting the effects of the squat-stand maneuvers on blood pressure, middle cerebral artery velocity, posterior cerebral artery velocity and end-tidal CO <sub>2</sub> levels. The data are presented under the no intervention, Indomethacin and hypocapnia experimental conditions .....	165
Figure 4.4.	Transfer function analysis of coherence, phase and gain for the group means of the middle cerebral artery velocity and posterior cerebral artery velocity driven oscillations during the three experimental conditions: No Intervention, Indomethacin, and Hypocapnia.....	167
Figure 5.1.	Typical trace for blood pressure, middle cerebral artery velocity and end-tidal CO <sub>2</sub> during spontaneous, 0.05 Hz and 0.10 Hz trials, in a long-term heart transplant recipients .....	187
Figure 5.2.	Middle cerebral artery velocity transfer function analysis of coherence, phase, and normalized gain in the very low frequency and low frequency for the group means of the spontaneous data for the three groups: age-match controls, long-term heart transplant recipients, and donor controls .....	190

Figure 5.3.	Middle cerebral artery velocity transfer function analysis of coherence, phase, and normalized gain at the driven frequencies of 0.05 Hz and 0.10 Hz for the three groups: age-match controls, long-term heart transplant recipients, and donor controls .....	191
Figure 6.1.	Typical trace for blood pressure, middle cerebral artery velocity and end-tidal CO <sub>2</sub> during spontaneous, 0.05 Hz and 0.10 Hz oscillatory negative pressure trials during a moderate supine cycling intensity .....	207
Figure 6.2.	Absolute values of the power spectrum densities for the mean arterial pressure and middle cerebral artery velocity with spontaneous and driven oscillations in blood pressure during moderate exercise in younger and older adults .....	215
Figure 6.3.	The absolute and relative delta changes from resting to exercise conditions in coherence, phase, absolute gain and normalized gain during driven oscillations in younger and older adults .....	216
Figure 6.4.	The augmentation in coherence to ~1.00 during the driven oscillations in blood pressure during moderate exercise in younger and older adults .....	218
Figure 6.5.	The transfer function analysis of coherence, phase, absolute gain and normalized gain at the driven frequencies of 0.05 Hz and 0.10 Hz for the younger and older adults during moderate exercise.....	219
Figure 7.1.	Schematic of the ascent protocol to 5050m.....	236
Figure 7.2.	Transfer function analysis of the cerebral pressure-flow relationship during spontaneous oscillations in blood pressure and cerebral blood flow velocities at sea level, upon arrival and following partial acclimatization to 5050m .....	246
Figure 7.3.	Transfer function analysis of the cerebral pressure-flow relationship during driven oscillations in blood pressure and cerebral blood flow velocities at sea level, upon arrival and following partial acclimatization to 5050m .....	247

## List of Abbreviations

AMP	Adenosine Monophosphate
ARI	Autoregulatory Index
BMI	Body Mass Index
BP	Blood Pressure
CARNet	Cerebral Autoregulation Research Network
CBF	Cerebral Blood Flow
CBV	Cerebral Blood Velocity
CO <sub>2</sub>	Carbon Dioxide
CVRi	Cerebrovascular Resistance Index
DC	Donor Control
F <sub>s</sub>	Sampling Frequency
g	Grams
HA	High Altitude
HF	High Frequency
HTR	Heart Transplant Recipient
Hz	Hertz
INDO	Indomethacin
LF	Low Frequency
MAP	Mean Arterial Pressure
MCA <sub>v</sub>	Middle Cerebral Artery Velocity
MHz	Mega Hertz
min	Minute
ml	Milliliter
mmHg	Millimeter of Mercury
MRI	Magnetic Resonance Imaging
M <sub>x</sub>	Mean Flow Index
n	Number of Subject
O <sub>2</sub>	Oxygen
OLBNP	Oscillatory Lower Body Negative Pressure
P <sub>a</sub> CO <sub>2</sub>	Partial Pressure of Arterial Carbon Dioxide
P <sub>a</sub> O <sub>2</sub>	Partial Pressure of Arterial Oxygen
PCA <sub>v</sub>	Posterior Cerebral Artery Velocity
P <sub>ET</sub> CO <sub>2</sub>	Partial Pressure of End-Tidal Carbon Dioxide
PPR	Projection Pursuit Regression
RoR	Rate of Regulation
TFA	Transfer Function Analysis
ULF	Ultra Low Frequency
VLF	Very Low Frequency

## **Acknowledgements**

I would like to thank Professor Philip Ainslie for his complete support, knowledge, guidance and mentorship throughout my MSc and PhD experiences. Throughout the process he has taught me more than just many valuable research skills and techniques but, also the level of work ethic, dedication, leadership and balance that it takes to excel both in the research laboratory and life in general.

A large thank you also goes to Dr. Shieak Tzeng from the University of Otago, the time that you spent advising on the intricacies of transfer function analysis to examine the relationship between blood pressure and cerebral blood flow. This set the foundation of my interest in exploring this field of research. I have truly enjoyed our conversations over the years and your guidance is greatly appreciated. I would also like to thank Dr. Mark Haykowsky from the University of Alberta for his assistance and effort for the long-term heart transplant recipients study. Without his efforts, this study would have never occurred.

Thanks to my committee and examination members: Dr. Neil Eves, Dr. Glen Foster, Dr. Mypinder Sekhon and Professor Ronney Panerai. I appreciated your contributions and feedback throughout this process. I would also like to thank my peers for the many informal physiological discussions that took place around the research labs at UBC Okanagan. These talks have helped shape my ideas and philosophy on what it takes to be a researcher.

Finally, I would also like to thank the Izaak Walton Killam Foundation and the Natural Sciences and Engineering Research Council for the pre-doctoral fellowship funding they provided that enabled me to pursue and complete my PhD.

## **Dedication**

Shannon, you are the light of my life, my true kindred spirit. The moment we met, I knew right then and there that you were the one. I am thankful for your love, and support each and every day. The journey we have been on throughout this PhD has been an adventure to say the least and there is no one else on the planet that I would want to have by my side for it. I love you with all of my heart and am ecstatic that we get to spend the rest of our lives together. Without your support and motivation, I would not be able to accomplish what I have and will in the future.

Piper, you are the precious energy that warms my heart each and every day. It has been an amazing experience to watch you learn, grow and develop from a little baby just two years ago into the smiling, giggling and dancing machine that greets me each and every day when I get home from the lab. Your enthusiasm is contagious and provides a bright light to all that know you. We are so blessed to have such a kind, considerate and caring person for our daughter.

Mom and Dad, your work ethic and dedication have been an inspiration to me throughout my entire life. I have always appreciated the sacrifices you have made for our family and willingness to put others first. It is an example I only wish I can emulate for Shannon and Piper.

Susan and Daryl, when I met Shannon I thought I had met the most fantastic woman on the planet and once I met her parents I knew where she got it from. I appreciate all of the time and energy you have given our family. I can only wish that Daryl were still here to have a wee dram of single malt with to celebrate the completion of this PhD. Although he left this world far too soon, he will never be forgotten.

## **Chapter One: Introduction**

### **1.1. Purpose of thesis**

A major limitation of the research to date examining the relationship between arterial blood pressure and cerebral blood flow (CBF) through the application of transfer function analysis (TFA) is that it has been performed under spontaneous conditions. Under these resting and spontaneous circumstances, there is very little power in the input signal (blood pressure), which makes linear interpretation of the output (CBF) metrics underlying this relationship tenuous. To date there have been several methods that have been proposed to enhance the input power by creating oscillations in blood pressure (e.g., squat-stand maneuvers, oscillatory lower body negative pressure [OLBNP], deep-breathing and passive leg raises) which are transmitted into the cerebrovasculature where buffering occurs. Most of the studies utilizing these methodologies have focused on the younger adult population, with little attention on older adult populations. The purpose of this thesis is to apply the driven methodologies that elicit the most effective oscillations in blood pressure (squat-stand maneuvers and OLBNP) to provide additional insight into the regulation of arterial blood pressure changes by the cerebrovasculature in both younger and older adult populations.

Prior to presenting the findings of the research chapters (Chapters 3-7) an extensive literature review (Chapter 1) will establish the relevant background material in the context of the thesis with particular focus upon: the anatomy of the cerebrovasculature; how CBF is measured; factors that influence CBF, and; finally, this section concludes with highlighting the relationship between arterial blood pressure and CBF. The second chapter in this thesis will highlight the specific instruments and methodologies that are utilized in the following research chapters. The research chapters of this thesis aim to accurately assess, quantify and describe the

relationship between arterial blood pressure and CBF across the aging spectrum. Chapter 3 gauges the reliability of utilizing methodologies that creates oscillations in blood pressure when assessing the pressure-flow relationship in both younger and older adult populations. Chapter 4 examines the effect of an acute increase in the cerebrovascular resistance index (CVRi) in young healthy adults, which is designed to mimic the chronic increases that occur with aging. In this context, for the first time, CVRi was increased via both pharmacological (Indomethacin) and non-pharmacological (hypocapnia) interventions. Chapter 5 assesses the relationship between blood pressure and CBF in long-term heart transplant recipients. This population provides the unique means to determine which aspect (if any) of the body (the younger donor heart or older recipient cerebrovasculature) are responsible for altering the cerebral pressure-flow relationship. Because of cardiac denervation, this approach also allows the investigation into the role of cardiac baroreceptor sensitivity in the regulation of CBF. Chapter 6 is the first study to examine the relationship between driven oscillations in blood pressure and CBF during a moderate exercise intervention in both young and old individuals. In this study, both younger and older adults performed supine cycling exercise within a specially designed negative pressure box which provides a novel means to perturb arterial blood pressure. In a field-based setting, Chapter 7 evaluates the cerebral pressure-flow relationship in healthy adults at high altitude (HA: 5050m). This extreme environment creates a desaturation of the arterial blood to similar levels as those experienced by patients with congestive heart failure or severe chronic lung disease. This is the first study to have examined the pressure-flow response in low-landers at sea-level baseline, during initial (first 2 days) and following partial acclimatization (after 2 weeks) to 5050m, and upon return to sea-level. Moreover, the partially acclimatized lowlanders were compared to those with a lifetime of HA exposure, the Sherpa population. The collective

findings from these five studies is then presented in the concluding chapter of this thesis (Chapter 8) and highlights: the regulatory relationship between blood pressure and CBF in both younger and older adults, and the need to utilize a methodology that creates oscillations in blood pressure (at the frequencies of interest) when assessing the cerebral pressure-flow response. At the end of Chapter 8, follows a section presenting the strengths and limitations of the presented findings and future research directions in this field are highlighted.

## **1.2. Literature Review**

The following sections of the chapter will provide an extensive literature review on: The anatomy of the cerebrovasculature (section 1.3); the measurement of CBF (section 1.4); factors that influence CBF (section 1.5). Finally, the literature review will conclude with a section outlining the underlying relationship(s) between arterial blood pressure and CBF regulation (section 1.6).

## **1.3. Anatomical aspects of cerebral circulation**

Although the brain weighs only 1200-1400 grams (~1.5-2% of body mass), it receives approximately 10-15% of resting cardiac output and accounts for 15-20% of the total resting oxygen consumption (reviewed in: <sup>4</sup>). The brain consumes ~3.5 mL of oxygen per 100 grams of brain mass which equates to 42-49 mL of oxygen every minute. <sup>5</sup> Despite the high metabolic demand of the brain, it has a limited capacity for substrate storage making precise regulation of CBF critical for maintenance of constant nutrient and oxygen supply. <sup>6,7</sup>

The brain receives blood via two sources: The internal carotid arteries and the vertebral arteries. Approximately 73-82% of the cerebral blood supply occurs through the internal carotid artery. <sup>8-12</sup> The internal carotid arteries branch within the circle of Willis to form the middle cerebral and anterior cerebral arteries. <sup>13</sup> These two vessels are the primary suppliers of blood to the forebrain (frontal and parietal lobes) and midbrain (temporal lobe) regions, which collectively encompass the anterior region of the brain. <sup>13</sup>

The remaining 18-27% of the global CBF arrives via the vertebral arteries. <sup>8-12</sup> The right and left vertebral arteries join together to form the basilar artery at the level of the brainstem (near the level of the pons), which connects to form the posterior portion of the circle of Willis

and is the main supplier of blood within the posterior cerebral arteries.<sup>13</sup> These vessels are responsible for supplying blood to the hindbrain (e.g., occipital lobe, cerebellum and medulla oblongata).<sup>13</sup>

The blood supplying the superficial white matter of the cortex drains into the medullary veins where it joins with the cortical veins.<sup>13</sup> The cortical veins run through the subarachnoid space and then enter the dural sinuses.<sup>13</sup> The dural sinuses eventually drain into the internal jugular vein.<sup>13</sup> The blood supplying the deeper white matter located within the corpus callosum and the gray matter of the brain, which will drain into the internal cerebral and basal veins, which together drain into the great vein of Galen.<sup>13</sup> The great vein of Galen drains into the straight sinus and onto the torcular herophili and also drains into the internal jugular vein.<sup>13</sup> The blood supplying the occipital region of the brain drains into either the transverse sinus or the basal vein.<sup>13</sup> The transverse sinus in turn empties into the internal jugular vein.<sup>13</sup>

#### **1.4. Measurement of cerebral blood flow**

The measurement and quantification of CBF has intrigued scientists for centuries.<sup>6,12,14-22</sup> The following section will provide an overview of the historical perspective of the measurement of CBF and the technological advancements in the field over the past century.

##### **1.4.1. Historical perspective**

Ever since William Harvey revolutionized the understanding of the circulatory system in 1628,<sup>23</sup> the field of cardiovascular physiology advanced from the Galenic mindset of the four humours of the body to the modern understanding of the heart functioning as the pump that sends blood throughout the body via the arterial system and returns blood via the one-way

valve venous system. Alexander Monro secundus in 1783<sup>6</sup> noted that maintaining blood flow to the brain must be of a relatively high importance in the body, as the internal carotid and vertebral artery cross sectional areas are much greater than that of the brachial artery even though the arm is much larger than the brain, in terms of both mass and size. This original notion has been shown to be accurate based upon modern *in vivo* measurement techniques, as the average combined cross-sectional area (~28 mm<sup>2</sup>) of the vessels delivering blood to the brain [internal carotid (~18 mm<sup>2</sup>)<sup>24</sup> combined with the vertebral (~10 mm<sup>2</sup>)<sup>25</sup> arteries], are approximately 60% greater than that of the brachial (~17.5 mm<sup>2</sup>)<sup>26</sup> artery. Some of the other key points that were made by Monro were: The brain is encased in a non-expandable skull; the substance of the brain itself is nearly incompressible; the volume of blood within the encapsulated brain should therefore be constant (or nearly so); and the continuous outflow of venous blood from the cranium makes way for the new blood to arrive via the internal carotid and vertebral arteries.<sup>6</sup> These findings were confirmed by one of Monro's pupils, George Kellie, in 1824<sup>27</sup> and have since become known as the Monro-Kellie doctrine.<sup>28</sup> The Monro-Kellie doctrine was eloquently stated by John Abercrombie in 1828<sup>21</sup> as:

*“The cranium is a complete sphere of bone, which is exactly filled by its components, the brain, and by which the brain is closely shut up from the atmospheric pressure, and from all influence from without except what is communicated through the blood vessels which enter it. In an organ so situated, it is probable, that the quantity of blood circulating in its vessels cannot be materially increased, unless something give way to make room for the additional quantity cannot be materially diminished, unless something entered to supply the*

*space which would become vacant... the blood circulating in these vessels must be divided in a certain ratio betwixt the arteries and veins of the brain; and it is probable that the healthy state of this organ will depend on the nice adjustment of circulation in these two systems. If we could suppose a case in which more than the usual amount of blood was accumulated in the one system, the necessary effect would be a corresponding diminution in the other because the whole mass of blood in the brain must, by the supposition, remain the same. Hence would arise a derangement of the circulation, such as could not occur in any other part of the body, because there is no other organ so situated as the brain.”*<sup>21</sup>

The next major development in CBF measurement occurred in the late 1870s, when Angelo Mosso developed a plethysmograph to detect CBF variations via a pressure transducer.<sup>22</sup> The transducer was placed over defects within an individual’s skull and thus enabled the recording of pressure variations due to a variety of stimuli, and became known as the ‘Mosso method’.<sup>22</sup> From this methodology, Mosso was able to conclude that CBF intimately related to brain function.<sup>22</sup> Mosso’s work from the late 19<sup>th</sup> century was able to describe many of the underlying themes that are still present in current research on CBF regulation. Moreover, Mosso was also not shy about discussing one of the major limitations in the field; namely, there can be a poor signal-to-noise ratio when indirectly measuring brain function.<sup>22</sup>

These notions by Mosso were further expanded upon by the work of Charles Roy and Charles Sherrington in 1890,<sup>15</sup> who determined that the by products of cerebral metabolism during cerebral activation are able to alter the local cerebrovasculature in terms of regional

diameter and blood supply. In doing so, they became the first people to describe the basis of neurovascular coupling (described in section 1.3.5). In 1895, Bayliss, Hill and Gulland<sup>14</sup> attempted to replicate the findings of Roy and Sherrington<sup>15</sup>, but were unable to do so. Instead they found that cerebral circulation followed passively along the same patterns as the rest of the systemic circulation.<sup>14</sup> They noted that every variation in the systemic circulation that occurred with breathing, abdominal compression, and muscular movements was also passively followed by that of the cerebral circulation.<sup>14</sup> They further went on to describe that every pleasurable emotion that elicits a rise in arterial blood pressure, elicits a concurrent rise in CBF; and every painful emotion will result in the opposite effects.<sup>14</sup>

Thus by the end of the 19<sup>th</sup> century, the basis of our early understanding of CBF had been established and chiefly included; the Monro-Kellie doctrine (the fluids that accompany the brain are encased in a rigid container and as such the volume tends to remain relatively constant);<sup>21</sup> cerebral metabolism affects CBF;<sup>15</sup> and perturbations to the systemic circulation will be observed in the cerebral circulation.<sup>14</sup> These notions have been shown to hold true to this day and it was not until the technological advancements of the mid 1940s that the next major breakthrough came in the assessment of CBF.

#### **1.4.2. Modern technological advancements**

The first absolute measurement of CBF was performed by Paul Dumke and Carl Schmidt in 1943<sup>12</sup> in 19 monkeys (*macacus rhesus*). They utilized a “simple bubble flowmeter”, where water is circulated in a temperature controlled bath (38-40°C) and blood from the basilar and carotid arteries are simultaneously passed through the meter on its way to the brain (Figure 1.1.).<sup>12</sup> Cerebral blood flow was calculated by injecting a ~0.2 cubic

centimeter air bubble into a known volume (~6 cubic centimeters) and measuring its movement across the tube, upon reaching the end of the tube the air bubble was removed via a trap. <sup>12</sup> Overall they found an average CBF of 63 ml/100g/minute. During this study, they also investigated the effects of inhaling anoxia, 100% oxygen, and 10% carbon dioxide (these findings will be discussed in section 1.3.1.) However, this method required such extensive surgery within the cerebrovasculature that applying it to the assessment of CBF in humans was not viable.

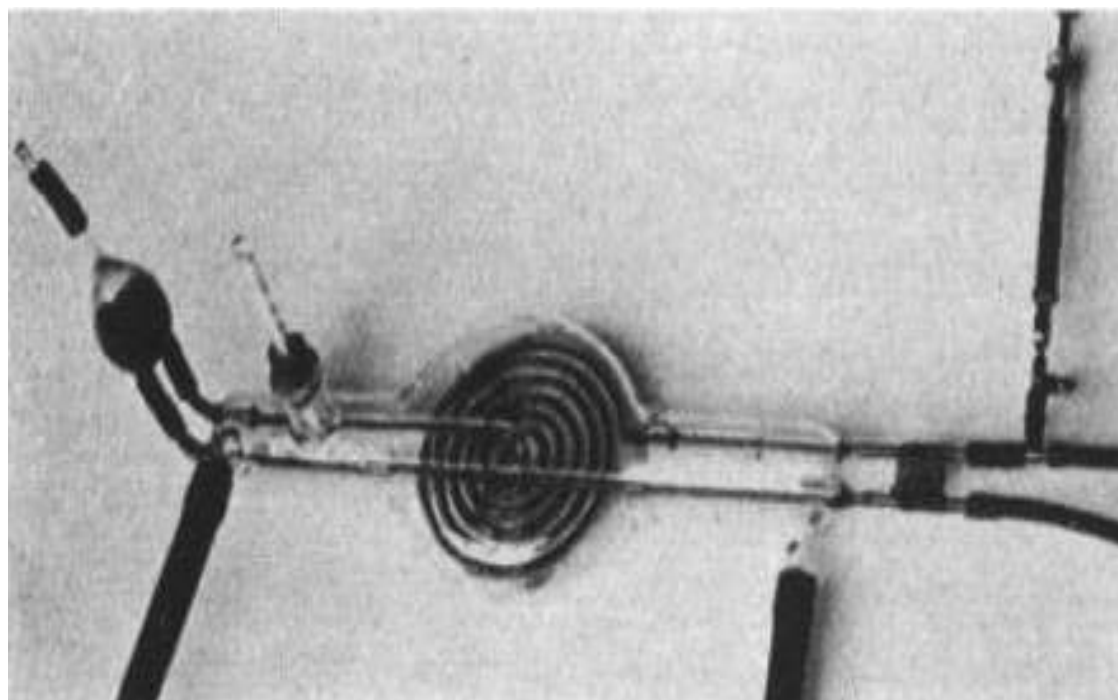


**Figure 1.1.** An image of the simple bubble flow meter used by Dumke and Schmidt in 1943 for the first true measurement of cerebral blood flow. <sup>12</sup> The blood would come in on the right hand side, where the air bubble would be injected. The trap on the left is where the air bubble would be collected prior to the blood re-entering the body. Permission to reproduce the image was not required by the *American Physiological Society*.

The first assessment of CBF in humans was performed by Seymour Kety and Carl Schmidt in 1945<sup>19</sup> through the use of low concentration of nitrous oxide inhalation (15%) and revolutionized the field (Figure 1.2.). This technique is based upon the notion that the rate at which the content of an inert gas in the cerebral venous blood approaches that of the inert gas in the arterial blood will be dependant upon the volume of the blood flowing through the cerebrovasculature.<sup>20</sup> The inert gas being used for this methodology should also be physiologically inert and is able to rapidly cross the blood-brain barrier.<sup>19</sup> The subject would inhale 100% oxygen for a period of 20 minutes prior to the assessment of CBF via 15% Nitrous Oxide / 21% Oxygen / 64% Nitrogen.<sup>19,20</sup>

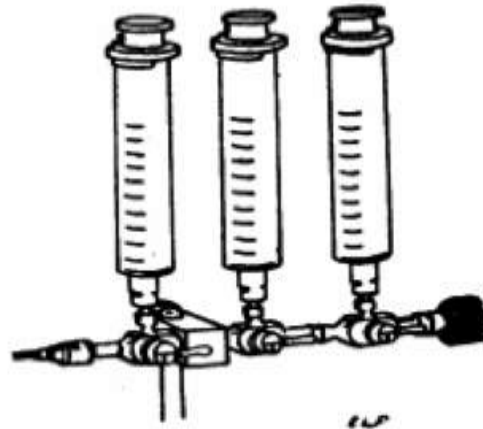
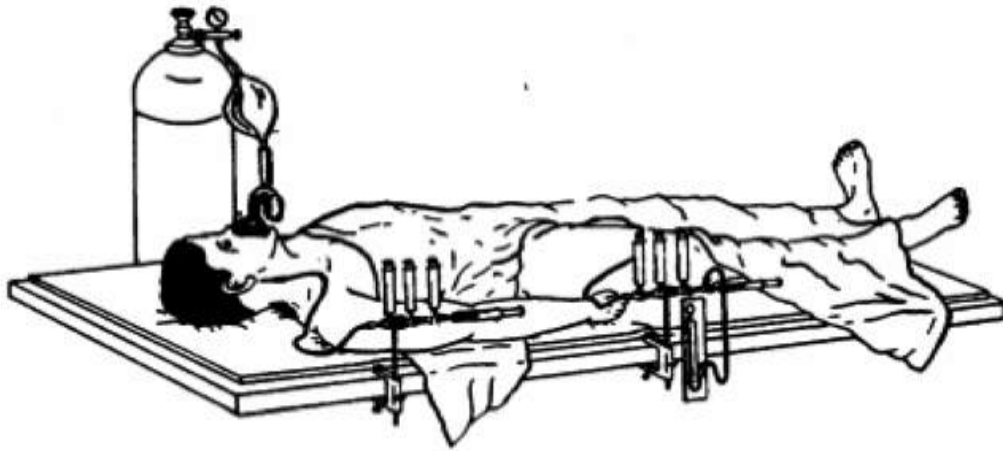


**Figure 1.2.** Illustration of the typical experimental protocol used in 1948 by Kety and Schmidt for the first CBF measurements in man.<sup>20</sup> The gas mixture was inhaled through the facemask and the blood samples were drawn from the radial artery and jugular vein. Image was reproduced with permission from the *Journal of Clinical Investigation*.<sup>20</sup>

Cerebral blood flow assessments were performed at 2, 4, 6, and 10 minutes (20 minutes is approximately the time it takes for the arterial and venous concentrations of nitrous oxide to be in equilibrium – Figure 1.3.) via simultaneous internal jugular venous and femoral artery samples and flow was calculated via modifying the Fick equation (Equation 1.1.):

**Equation 1.1.** 
$$CBF = \frac{100 Q_t}{(A-V)t}$$

Where: CBF is cerebral blood flow (in ml/100g brain mass/minute);  $Q_t$  is the quantity of oxygen consumed over time (expressed as ml/100g brain mass);  $A$  and  $V$  represent the arterial and cerebral venous oxygen content as percent of volume;  $t$  is time in minutes. Brain mass was assumed to be 1400 grams. <sup>19,29</sup>

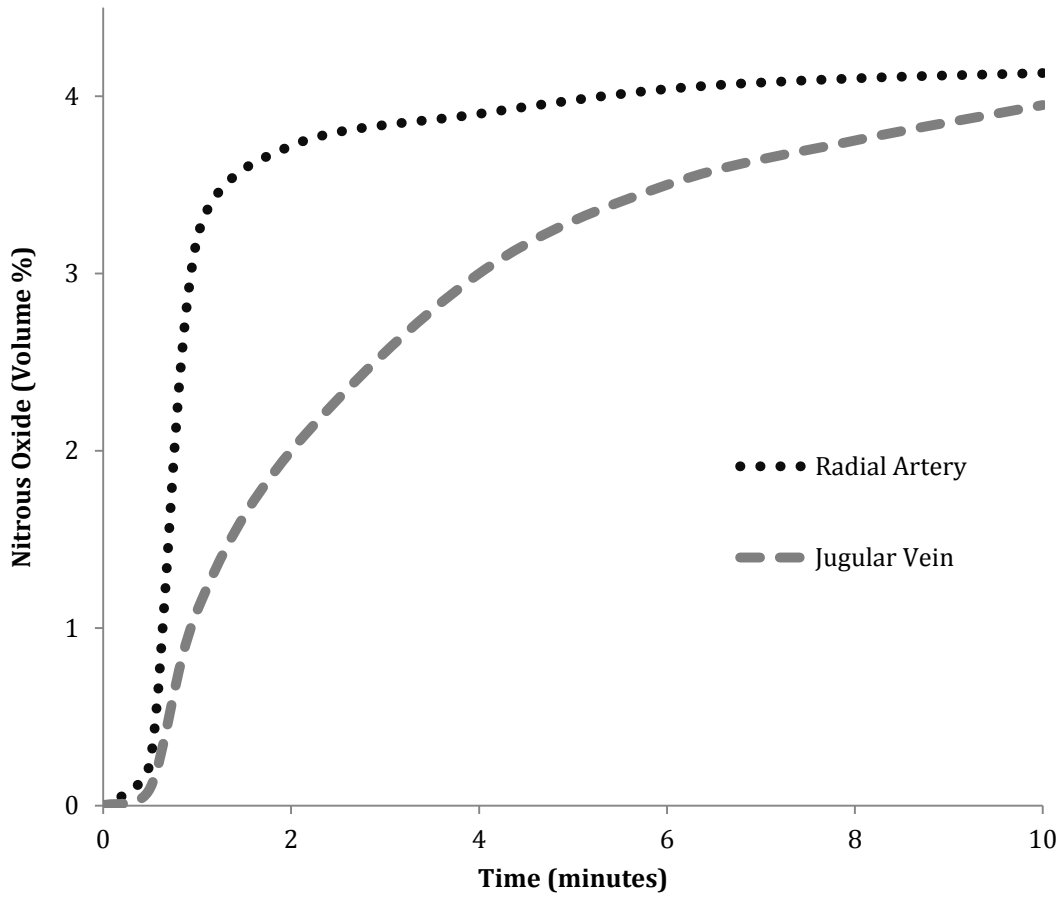


**Figure 1.3.** Typical sampling of nitrous oxide concentration (as measured by volume %) from the radial artery and jugular vein during the Kety-Schmidt method during a 10-minute sampling period while inhaling 15% nitrous oxide. Modified from: <sup>20</sup>.

The authors then used the same general principle and applied it to any substance that is removed from the blood by the brain (such as nitrous oxide). Prior to inhalation, both the arterial and venous components will have a concentration of 0 and will increase with time (Figure 1.3.). The arterial concentration will rise more rapidly than venous with the maximal difference occurring within the first 30 seconds.<sup>19,20</sup> Therefore the same  $(A-V)t$  formula is used for calculating CBF via oxygen, but will be represented by the area between the arterial and venous nitrous oxide curves from time 0 to time t (Equation 1.2.).

**Equation 1.2.** 
$$CBF = \frac{100 Q_t}{\int_0^t (A-V) dt}$$

Where: CBF is cerebral blood flow (in ml/100g brain mass/minute);  $Q_t$  is the quantity of nitrous oxide taken up by the brain from the beginning of inhalation time to time t (expressed as ml/100g brain mass); A and V represent the arterial and cerebral venous nitrous oxide content as percent of volume;  $dt$  is change in time from the start of inhalation to time t in minutes.

Since the nitrous oxide concentration does not meet the maximal difference between arterial and venous samples until half-way through the first minute, the theoretical value at which the  $(A-V)$  difference would be at time 0 needs to be derived by a semi-logarithmic graph that is then extrapolated back to time 0.<sup>19,20</sup> Once the corrected integral for time 0 and the solubility index for nitrous oxide are determined, they can then be used to calculate CBF. From this methodology and set of calculations, Kety and Schmidt in 1945<sup>19</sup> were able to determine that global CBF based on 11 subjects. They observed a global CBF in a ‘normal’ man was ~66 ml/100g/minute (Note: they only had one healthy subject, the other 10 had co-morbidities such as multiple sclerosis, hypertension, hypochromic anemia, pneumonia and rheumatic fever).

Across this range of medical conditions, Kety and Schmidt observed that CBF varied with a peak of ~74-77 ml/100g/minute (with hypertension and rheumatic fever) to a low of ~41-50 ml/100g/minute (with gastric neurosis and multiple sclerosis).<sup>19</sup> In 1946 and 1947, Fredrick Gibbs and his co-workers performed the first measurements of CBF via injection of Evans blue dye into the internal carotid artery, and sampling from the internal jugular vein.<sup>30,31</sup> Through this methodology they recorded a global CBF in seven healthy individuals of  $44 \pm 15$  ml/100g/minute, which is consistent with the previous work by Kety and Schmidt<sup>19,31</sup> They also demonstrated that hypocapnia (CO<sub>2</sub> level obtained was not stated) caused a 32% reduction in CBF, whereas hypercapnia (via 5-10% CO<sub>2</sub> inhalation) elevated it by 40%.<sup>31</sup> By 1948, Kety and Schmidt had performed 34 assessments of CBF on 14 healthy men and were able to report that mean global CBF was  $54 \pm 12$  ml/100g/minute with a mean cerebral oxygen consumption of  $3.3 \pm 0.4$  ml/100g/minute.<sup>20</sup>

In the 1950s, Neils Lassen and Ole Munck advanced the nitrous oxide method for assessment of CBF through the inhalation of inert gas containing the radioactive isotope <sup>85</sup>Krypton.<sup>32</sup> This isotope was selected since cerebral uptake occurs strictly through diffusion and solubility, which does not differ from subject to subject. They utilized a similar methodology as described by Kety and Schmidt<sup>19,20</sup> and also determined global CBF through the Fick method.<sup>32</sup> The findings from this study confirmed that of Kety and Schmidt,<sup>20</sup> as they observed global CBF varied from 33-67 ml/100g/minute and cerebral oxygen consumption varied from 2.4 to 4.3 ml/100g/minute.<sup>32</sup>

In the early to mid 1960s, the first regional CBF measurements were made possible by modifying the methods of Gibbs, Maxwell and Gibbs.<sup>30,31</sup> Here, the authors injected 3-5 millicuries of radioactive isotopes (<sup>85</sup>Krypton or <sup>133</sup>Xenon) dissolved in 2-3 ml of saline into the

internal carotid or vertebral arteries. <sup>33,34</sup> The injection occurred in a stepwise fashion over a period of 2.5 to 3.5 minutes. <sup>34</sup> The build-up and subsequent clearance of the isotopes were monitored for 15 minutes by collimated scintillation detectors at a depth of less than 5 mm over the region of interest of the cerebral cortex. <sup>33,34</sup> The first measurements made in man determined a regional blood flow of 43-51 ml/100g/minute in the middle frontal gyrus. <sup>34</sup> By 1965, “regional” CBF measures were reported for the: temporal region ( $48.7 \pm 6.3$  ml/100g/minute); pre-central region ( $50.0 \pm 5.0$  ml/100g/minute); central ( $51.7 \pm 6.2$  ml/100g/minute); and post-central region ( $48.9 \pm 4.4$  ml/100g/minute). <sup>35</sup> The same study <sup>35</sup> reported the global CBF to be  $49.8 \pm 5.4$  ml/100g/minute, and compares well with the values presented in follow up study ( $50.0 \pm 5.2$  ml/100g/minute) by the same research group in 1971.

36

The problem with the regional and global CBF measures as described previously<sup>19,20,30,32-36</sup> is the time scale (10-20 minutes per measure) upon which the measures are made precludes any information about ‘dynamic’ CBF changes. In 1982, Rune Aaslid, Thomas-Marc Markwalder and Helen Hornes<sup>37</sup> rectified the time scale issue for estimation of CBF through the use of non-invasive transcranial Doppler ultrasound (Figure 1.4.). Transcranial Doppler ultrasonography is able to provide a real-time index of CBF by using a 1 to 2 MHz probe placed over the acoustic windows provided by thin bones of the temporal region of the skull. <sup>37,38</sup> This window enables the observation of the Doppler shift (difference between the transmitted and received signals – Figure 1.5.) of the red blood cells as they pass through large intracranial vessels (middle, anterior and posterior cerebral arteries). <sup>37,38</sup>



**Figure 1.4.** The first transcranial Doppler, the “UrDoppler” as first constructed by Rune Aaslid in December of 1981 at the University of Berne, Switzerland, and was still in clinical use in the early 21<sup>st</sup> century.

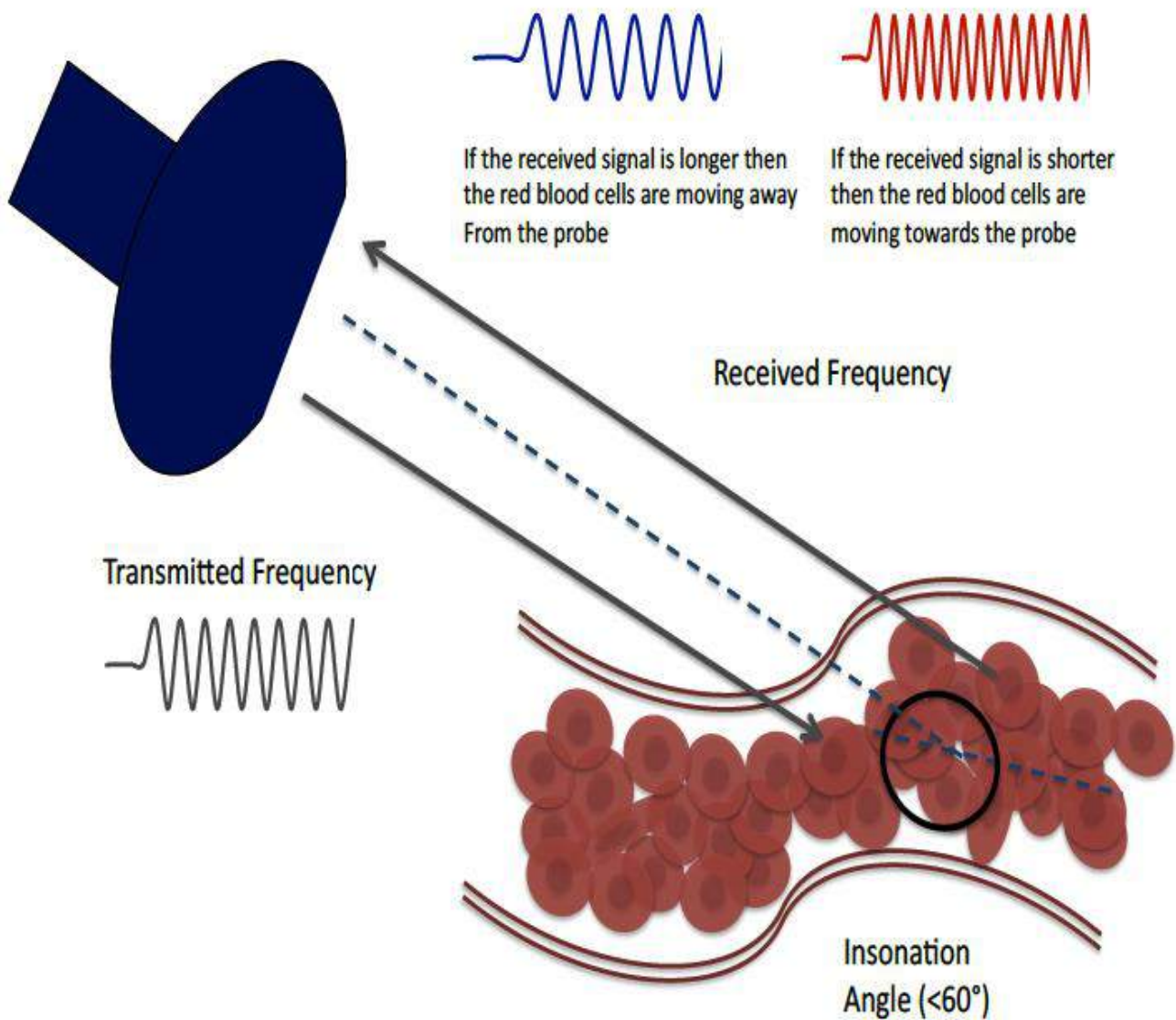


**Figure 1.5.** Example of the Doppler shift. The frequency difference between the transmitted signal and the received signal is used to determine the direction and velocity of the red blood cells.

The Doppler shift is used to determine the velocity of the red blood cells via the following equation (Equation 1.3.):

**Equation 1.3.** 
$$\text{Doppler shift} = 2 \times Ft \times V \times \cos\theta / C$$

Where:  $Ft$  is the transmitted frequency (2 MHz);  $V$  is the velocity of the reflector (red blood cells);  $\cos\theta$  is the correction factor based on the angle of insonation; and  $C$  is the speed of sound in the blood (1540m/s).

Based on this method, Aaslid, Markwalder and Hornes<sup>37</sup> were the first to be able to record the velocity of the red blood cells in the: middle cerebral artery (MCAv:  $62 \pm 12$  cm/s); anterior cerebral artery ( $51 \pm 12$  cm/s); and posterior cerebral artery (PCAv:  $44 \pm 11$  cm/s) in healthy individuals from 20-65 years old. Since this initial study,<sup>37</sup> there have been in excess of 6500 studies that have used transcranial Doppler ultrasound to assess cerebral blood velocity (CBV) across a wide range of conditions and populations including; alterations to partial pressures of oxygen<sup>39-42</sup> and carbon dioxide; <sup>42,43</sup> intracranial pressure and cerebral perfusion pressure; <sup>44</sup> neurovascular coupling; <sup>45</sup> changes in posture; <sup>46</sup> during acute exercise; <sup>47-49</sup> chronic exercise; <sup>50,51</sup>; throughout healthy aging; <sup>49-51</sup> and in clinical populations such as heart transplant recipients. <sup>48,52-54</sup> The greatest benefit to this methodological approach to CBF measurement is that it is non-invasive, highly reproducible and can provide measurements with high temporal resolution. <sup>38</sup> The limitation to this methodology is that it only provides an index of flow, and is not a true measurement of flow (as provided by the Kety-Schmidt method, for example <sup>19,20</sup>); as such, dynamic changes in diameter of the insonated vessels would impact the index of flow as per Poiseuille's law (Equation 1.4):

**Equation 1.4.**

$$F = (P_1 - P_2) \pi r^4 / 8 \mu L$$

Where: F is flow;  $P_1$  is the inflow pressure;  $P_2$  is the outflow pressure; r is the vessel radius;  $\mu$  is the viscosity of the fluid; and L is vessel length.

There are several other recent advancements in the field of CBF measurement such as: near infrared spectroscopy; positron emission tomography; single photon emission computed tomography; magnetic resonance imaging with arterial spin labelling; and volumetric Doppler ultrasound. These methodologies will be briefly describe below:

*Near infrared spectroscopy (reviewed in: <sup>55</sup>):*

This is a non-invasive bedside technique that provides an indication of cerebral oxygenation levels, through the use of light emitted in the near infrared band (700 to 1000nm). The light emitter is placed on the skin next to the sensor, thus enabling the light to be directed perpendicularly through the brain (to a depth of 7-8cm) where it is reflected back to the sensor. The reflected signal will give an indication of the combined oxygenation level of the arterioles, capillaries and venules and as such it is not the most suitable tool for overall CBF but is useful for determining a change in overall oxygenation levels in real time. The advantage to this methodology is that it can provide a bedside measure of alterations to cerebral oxygenation; however, the poor spatial resolution and inability to provide a measurement of CBF limit its applications for the quantification of CBF.

*Positron emission tomography (reviewed in: <sup>56</sup>):*

This is a minimally-invasive technique that utilizes a positron-emitting radioisotope ( $^{15}\text{O}_2$ ,  $\text{C}^{15}\text{O}_2$ ,  $\text{H}_2^{15}\text{O}$  – administered via intravenous injection or inhalation) and then CBF is calculated through the imaging of the isotopes. After steady-state has been achieved, a 1-2 minute scan is performed and the regional maps of the brain for CBF; intracranial velocity; and the cerebral metabolic rate of oxygen, glucose and lactate are able to be computed. The greatest advantage to this technique is that the both white and gray matter can be imaged with great accuracy and reproducibility (<8% variance over multiple days of measures) <sup>57,58</sup>, but the largest limitations are that it is not able to be performed by the bedside, involves administration of a radioactive substance and has poor time resolution.

*Single photon emission computed tomography (reviewed in: <sup>56</sup>):*

This is also a minimally-invasive technique that is utilized to generate 3-dimensional images of the cerebral hemodynamics that can be made at the bedside. A retention tracer is administered and then the images are collected by a series of multiple detector cameras over a period of 10 to 15 minutes. The noise from the scattering of photons in the body can affect the quantification of the voxels of the acquired images. The images obtained provide an index of cerebral perfusion that can be compared to normal control images to note abnormalities. The limitations of this technique are that it has poor time resolution, requires radiation, and a correction factor is required to have the images relate back to CBF.

*Magnetic resonance imaging with arterial spin labelling (reviewed in: <sup>56</sup>):*

This is a non-invasive technique that utilizes the detection of magnetically labelled water (spin labelling) to provide a measure of CBF. The labelling occurs at the carotid level of the brain then the bolus is observed within the region of interest within the brain. Multiple paired images are made over a period of 5 to 10 minutes of the labelled and control conditions (observation of the region of interest in the brain without any spin labelled water present), which are subsequently averaged together to get a sufficient signal-to-noise ratio, which is suitable for interpretation. The major limitations of this method are that the difference between the labelled and control images is typically only about 1% and therefore are not able to accurately detect changes in flow of less than 10 ml/100g/minute, it is difficult to obtain blood pressure measures while in the scanner and that it has poor time resolution. The greatest benefit to this technique is that it does not require the use of a radioactive tracer and it provides detailed information on regional perfusion.

*Volumetric Doppler ultrasound (reviewed in: <sup>56</sup>):*

This is a non-invasive technique that utilizes Doppler ultrasound (based upon the principle described in the section on transcranial Doppler ultrasound), but has the added benefit of being able to track the cross-sectional area of the insonated vessel (internal carotid and/or vertebral arteries). This method is able to provide a real time assessment of CBF to the anterior (internal carotid artery) and posterior (vertebral artery) of the brain, as both velocity and area are known quantities. In order for the velocity of the red blood cells to be valid the insonation angle must be held constant and be kept less than 60 degrees. For accurate repeat measures, the same area of the vessel and insonation angles should be replicated. The greatest limitation of

this methodology is that it requires a trained sonographer, is very dependant upon the anatomical locations of the vessels of interest (e.g., if the bifurcation is very superior then the internal carotid artery is unable to be insonated) and is unable to be performed if the neck of the subject is not relatively stationary. Another limitation that limits the duration and reliability of sampling is that the probe is still hand-held rather than fixed in place.

Based upon the strengths and weakness of each of the previously mentioned methodologies to assess CBF, transcranial Doppler ultrasound was selected for use in the studies presented this thesis due to the availability, high time resolution, highly reproducible results, bedside application, portability and robust ability to maintain the signal quality over time and throughout movement to provide an index of CBF. This method for the use of transcranial Doppler ultrasound is covered in detail in section 2.1.1.

## 1.5. Factors that influence cerebral blood flow

The following section of the thesis will highlight some of the key modulators of CBF, namely: Arterial blood gases; intracranial pressure; cerebral perfusion pressure; local metabolism; neurogenic innervation; neurovascular coupling; influence of posture; effects of acute and chronic exercise; aging, and selected pathologies.

### 1.5.1. Arterial blood gases

#### *Carbon Dioxide*

Out of all components that contribute to the regulation of CBF it has been shown that the partial pressure of arterial carbon dioxide ( $P_aCO_2$ ) has the greatest impact (reviewed in: <sup>59,60</sup>). The blood-brain barrier is highly permeable to the small non-polar carbon dioxide molecules, enabling it to readily diffuse from the blood stream into the cerebrospinal fluid and extra-cellular fluid. Once in these fluids, carbon dioxide dissociates within the bicarbonate buffer system and causes large swings in extracellular pH via the chemical reaction:



Once carbon dioxide is dissociated, it forms  $H^+$  and  $HCO_3^-$ , which will lead to decreases in pH during hypercapnia (increases in  $P_aCO_2$ ) and increases in pH with hypocapnia (decreases in  $P_aCO_2$ ).<sup>29</sup> During hypercapnia, the decreased pH in the extracellular fluid leads to a vasodilatory response and thus increases CBF. In contrast, increases pH associated with hypocapnia results in vasoconstriction and a decrease in CBF.<sup>29</sup>

It was initially proposed that the pial vessels were the only site where the alterations to cerebrovascular resistance (and thus changes in blood flow) occurred.<sup>61,62</sup> This notion held true during early magnetic resonance imaging (MRI) work as a 1.5 Tesla MRI revealed that there were no changes to the middle cerebral artery diameter during both hypercapnia<sup>63</sup> and hypocapnia.<sup>63,64</sup> However, more recent work with 3 Tesla<sup>65</sup> and 7 Tesla<sup>66</sup> MRI have revealed that minor changes to  $P_aCO_2$  ( $\pm 8$  mmHg from eucapnia) do not affect middle cerebral artery diameter.<sup>67</sup> Whereas changes greater than 8 mmHg from eucapnia, resulted in elevations (6-8%) in the diameter of the middle cerebral artery during a +10-15 mmHg hypercapnic stimulus,<sup>65,66</sup> and decrease the diameter 4% during a -13 mmHg hypocapnic stimulus (Figure 1.6.).<sup>65</sup> Thus it appears as though there is a physiological range in which  $P_{ET}CO_2$  has a negligible effect on the discrepancy between CBF and CBV as indexed by transcranial Doppler.<sup>67</sup>

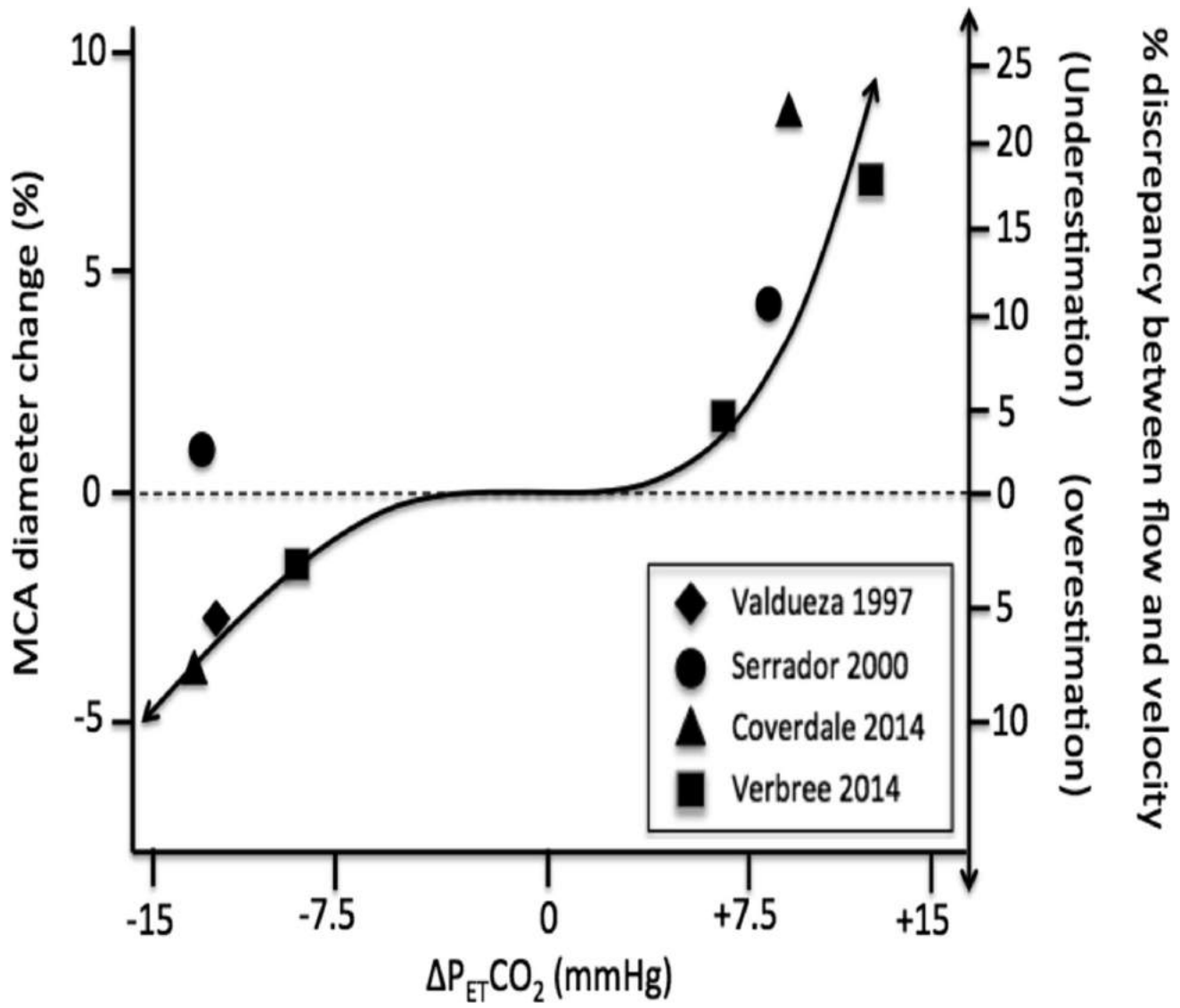


**Figure 1.6.** The previously reported middle cerebral artery diameter changes (left y-axis) as they relate to over and under estimation of cerebral blood flow (right y-axis) with respect to alterations in end-tidal CO<sub>2</sub> (x-axis).<sup>67</sup> Permission to reproduce the figure was not required by the *Journal of Applied Physiology*.

In 1987 Faraci, Heistad and Mayhan<sup>68</sup> revealed in cats, that the large arteries of the neck (internal carotid and vertebral arteries) are sensitive to changes in carbon dioxide and account for approximately 33% of the total change in vascular resistance. Comparatively, research in humans has also revealed evidence that the large arteries of the neck also respond to alterations in  $P_aCO_2$ .<sup>42</sup> Similar to the recent MRI data, using vascular ultrasound, it appears as though the large arteries of the neck do not measurably change in diameter with modest changes in  $P_aCO_2$  from eucapnia ( $\pm 10$  mmHg).<sup>42</sup> In contrast, alterations in  $P_aCO_2$  of  $\pm 25$  mmHg lead to 11.5% increase (hypercapnia) and a 6.5% decrease (hypocapnia) change of internal carotid artery diameter.<sup>42</sup> Thus there is growing evidence that the entire cerebrovascular system is responsive to alterations in pH induced via alterations to  $P_aCO_2$  and not just at the level of the pial vessels (reviewed in:<sup>59</sup>).

Broadly consistent to the notion that diameter changes are greater with large ( $>10$  mmHg) hypercapnic than hypocapnic alterations to  $P_aCO_2$ , there is also evidence of a similar hysteresis effect on CBF (reviewed in:<sup>59</sup>). Hypercapnic increases in  $P_aCO_2$  results in a CBF increase of  $\sim 2-5\%/mmHg$ ,<sup>29,42,65</sup> whereas hypocapnic decreases in  $P_aCO_2$  lead to  $\sim 1-2\%/mmHg$  reduction in CBF.<sup>29,42,65</sup> Kety and Schmidt first demonstrated this curvilinear response to both pH and  $P_aCO_2$  in 1948 (Figure 1.7.).<sup>29</sup> Recently, it has been suggested that the mechanism for the disproportionate changes in flow could possibly be due to a large shear-stress mediated release of endothelial nitric oxide that coincides with the increased flow associated with hypercapnia.<sup>69,70</sup> In contrast, in response to hypocapnia, there is a reduced if not absent shear stress.<sup>42,71</sup>

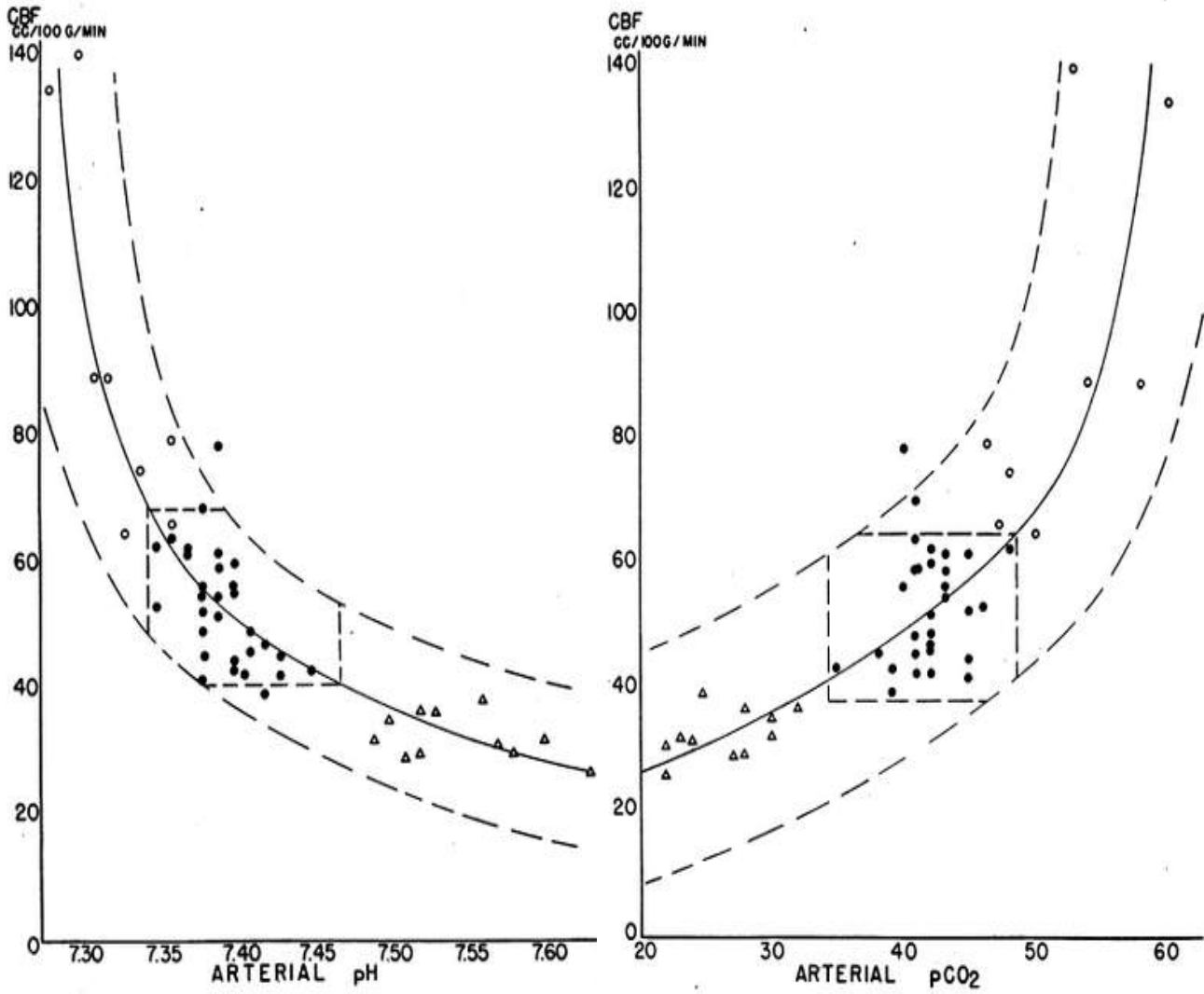


**Figure 1.7.** The relationship between cerebral blood flow and arterial pH (left) and arterial CO<sub>2</sub> (right). The filled in circles represent normocapnia, open circles are breathing 5-7% CO<sub>2</sub> and triangles represent hyperventilation. The central line represents the mean data, dotted lines are 98% confidence intervals.<sup>29</sup> Permission to reproduce the figures was provided by the *Journal of Clinical Investigation*.

## Oxygen

The brain is less sensitive to changes in arterial partial pressure of oxygen ( $P_aO_2$ ) than  $P_aCO_2$ . There is a semi-logarithmic relationship between  $P_aO_2$  with CBF (reviewed in: <sup>59,60</sup>). Increases in  $P_aO_2$  above euoxemia have little effect on CBF, whereas extreme hypoxemia ( $P_aO_2 < 50$  mmHg) results in a substantial increase in CBF to ultimately maintain oxygen delivery. <sup>12,29,42</sup> Dumke and Schmidt in 1943<sup>12</sup> were the first to demonstrate this notion. They observed a small reduction in CBF of ~8% when 100% oxygen was inhaled by the macaques monkey, whereas anoxemia elicited nearly a 100% increase in CBF. <sup>12</sup> Since anoxemia is the *extreme end* of the physiological spectrum of hypoxemia, the breakpoint for the CBV *versus* arterial oxygen tension relationship has been investigated and shown to occur when  $P_aO_2$  falls below 50 mmHg (Figure 1.8). <sup>42</sup>

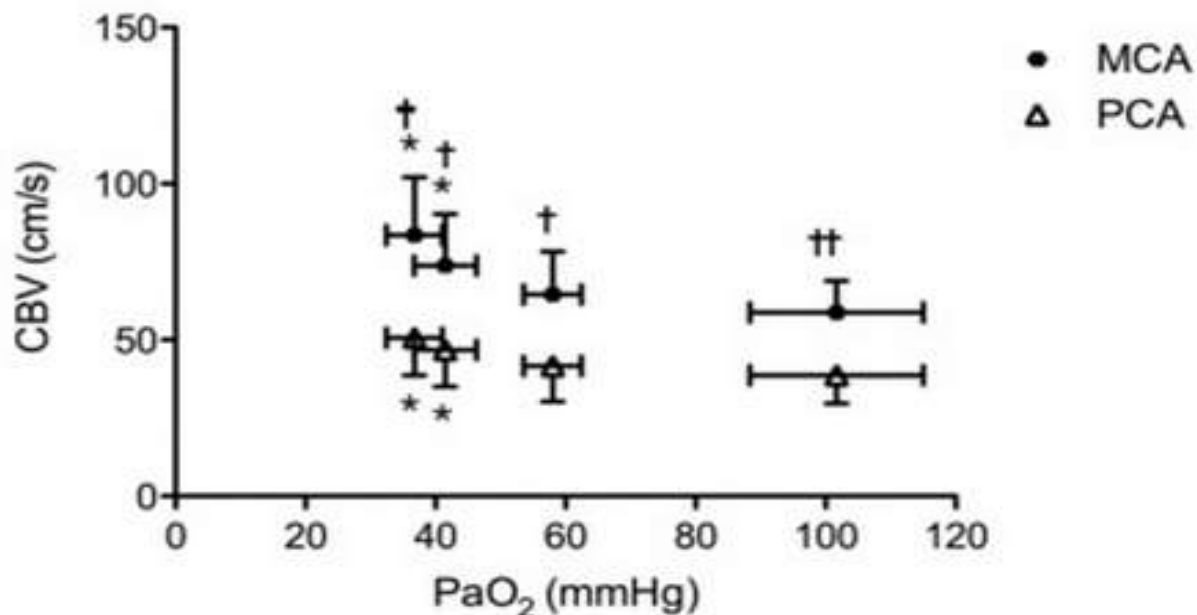


**Figure 1.8.** The relationship between cerebral blood velocity and steady-state changes in arterial  $O_2$ . The filled in circles represent the middle cerebral artery (MCA) and open triangles represent the posterior cerebral artery (PCA). <sup>42</sup> Permission to reproduce the figure was provided by the *Journal of Physiology*.

In 1948, Kety and Schmidt<sup>29</sup> investigated the effects of altered oxygen tensions (hypoxia – FiO<sub>2</sub>: 10%; normoxia – FiO<sub>2</sub>: 21%; and hyperoxia – FiO<sub>2</sub> 85%) on CBF and oxygen consumption. They observed a +35% increase in CBF during hypoxia (despite a 4 mmHg decrease in PaCO<sub>2</sub>), and a -13% reduction in CBF during hyperoxia.<sup>29</sup> Despite the large changes in CBF levels across the study interventions, they noted that there was no change in the level of cerebral oxygen consumption and extraction rates were maintained at ~35-40%.<sup>29</sup> However, more recent data from blood oxygen level dependant MRI studies have revealed that the reduced oxygen content present when the FiO<sub>2</sub> is reduced to 8-12% will lead to a >50% increase in the oxygen extraction fraction rates.<sup>72,73</sup> An even more recent study has been performed in elite breath-hold divers (mean breath hold time of 316 ± 60 seconds; P<sub>a</sub>O<sub>2</sub> 29.5 ± 6.5 mmHg).<sup>74</sup> This study revealed that global oxygen delivery is maintained throughout the breath-hold maneuvers despite these extremely low arterial oxygen levels.<sup>74</sup> Combined, these findings indicate that increases to global CBF act to maintain oxygen delivery; thus, the oxygen demands of the brain are met even during the most physiological extreme conditions.<sup>12,29,42,73,74</sup>

### **1.5.2. Intracranial pressure**

As proposed in the Monro-Kellie doctrine,<sup>21</sup> the fluids within the brain are encased in a rigid container; as such, the internal volume tends to remain relatively constant. This means that in order to maintain a normal pressure within the rigid skull, if there is an increase in either the blood or cerebrospinal fluid volume inside the cranium then there should be a subsequent decrease in the other and thus normal intracranial pressure should be maintained between 0 and 15 mmHg.<sup>75</sup> The first accurate descriptions of the effects of intracranial pressure on the cerebrovasculature were reported by Roy and Sherrington in 1890,<sup>15</sup> and Bayliss and Hill in

1895.<sup>14</sup> They noted that intracranial pressure does not solely depend on the direct tension of the cerebral arteries, but is more closely related to the pressure within the cerebral capillaries and veins.<sup>14</sup> They concluded that the pressure in the venous sinuses (as measured in the Torcula Herophili) could be utilized as a surrogate for intracranial pressure; however, it was also noted that if the intracranial pressure exceeds that of the venous sinus then the cerebral circulation would be disrupted.<sup>14,15</sup> This disruption occurs because the increase in intracranial pressure could be severe enough to increase the transmural pressure on the cerebral vessels and could cause them to collapse. Since cerebral perfusion pressure is equal to the difference between mean arterial and intracranial pressure, the worst-case scenario for an increase in intracranial pressure would be if it exceeds that of the mean arterial pressure. In this case CBF would cease and the subsequent build up of intracranial pressure would cause brain herniation or cerebral ischemia, or both.<sup>75</sup>

### **1.5.3. Cerebral perfusion pressure**

Cerebral perfusion pressure is the balance point between the pressure driving blood to the brain (mean arterial pressure) and the intracranial pressure. It was originally proposed by Bayliss and Hill in 1895,<sup>14</sup> that increases to mean arterial pressure (and thus cerebral perfusion pressure) will result in an increase to CBF and a reduction in arterial pressure will reduce it. This notion prevailed until 1959, when a review paper proposed that CBF is maintained at approximately 50 ml/100grams brain mass/minute across a wide range of cerebral perfusion pressures (50-150 mmHg – Figure 1.9.).<sup>16</sup> In 1973, Strandgaard and colleagues<sup>76</sup> reported the upper limit of the cerebral autoregulatory curve in hypertensive humans occurs in the mean arterial pressure range of 150-200 mmHg. This work was further expanded upon in 1978 by

Kontos *et al.*,<sup>77</sup> where they used a cat model to identify changes in pial vessel diameter to alterations in arterial pressure. They demonstrated that when mean arterial pressure decreased below 70 mmHg, the smallest pial vessels (<100 microns) dilated more than the larger pial vessels (>200 microns).<sup>77</sup> Conversely, when the mean arterial pressure was increased to ~170-200 mmHg, the small pial vessels dilated while the larger pial vessels were constricted.<sup>77</sup> At pressures above 200 mmHg, all of the pial vessels dilated, regardless of size.<sup>77</sup> These findings indicate that the responses of the cerebrovasculature to alterations in arterial pressure are likely due to a highly complex integration of varying responses throughout the entirety of the cerebrovasculature.<sup>78</sup>

Recent research, however, has shown that the original work by Bayliss and Hill,<sup>14</sup> is likely a more accurate and apt description for the relationship between cerebral perfusion pressure and CBF. There is evidence that the autoregulatory window is not quite as robust as initially suspected and that the blood pressure range does not extend from 50-150 mmHg as speculated,<sup>17</sup> but is more likely only encompasses a 10 mmHg around a mean arterial pressure window (85-95 mmHg) in which CBV is relatively constant (reviewed in:<sup>59</sup>). If cerebral perfusion pressure is lower than ~85 mmHg there will be a subsequent reduction in cerebrovascular resistance causing vasodilation in order to maintain oxygen delivery via an increase CBF.<sup>59</sup> If CBF falls too low (below 15 ml/100 grams brain mass/ minute) the individual is put at risk of suffering an ischemic stroke (reviewed in:<sup>79,80</sup>). Conversely, if cerebral perfusion pressure rises too far above the plateau region damage to the cerebral vessels could occur which would end up resulting in a cerebral haemorrhage (reviewed in:<sup>79,80</sup>). In a recent review article,<sup>81</sup> it was highlighted that the cerebrovasculature is better able to buffer transient increases in cerebral perfusion pressure and is more pressure-passive in response to

reductions in cerebral perfusion pressure. This indicates that brain has a greater protective response mechanism to over perfusion rather than under perfusion, as under perfusion can be compensated for by increasing oxygen extraction from the blood, at least to a certain extent (refer to section 1.5.1. for further discussion on this topic).<sup>72,73</sup>

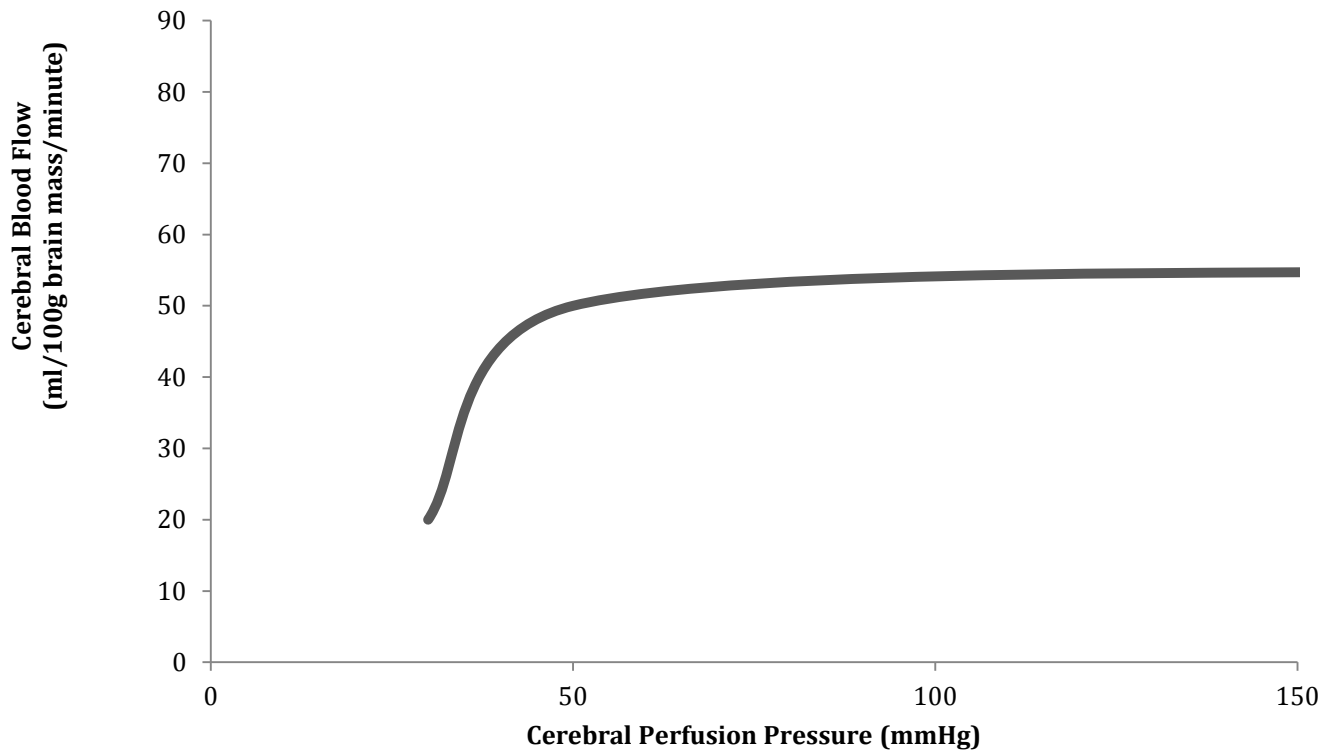


**Figure 1.9.** The cerebral autoregulatory curve as first proposed by Dr. Niels Lassen in 1959. Modified from:<sup>16</sup>.

#### 1.5.4. Neurogenic factors

There is an extensive network of both sympathetic and parasympathetic nerves that innervate the cerebral blood vessels and can be broadly categorized into two main categories: intrinsic and extrinsic.<sup>59,82,83</sup>

The intrinsic innervation pathways are present in the deeper levels of the parenchyma, where they interact with the cortical microvessels and astrocytes.<sup>82,83</sup> Pharmacological, anatomical and molecular studies have revealed resounding evidence that the connections between the intrinsic neurons and the microvessels and/or astrocytes cause the release of vasoactive mediators which have specific receptor sites located on the local endothelial cells and/or upstream smooth muscle cells; these vasoactive mediators can cause either constriction or dilation when activated. Additional receptors are located on the astrocytes and thus provide an additional means to alter vessel tone (reviewed in:<sup>82,83</sup>). The functional role of these intrinsic nerves have been difficult to define in humans (reviewed in:<sup>59</sup>).

The extrinsic innervation pathways are present outside of the parenchyma. The three main sources of the extrinsic innervation are; 1) trigeminal ganglion; 2) sphenopalatine ganglion; and 3) superior cervical ganglion.<sup>59,83</sup> Unilateral<sup>84</sup> and bilateral<sup>85-87</sup> cervical ganglion excision has resulted in increases to CBF, which provides convincing evidence that the sympathetic nervous system is involved in cerebral vessel tone and blood flow regulation. Thus, the sympathetic control of CBF has been speculated to be involved in increasing vessel tone as a protective mechanism in acute hypertensive states,<sup>59,83</sup> possibly to reduce intracranial pressure (as per the Monro-Kellie doctrine<sup>21</sup>). When chronic hypertension occurs, cerebrovascular remodelling occurs through a multitude of factors with the end-result being increased cerebrovascular resistance and reduced CBF (reviewed in:<sup>88</sup>). It has also been

speculated that the parasympathetic innervation of the cerebrovasculature was involved in counteracting the vasoconstriction of the sympathetic nervous system through activation of the trigeminal nerves.<sup>83</sup>

The extracranial cerebral blood vessels (internal carotid and vertebral arteries) are also highly innervated with both sympathetic and parasympathetic fibres and therefore have the ability to be involved in the neural regulation of CBF.<sup>59,89</sup> The specific role of this innervation has yet to be clearly proven; however, it has been speculated that neurogenic innervation encompassing the cerebrovasculature limits the amount of turbulent blood flow in the winding segments of the extracranial vessels.<sup>59</sup> The increase in turbulence, could in turn cause a drop in downstream perfusion pressure as per Poiseuille's law (Equation 1.4.).

Thus there is evidence that the entire length of the cerebrovasculature (from the microvessels and their surrounding astrocytes to the large extracranial vessels) is highly innervated with both sympathetic and parasympathetic nerve fibres, which enables the cerebrovasculature to respond to changes in arterial blood pressure uniformly.<sup>59</sup> When there are large increases in mean arterial pressure (up to 170 mmHg), cerebral SNA is likely activated in order to constrict and limit over perfusion damage.<sup>77</sup> However, if the increases to mean arterial pressure are too high (>200 mmHg), the cerebrovasculature is no longer able to constrict to counter the increases in pressure and becomes more pressure-passive.<sup>77</sup> Conversely, when there is a decrease in mean arterial pressure there is a vasodilatory response within the cerebrovasculature.<sup>16,59,77</sup> These findings once again highlight the notion that regulation of the cerebrovasculature likely occurs through a highly complex integration across the entire length of the cerebrovasculature.<sup>78</sup>

### 1.5.5. Neurovascular coupling

In the late 1800s, research performed by Angelo Mosso<sup>22</sup> as well as that of Roy and Sherrington<sup>15</sup> revealed the notion that with an increase in neuronal activity in the brain, there is a subsequent increase in CBF. This coupling of neuronal activity and alterations to CBF was later termed “*neurovascular coupling*”. Before describing the mechanisms underlying neurovascular coupling, the blood-brain barrier and neurovascular unit will be described.

#### *Blood-brain barrier (Figure 1.10.)*

Paul Ehrlich discovered the blood-brain barrier in 1885 when he noted that intravital dyes that were injected intravenously would stain the peripheral organs but could not penetrate into the brain and spinal cord. This idea was confirmed in 1900 by Max Lewandowski, when he concluded that the capillaries within the brain are able to hold back certain molecules. (reviewed in: <sup>90,91</sup>). It took another 67 years, and the advent of the electron microscope, before the root causes for the earlier notions of Ehrlich and Lewandowski were finally revealed; astrocyte end-feet; pericytes; and the tight junctions between endothelial cells, combined make a barrier that is relatively impermeable to anything other than small molecules. <sup>92</sup> The blood-brain barrier is able to be overcome by small non-polar and lipid soluble molecules, but typically prevents the crossing of large polar molecules; molecules that establish hydrogen bonds; or molecules that have rotatable bonds, these type of large molecules (i.e., Glucose) are selectively regulated through active transport (reviewed in: <sup>90,91,93,94</sup>). In the 1980s, numerous studies were able to demonstrate that the astrocytes are able to influence the level of transendothelial resistance and modulate the role of the pericytes. <sup>95-97</sup> The role of the pericytes in the blood-brain barrier is to regulate the gene expression patterns of the endothelial cells.

These essentially prevents endothelial transcytosis which increases the permeability of the blood-brain barrier to water, and also helps to induce the astrocyte end-feet polarization as they surround the pial vessels.<sup>94,98,99</sup> The astrocytes are situated between the neurons and capillary endothelium and envelope more than 99% of the endothelium, as such they are in an ideal position to assist in the regulation of CBF (as regulated at the pial arterioles) to meet metabolic demand.<sup>90,93,94,99-101</sup> In addition to controlling the blood-brain barrier and the local regulation of blood flow, astrocytes are also involved in the regulation of ion and water concentrations, proliferation of stem cells and clearance of neurotransmitters (reviewed in:<sup>91</sup>).

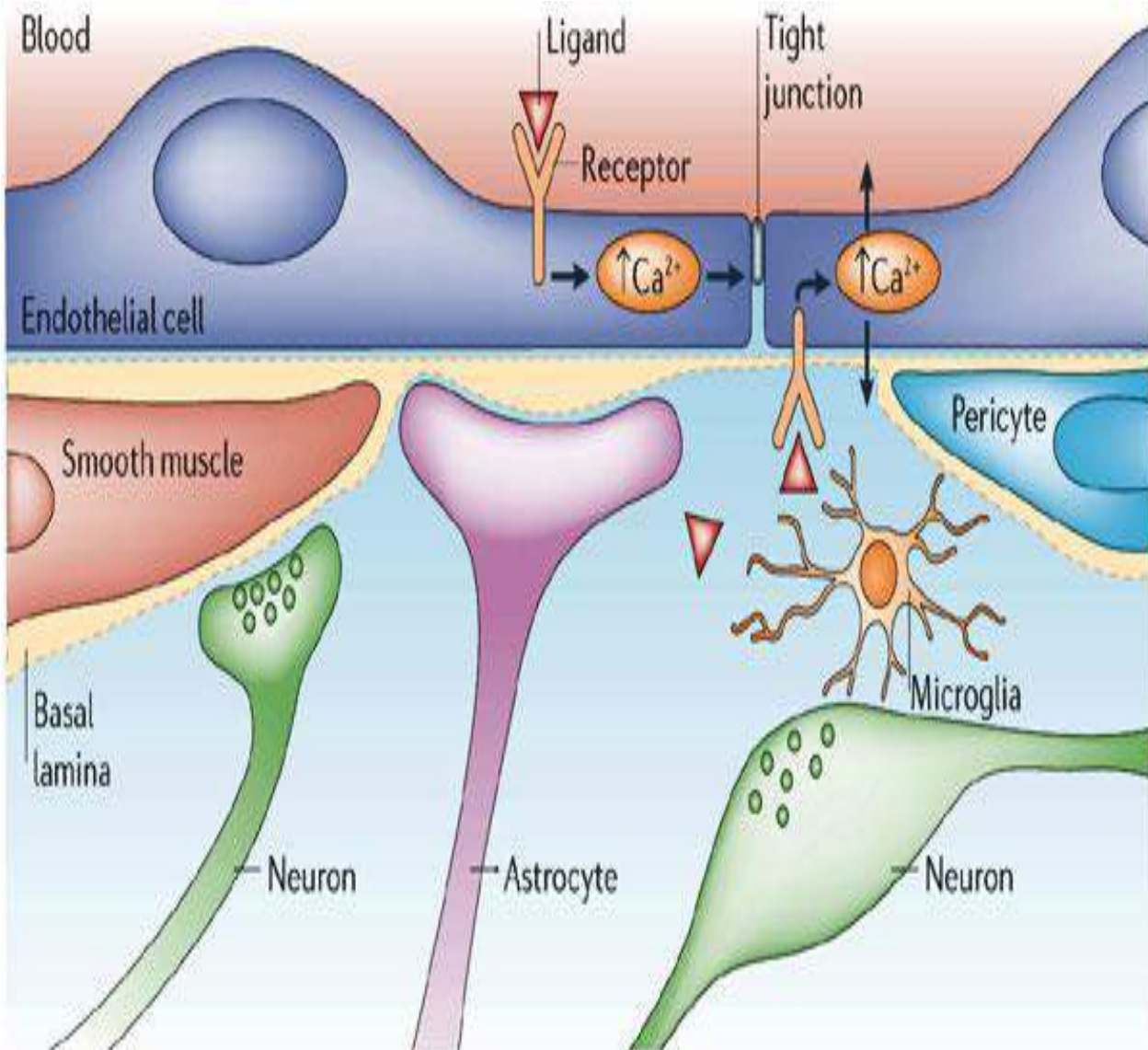


**Figure 1.10.** A section of the capillary cell wall, that highlights the main cells (astrocytes, pericytes and endothelium) responsible for the relatively impermeable blood-brain barrier. Image originally created by Abbott *et al.*,<sup>94</sup> and was reproduced with permission from the *Nature Publishing Group*.

### *Neurovascular unit*

The neurovascular unit is composed of the neurons, astrocytes, smooth muscle cells of the blood vessels, pericytes, endothelial cells and extracellular matrix.<sup>91,93,94,99,102</sup> The components of this system interact with each other through a cascade of events to regulate CBF to meet the metabolic demands of the local neurons, and guide the inflammatory response cells to where they are needed.<sup>93,99</sup>

When there is an adequate supply of oxygen, glucose and the other nutrients required by the brain are in abundant supply, the smooth muscle cells and pericytes will be in a state of basal tone.<sup>91,94,102</sup> When the neuron is activated, it will send a signal to the astrocyte via the release of glutamate, which results in the increase of calcium within the astrocyte. This initiates a chain reaction within the astrocyte that will lead to the release of vasoactive substances from the end-feet causing the pericytes and vascular smooth muscle cells to hyperpolarize, resulting in either vasodilation (when adenosine, nitric oxide, or arachidonic acids are released) or vasoconstriction (when endothelin or thromboxane are released) of the local vasculature.<sup>94,102</sup> Vasodilation causes a reduction in vascular resistance and thus flow is increased to meet the local demand for metabolites, conversely vasoconstriction increases the local vascular resistance and will result in a decrease in blood flow to the area.

### *Neurovascular coupling*

As mentioned previously, the brain requires a steady supply of glucose and oxygen to metabolize in order for it to function effectively. When there is an increase in neuronal activity within a region of the brain, this causes an increase in metabolism within the same region. This in turn increases the supply demand of the necessary substrates (namely glucose and oxygen) to

occur and an increase in delivery must happen. Thus either through increases in CBF or extraction of the nutrients from the blood (or both) must occur within this activated cerebral region.<sup>103</sup> There are at least four pathways that can lead to the localized increase in CBF; 1) the release of metabolite by products that cause local vasodilation; 2) regulation by astrocyte activation; 3) release of nitric oxide due to shear stress; and 4) direct neural activation of the vasculature.

The first pathway for the increased blood flow (or nutrient delivery) was initially proposed by Roy and Sherrington in 1890.<sup>15</sup> When there is an active region of the brain, a local build up of metabolic by products results will enter the extracellular fluid, and cause vasodilation. In their seminal work it was stated:

*“We conclude then, that the chemical products of cerebral metabolism contained in the lymph which bathes the walls of the arterioles of the brain can cause variations of the calibre of the cerebral vessels; that in this re-action the brain possesses an intrinsic mechanism by which its vascular supply can be varied locally in correspondence with the local variations in functional activity.”<sup>15</sup>*

This notion as proposed over 100 years ago (and before the advent of true measures of CBF<sup>19</sup>) has been shown to hold true. For example, a study performed by Andrea Fergus and Kevin Lee,<sup>104</sup> demonstrated that the hippocampal neurons release nitric oxide that is directly involved in the parenchymal microvessel regulation. These data provides evidence that the by products produced by local neuron metabolism does indeed contribute to the coupling of CBF changes with neuronal activation.<sup>104</sup>

The second proposed mechanism for neurovascular coupling was previously described (see: *neurovascular unit*) that the astrocytes were actively involved in the local regulation of CBF.<sup>105</sup> This mechanism results from the local neurons releasing glutamate, which activates the uptake of calcium by the astrocyte. The uptake of calcium by the astrocyte in turn activates the pericytes and endothelium to release vasoactive modulators, including vasodilators (adenosine; nitric oxide; and arachidonic acids) or vasoconstrictor (endothelium).<sup>99,105</sup>

The third proposed mechanism for neurovascular coupling is based upon shear stress (reviewed in:<sup>91</sup>). Shear stress results from the frictional drag as a result of blood flow across the vessel wall, and the magnitude of the shear stress is proportional to the flow rate and viscosity and inversely proportional to the cubed power of the radius.<sup>91</sup> Therefore, when there is an increase the blood flow, there will be a subsequent increase in the shear stress experienced by the local vasculature. This in turn will cause activate the shear stress receptors in the endothelial cells, which in turn cause the release of nitric oxide, which acts as a local vasodilator.<sup>69,70</sup>

The final mechanism proposed to explain neurovascular coupling is that of direct sympathetic and parasympathetic activation of the blood vessels. The entire length of the cerebrovasculature - from the internal carotid and vertebral arteries all the way to the pial vessels - are innervated by adrenergic (sympathetic) and cholinergic (parasympathetic) fibres.<sup>59,82,83,101</sup> There is growing evidence that the sympathetic nervous system contributes to buffering surges in cerebral perfusion pressure, via increasing vasoconstriction of the cerebrovasculature tree (reviewed in:<sup>59</sup>). This global neural innervation is likely a protective mechanism to limit the volume of blood entering the brain, via the Monro-Kellie doctrine,<sup>21</sup> which could possibly prevent a cerebral haemorrhage from occurring. There is limited human

data on the effects of parasympathetic innervation of the cerebrovasculature, but a recent study by Hamner *et al.*,<sup>106</sup> demonstrated that cholinergic blockade results in very similar autoregulatory changes as that of adrenergic blockade. Such findings have been indicated as a possible balance between the sympathetic and parasympathetic nervous systems that enables the optimal modulation of CBF to both rising and falling cerebral perfusion pressures.<sup>106</sup>

It is well known that visual stimulation will increase blood flow in the occipital lobe, and provides an effective manner in which neurovascular coupling can be assessed.<sup>45,107,108</sup> The increase in posterior cerebral artery blood flow is initiated within the first second of the eyes being opened and continues to reach a peak response in approximately 11.5 seconds, whereas the velocity in the middle cerebral artery remained relatively unchanged.<sup>45,108</sup> These findings indicate that the overall mechanism for neurovascular coupling is likely a combination of all four previously proposed mechanisms – the initial increase is likely occurring too quickly for it to be solely based upon: metabolic by products; release of vasodilators from the astrocytes; or shear stress as these have a latency of approximately 3 seconds (initial increase) to 6-12 seconds (peak response).<sup>109</sup> Thus indicating that direct neural innervation likely plays an initial role and the peak CBF response is likely a combination of all four mechanisms.

#### **1.5.6. Local metabolic factors**

As already mentioned, there are numerous local metabolic factors that can influence CBF regulation: Carbon dioxide; oxygen; adenosine; nitric oxide; arachidonic acids; endothelin; and thromboxane. The effects of alterations to  $P_aCO_2$  and  $P_aO_2$  have been already extensively discussed (see section 1.3.1. Arterial blood gases), as such they will be omitted from this section. The following section will focus on the main local markers of vasodilation

(adenosine, nitric oxide, arachidonic acids) and the main vasoconstrictors (endothelin-1 and noradrenaline).

### *Adenosine*

Adenosine has been shown to be a potent vasodilator of the cerebrovasculature, as activation of the adenosine<sub>2A</sub> receptors has been shown to result in the dilation of the pial vessels.<sup>109,110</sup> However, basal levels of adenosine have been shown to be inadequate to alter the resting tone of the cerebrovasculature.<sup>111</sup> Thus, it appears as though only when there are either high levels of metabolism in the brain, marked hypoxemia, or glucose/oxygen supply is decreased (hypoxia/ischemia), are there large enough releases of adenosine into the extracellular space to directly cause alterations to CBF.<sup>111</sup> Alternatively, it is possible for the adenosine<sub>2B</sub> receptors to be activated – which results in an increase of intracellular calcium in the astrocytes – and thus indirectly lead to increases in CBF via a calcium based mechanism.<sup>109,110</sup> In either case, when there is activation of adenosine<sub>2A</sub> or adenosine<sub>2B</sub> receptors, the end result will be an increase in CBF to increase the delivery and/or uptake of the cerebral metabolites.<sup>110</sup> Administration of the adenosine receptor antagonist, caffeine results in a 20-30% reduction in CBF (reviewed in:<sup>112</sup>). However, the reduction in CBF due to the administration of caffeine is likely offset by an increase in oxygen and glucose extraction rate or an increase in the rate of anaerobic metabolism.<sup>112</sup>

### *Nitric Oxide*

In 1980, published in a letter in *Nature*, Robert Furchgott and John Zawadzki<sup>113</sup> first described that there is a relaxation factor associated with the endothelial cells. This discovery

was made through the accidental misreading of preparation directions of a rabbit aorta by a technician in 1978.<sup>114</sup> As a result, the endothelium was not mechanically washed out of the aorta and when acetylcholine was added, the potent effect of the endothelium-derived vasodilator was observed.<sup>114</sup> It was not until 1986 that Robert Furchgott first identified the endothelium derived relaxing factor as nitric oxide.<sup>114</sup>

Nitric oxide is produced via nitric oxide synthase of L-arginine and can be derived from either the endothelium or neurons. In the cerebrovasculature, basal levels of nitric oxide have been shown to be important in controlling CBF as we age (reviewed in:<sup>115</sup>). In younger adults (mean age 25 years), infusion of a nitric oxide inhibitor has little-to-no impact on CBF (but does increase mean arterial pressure), indicating that nitric oxide pathway is not vital in controlling CBF in young adults.<sup>116</sup> Contrasting this finding, are the older population (mean age 70 years) where the nitric oxide blockade has been shown to decrease CBF by ~22% and cerebrovascular resistance increases by ~40%.<sup>116</sup> The authors of this study speculated that these findings do indeed confirm that the nitric oxide pathway is important in the control of CBF, but only in an elderly population where endothelial dysfunction and/or atherosclerosis may be present.<sup>116</sup>

### *Arachidonic Acid*

The cellular membranes of the brain are densely covered in phospholipids, which are utilized to derive arachidonic acids. Arachidonic acids are the principal substrate utilized in the formation of prostaglandins in the brain, via the cyclooxygenase pathways.<sup>117</sup> Cyclooxygenase can act either through the astrocytes and their end-feet (cyclooxygenase 1 pathway); or the neurons (cyclooxygenase 2 pathway), with both pathways resulting in formation of

prostaglandins. <sup>118</sup> The build up of prostaglandins, will cause the relaxation of local vascular smooth muscle, which in turn causes vasodilation and is a large modulator of basal tone. <sup>118</sup>

Prostaglandin formation can be inhibited through the use of nonsteroidal anti-inflammatory medications such as Indomethacin, Naproxen and Ibuprofen. <sup>117,119</sup> Indomethacin and Naproxen are potent and reversible non-selective cyclooxygenase inhibitors that are able to cross the blood brain barrier and inhibit both cyclooxygenase 1 and 2 pathways. They have been shown to lower CBF by 20-35% <sup>119-122</sup> and elevate cerebrovascular resistance without altering metabolic rate, <sup>119,120,123</sup> plasma catecholamines, <sup>123,124</sup> or  $P_aCO_2$ . <sup>18,124,125</sup> In contrast, although Ibuprofen is also a non-selective cyclooxygenase inhibitor, it appears to have little-to-no effect on CBF of newborn piglets. <sup>126</sup> All three of these anti-inflammatory drugs have been shown to cross the blood-brain barrier, <sup>127</sup> thus it appears as though Indomethacin and Naproxen may have an additional pathway (likely the inhibition of cyclic AMP – dependent protein kinases) <sup>128,129</sup> in which they decrease CBF and increase cerebrovascular resistance.

### *Endothelin-1*

Endothelin is a family of amino acid peptides that are produced in the neurons, astrocytes and endothelial cells. They act as potent vasoconstrictors on smooth muscle cells, and work as a feedback system with nitric oxide to regulate the tone of the pial vessels.<sup>130</sup> Endothelin-1 is released during periods of increased shear stress<sup>131</sup> and hypertension<sup>130</sup> and likely acts as a protective mechanism to prevent over-perfusion of the brain.<sup>130</sup> In vitro animal studies have shown that the application of endothelin-1 agonists can result in extreme decreases in CBF (68 to 93% reductions), which results in irreparable ischemic damage to the cerebrovasculature.<sup>132-135</sup> In contrast, the administration of an endothelin-1 antagonist has been shown to increase CBF (45 to 60% elevations) in cerebral ischemic animal models.<sup>136-138</sup> Comparable data in humans has not been established.

### *Noradrenaline*

Noradrenaline is the principle neurotransmitter released by sympathetic nerve activity. In vitro studies of the middle cerebral artery and pial vessels in cats has revealed that noradrenaline administration results in a contraction (up to 40% reduction in diameter) of the vessel.<sup>89,139</sup> In humans it has been suggested that measuring the spill-over rate of noradrenaline released from the brain will provide an indication of the influence of the sympathetic nervous system on the cerebrovasculature.<sup>140</sup> In a recent study by Trangmar et al.<sup>141</sup> it was shown that during intense cycling exercise (80-100% of maximal work rate), there is an increase in the release of noradrenaline, concomitant to the reduction in  $P_aCO_2$ . It was speculated – although not established - that both of these factors (increased noradrenaline release and a decline in  $P_aCO_2$ ) play a physiological role in the decline in CBF during intense exercise.<sup>141,142</sup>

### 1.5.7. Posture

Movement from a supine to standing position can result in a reduction of ~1.5 litres of central blood volume.<sup>63,143</sup> Initially (within the first 15 seconds) there is an increase in cardiac output (+30%) and a reduction in mean arterial pressure (-45%).<sup>144</sup> The transient drop in mean arterial pressure is sensed by the arterial baroreceptors which increases the sympathetic output from the central nervous system to increase total peripheral resistance and heart rate as a compensatory response. If this response is either delayed or incomplete then dizziness, light-headedness, nausea or syncope could occur.<sup>46</sup> Conversely, when there is a change from supine to head down tilt, mean arterial pressure has been shown to increase.<sup>145</sup> Cerebral blood flow is initially altered with the change in posture,<sup>146,147</sup> but within 5-10 minutes of the tilt-table posture change (either head up or head down tilt) both the anterior and posterior CBF is comparable to supine measures<sup>46,146,148</sup> and are maintained even with prolonged bed-rest (up to 10 days).<sup>149</sup> This maintenance of CBF occurs despite increases to CVR<sub>i</sub> that occurs only in head down tilt.<sup>46</sup>

These alterations to CBF during initial posture change have been thought to manifest from as a result of the alteration to P<sub>a</sub>CO<sub>2</sub>.<sup>150,151</sup> When a subject moves from the supine to upright position, it has been shown that P<sub>a</sub>CO<sub>2</sub> decreases by ~3 mmHg and results in a decrease in the velocity of the middle cerebral artery ~10%.<sup>150,151</sup> The changes to CBF likely occurred as a result of reduced ventilation/perfusion matching within the lung<sup>150,151</sup> when the subject is upright.

However, the alterations in CBF with posture change do not appear to impact the neurovascular coupling within the posterior cerebral circulation,<sup>108</sup> or the TFA gain in the anterior circulation.<sup>150</sup> Combined, these results appear to indicate that the altering posture from

supine to upright positions, may reduce the overall CBF but does not impair the ability of the cerebrovasculature to regulate CBF.<sup>46,108,150,151</sup> These findings could occur because the changes to  $P_a\text{CO}_2$  are not the only factor affecting CBF regulation with posture change.<sup>150,151</sup> These findings could also be a result of the larger intracranial compliance (2.8 fold increase) that occurs when a subject is upright.<sup>147,152</sup> The increase in intracranial compliance is due to a combination of the shift in cerebrospinal fluid from the cranium to the spinal canal,<sup>147,152,153</sup> which offsets the increased resistance of the venous outflow due to jugular collapse upon standing<sup>152,154</sup> and thus enables the maintenance of CBF regulation in spite of the marked influence of posture on CBF.

### **1.3.8. Aging**

Over the course of normal healthy human aging, physiological changes occur that result in the structural and functional alterations of the cerebrovascular system, such as white matter loss<sup>155</sup>; hormonal changes<sup>156</sup>; and a progressive loss of cortical neurons.<sup>157,158</sup> As a result of these alterations there is an observed reduction in CBF, which likely reflects a decrease in global cerebral perfusion.<sup>51</sup> Cross sectional studies have revealed that with healthy aging, CBF declines approximately 25-40% between 30 and 89 years of age.<sup>51,156,159</sup> Similar findings were reported in a longitudinal study by Fotenos *et al.*;<sup>155</sup> namely, there is a reduction in whole-brain volume of 0.45% per year after 30 years of age. Despite these declines to CBF and whole-brain volume, there is magnetic resonance imaging evidence to suggest that the cerebral metabolic rate is unchanged with aging.<sup>157,158</sup>

### **1.5.9. Acute exercise**

Numerous studies have revealed that CBF is elevated by approximately 10-30% during a sub-maximal exercise bout (reviewed in: <sup>160,161</sup>). The elevated CBF levels are likely a result of the raised oxygen requirements of the brain and mild elevations in  $P_aCO_2$ . <sup>48,160,162</sup> After the anaerobic threshold is reached (60-70% of  $VO_{2Peak}$ ; respiratory exchange ratio >1.0), CBF returns towards baseline levels and can even be reduced below baseline values due to hyperventilation-induced hypocapnia. <sup>48,162,163</sup> This response occurs in spite of the continued elevations in arterial blood pressure, cardiac output and increasing oxygen consumption demands of the brain. <sup>162,163</sup> Therefore, the hypocapnia that occurs as a result of exercise-induced hyperventilation seems to be a greater governor of CBF than cerebral metabolism, blood pressure and cardiac output at exercise above aerobic threshold. <sup>164</sup>

### **1.5.10. Chronic exercise**

With a lifetime of regular endurance training, it has been shown to result in an increase in CBF of approximately 17% across the aging spectrum, which equates to the cerebrovasculature of trained individuals to be nearly a decade 'younger' than their sedentary counterparts. <sup>51</sup> It has also been shown that individuals who have led an active lifestyle have greater brain tissue density, <sup>165</sup> which coincides with a reduction in the degradation of the white matter of the brain<sup>166</sup> when compared to similar age sedentary controls. It has been reported that masters athletes (~75 years old) have lower CVRi along with the reduced decline in CBF as compared to sedentary individuals. <sup>153</sup> It was speculated that the underlying mechanisms for these improvements in CBF were due to the numerous cardiovascular benefits that are associated with regular physical training. <sup>51,153</sup> These cardiovascular benefits include increased vascular

compliance and stroke volume, with a decrease in aortic stiffness (reviewed in: <sup>153</sup>). These results also demonstrate that ‘normal’ is really only a point of reference for comparison as living a healthy and active lifestyle can potentially delay pathological disorders that result in age-associated cerebrovascular related brain diseases. <sup>51</sup>

### **1.5.11. Selected pathology - heart transplantation**

Cardiac allograft surgery is a life saving intervention for certain individuals with end-stage heart failure. When Dr. Christiaan Barnard performed the first successful heart transplant surgery on December 3, 1967, the patient survived for just 18 days. <sup>167</sup> The longevity of recipients has greatly increased with modern medical practices, and now heart transplant recipients have a current mean survival expectancy of over 10.5 years. <sup>168</sup> The vastly improved survival outcomes after surgery have led to alterations in the patient’s long-term functional outcomes. For example, neurological impediments develop in approximately 60-80% of heart transplant recipients, <sup>52,169-171</sup> and have a 14-18% greater occurrence rate of cerebral haemorrhage or ischemic stroke. <sup>81,169,171,172</sup> The exact mechanism for these alterations remains to be revealed. There is speculation, however, that the adverse events may be the result of taking life-long immunosuppressant medications, <sup>173</sup> or could be an outcome of vascular remodelling related to the chronic under perfusion of the cerebrovasculature that is associated with end-stage heart failure. <sup>170,171,174</sup>

To date, only four studies have quantified CBF after cardiac allograft surgery: three studies examined the response in acute recipients at rest (<6 months post transplant); <sup>52-54</sup> and one in long-term recipients (>6 years post transplant). <sup>48</sup> The first study was performed by Gruhn *et al.* <sup>52</sup> where they reported CBF was ~30% lower reduced in end-stage heart failure

patients and by the first month post allograft surgery they were comparable to age-matched controls and they remained elevated at their six month review. Massaro *et al.*,<sup>53</sup> speculated that hematocrit levels may have been reduced after the surgery and that would reduce the blood viscosity and could possibly be the reason CBF increased. In their follow-up study, it was reported that CBF increased over 50% within the first month after surgery and was not related to hematocrit levels.<sup>53</sup> This lack of a hematocrit-CBF relationship has also been demonstrated in healthy populations.<sup>175</sup> The third study,<sup>54</sup> was actually being performed on 52 advanced heart failure patients, 4 of whom happened to under go heart transplant surgery. In this subsection of patients it was noted that global CBF was 25% higher by their 4-month follow-up appointment.<sup>54</sup> The most recent study in the area was performed in long-term heart transplant recipients at rest and during an incremental maximal exercise test.<sup>48</sup> The key finding from this study was that the long-term heart transplant recipients had similar CBF responses as their age-matched controls (but CBF was reduced compared to donor heart controls) during both rest and incremental cycling exercise.<sup>48</sup> Thus it appears as though the older cerebrovasculature of the recipient is the primary cause of the cerebral hypoperfusion rather than a younger cardiac allograft.

## **1.6. Underlying relationships between arterial blood pressure and cerebral blood flow regulation**

Throughout the studies presented in this thesis there will be extensive discussion and interpretation on the relationship that exists between arterial blood pressure and CBF. This relationship is commonly referred to as '*cerebral autoregulation*' and pertains to the maintenance of adequate CBF (~50ml/100g brain mass/minute) via the alterations in cerebrovascular resistance across a wide range of perfusion pressures.<sup>16</sup> In the following sections of the thesis, the concepts of static and dynamic cerebral autoregulation, assessment methodologies, rationale for the methodology utilized throughout the research chapters, and the factors influencing TFA for the assessment of dynamic cerebral autoregulation will be discussed.

### **1.6.1. Cerebral autoregulation**

The concept of cerebral autoregulation was first proposed by Neils Lassen in his 1959 seminal publication "*Cerebral blood flow and oxygen consumption in man*",<sup>16</sup> where he concluded:

*“The cerebral perfusion in normal man varies only moderately, the most important regulating factor probably being the tissue carbon dioxide tensions and the direct reaction of the muscular cells of the cerebral arteries in response to variations of the distending blood pressure. The cerebral circulation has also been studied in many disease entities, and it appears in general that the cerebral perfusion is ample relative to the cerebral metabolism. Of particular interest is the finding of adequate over-all cerebral perfusion in so called cerebral*

*arteriosclerosis. Only in severe hypotension and during marked hyperventilation has total cerebral perfusion been found to be critically lowered.”*<sup>16</sup>

Based on this review paper, it was proposed that the CBF will be maintained at near normal levels during cerebral perfusion pressures of 50-150 mmHg and this concept has persisted in the literature to this day.<sup>176-182</sup> Despite the conclusion by Bayliss, Hill and Gulland who some 60+ years prior to Lassen’s seminal work, who noted:

*“In all physiological conditions a rise in arterial pressure accelerates the flow of blood through the brain, and a fall slackens it.”*<sup>14</sup>

Thus it is not surprising that there were some major issues that were associated construction of the Lassen autoregulatory curve (Figure 1.9.). These were highlighted by Heistad and Kontos in the *Handbook of Physiology* in 1983,<sup>183</sup> with the main concerns being: 1) it was constructed based upon data sets that typically would not have been classified as ‘normal man’ (drug induced severe hypotension; drug induced moderate hypotension; normal pregnant women; drug induced hypertension; hypertensive toxemic pregnancy; and essential hypertension); 2) the drugs that were administered to elicit blood pressure changes caused cerebral vasodilation, thus confounding the findings; 3) the data from some of the points used to plot the figure did not correspond to that of the data presented within the cited papers; 4) the data plotted for the figure were all from separate between subject data sets; 5) alterations to CO<sub>2</sub> tensions in the blood were not controlled for; and 6) the cited studies that did involve a change in mean arterial pressure also elicited a change in CBF, indicating that within individual

subjects the 'plateau' was not as all encompassing as stated by Lassen. When Heistad and Kontos reconstructed the curve for the autoregulatory plateau (Figure 1.11), they noted little evidence for a true 'plateau' but instead noted a hysteresis effect on the regulation of CBF.<sup>183</sup> They observed a change in CBF of ~7% per 10 mmHg swing in mean arterial pressure over most ranges, but during hypertension it was just a 2% change in flow for every 10 mmHg pressure swing. This concept has recently been confirmed through a meta-analysis.<sup>81</sup> However, just because there is not a prolonged plateau does not necessary mean that cerebral autoregulation does not occur.<sup>184</sup> For example, recent research has shown that there appears to be a brief plateau of ~10 mmHg around a mean arterial pressure of 90 mmHg that occur during oscillations slower than 12.5 seconds (0.08 Hz – Figure 1.12.).<sup>185,186</sup> Also, if the cerebrovasculature was a truly pressure passive system then we would observe equal changes to CBF in response to a given hypotensive or hypertensive stimuli. A second hypothesis in regards to the hysteresis nature for the relationship between arterial blood pressure and CBF is that there could be different mechanisms underlying the relationship during hypertension (refer to section 1.3.3.).<sup>77</sup> This symmetry does not seem to occur. For example, the brain typically has a relatively blunted CBF increase during hypertensive events and experiences larger changes in CBF when hypotensive alterations occur (reviewed in:<sup>81</sup>). Thus it appears as though the work by Bayliss, Hill and Gulland in describing CBF regulation in 1895<sup>14</sup> was a more apt description than that provided by Niels Lassen in 1959.<sup>16</sup>

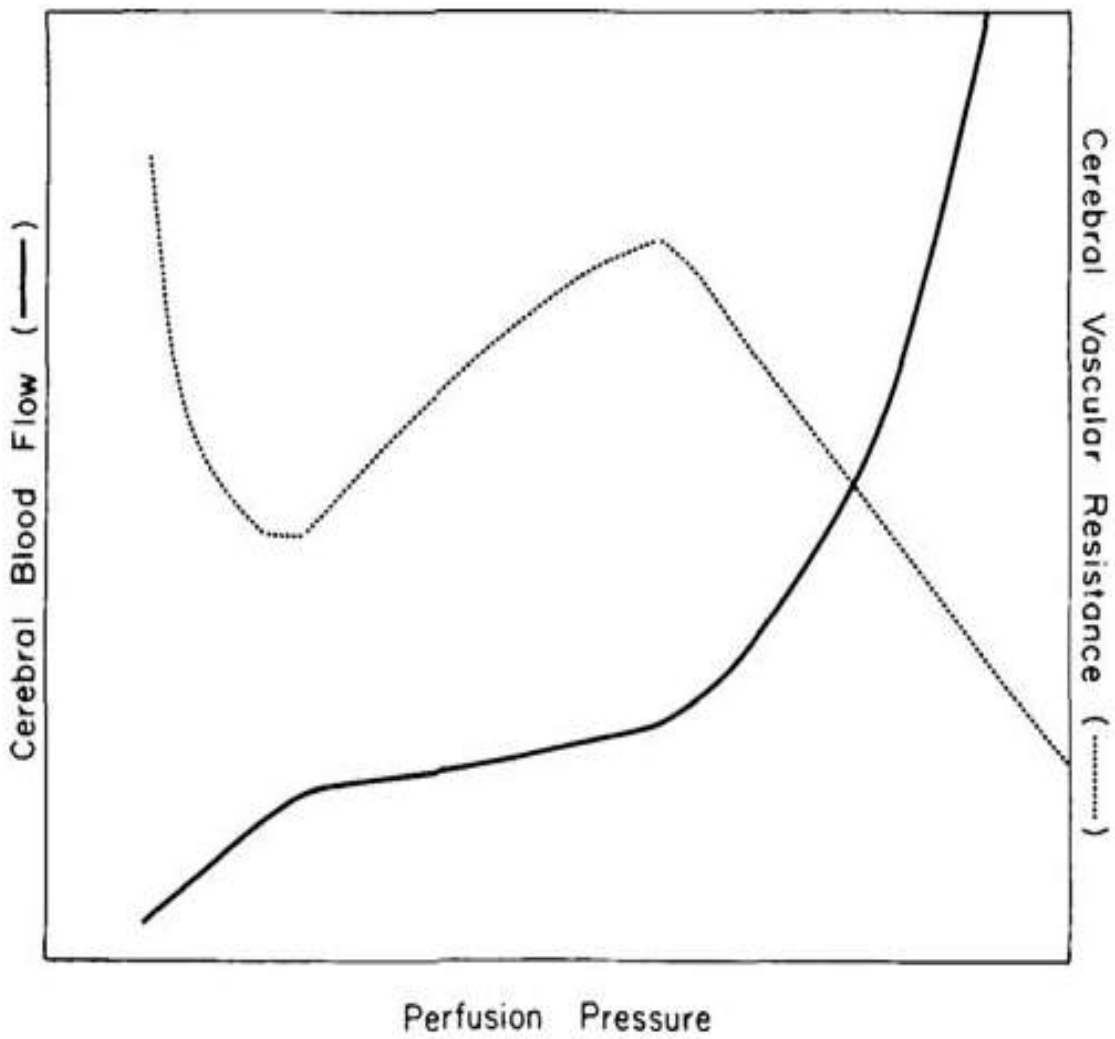


**Figure 1.11.** The relationship between cerebral perfusion pressure and cerebral blood flow (solid line) and cerebral vascular resistance (dotted line). Image from: <sup>183</sup>, permission to reproduce the image was not required by the *American Physiological Society*.

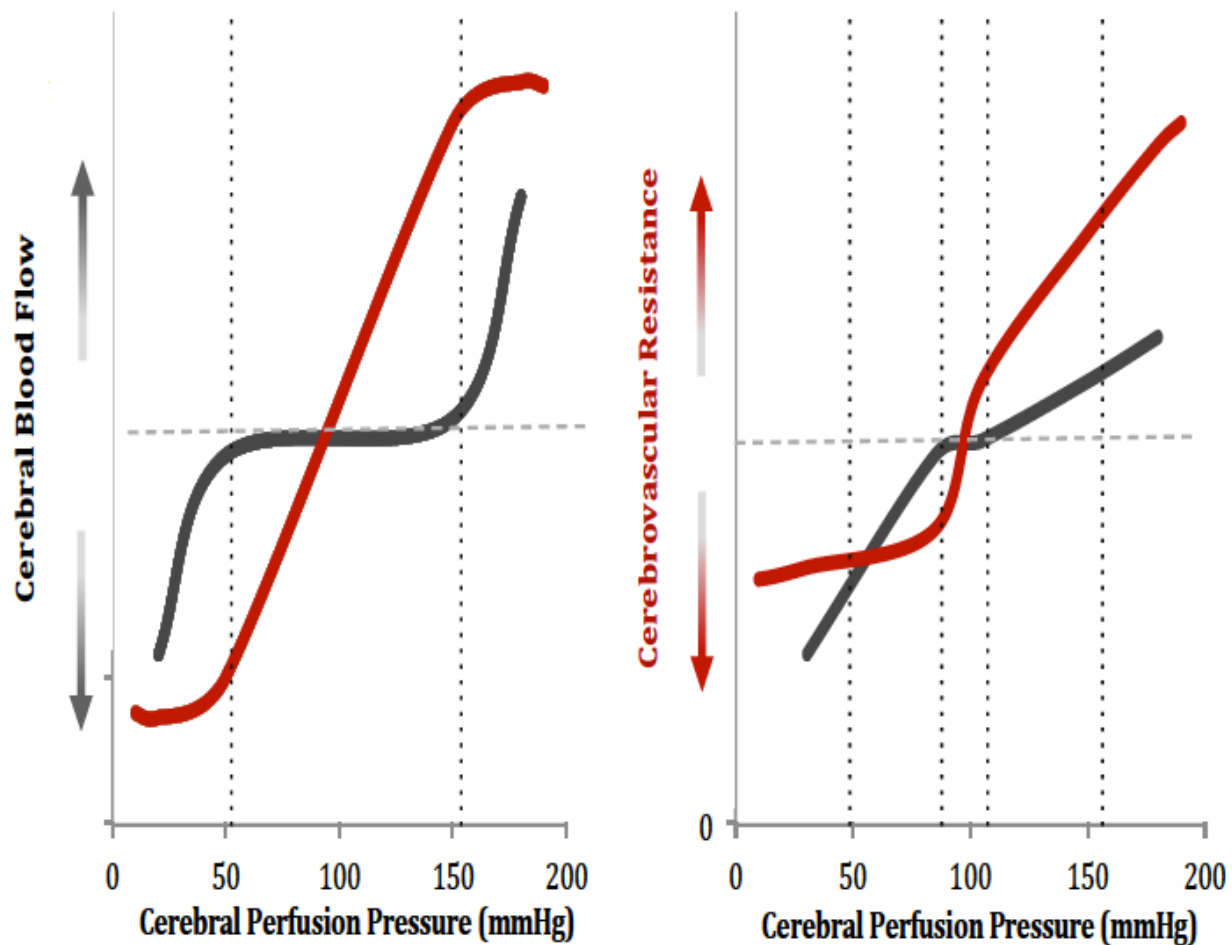


**Figure 1.12.** The left panel is a modified representation of the classic cerebral autoregulation curve that was first presented by Lassen in 1959<sup>16</sup> and updated by Paulson in 1990, with changes in cerebral blood flow (black trace) resulting from alterations to cerebrovascular resistance (red trace).<sup>17</sup> The right panel is the current view on the cerebral autoregulation curve as updated by the work of Numan et al.,<sup>81</sup> and Tan et al.<sup>185,186</sup> This image was modified from:<sup>59</sup>

### 1.6.2. Static vs. dynamic cerebral autoregulation

The previously mentioned studies<sup>14,16,81</sup> were all assessed through steady-state (>5 minutes) measurements of blood pressure and CBF. The implementation of the transcranial Doppler<sup>37</sup> in 1981 enabled a much higher time resolution (e.g., beat-to-beat vs. minutes) to be

achieved, an approach that allows the dynamic nature of CBF regulation to be observed.<sup>18,176,187-189</sup> These observations have revealed that the relationship between arterial blood pressure and CBF is frequency dependant in nature, with the brain acting as a high-pass filter.<sup>18,125,187,189,190</sup> Within a high-pass filter, slower oscillations are filtered (i.e., effectively buffered) and higher frequency oscillations are passed through unimpeded (i.e., ineffective buffering). In the case of the cerebrovasculature, oscillations in blood flow that are slower (<0.20 Hz – e.g. below resting respiratory rate) are buffered whereas faster oscillations ~1 second (~1 Hz – e.g. resting heart rate) are passed through relatively unimpeded.<sup>18,176,178</sup>

Traditionally, the literature had considered the steady-state (static)<sup>16,17</sup> and high-pass filter (dynamic)<sup>18,176,188,189</sup> models of cerebral autoregulation to be two separate entities. More recently, however, it has been suggested that cerebral autoregulation occurs on a continuum where steady-state (0 Hz) measures are really just part of the ultra low frequency spectrum of the dynamic regulation of arterial blood pressure by the cerebrovasculature (Figure 1.13).<sup>125,184-186</sup> The frequency bands of interest in terms of the relationship between arterial blood pressure and CBF are thought to be the ultra low frequency (ULF: <0.02 Hz); very low frequency (VLF: 0.02-0.07 Hz); low frequency (LF: 0.07-0.20 Hz); high frequency (HF: >0.20 Hz). Throughout the research chapters of this thesis, the VLF and LF ranges will be investigated. The cerebral pressure-flow relationship during steady-state is able to be described by Poiseuille's law (Section 1.2.2. – Equation 1.4.).<sup>184</sup> However, during higher frequency oscillations (e.g. VLF, LF and HF) this may not necessarily be the case and an incorrect use of this steady-state law could result in inappropriate interpretations (Figure 1.13).<sup>184</sup> Under steady-state conditions, this law holds true because the arterial baroreflex (and to some extent the cerebrovasculature – refer to section 1.3.5.) is able to buffer slower changes (>10-20

seconds in duration) and maintain blood pressure at a relatively constant level, and CBV follows suit. However, more rapid and dynamic changes to blood pressure (<5 seconds in duration) are passed along relatively unimpeded through the systemic and cerebral vasculature.<sup>184</sup> These brief and robust changes in blood pressure can cause the compliance of the vessels to be altered (dilation with reduced blood pressure and constriction with increases), which in turn adds an additional paradigm to be considered when assessing or interpreting the dynamics or the cerebral pressure-flow relationship (Figure 1.13.).<sup>184</sup>

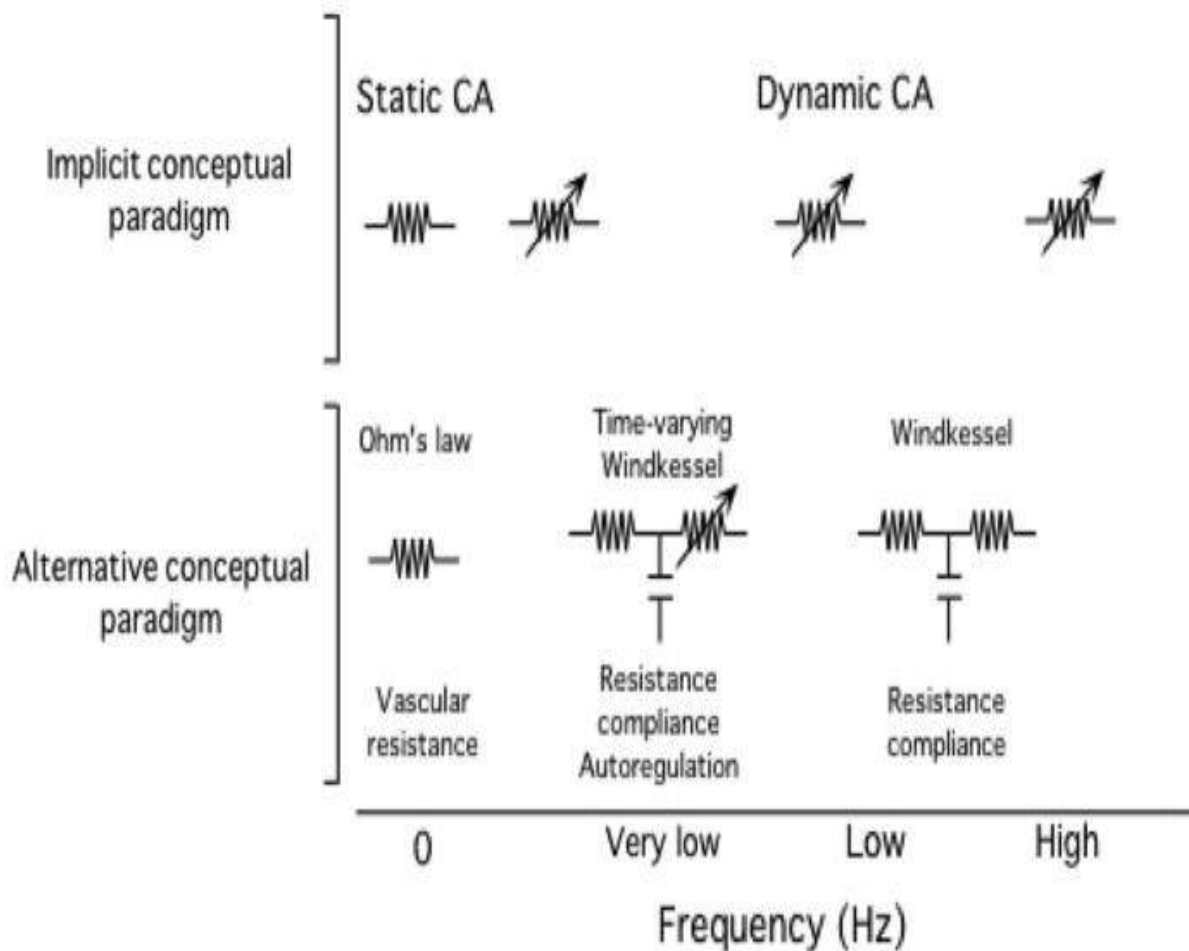


**Figure 1.13.** A schematic diagram illustrating two theoretical models that can influence the interpretation of cerebral autoregulation data. The top panel shows the common interpretation that cerebral autoregulation is the main regulator of the cerebral pressure-flow relationship. The bottom panel highlights an alternative model that enables input from vascular properties such as resistance and compliance, in conjunction with cerebral autoregulation as factors that can impact the cerebral-pressure flow relationship as proposed by Tzeng and Ainslie.<sup>184</sup> Image from:<sup>184</sup>. Permission to reproduce the image was not required by the *European Journal of Applied Physiology*.

### **1.6.3. Key studies on dynamic relationship between blood pressure and cerebral blood flow**

#### *Rate of regulation and autoregulatory index*

The first major study to directly assess the dynamic relationship between blood pressure and CBF was performed on 10 healthy subjects (5 male / 5 female) by Rune Aaslid and associates in 1989.<sup>176</sup> In their study, they utilized transcranial Doppler to characterise the beat-to-beat changes of CBV during a rapid thigh-cuff deflation. When the cuff was deflated there was a sudden decrease (~20 mmHg) in mean arterial pressure occurring within 0.2 seconds and reached a trough in approximately 5-7 seconds. The rate of change of cerebrovascular resistance to the initial hypotensive insult is quantified with regression. A slope change of 0.15 or greater was indicative of an effective autoregulatory response (hypocapnia trace in Figure 1.14.) and a slope below 0.15 was an impaired response (hypercapnia trace in Figure 1.14.). As blood pressure is suddenly decreased following thigh-cuff deflation, the cardiac and vascular baroreceptors are activated and mitigate the decline and return blood pressure to resting levels over the next 15-20 seconds. The authors noted that the CBV response to this gradual return in blood pressure under normocapnic (37.1 mmHg), hypocapnic (22.2 mmHg) and hypercapnic (46.9 mmHg) conditions. They found that during hypocapnia the CBV returned back to baseline (and even overshoot) within the first 4 seconds post-deflation, whereas during hypercapnia the CBV response tracked that of blood pressure and during normocapnia the CBV response (8-12 seconds) was faster than that of blood pressure but not nearly as rapid as when carbon dioxide was reduced (Figure 1.9.) This method of CBF regulation assessment was termed the *rate of regulation* (RoR).

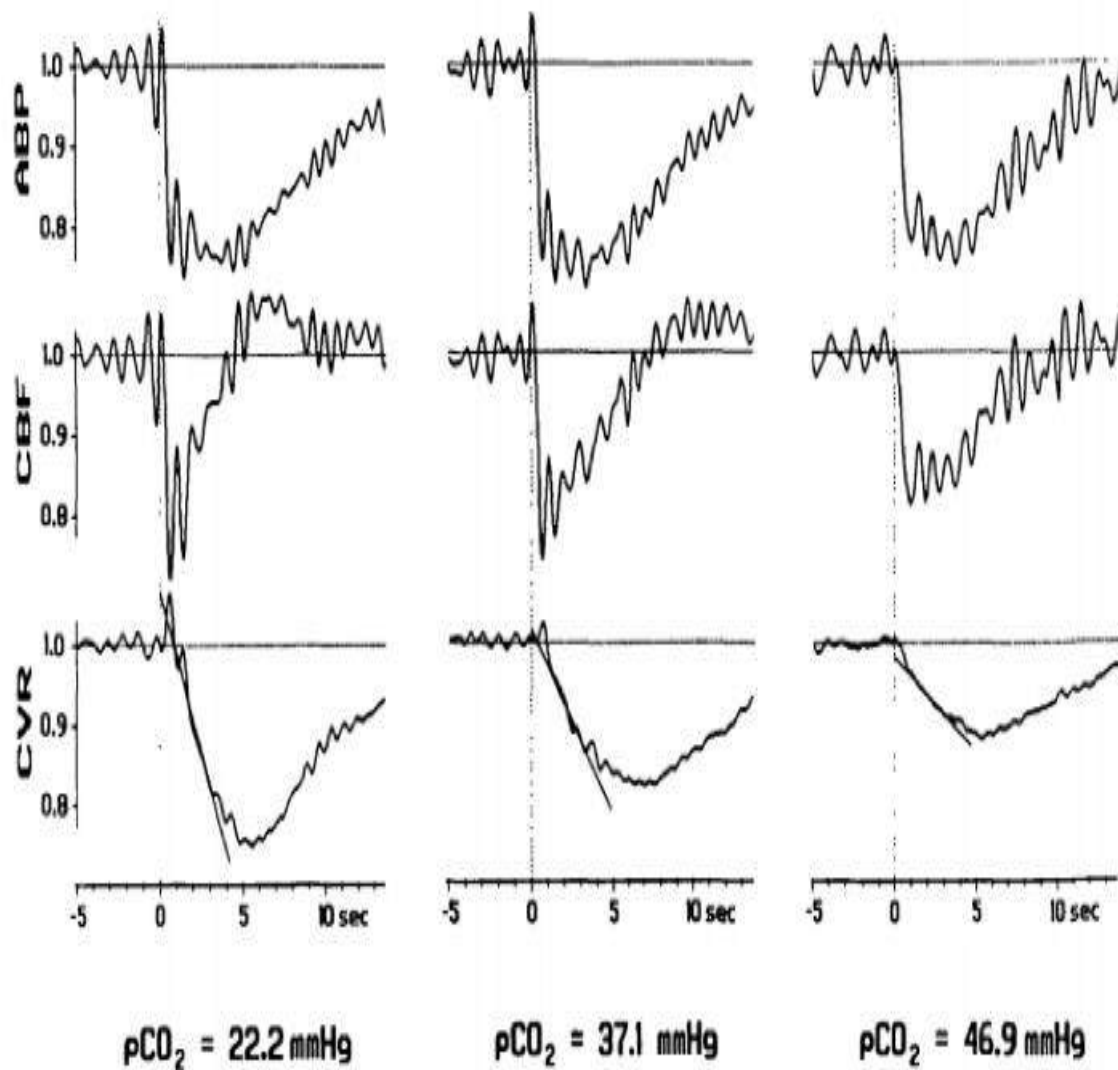


**Figure 1.14.** The typical arterial blood pressure (ABP), cerebral blood flow (CBF) and cerebrovascular resistance (CVR) responses to the thigh cuff deflation during hypocapnia (left), normocapnia (middle) and hypercapnia (right). The tracings are based upon normalized values for the 4 seconds prior to deflation. Image from: <sup>176</sup>, reproduced with permission from *Stroke*.

The concept of the rate of regulation was expanded by Tiecks and colleagues in 1995<sup>188</sup> when they proposed the autoregulatory index as a way of quantifying the gradual return of CBV after the peak response to the sudden hypotensive insult had been reached. In this study, thigh cuff deflation was once again utilized to induce a large and sudden decrease in arterial blood pressure. The novelty in this study was that these dynamic CBV regulation findings were compared to individuals under general anaesthesia with either intact (via propofol) or impaired (via isoflurane) CBF autoregulation. The findings from these tests were used to construct a mathematical quantification model (within a 30-second window) that related to the gradual return of CBV post hypotension and converted it into a 0-9 autoregulatory index (ARI) scale (Figure 1.15.)

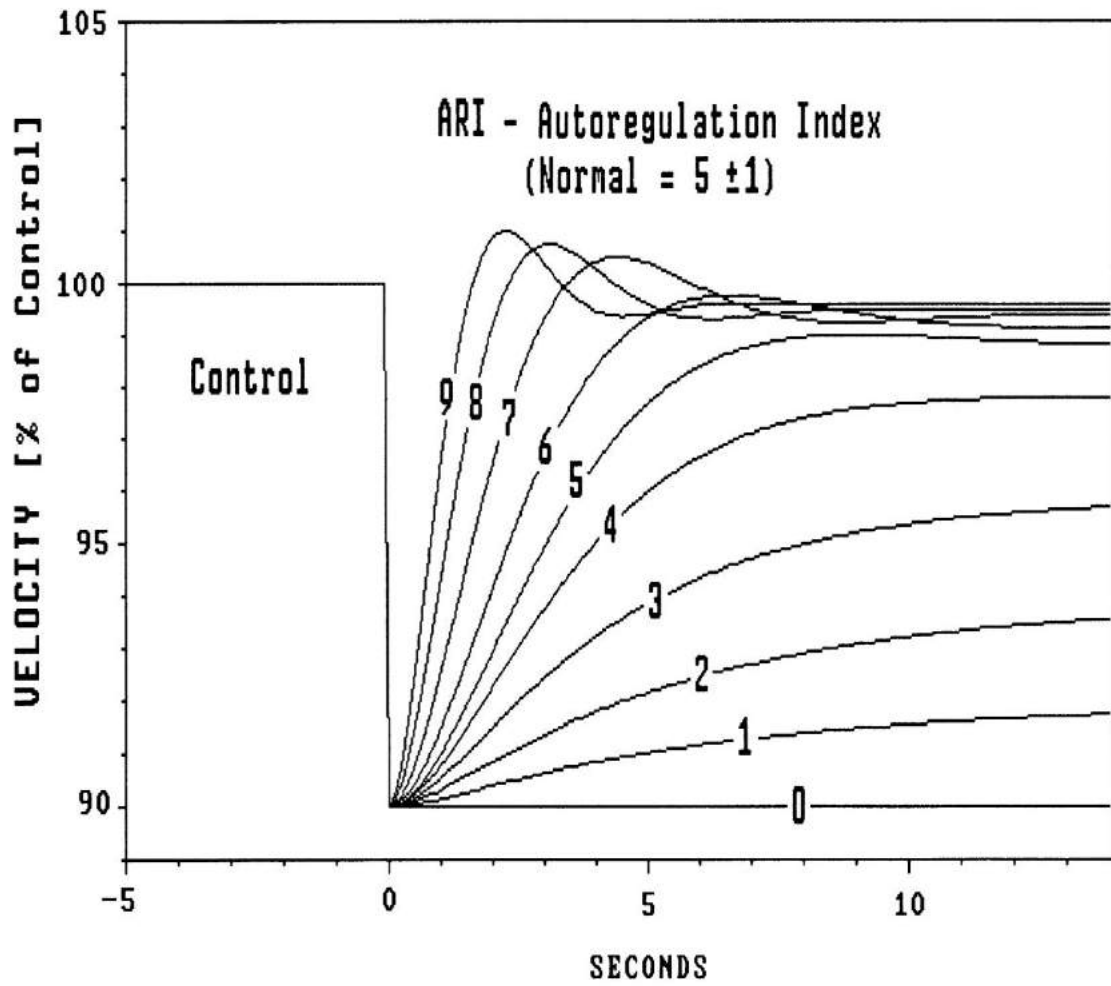


**Figure 1.15.** Quantification of the cerebral blood flow response to a thigh cuff deflation on the autoregulatory index scale. Image from: <sup>188</sup>, reproduced with permission from *Stroke*.

Since the CBF reduction post thigh cuff deflation is typically less pronounced than that of mean arterial pressure, the transient decrease in blood pressure results in a concomitant reduction to cerebrovascular resistance.<sup>184</sup> The RoR utilizes the assumption that these transient reductions to cerebrovascular resistance reflect the autoregulatory properties of the cerebral vessels in a linear fashion.<sup>176</sup> The steeper the RoR slope, the more robust the cerebral autoregulatory properties are thought to be, the cut-off point within for determining an intact response is a slope of 0.15.<sup>176</sup> After the peak reduction has occurred, the ARI model assumes that the cerebral arterioles actively regulate to increase cerebrovascular resistance on a beat-to-beat basis to return CBF back to normal levels.<sup>188</sup> Once again these alterations to blood pressure and CBF are thought to reflect the autoregulatory properties of vascular responses in a linear fashion, with a higher ARI value (>5) being indicative of an intact response.<sup>188</sup>

In 2003, Panerai *et al.*,<sup>191</sup> compared the traditional ARI with an autoregressive-moving average ARI. They performed a 10-minute resting period and three five-minute bouts of driven breathing at 6, 10 and 15 breaths per minute in 15 healthy subjects were performed, which created oscillations in blood pressure without a thigh cuff deflation test. The autoregressive-moving average ARI functions by using a least-squares method to estimate the appropriate model coefficients, taking into account only the first 6 seconds of each step response as per the RoR model proposed by Aaslid *et al.*<sup>176</sup> The main findings from this study were that the autoregressive-moving average ARI yielded significantly less variability as compared to the ARI ( $15 \pm 8\%$  vs  $30 \pm 21\%$ , respectively) and respiration had little effect on the results (although  $P_{ETCO_2}$  was not significantly different between spontaneous and driven respiration rates). Therefore the authors concluded that since the autoregressive-moving average ARI provided greater stability and reduced variability, it should be utilized as an assessment tool for

dynamic cerebral autoregulation in place of the traditional ARI and RoR models. In more recent publications, this research group has examined the autoregressive-moving average ARI with the impulse response<sup>192-194</sup> in place of thigh cuff deflation and deep breathing techniques.

### *Transfer function analysis*

The main assumption of TFA is that information from the time-domain can be converted into the frequency-domain without any information being lost (refer to section 2.2.1). For example if someone is breathing at 20 breaths per minute, each breath takes ~3 seconds to complete; therefore, 1/3 of a breath happens every second which equates to 0.33 Hz (Hertz = cycles per second). Another example in the human body where frequency dependent changes occur are the Mayer waves.<sup>195</sup> Mayer waves are oscillations in blood pressure that occur approximately every 10 seconds (~0.10 Hz) in healthy humans, and are linked to efferent sympathetic nerve activity in response to changes in blood pressure.<sup>195</sup> When the blood pressure waveform is processed with TFA, there are corresponding spikes in the power spectrum at these frequencies.

In 1990, Cole Giller<sup>187</sup> was the first to utilize a fast Fourier transform to decompose the beat-to-beat arterial blood pressure (input) and CBV (output) waveforms into their harmonic sine wave components (power spectrums). The power spectrums of the input and output variables are then further processed with a cross-spectral analysis, which yields three main outcome variables: coherence, gain and phase. The statistical correlation of the two waveforms was assessed with linear TFA to determine the coherence between the two signals. Coherence is similar to a correlation coefficient: 1.0 indicates perfect correlation (input and output are directly related) and 0.0 indicates no correlation (no relationship between input and output

variables, extremely high noise in the signals, multiple inputs for a single output, non-linearity of the relationship).<sup>18</sup> The amplitude modulation (gain) was also assessed to determine how the blood pressure waveforms were being regulated by the cerebrovasculature. Studies have indicated that the gain measure can be presented in either absolute (cm/s/mmHg), normalized to MCAv (%/mmHg) or normalized to both CBV and blood pressure (%/%).<sup>125</sup> It was discovered that cerebrovasculature acted as a high-pass filter, where the brain was able to modify the slower oscillations in blood pressure but not the faster ones.<sup>18,187,189,190,196</sup> It was also observed that patients with a subarachnoid haemorrhage had a higher coherence and gain values than normal control subjects,<sup>187</sup> which was surmised to mean that these patients had an impaired cerebral autoregulatory response.

Birch *et al.*,<sup>189</sup> used the fast Fourier and TFA methods proposed by Giller<sup>187</sup> to assess the relationship between blood pressure and CBV; however, instead of reporting the coherence and gain values, the focus in this study was on the phase lead (timing) of the MCAv compared to the blood pressure during squat-stand maneuvers at 0.05 Hz (20-second cycles: 10 seconds squatting, 10-seconds standing) during hypocapnia (25.9 mmHg), normocapnia (37.4 mmHg), and hypercapnia (50.6 mmHg) (Figure 1.16.). It was observed that the phase lead of the CBF velocity was markedly longer during hypocapnia (1.05 radians), than both normocapnia (0.80 radians) and hypercapnia (0.24 radians), while the amplitude change in blood pressure was unaltered. Based upon these findings, it was suggested future studies should examine all three metrics of TFA for the best interpretation of the cerebral pressure-flow relationship.

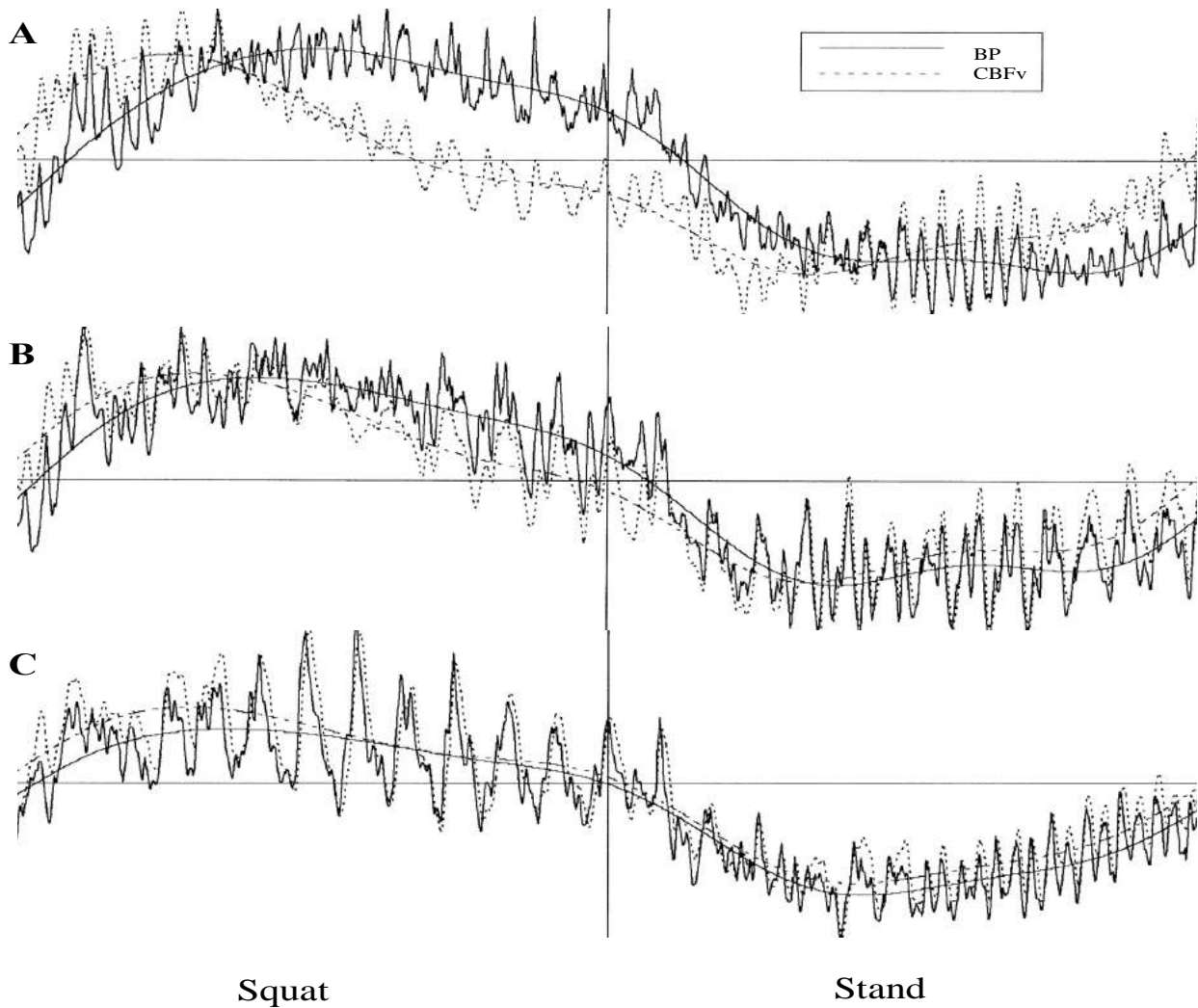


**Figure 1.16.** Typical waveforms from the 0.05 Hz squat-stand maneuvers for blood pressure (BP: solid line) and cerebral blood flow velocity (CBFv: dashed line) during hypocapnia (A), normocapnia (B) and hypercapnia (C). Note the phase lead of cerebral blood flow on the blood pressure changes in hypo- and normocapnia. This trend is abolished with the cerebral dilation associated with hypercapnia. Image modified from: <sup>189</sup>, reproduced with permission from *Stroke*.

Also in 1995, Diehl *et al.*,<sup>196</sup> attempted to assess the phase relationship between CBV and arterial blood pressure through driven blood pressure oscillations. Instead of performing the squat-stand maneuvers that were proposed by Birch *et al.*,<sup>189</sup> Diehl and colleagues<sup>196</sup> performed 1-minute of deep breathing at a rate of six breaths per minute (0.10 Hz). The findings from their study revealed that the phase lead in normal healthy controls was  $1.23 \pm 0.52$  radians. They compared these findings to patients with impaired autoregulation as reflected in a reduced phase lead compared to the controls; occlusive cerebrovascular diseases ( $0.90 \pm 0.61$  radians) or arteriovenous malformations ( $0.47 \pm 0.23$  radians). Unfortunately, this study did not explain the details of their fast Fourier transform nor TFA methodologies which were likely under powered due to their short collection time (60 seconds) and lack of windowing (for details on appropriate fast Fourier transform and TFA methodologies, please refer to section 2.2.). There was also no report of the reductions to  $P_{ETCO_2}$  that occurred with the deep breathing maneuvers. However, similar methodologies used in another study revealed decreases in  $P_{ETCO_2}$  of ~8-10 mmHg<sup>197</sup> have a profound effects on the cerebral pressure-flow relationship (Figures 1.14 and 1.16).

In 1998, Ronney Panerai and colleagues<sup>198</sup> utilized the TFA methodologies proposed by Giller *et al.*,<sup>187</sup> and Birch *et al.*,<sup>189</sup> to examine the autoregulatory properties of 83 neonates (gestational age ~30 weeks). The findings from this study revealed paradoxical results (Figure 1.17, below). In the traditional high-pass filter model of the cerebral pressure-slow relationship gain increases and phase decreases from 0.02-0.20 Hz. The findings from this study revealed an intact gain response, with an impaired phase response in the neonates. The authors of this study issued caution about interpreting the findings from figure 1.17, as diameter of the middle cerebral artery in the neonates may experience changes in cross-sectional area with fluctuations

in blood pressure (which could alter both phase and gain findings). However, they also stated that the use of TFA is appropriate to assess the relationship between blood pressure and CBV as the pressure-flow response can be approximated as a linear system.

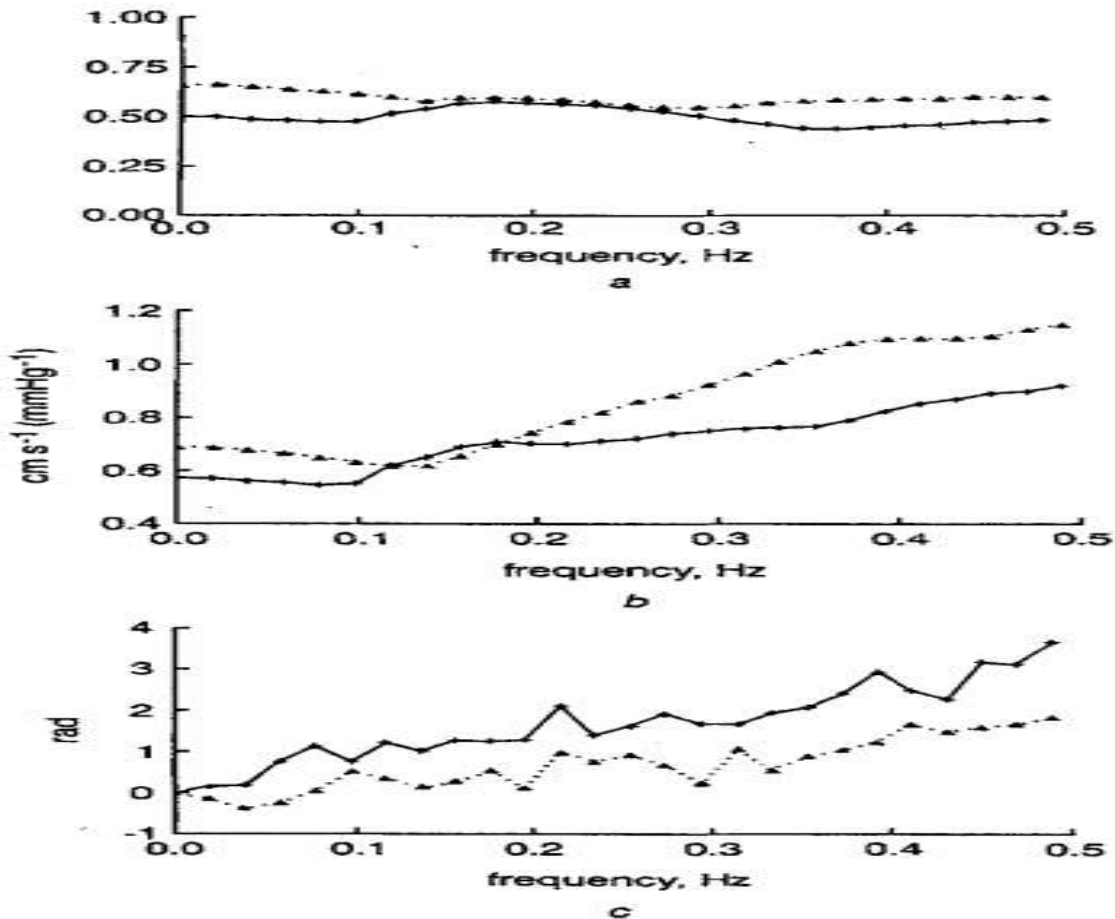


**Figure 1.17.** Findings from the study assessing the frequency dependant nature of cerebral autoregulation in neonates by Panerai *et.al.*<sup>198</sup> Coherence is represented in (a), the neonates with impaired autoregulation are represented in the dotted line and neonates with intact autoregulation are represented in the solid lines. In a typical high-pass filter model, gain (b) increases and phase (c) decreases from 0.01-0.20 Hz. Note the paradoxical relationship between the increase in gain (b) and increases in phase (c) within the neonatal findings. Image from:<sup>198</sup>, permission to reproduce the image was provided by *Medical & Biological Engineering & Computing*.

Rong Zhang and coworkers built upon the previous work of Giller<sup>187</sup>, Birch *et al.*,<sup>189</sup> and Panerai *et al.*,<sup>198</sup> in their seminal work “*transfer function analysis of dynamic cerebral*

*autoregulation in humans*” published in 1998.<sup>18</sup> In this study it was observed that coherence was reduced ( $<0.50$ ) in the frequency range below 0.07 Hz – this region was termed the VLF and has a myogenic influence on CBF regulation (as evidenced by cholinergic blockade<sup>106,185</sup> and ganglion blockade<sup>199</sup> studies). In contrast there was an elevated coherence, high gain and minimal phase lead in the frequencies above 0.20 Hz - this region was termed the HF and is influenced by normal respiration rates.<sup>200</sup> The intermediate frequency range between the VLF and HF – termed LF: 0.07-0.20 Hz – is likely under some sympathetic influence [as noted with in studies with sympathetic agonist drugs – midazolam;<sup>201</sup> sympathetic antagonist drugs – prazosin;<sup>202</sup> and are associated with Mayer waves<sup>200</sup>]. Therefore the regulatory properties of the cerebrovasculature were noted to have the characteristics of a high-pass filter; namely, coherence and gain were increasing and there was a reduction in phase lead (Figure 1.18).<sup>18,184</sup> Thus it appears as though there is an optimal window in which the cerebrovasculature is able to actively regulate alterations in blood flow (the VLF: 0.02-0.07 Hz and LF: 0.07-0.20 Hz frequency bands).<sup>18,125,184,190</sup>

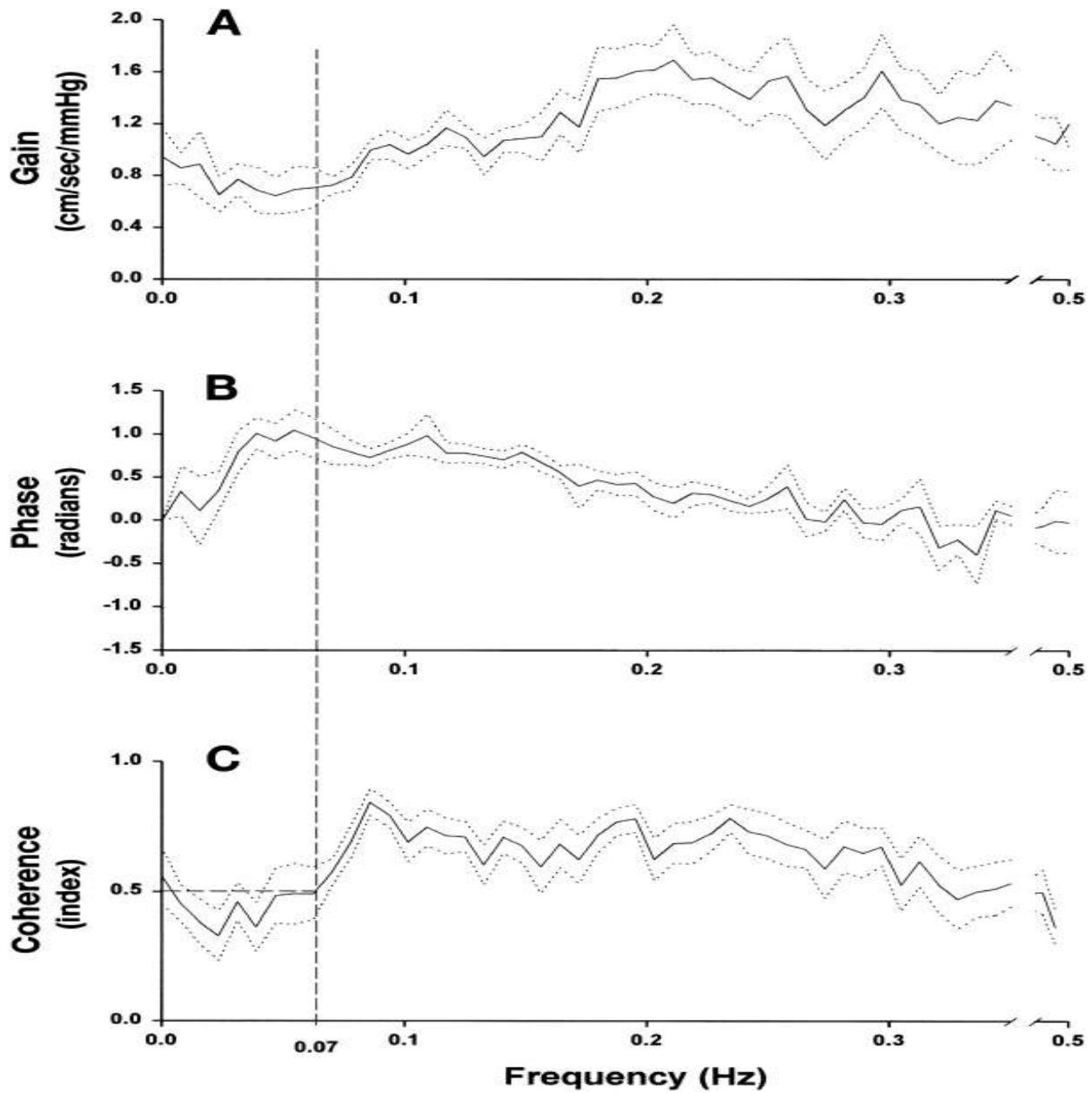


**Figure 1.18.** Group averaged TFA data (mean  $\pm$  standard error) for gain (A), phase (B) and coherence (C) in the study by Zhang *et.al.*,<sup>18</sup> Note the low coherence in the VLF (<0.07 Hz), rising gain and decreasing phase in the LF (0.07-0.20 Hz), and phase  $\sim$ 0 radians and consistently elevated gain in the HF (>0.20 Hz). Image from:<sup>18</sup>, permission to reproduce the image was not required by the *American Physiological Society*.

Since TFA is a linear process in which the input (blood pressure) and output (CBV) are assessed, the coherence function is of utmost importance (refer to section 2.2.2.). A high coherence (e.g. close to 1.0) indicates that the system is linear and thus the changes to phase and gain are interpretable, whereas a low coherence ( $<0.50$ ) could be a result of a multitude of factors.<sup>18,125,184</sup> Namely, the low coherence could occur due to a poor signal-to-noise ratio, the system is non-linear, there are multiple inputs that regulate the output variable; or quite simply there is just no relationship present between the input and output variables. As such, phase and gain values are typically not reported when coherence is below 0.50.<sup>18,125,184,190,200</sup> To address this concern, numerous methodologies to drive blood pressure (and thus improve coherence by maximizing the signal-to-noise ratio) have been proposed: deep breathing;<sup>196,200</sup>; OLBNP;<sup>199,203</sup>; squat-stand maneuvers;<sup>190</sup> and passive leg raises.<sup>204</sup>

Of these proposed driven methodologies, the squat-stand maneuvers as proposed by Claassen and colleagues elicited the greatest oscillations in blood pressure (Figure 1.19.) within the high-pass filter frequency range ( $<0.20$  Hz) of the cerebrovasculature. These large swings in blood pressure not only could be used to increase the statistical reliability of the phase and gain metrics but also did so in a physiologically relevant manner (as the amplitude of these swings represent challenges that the cerebrovasculature endures on a daily basis). When an individual squats down, the muscles of the legs are engaged which increases the skeletal muscle pump and results in a large transient increase in venous return and blood pressure within 2-3 seconds. Upon standing the muscles of the leg are relaxed, decreasing the pressure applied to the veins, enabling venous pooling to increase and results in a subsequent decrease in blood pressure. These large swings in mean arterial pressure (up to 40 mmHg) were performed at frequencies within the high-pass filter range (0.025, 0.05 and 0.10 Hz) and are transmitted to

the cerebrovasculature.<sup>190</sup> The swings in blood pressure were larger at 0.05 Hz and 0.10 Hz as compared to 0.025 Hz. This was likely due to the extended time interval of the 0.025 Hz (20 seconds squat - 20 seconds stand) was sufficiently prolonged such that the baroreceptors were able to counter-regulate the transient blood pressure change. These large oscillations result in greatly increased coherence values at the frequency of interest (can be >0.99), which is believed to occur as a result of an improved signal-to-noise ratio.

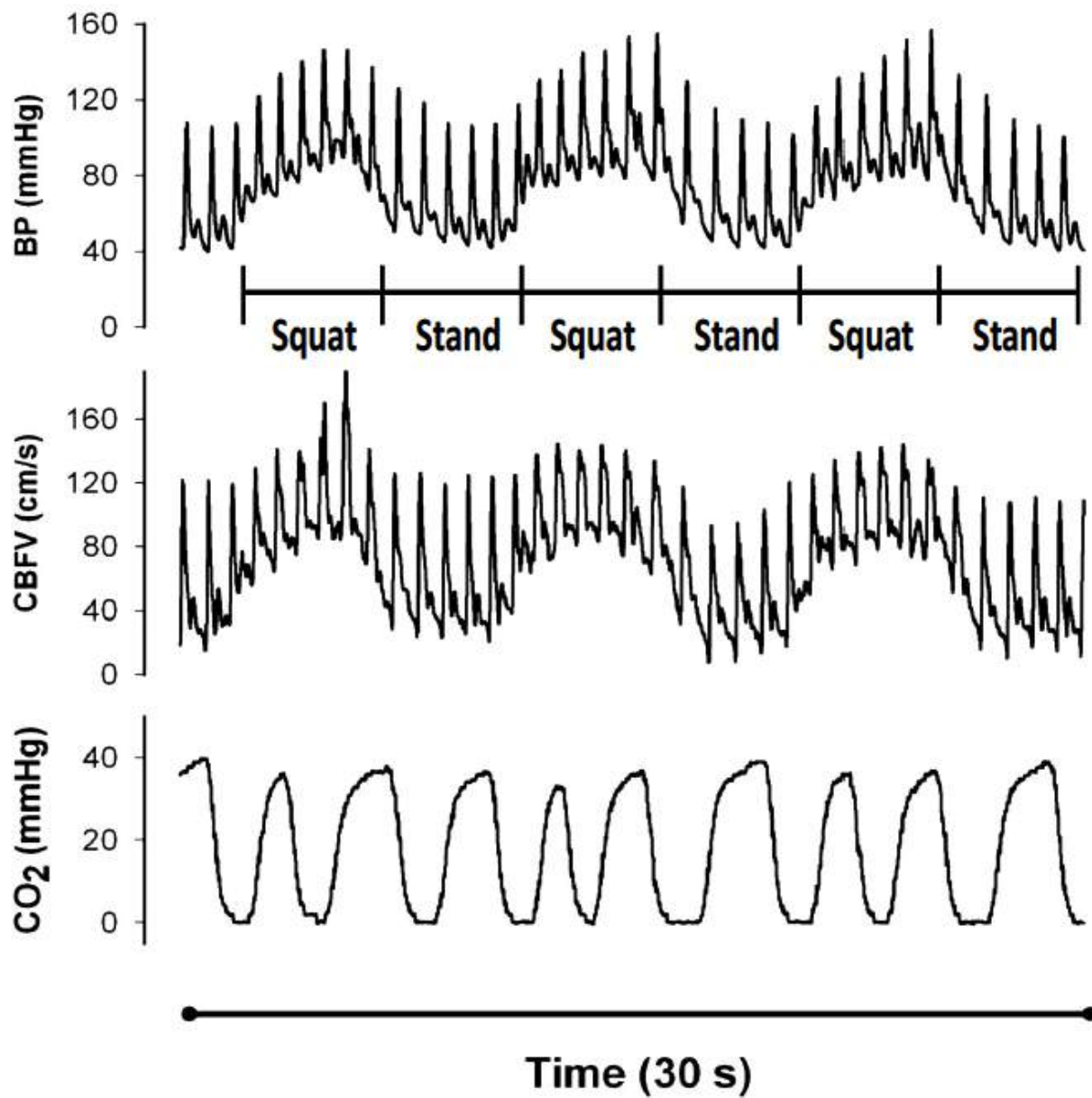


**Figure 1.19.** Trace from a typical subject performing repeated squat-stand maneuvers at 0.10 Hz for blood pressure (top) cerebral blood flow (middle) and end-tidal CO<sub>2</sub> (bottom). Image modified from: <sup>190</sup>. Permission to reproduce the image was not required by the *American Physiological Society*.

### *Mean flow index (Mx)*

Marek Czosnyka and his research group have proposed that the continuous analysis of slow spontaneous fluctuations (20 seconds to 3 minutes) in CBV through a cerebral autoregulation monitoring algorithm (Mx) within the time-domain and can be used to determine the ability of the cerebrovasculature to regulate blood flow against pressure fluctuations.<sup>78,181,205-209</sup> The Mx utilizes a moving correlation coefficient of 30 consecutive samples that compares cerebral perfusion pressure and CBV over a series of 5-minute intervals.<sup>209</sup> This enables a continuous monitoring of cerebral autoregulation to occur, instead of the “*snapshot*” monitoring that other traditional assessment tools (e.g., thigh cuff deflation for RoR and ARI – exception being the ARI impulse response associated with real arterial blood pressure and flow) utilize.<sup>205</sup>

A high Mx value indicates that CBV is responding in a more pressure passive manner to alterations in blood pressure.<sup>78</sup> Mx values above 0.30 are taken as an indication of impaired cerebral autoregulation that could result in very unfavourable outcomes for a traumatic brain injured patient (e.g. mortality)<sup>78,209</sup>. However, values between 0.05 and 0.30 indicate that there is a modest impairment of autoregulation but mortality from a traumatic brain injury is unlikely. Values below 0.05 indicate an intact cerebral autoregulatory system.<sup>78,209</sup>

### *Projection pursuit regression*

Projection pursuit regression (PPR) was first coined by Friedman and Stuetzle in 1981.<sup>210</sup> This assessment tool performs a non-parametric multiple regression analysis and was initially designed to be used to assess complex data sets such as air pollution metrics.<sup>210</sup> The multiple regression analysis during PPR is performed as a sum of smooth linear ridge functions, which are created without a defined *a priori* predictor.<sup>210</sup> The PPR creates the optimal linear combination that results in the least sum of squares as they relate to each ridge function based upon the data set. The data set is not split during PPR, as such more complex models are able to be assessed ( $R^2$ ) and graphically viewed.<sup>210</sup>

Although this statistical methodology has been around since 1981,<sup>210</sup> it was not applied to the relationship between blood pressure and CBF until 2012.<sup>186</sup> The application of PPR to the cerebral pressure-flow relationship proved to be novel approach to assess the independent (blood pressure) and dependant (CBV) variables, and revealed that the high-pass filter model of CBF regulation persists.<sup>186</sup> The ridge functions, although potentially ‘forced’ through the data, revealed that driven oscillations in blood pressure are linearly passed along to the cerebrovasculature at frequencies above 0.04 Hz, as noted by the increasing slope of the autoregulatory range (Figure 1.20.).<sup>185,186</sup> Only at the lowest frequency (0.03 Hz) was there an extended autoregulatory zone of ~10 mmHg,<sup>186</sup> which was lost when a cholinergic blockade was administered.<sup>185</sup> These findings are useful as, at least with this approach, they confirm that there is likely a myogenic influence within the VLF.

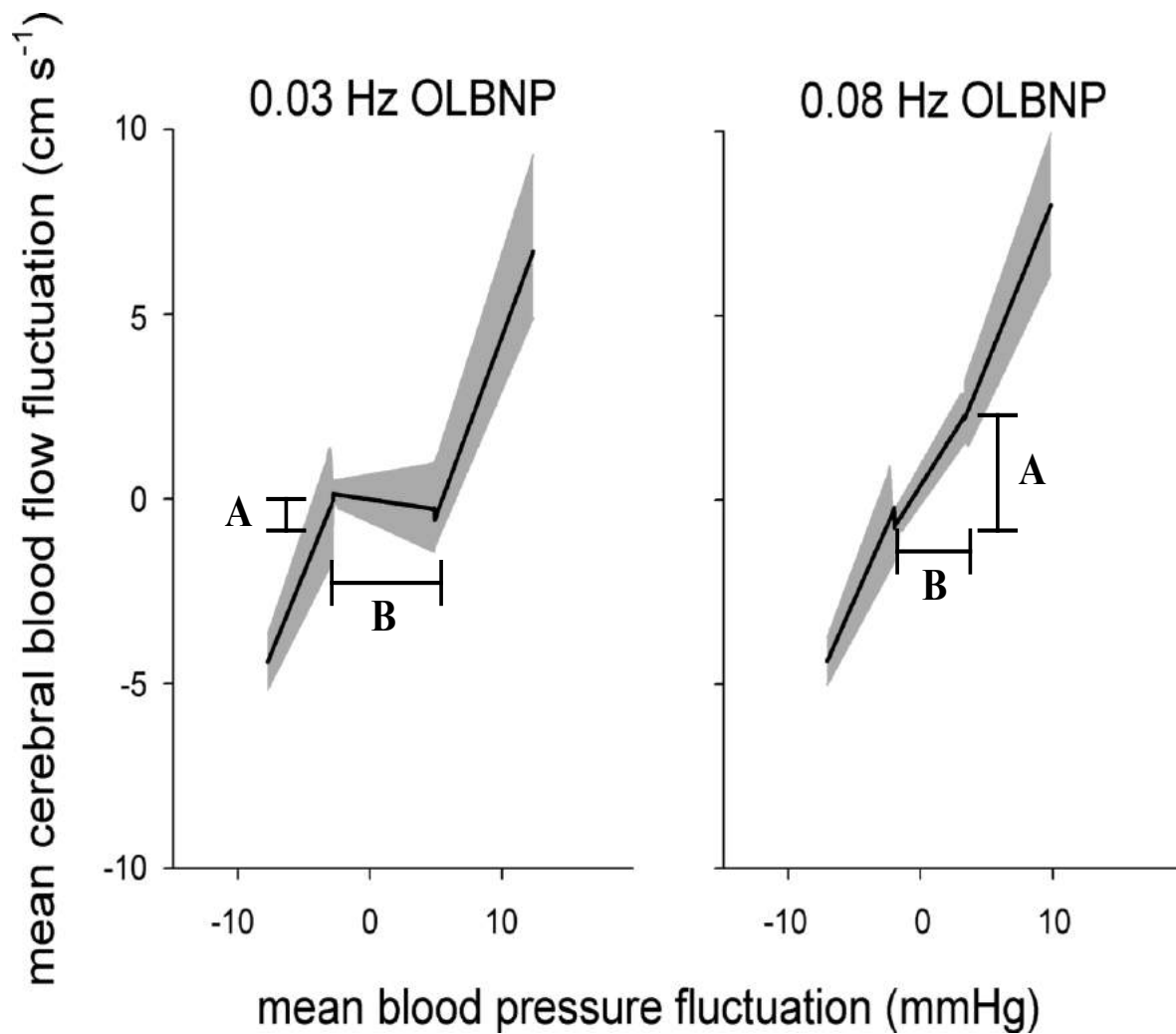


**Figure 1.20.** Ridge functions for the cerebral pressure-flow relationship at 0.03 Hz (left) and 0.08 Hz (right). The autoregulatory gain (A) and autoregulatory range (B) are represented for both frequencies. The shaded area indicates the 95% confidence interval range. Note the linearity of the relationship between cerebral blood flow and mean arterial pressure at 0.08 Hz (right panel). Image modified from: <sup>186</sup>. Permission to reproduce the image was not required by the *American Physiological Society*.

#### 1.6.4. Comparison of commonly used methodologies to assess this relationship

The term '*cerebral autoregulation*' is an all-encompassing concept that entails much more than just the relationship between mean arterial pressure and CBF (as highlighted in section 1.3.). As such, the mechanisms underlying cerebral autoregulation are not as simple as just occurring as a result of alterations to cerebrovascular resistance to maintain a steady-state CBF. If this was the case, then any measurement tool (RoR/ARI, TFA, Mx, PPR) used to assess cerebral autoregulation should reveal the same outcomes, unfortunately they do not and currently there is no '*Gold Standard*' assessment tool.<sup>125</sup> As previously explained, RoR and ARI quantify either the cerebrovascular resistance rate of change post thigh cuff deflation (RoR) or the measure of latency and gain within 30-second of a hypotensive stimulus for the cerebral autoregulatory system (ARI).<sup>176,188</sup> In both systems of assessment, slower or weaker values indicate a autoregulatory impairment. TFA applies a linear input-output model to assess the dynamic cerebral-pressure flow relationship within the frequency domain and provides metrics for the linear correlation (coherence), timing (phase) and amplitude changes (gain).<sup>18,187,189</sup> The Mx utilises a correlation coefficient based upon linear regression to relate spontaneous fluctuations in blood pressure and CBV across a series of moving windows.<sup>181,208,211</sup> Mx values  $>0.05$  related to poor outcomes and values  $>0.30$  and index of possible mortality in the context of traumatic brain injury.<sup>181,205,211,212</sup> Finally, PPR uses a series of ridge functions (Figure 1.20.) to quantify the blood pressure and CBV relationship in a non-linear fashion, and provides a measure of explained variance between the two signals (but no indication for phase or gain changes).<sup>185,186</sup> Thus the question remains: *How well do some of these commonly used metrics converge and how compatible are they?*

A recent study by Tzeng *et al.*,<sup>125</sup> “*Assessment of cerebral autoregulation: the quandary of quantification*” set about trying to systematically examine RoR, ARI and TFA metrics and determine how interchangeable they are. It was found that most of the metrics are actually either unrelated or only have a weak-to-moderate correlation (Figure 1.21.) - finding supported in a previous review.<sup>212</sup> For example, RoR and ARI which are both measuring the step change CBV response to a hypotensive stimulus only had coefficient of determination of 0.34.<sup>125</sup> The only strong correlations ( $R^2 > 0.50$ ) occurred from mathematically related constructs (gain vs normalized gain).<sup>125</sup> In other studies, the Mx is only weakly correlated to ARI ( $R^2 = 0.16$ ), but unrelated to any of the spontaneous TFA metrics.<sup>207</sup> On the other hand PPR has been shown to have comparable results to TFA coherence and gain metrics, especially when the frequency of interest is  $>0.04$  Hz.<sup>185</sup>

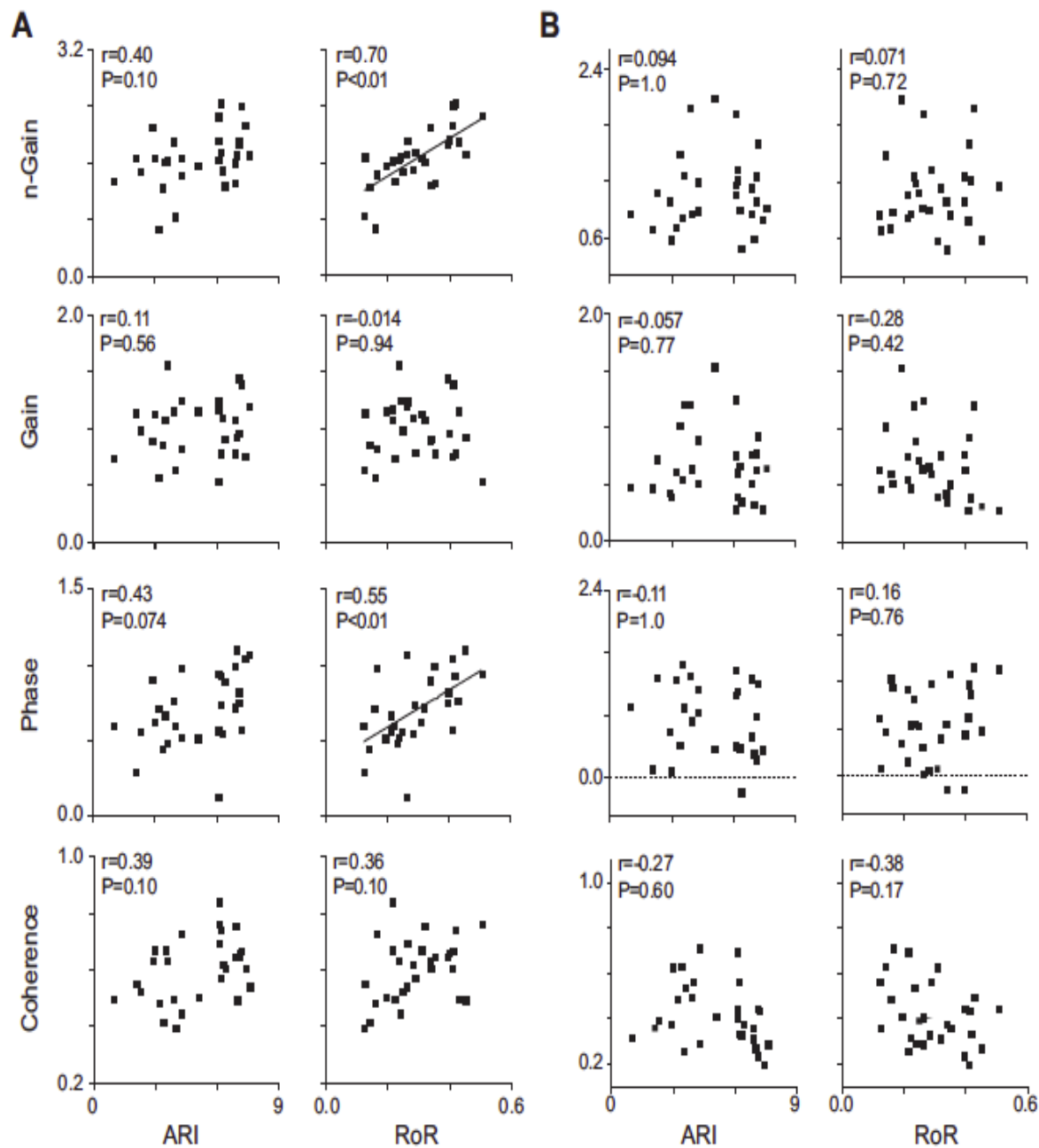


**Figure 1.21.** Between subject relationships for the transfer function analysis metrics and either RoR (rate of regulation) and ARI (autoregulatory index). Left panel (A) is for LF (0.07-0.20 Hz) and right panel (B) is for VLF (0.02-0.07 Hz). Note how few significant correlations are present between the assessment metrics. Image is from: <sup>125</sup>. Permission to reproduce the image was not required by the *American Physiological Society*.

There were several explanations as to why there was a general lack of convergence in these measures. For instance, single large abrupt changes to blood pressure (as indexed with

RoR and ARI) may be recording a different aspect of the autoregulatory response as compared to Mx, PPR and TFA. <sup>125,207</sup> The amplitude of the spontaneous and rhythmically driven blood pressure changes may also influence the nature of the cerebrovascular responses. <sup>125</sup> Although RoR and ARI are both examining the CBF response to a strong hypotensive event, RoR is an index of the “*pace*” of cerebral autoregulation whereas ARI is an index of the restorative properties of autoregulation, therefore they are actually reporting on two separate entities that may have different underlying properties and mechanisms. <sup>125</sup>

Thus, the combination of a lack of metric congruency and the fact that there is no real ‘*gold standard*’<sup>125,213</sup> for researchers to go by when quantifying the relationship between blood pressure and CBF, leads researchers to choose which metric best fit the needs of their particular study. The following section outlines the rationale for the use of TFA in the thesis research chapters.

### 1.6.5. Rationale for the use of transfer function analysis

Although there are very few relationships in physiology that are truly linear in nature, most systems can be approximated through a linear black-box model and the cerebral pressure-flow response falls within this category.<sup>198</sup> The data presented by Tan et al.,<sup>185,186</sup> exemplifies this notion. Their ridge models have demonstrated that as the frequency of driven oscillations increased above the rate at which the baroreceptors are able to modulate blood pressure, CBF regulation is relatively linear in nature (right panel, Figure 1.20.). Also, when methodologies are employed that create large oscillations in blood pressure, these in turn are passed along into the cerebrovasculature and, as mentioned, can lead to dramatic increases in TFA coherence (due to enhanced signal-to-noise ratio) and can '*linearize*' the system.<sup>190,196,200,203,214</sup> These combined notions indicate that although the pressure-flow relationship may in of itself not be truly linear in nature, it can be approximated in a linear fashion (as highlighted by coherence values that can exceed 0.99 during squat-stand maneuvers – see research Chapters 3-7).

The TFA also enables a greater context of interpretation for the researcher to examine. For instance, not only does TFA clearly demonstrate the high-pass filter model of the cerebrovasculature, it allows the researcher to quantify alterations to both the timing and amplitude modulation as they pertain to the particular research question.<sup>18,187,190,215</sup> Thus, when the appropriate methodologies are employed, linear TFA is an appropriate tool for the evaluation and quantification of the relationship between arterial blood pressure and CBV,<sup>125</sup> and as such will be utilized throughout this thesis.

The utilization of TFA is also one of the most wide-spread assessment tools for examining the dynamic relationship between arterial blood pressure and CBV.<sup>213,216</sup> There are currently in excess of 15 research centres around the globe that are utilizing this technique to

assess the cerebral pressure-flow relationship, and there is good accuracy for these centres to be able to distinguish between intact and impaired autoregulatory systems.<sup>213</sup> Spontaneous TFA has also been shown to have a fair reliability for assessing both phase and gain measures, across cerebral hemispheres and over multiple testing periods (intraclass correlations <0.60).<sup>217</sup> Furthermore, the numerous studies published utilizing TFA, enables findings from this thesis to be readily compared and contrasted with the current literature in the field.

It should also be noted that this thesis will not directly discuss cerebral autoregulation *per se*, as the term '*cerebral autoregulation*' is a much more all encompassing concept than just the relationship between mean arterial pressure and CBF. Instead, this thesis will present the data and its interpretations based merely as they regard to the relationship that exists between blood pressure and CBF in the VLF and LF ranges. The black-box nature of TFA does not adequately enable further claims to concretely prove that the only appropriate input for CBF assessment is blood pressure (Figure 1.13.).<sup>184</sup>

## **Chapter Two: Methodological Overview**

The following chapter will provide a methodological review on: 1) the instruments used to collect the data presented in this thesis; and 2) the methods used to describe underlying relationship between arterial blood pressure and CBV. The instrumentation and assessment methodologies will be referenced within the individual research chapters (Chapters 3-7).

### **2.1. Instrumentation**

The key instruments utilized to collect the data presented in the research chapters of the thesis were transcranial Doppler ultrasound, finger photoplethysmography, electrocardiography, and a respiratory gas analyzer. These instruments are described in detail below.

#### **2.1.1. Transcranial Doppler ultrasound**

*Principles underlying transcranial Doppler ultrasound [reviewed in: <sup>38</sup>]*

The basic principle of transcranial Doppler ultrasound is that a transmitter emits a pulsed ultrasound wave from Doppler probe at 1.5-2 MHz. The sound wave is transmitted through the thin acoustic windows of the temporal region of the cranium to assess a target vessel (middle or posterior cerebral arteries). The wavelength of 1.5-2 MHz provides the optimal resolution-to-penetration depth ratio for imaging the deep cerebral vessels. A higher frequency signal (as used in diagnostic tissue ultrasound ~8-15 MHz) would not have the ability to penetrate as deep (only 3-4 cm) into the cerebral tissue and not reach the vessels of interest. The transmitted ultrasound beam contacts the red blood cells within the target vessel and a portion of the signal is reflected back to the transducer, where it is recorded. The

difference between the frequency of the transmitted and received signals is known as the Doppler shift (For more information please refer to section 1.4.2.). The frequency data from the Doppler shift is then processed through a fast Fourier transform to convert the data from the frequency domain (ultrasound waves) into the time domain (velocity trace), where it can be utilized to calculate the velocity of the red blood cells within the cerebral vessel of interest. Since the transmitted signal from the transducer and the speed at which sound travels through the blood stream are constant values, the only real variables in the equation Doppler shift are the insonation angles of the Doppler probe in relation to the vessel of interest and the velocity of the red blood cells themselves.

The insonation angle is of critical importance to the precision of the measure, as the error associated with the Doppler shift is a result of the cosine of the insonation angle (Figure 2.1.). For optimal signal quality the ideal angle of insonation should be between 0 and 30 degrees (cosine range 1.00 to 0.87); however, as long as the insonation angle is below 60 degrees (cosine of 0.50) the signal is deemed adequate for assessment (reviewed in: <sup>56</sup>). When insonating the middle cerebral artery through the middle portion of the temporal window, the insonation angle is virtually inline (<15 degrees) with the probe (Figure 2.2.); this low angle helps create optimal signal quality. Similarly, the PCAv can be acquired with a low angle of insonation from the anterior portion of the temporal window (Figure 2.2.). The summation of the Doppler shift reflected from each of the red blood cells within the insonated region of the target vessel is used to make a 2-dimensional Doppler waveform (Figure 2.3.). The envelope placed on this waveform is used to determine the velocity of blood within the target vessel and is recorded for future analysis.

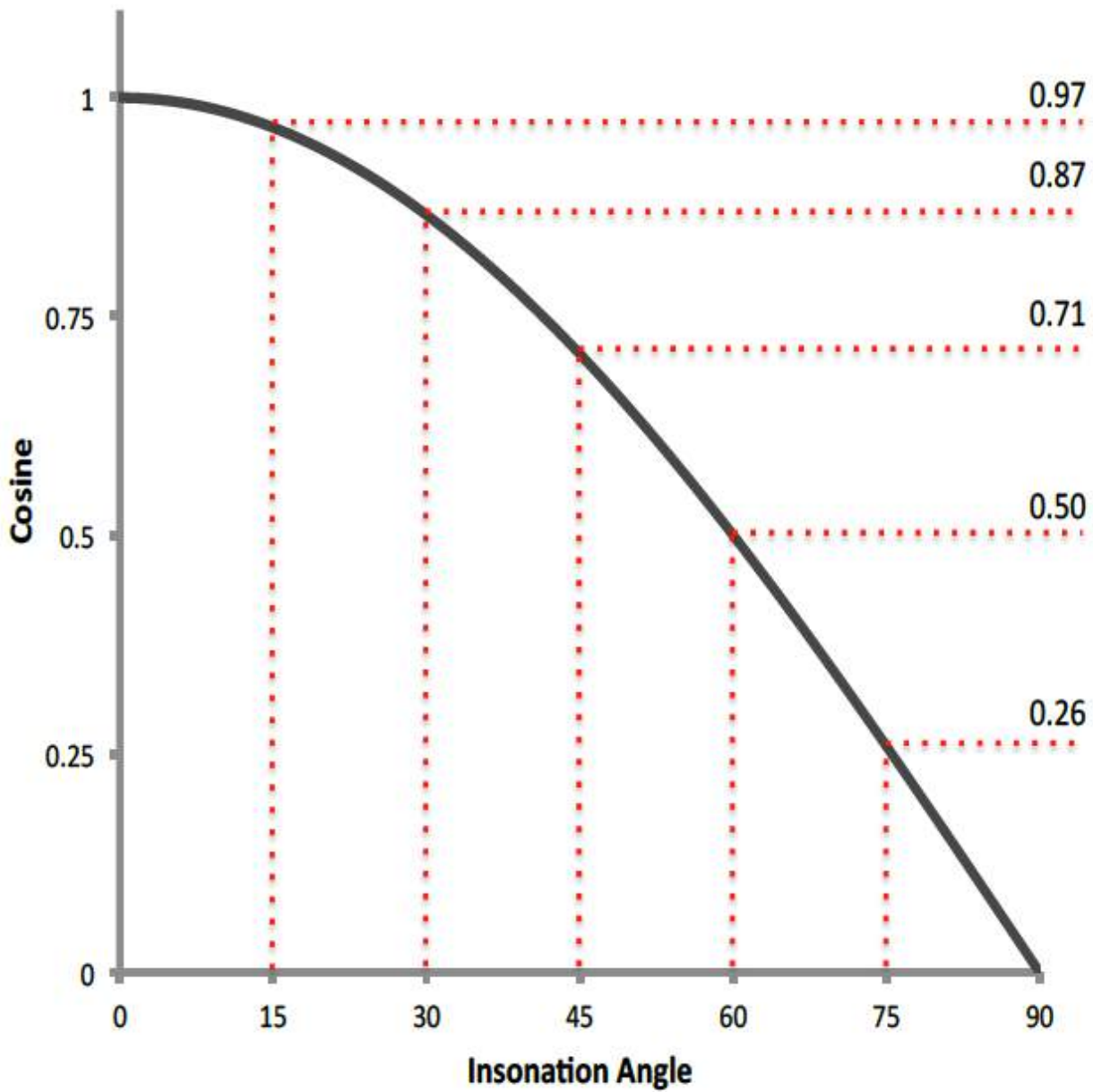


**Figure 2.1.** The relationship between the angle of insonation and the cosine of that angle. The cosine of a 15 degree insonation angle is 0.97, indicating that 97% of the frequency shift within the signal is being transmitted back to the receiver. At insonation angles >60 degrees, there is less than 50% of the signal being received and at 90 degrees; therefore, no signal will be recorded.

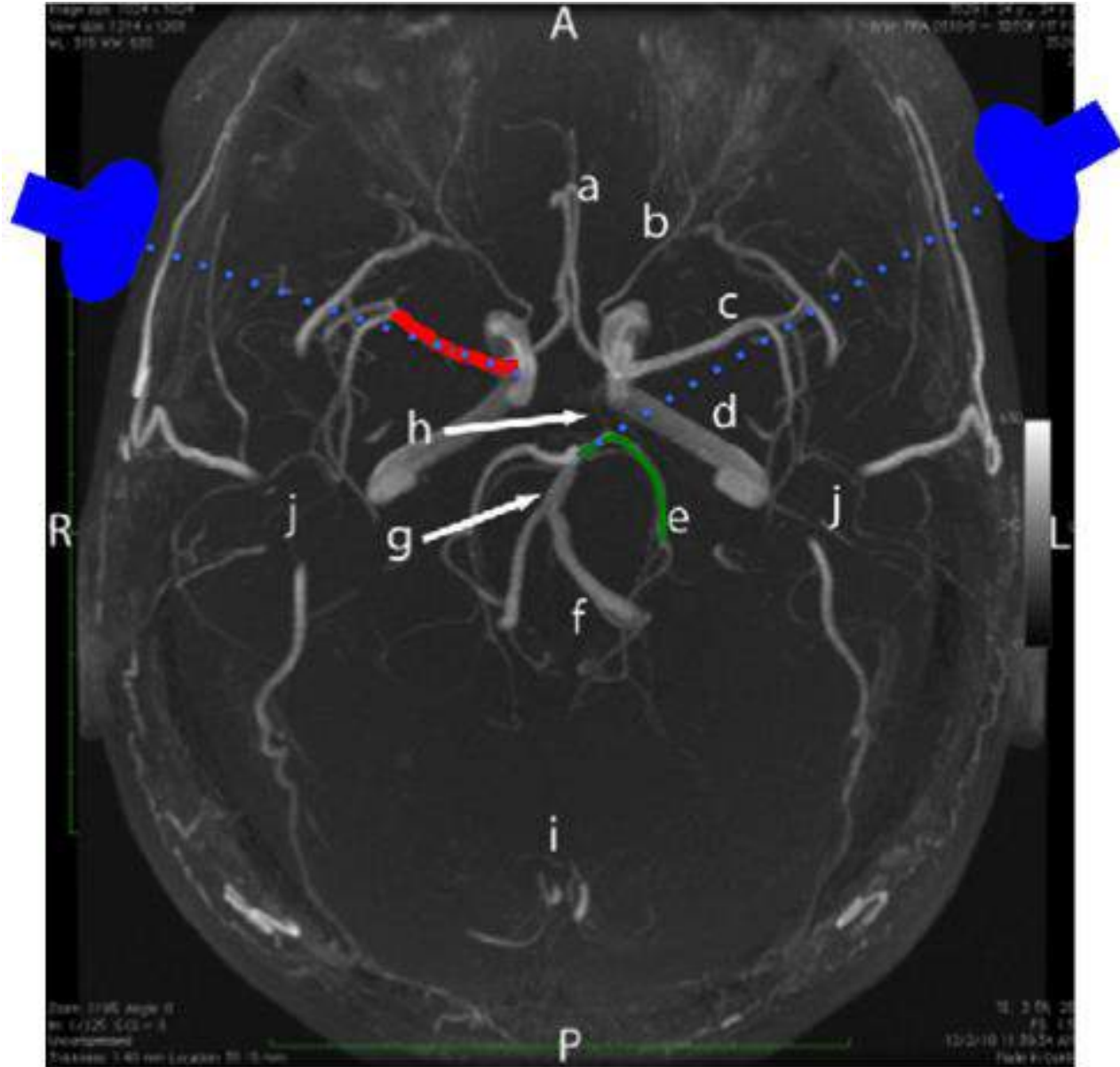


**Figure 2.2.** Example of insonation angles and probe placement for the middle cerebral artery (highlighted in red on the left: c) and the posterior cerebral artery (highlighted in green on the right: e). A denotes anterior and P denotes posterior. Note the insonation angles are very close to 0 degrees which optimizes the signal quality and mitigates any issues associated with the cosine correction factor. Image modified from: <sup>38</sup>. Permission to reproduce the image was provided by the *Journal of Neuroscience Methods*

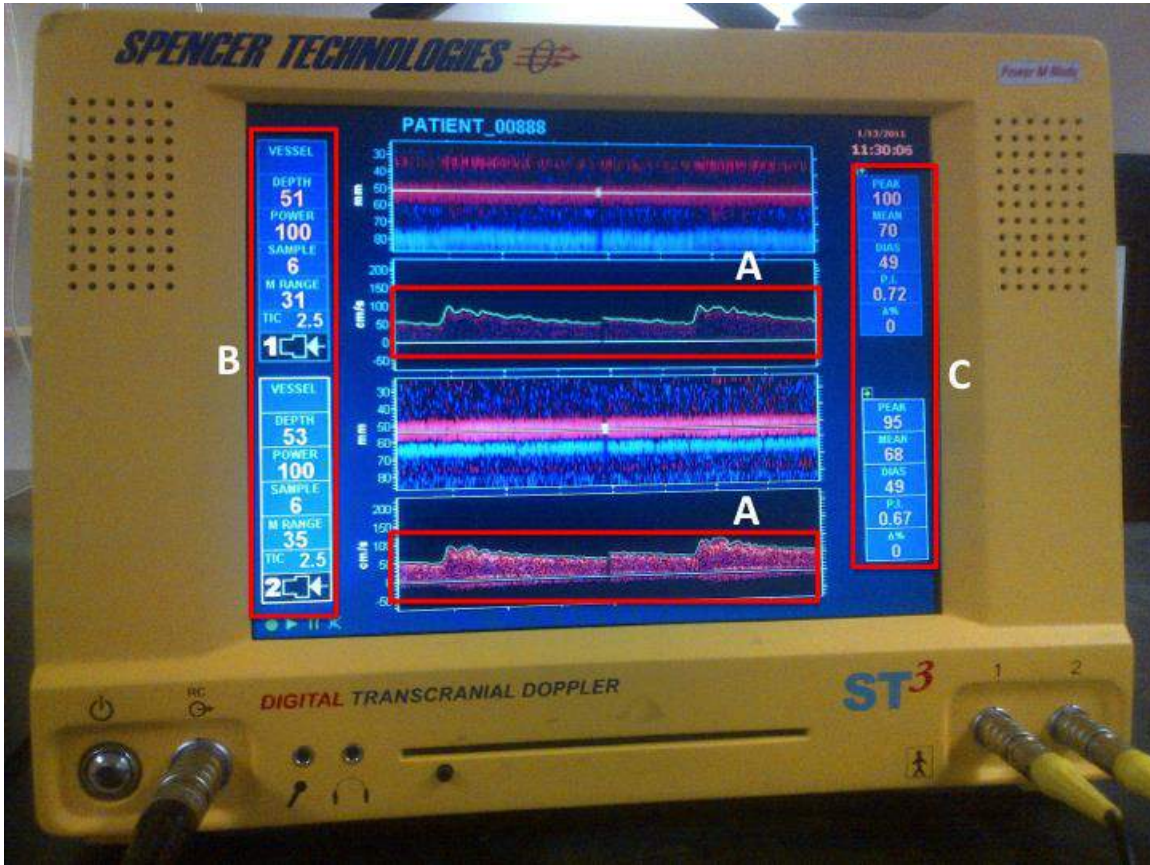


**Figure 2.3.** Example the 2-dimensional waveform created by the spectral analysis of the Doppler shift from the red blood cell velocity and the surrounding envelope (A). The envelope data can be exported in real time for future analysis. The depth of the insonated vessel (in millimeters), and % power of the M-mode are highlighted on the left side of the display (B). The peak systolic, mean and minimum diastolic velocity (in cm/s) of the insonated red blood cells are displayed on the right side of the display (C), along with the pulsatility index [calculated as:  $(\text{systolic}-\text{diastolic})/\text{mean}$ ] which gives an index of the local resistance in the artery of interest as well as the variability of the blood velocity.

### *Technique of transcranial Doppler ultrasound*

The method for insonation of a cerebral vessel is summarized as follows. First, acoustic gel is generously applied to the temporal window of the subject and is also applied to the transcranial Doppler probe in order to enable signal conduction. Next, the probe is positioned over the appropriate portion of the temporal window that enables the best angle to insonate the vessel of interest and is secured to an adjustable headband. The headband will hold the probe in place and maintain the signal quality throughout the data collection periods. An experienced sonographer will then identify the vessel of interest based upon their technical skill and knowledge of the anatomical structure of the cerebral vessels (reviewed in: <sup>38</sup>). The sonographer needs to have an understanding of the basal structure of the circle of Willis (middle and posterior cerebral branches), common insonation depths for the vessel of interest (middle cerebral artery 30-65 mm – M1 segment 45-55 mm; P1 segment of the posterior cerebral artery 55-75 mm). <sup>218</sup> Approaches are also required in which to confirm the insonated vessel is indeed the vessel of interest (the middle cerebral artery will diminish with carotid occlusion whereas the PCAv will be unaltered; and PCAv will increase by up to 20% with activation of the occipital lobe whereas velocity in the middle cerebral artery will increase much less (<5%).

### *Validity of transcranial Doppler ultrasound*

Early MRI studies (1.5 Tesla) demonstrated that the middle cerebral artery diameter was relatively constant with elevations and reductions in  $P_{ET}CO_2$  (range: 23-60 mmHg). <sup>63,64</sup> However, the voxel size in these early studies appear to have been too large to detect the changes in the diameter of the middle cerebral artery as more recent work with both a 3 Tesla <sup>65</sup>

and 7 Tesla.<sup>66</sup> MRI have revealed that the middle cerebral artery diameter is altered when  $P_{ETCO_2}$  changes are greater than  $\sim 8$  mmHg (reviewed:<sup>67</sup>). Therefore, if  $P_{ETCO_2}$  levels are maintained near eucapnia, CBF and CBV (as indexed by transcranial Doppler) appear to be robust and accurate indices for CBF.<sup>67</sup> When  $P_{ETCO_2}$  exceeds 8 mmHg from eucapnia, the middle cerebral artery diameter can dilate  $\sim 6-8\%$ <sup>65,66</sup> which could lead to an over estimation of CBF by  $\sim 25\%$ .<sup>67</sup> Conversely when there is a reduction to  $P_{ETCO_2}$  the middle cerebral artery diameter can constrict approximately  $4\%$ <sup>65</sup> which would result in an overestimation of CBF by  $\sim 10\%$ .<sup>67</sup> Therefore it appears as though large increases in  $P_{ETCO_2}$  have a greater effect on transcranial Doppler ultrasound indices of CBF than reductions in  $P_{ETCO_2}$ . Whether or not smaller changes in diameter could be detected with higher resolution MRI remain unknown. Interesting, however, the % change in the diameter of the middle cerebral artery per mmHg changes in  $P_{ETCO_2}$  is comparable to the % change in the diameter of the internal carotid artery.<sup>42</sup> Such findings are consistent with the notion that the entire cerebrovascular tree is sensitivity to changes in  $P_aCO_2$ . Collective, these recent findings reinforce the vital need of any study reporting CBV values from a transcranial Doppler ultrasound to monitor  $P_{ETCO_2}$  closely throughout the experiment.

Transcranial Doppler indices have been compared with the Kety-Schmidt method during cardiopulmonary bypass<sup>219</sup> where it was revealed that there was a minimal bias (less than 8%). However, it should be noted that  $P_aCO_2$  levels were unchanged during this experiment, which helps confirm the findings in Figure 1.6.<sup>67</sup> Specifically, this finding further highlights the notion that the transcranial Doppler indices for CBF are robust as long as  $CO_2$  levels are maintained near eucapnic levels. Therefore the use of transcranial Doppler ultrasound to monitor and report on CBF indices is still a useful, powerful and valid measure that can be

used to advance the research of cerebrovascular physiology. In the event that CO<sub>2</sub> levels are being manipulated, a parsimonious interpretation of transcranial Doppler data is needed.

### **2.1.2. Finger photoplethysmography**

Finger photoplethysmography is a non-invasive tool that is able to continually monitor blood pressure, stroke volume and cardiac output. This approach works by monitoring the infrared photoplethysmograph signals that detect light reflected off of the blood moving through the finger.<sup>220</sup> In vivo, this concept enables the measurement of the absorption of light by the red blood cells and gives an indication of the diameter of the fingers small arteries.<sup>220</sup> The small artery diameter is thought to be constant as it opposes changes in artery volume.<sup>221,222</sup> A fast pressure servo controlled monitor continually tracks the changes in the diameter and volume of the vessels, which is used to create an index of blood pressure within the finger.<sup>221-223</sup> The signal from the finger is then digitally filtered and the brachial intra-arterial waveform is recreated by applying a correction algorithm that compensates for the pressure gradient between the finger and the upper arm.<sup>222</sup>

One of the most common and robust commercially available products that utilize photoplethysmography is the Finometer (Figure 2.4).<sup>221-223</sup> It has been shown to comply with the American Advancement of Medical Instrumentation standards (the accuracy is within 5 mmHg of intra-arterial blood pressure recordings) and further use of the physio-cal calibration tool ensures that the non-invasive recordings track the arterial blood pressure waveforms accurately throughout prolonged experimental procedures.

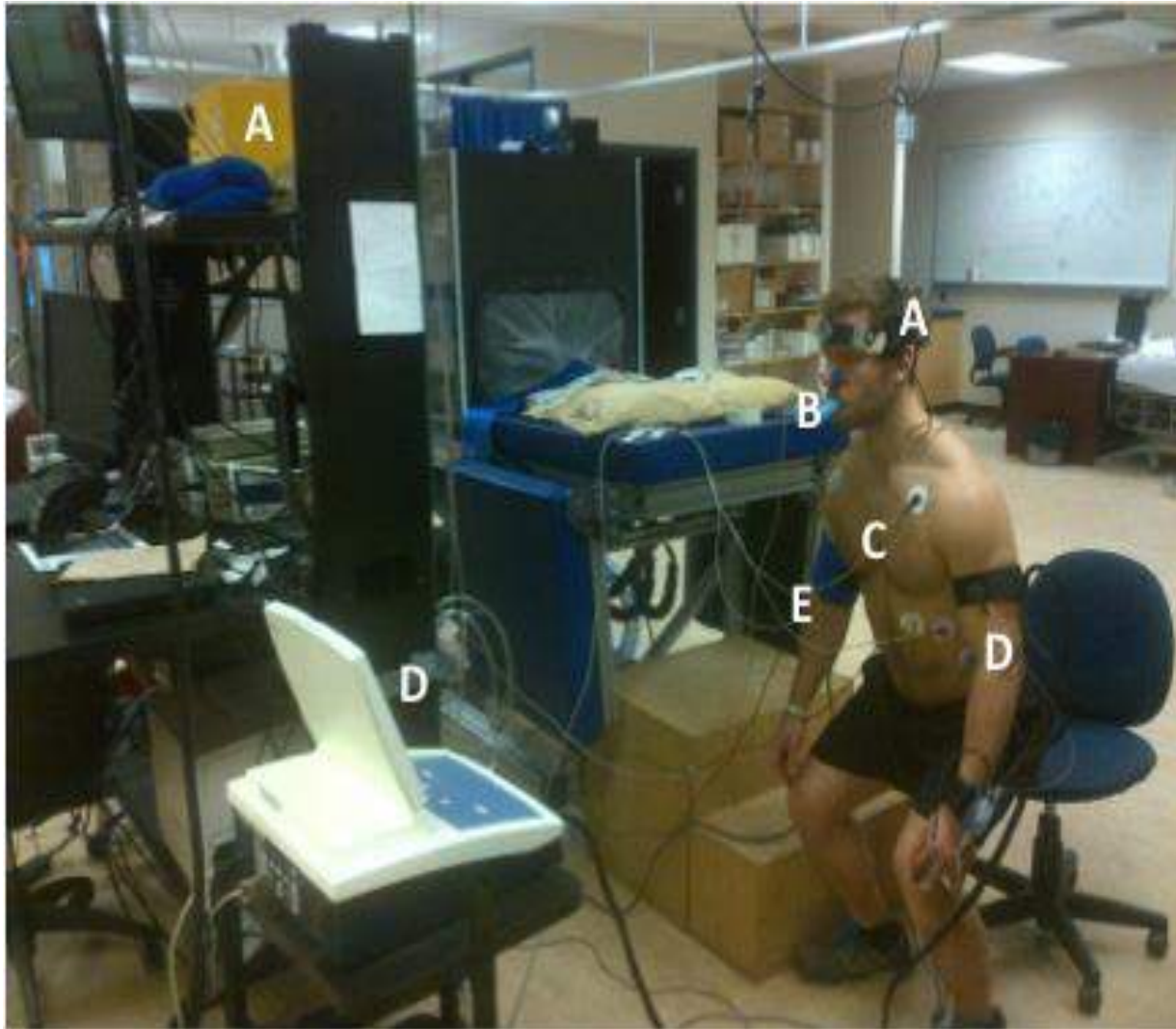


**Figure 2.4.** An example of a typical experimental set up. The transcranial Doppler (A) is continually recording cerebral blood velocity with the probes fixed in place with a head frame (A) to ensure the insonation angle of the vessel of interest is maintained throughout the experiment. The end-tidal gases are sampled (B), which provides an index for monitoring the arterial carbon dioxide levels. A 3-lead electrocardiogram (C) records the electrical activity of the heart. A Finometer (D) continually monitors blood pressure and is height corrected to the brachial region. The finometer blood pressure measures are also checked against intermittent automated blood pressure recordings with the SunTech Tango+ (E).

### 2.1.3. Electrocardiography

Electrocardiography is the process of monitoring and recording the electrical activity of the heart through leads placed on the surface of the body. As the cardiac tissue contracts and relaxes; calcium, potassium and sodium ions are exchanged which results in the depolarization (contraction) and repolarization (relaxation) of the cardiac tissue. The exchange of these ions creates an electrical signal (Figure 2.5) that is detected by electrodes placed at specific location on the surface of the body (Figure 2.4). There are 5 distinct waves within the electrocardiogram, each representing a different aspect of the cardiac cycle. The P wave occurs when the atria depolarization, QRS complex occurs with ventricular depolarization (and repolarization of the atria), and the T wave represents the repolarization of the ventricles. The interval between one R wave and the adjacent R wave (R-R interval) is typically used to determine heart rate and is the interval for sampling beat-to-beat blood pressure and CBV data.

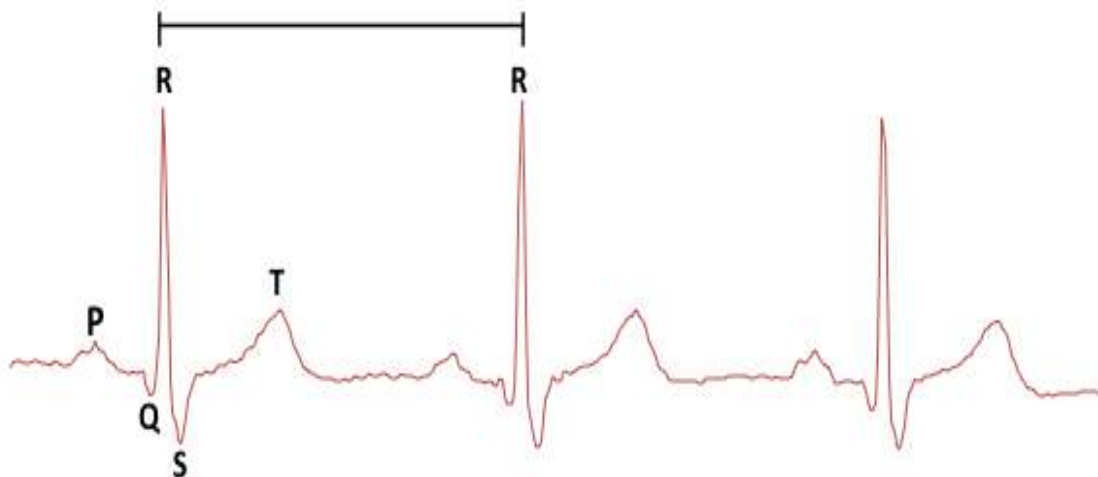


**Figure 2.5.** Example a typical electrocardiogram trace during a data collection. The P,Q, R,S,T waveforms and R-R interval are labelled for identification.

#### 2.1.4. Gas analysis

The  $P_{ET}O_2$  and  $P_{ET}CO_2$  samples reported in the thesis research chapters were obtained using an ADInstruments gas analyzer (model ML 206). The expired gases are sampled at the mouth (Figure 2.4) and a small pump within the gas analyzer draws a sample into the transducer where the measurements of percent oxygen and carbon dioxide are performed. The obtained percentages are then used to calculate the respective  $P_{ET}O_2$  and  $P_{ET}CO_2$  values.

The percentage of inspired and expired  $O_2$  measurements are obtained through a visible spectrum (760 nm) transducer with absorption spectroscopy. A narrow band of light is projected by a laser diode across the incoming gas sample and a detector records the emission levels within the oxygen spectrum. As the oxygen concentration levels increase, the energy absorbed by the oxygen molecules within the sample also increases and thus there is a decrease in light received by the detector. Conversely, when oxygen levels are decreased, there are fewer gas molecules to absorb the light and the detector will receive more light.

The percentage of inspired and expired  $CO_2$  measurements is made using a non-dispersive infrared transducer, which works on a similar principle as the absorption spectroscopy described above. An infrared lamp is projected through a gas sample and any gas molecules that are the same size as the infrared light wavelength (in this case  $CO_2$ ) are absorbed. Close to the end of the sampling tube there is an optical filter, which absorbs all wavelengths of light except that of  $CO_2$ . Finally, at the end of the sample tube, there is an infrared detector that will record the amount of light that was not absorbed by the  $CO_2$  molecules or optical filter. The difference in the amount of light projected and absorbed is proportional to the number of  $CO_2$  molecules in the sample.

## 2.2. Signal Processing

Signals are mathematical representations for the functions of one or more independent variables. <sup>224,225</sup> For example, blood pressure can be represented as the arterial pressure in mmHg as a function of time. Similarly, CBV can be represented as the speed of the red blood cells in the cerebrovasculature in cm/s as a function of time. The interpretation and analysis of these acquired signals occur via signal processing. Blood pressure and CBV are continuous analog signals in the body; the first step in signal processing is to convert these signals into discrete digital signals. This is done by converting the analog system (mmHg or cm/s) into a digital signal, such that the pressure or velocity is converted into a voltage and tracked over discrete time periods (in the case of this thesis the sampling period during data collection was 1000 Hz which equates to a sample occurring every 0.001 seconds for a period of 5 minutes). These signals are then converted into beat-to-beat data by taking the mean value of all of the data points from each blood pressure (or CBV) as sampled from each R-R interval.

A linear system is any process that results in an output signal (CBV) being produced as a result of an input signal (blood pressure) (Figure 2.6.) as long as certain criteria are met which will be discussed below. As discussed in Chapter one, within the cerebrovasculature the regulation of may (or may not, depending on how it is assessed) be an entirely linear system in nature (refer to section 1.6.3). Regardless, the cerebrovasculature can be approximated as such because it meets the needs of a linear system, namely it possesses: homogeneity and additivity. <sup>225</sup> Homogeneity occurs when the amplitude of the input variable is altered, this change is reflected (to some extent) in the output variable. <sup>225</sup> As described in section 1.5.3., when there is a change in cerebral perfusion pressure (which is highly influenced by blood pressure) there is a subsequent change in CBF, thus demonstrating homogeneity within the cerebrovasculature.

Additivity is when additional signals can influence the input signal, which will result in alterations to the output signal.<sup>225</sup> The cerebrovasculature is additive in nature, as alterations in  $P_aO_2$  and  $P_aCO_2$ , in conjunction with alterations to cerebral perfusion pressure, can result in further changes in CBF.<sup>74</sup> Thus, the cerebrovasculature has been shown to meet the requirements of a linear system<sup>225</sup> and, therefore, is able to be assessed with linear systems analysis methods such as TFA.

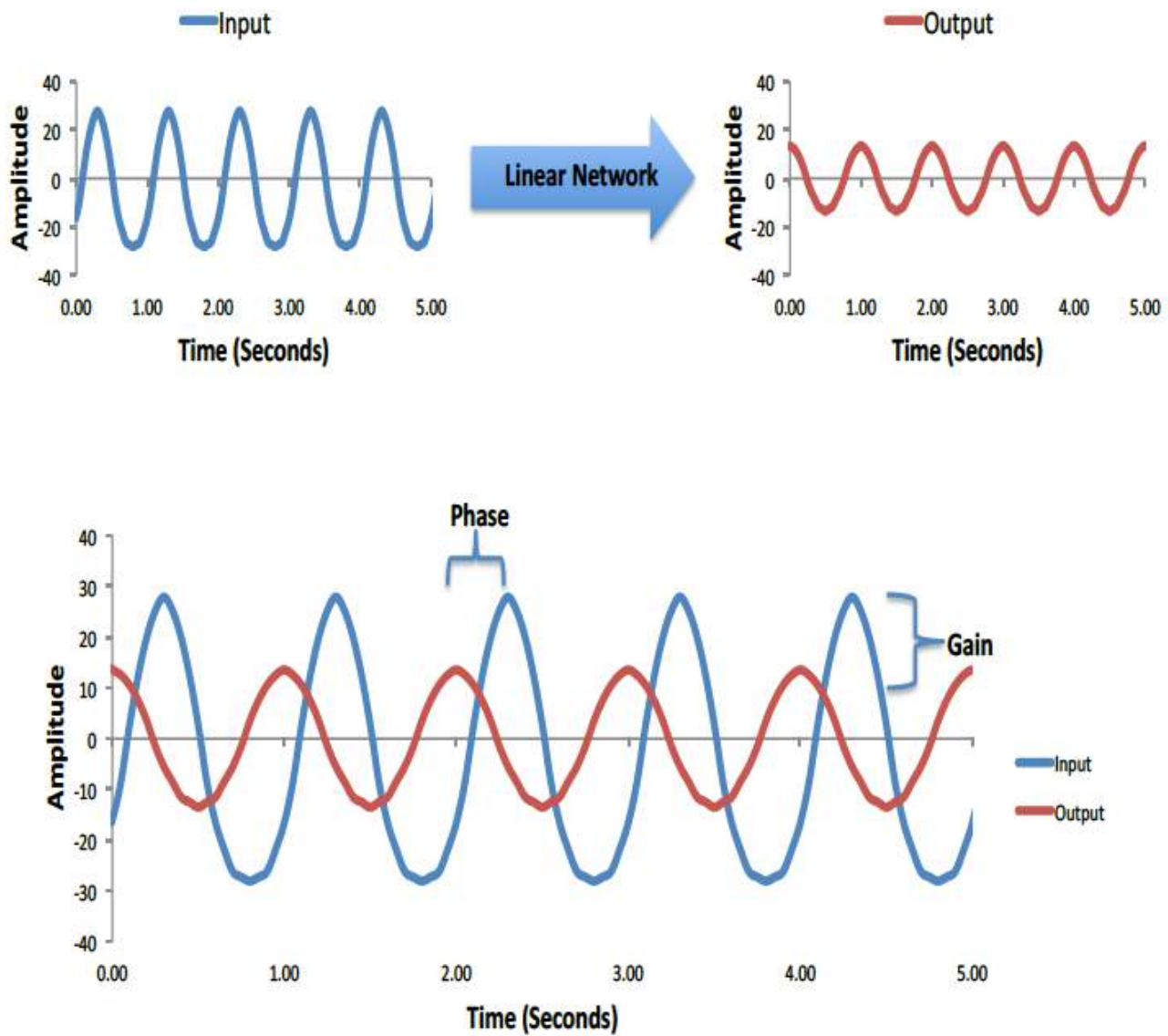


**Figure 2.6.** Example of the relationship between the input and output signals at 1 cycle per second (1 Hz), represented in the time-domain waveform for a linear system (top traces). Note: Although the overlaid signals in the bottom trace are both at 1 Hz, the processing that occurs within the linear system can lead to changes in phase (e.g. time lead of the output trace) and gain (reduction in the amplitude of the signal) at the given frequency.

### 2.2.1. Fourier transform

Before the input and output data are compared with TFA, they first must be transformed from the time-domain (seconds) into the frequency-domain (Hertz) (Figure 2.7). This process enables the identification of the signal's frequency spectrum (or power spectrum) (Figure 2.8).<sup>225</sup> The power spectrum encodes the information about the components of the frequency, phase and gain of the signal's sinusoidal waveforms. The shape of any continuous analog time-domain waveform can be recreated by a series of sinusoidal waveforms, which can be represented in the frequency-domain (Figure 2.8.).<sup>225</sup> In order for the discrete digital signal (i.e., beat-to-beat blood pressure or CBV) to be transformed from the time-domain into the frequency domain, it must first be spline interpolated (i.e., remade into a continuous waveform to provide a uniform time-base given the high degree of R-R variability). After the data is spline interpolated, it can be re-sampled at a reduced rate (in the case of this thesis the original 1000 Hz data is re-sampled to 4 Hz). This is done to smooth the data and reduce the noise in the signal. The resampling also needs to be done at a minimum rate of at least double the frequency present in the signal to avoid aliasing, which occurs when the data are under sampled (Nyquist frequency – Figure 2.9.). After the data has been resampled, the recordings are subdivided using the Welch algorithm<sup>226</sup> into five successive windows (in this thesis the Hanning windows are 100 seconds in duration and create a resolution of ~0.01 Hz) that overlap by 50%. Windowing the data creates a main lobe (centre of the smoothing window) and side lobes on either side of the main lobe. The main lobe of the window limits the frequency resolution of the window, with a narrower main lobe providing better spectral resolution but limits amplitude accuracy. The side lobes of the window can directly affect the frequency components of adjacent bins through spectral leakage. Utilizing a method where the data are

binned into successive windows, which minimizes the spectral leakage as the outer limits of the windows are overlapped. Overlapping the windows by 50% mitigates coefficient of variation within the estimates.<sup>225</sup> The Hanning window enables the optimal arrangement for maximizing frequency resolution and amplitude accuracy. Other windows could have been utilized that would create a better frequency resolution but would come at the cost of amplitude accuracy (uniform window), or could optimize amplitude accuracy at the expense of frequency resolution (flat-top window). The data within the windows are linearly detrended (which means that each window is looped on itself to create an infinite length sample).<sup>225</sup> The linearly detrended and windowed data is then passed through the Fourier transform which acts as a set of parallel filters to yield the power spectrum data (Figure 2.8. – middle traces). The power spectrum indicates the number of data points that are present within any given frequency bin and the bins are averaged across the 5 overlapped windows. The first frequency bin occurs at the direct current (0 Hz) and the last sample point is  $F_s/2 - F_s/N$  (where  $F_s$  is the sampling frequency and  $N$  is the number of samples). Initially, the power spectrum is two-sided; however, since the negative values are not utilized in the analysis, all of the positive power spectrum values (except direct current) are multiplied by 2.<sup>225</sup> This results in a power spectrum where the values are proportional to the amplitude squared of each frequency bin. The final results of the power spectrum data are now ready to be processed through the cross-spectral analysis (Figure 2.8) to yield the transfer function. The settings used for the Fourier transform utilized in this thesis meet the specifications and guidelines as outlined for signal processing by the Cerebral Autoregulation Research Network.<sup>213</sup>

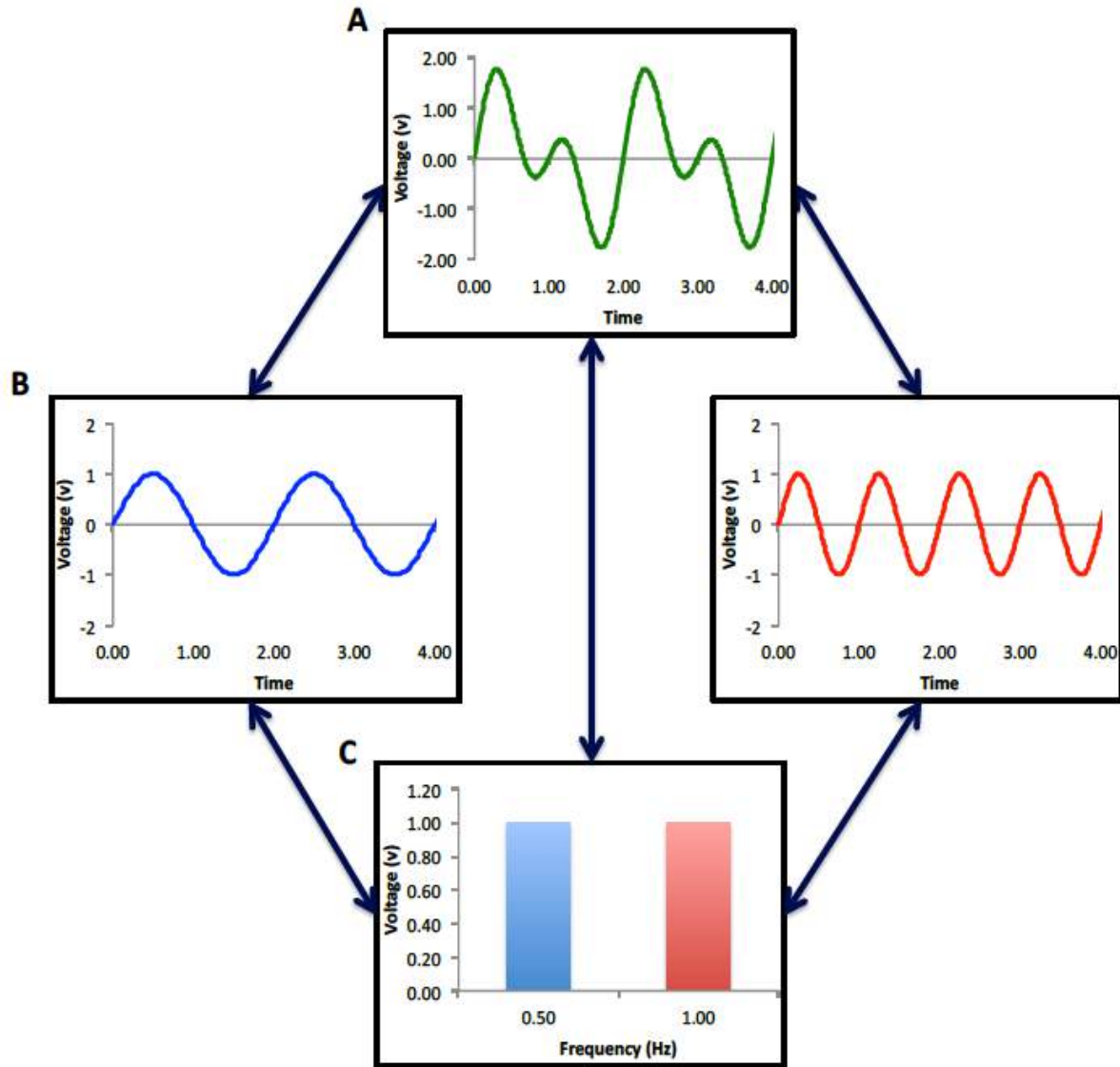


**Figure 2.7.** Example a time-domain waveform (A) that is composed of two sinusoidal waveforms (B). The frequency-domain representation (C) of the time-domain waveform (A) is represented at the bottom of the figure.

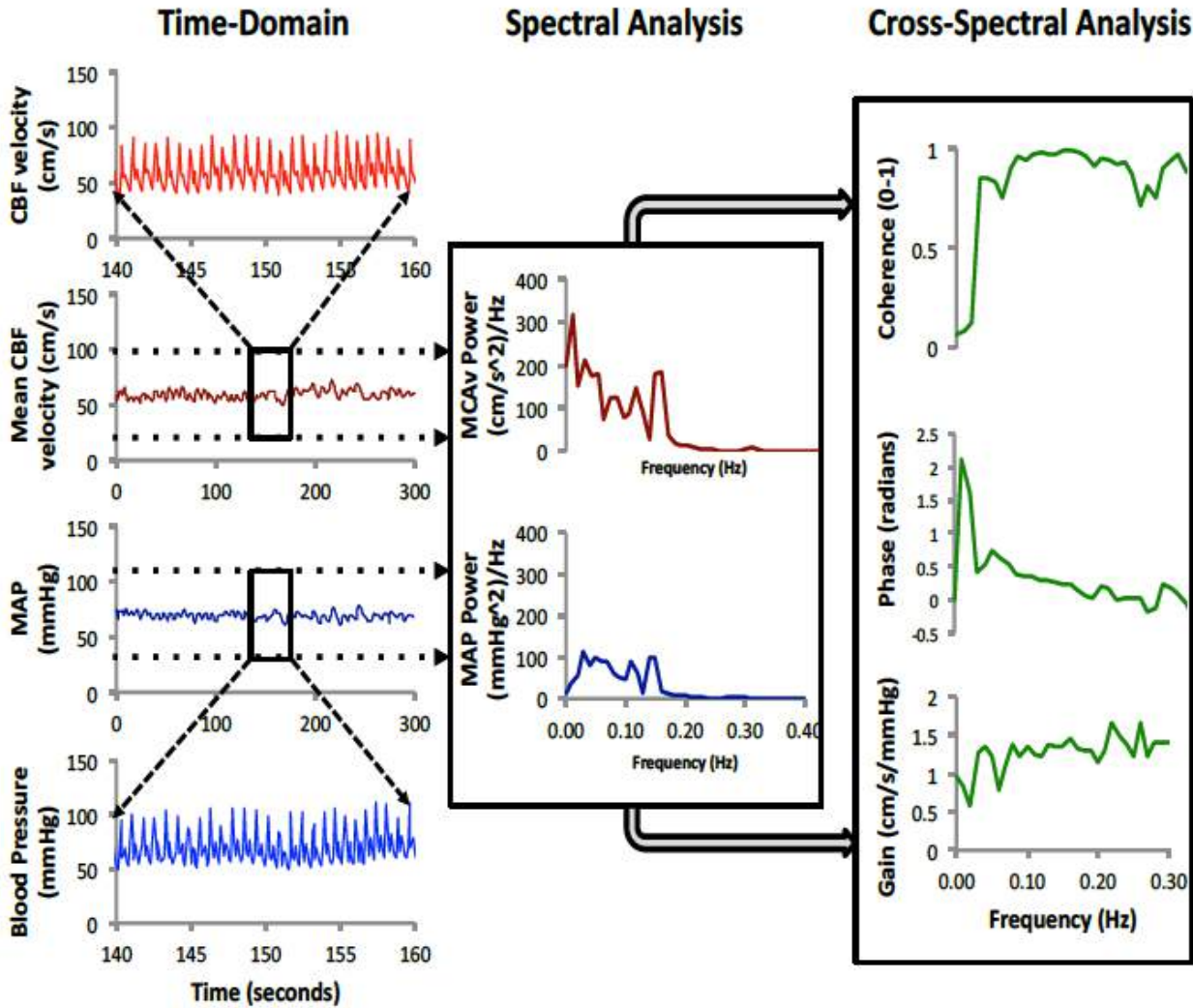


**Figure 2.8.** The velocity envelope for the cerebral blood velocity (red trace on left) and blood pressure (blue trace on left) are sampled from the R-R interval to create mean beat-to-beat data. A Fourier transform is applied to the time-domain data to create the frequency-domain spectral analysis (MCAV and MAP power spectrums in the middle trace). A cross-spectral analysis is applied to the power spectrums of the mean arterial pressure (blue trace in middle) and the cerebral blood flow velocity (middle or posterior cerebral artery; red trace in middle) to create the transfer function. The transfer function is then utilized to calculate the coherence (top green trace on right), phase (middle green trace on right) and gain (bottom green trace on right). Although the absolute values are shown in this figure the same principles can be applied to the normalized data (%), which enables the calculation of a normalized gain value from the transfer function analysis. Normalization is used when the applied interventions (e.g., between group comparisons) create changes in the either the absolute blood pressure or cerebral blood flow velocity.

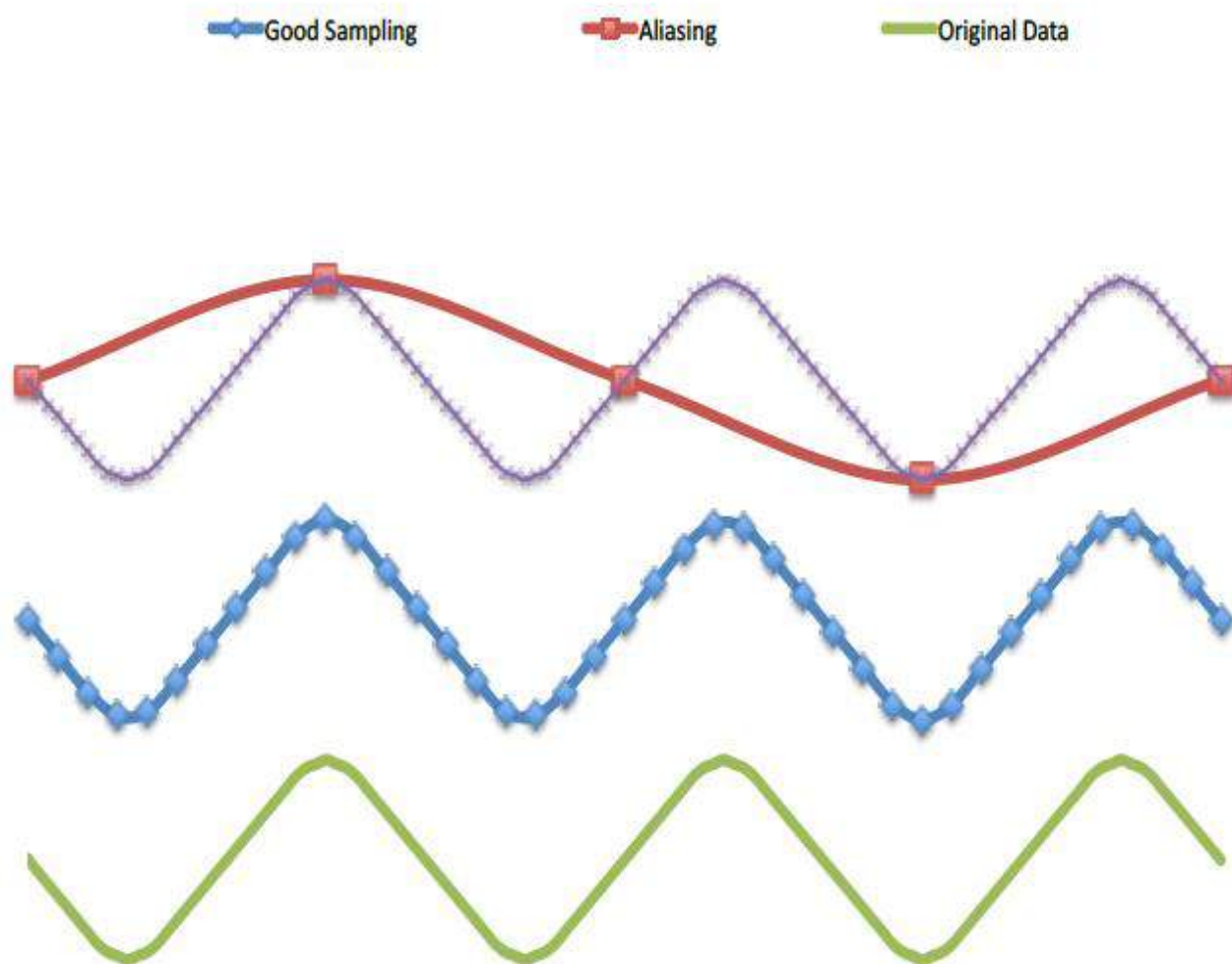


**Figure 2.9.** Example of aliasing in the data due to under sampling the signal. The resampling also needs to be done at a minimum rate of at least double the frequency present in the signal to avoid aliasing, which occurs when the data are under sampled. The original signal (green) is appropriately sampled in the middle trace (blue) but under sampled in the top trace (red) creating aliasing in the data, which confounds the interpretation of the data.

### 2.2.2. Transfer function analysis

TFA utilizes a cross-spectral analysis (Figure 2.8) to establish the relationship between two time series (blood pressure and CBF) as a function of the power spectrum frequency bins. The purpose of this analysis technique is to establish the correlation (coherence), time lag (or lead – CBF has been shown to change prior to mean arterial pressure at frequencies below 0.20 Hz. <sup>18,189,190</sup> for more details please refer to section 1.6.3.) as indexed through the phase metric, and amplitude modulation (gain) between the two signals. The cross-spectrum transfer function ( $H(f)$ ) is calculated as follows (equation 2.1):

**Equation 2.1.** 
$$H(f) = S_{AB}(f) / S_{AA}(f)$$

Where:  $H(f)$  is the transfer function;  $S_{AA}(f)$  is the autospectrum of changes in mean arterial blood pressure; and  $S_{AB}(f)$  is the cross-spectrum between the mean arterial blood pressure – and cerebral blood velocity signals.

### 2.2.3. Coherence

Coherence [ $\Upsilon^2(f)$ : Figure 2.8 – top right panel] is comparable to a squared correlation coefficient and in and of itself, the squared coherence value is utilized to index the reliability of the transfer function and can relate the linearity of the input/output relationship.<sup>18</sup> A value of 1.0 indicates a perfect correlation between the input (blood pressure) and output (CBV) variables. Whereas a value of 0.0 indicates there is no correlation between the variables. More specifically, however, this could mean that there is no relationship between input and output variables, extremely high noise in the signals, multiple inputs for a single output, or non-linearity of the relationship.<sup>18</sup> The calculation for determining the squared coherence ( $\Upsilon^2(f)$  – equation 2.2.) is as follows:

**Equation 2.2.**

$$\Upsilon^2(f) = \frac{|H(f)|^2 \times S_{AA}(f)}{S_{BB}(f)}$$

Where:  $\Upsilon^2(f)$  is the squared coherence function;  $|H(f)|$  is the transfer function magnitude;  $S_{AA}(f)$  is the autospectrum of changes in mean arterial blood pressure; and  $S_{BB}(f)$  is the autospectrum of changes in cerebral blood velocity.

Under spontaneous conditions, coherence tends to be reduced in the VLF band (0.02-0.07 Hz) and is elevated at frequencies above 0.20 Hz (for detailed explanation refer to section 1.6.3).<sup>18</sup> Mathematically, the phase and gain values for a 5-minute data collection are interpretable when coherence exceeds 0.20. This is due to the degrees of freedom present in the sampling duration (e.g. for a 15-minute sampling period, the minimum coherence would be 0.06).<sup>227</sup> However, under these circumstances although the coherence is mathematically interpretable at a level of 0.20 (or 0.06), it still means that more than 80% of input and output signals power spectra are possibly unrelated due to noise in the signals. As a result, the phase

and gain values presented in the research chapters (Chapters 3-7) are not reported when coherence is below 0.50, which is consistent with the approaches of numerous studies in the field.<sup>18,125,184,190,200</sup> Another method that can be used to enhance the coherence, and thus interpretability of the phase and gain metrics is to utilize a methodology that creates oscillations in blood pressure at the frequency of interest. Oscillating blood pressure will increase the power in the autospectra of the input signal, which in turn is passed through the cerebrovasculature in a linear fashion and results in an increase in the power of the CBV autospectra. This approach amplifies the input (and output signals), which results in a vastly improved signal-to-noise ratio and thus improves the coherence as well as the understanding of the phase and gain metrics. Numerous methods have been proposed to accomplish this task; deep breathing;<sup>196,200</sup>; OLBNP;<sup>199,203</sup>; squat-stand maneuvers;<sup>190</sup> and passive leg raises.<sup>204</sup> Of these proposed methods, the OLBNP<sup>203,228,229</sup> and squat-stand maneuvers<sup>190,230-232</sup> elicit the greatest elevations in coherence. Chapter three will provide further description and comparisons between these two methodologies. The next portion of this methodology section will highlight the physiologically interpretable metrics (phase and gain) of the cross spectral analysis (Figure 2.8).

#### **2.2.4. Phase**

The phase shift [ $\Phi(f)$ : Figure 2.8 – middle right panel] is utilized to determine how much the output signal either leads (as is the case with the cerebral pressure-flow relationship at frequencies below 0.20 Hz) or lags behind the input signal (as is the case with heart rate variability analysis). The relationship between any two sine waves can be expressed as part of a circle [therefore can be expressed in either radians (up to 6.28) or degrees (up to 360 degrees)]

and are calculated from the real and imaginary components of the complex transfer function (equation 2.3):

**Equation 2.3.** 
$$\Phi(f) = \arctangent (H(f)_I / H(f)_R)$$

Where:  $\Phi(f)$  is the phase shift;  $H(f)_I$  is the imaginary component of the transfer function; and  $H(f)_R$  is the real component of the transfer function.

The main issue with the phase metric is when wrap-around occurs – this involves the addition of large negative phase values to the real phase shift.<sup>125</sup> This typically happens when the coherence values are reduced (often this occurs within the VLF band of 0.02-0.07 Hz), as a result the actual phase value can be distorted significantly.<sup>125</sup> There are numerous methods that have been proposed to deal with the phase wrap-around, such as: only implementing the data points that are associated with a coherence above 0.50 as very few data points (<1%)<sup>125</sup> may be affected; it has also been proposed that adding 2 Pi (6.28 radians) to the large negative values could fix this issue;<sup>125</sup> however, the most robust method appears to be utilising an approach that involves oscillating blood pressure (which avoids any phase wrap-around) at the frequency of interest and sampling the subsequent point estimate value phase.<sup>189</sup>

Associated with the phase metric is the concept of phase lead. This notion indicates that the cerebrovasculature is able to respond to slow oscillations in blood flow prior to these changes occurring within the systemic vasculature. The first paper to definitively demonstrate the notion of phase lead was performed by Birch *et al.*<sup>189</sup> in 1995. In this study, they utilized squat-stand maneuvers to induce oscillations in BP and CBF at 0.05 Hz during hypocapnia (1.05 radians), eucapnia (0.80 radians) and hypercapnia (0.24 radians) [see figure 1.16]. They speculated this response was indicative of the autoregulatory mechanisms, however they noted

that the linear approach for modeling this system may not be the most appropriate to quantify the extent of the autoregulatory response as such it should be used to strictly explain the relationship as it pertains to the linear model employed.

Richard Hughson *et al.*<sup>233</sup> performed a follow-up to this initial work by Birch *et al.*,<sup>189</sup> [as well as the deep breathing studies by Diehl *et al.*,<sup>196</sup> who reported similar findings for phase lead] in order to quantify the mechanisms responsible for the phase lead. In this study they explored this phenomena via 3 components of Ohm's law (pressure, flow and resistance). Perfusion pressure was quantified via a Finapres that was height corrected to the brain, CBF was indexed via transcranial Doppler ultrasonography of the middle cerebral artery, and resistance was calculated as CPP/CBV. To enhance blood pressure variability they utilized a tilt table, which enabled them to manually tilt the subject from supine to 45 degrees head-up on 10 second cycles (with the change occurring in less than 2 seconds). It was through this methodology that they were able to demonstrate that the phase lead observed within the cerebrovasculature is indicative of the lag in the cerebrovascular resistance as it responds to an increase in CPP more slowly than a decrease in CPP. They concluded that this is likely a protective mechanism for maintaining CBF, as this mechanism provides a very valuable physiological adaptation to prevent fainting during rapid body adjustments that would otherwise alter perfusion of the cerebrovasculature. Therefore they deduced that the phase lead occurs as a result of a consequence of the phase lag associated with the changes to cerebrovascular resistance.

In 2011, Tzeng *et al.*,<sup>229</sup> took this concept even further by evaluating the role that arterial vessel compliance plays on this relationship. They employed a Windkessel model that was able to quantify the upstream capacitance of the intra- and extracranial vessels to quantify

the response of the mechanical properties of the cerebrovasculature (in addition to the current concepts associated with the myogenic tone of the vessels). In this study they were able to demonstrate that the phase lead of the cerebrovasculature is not solely related to the changes in resistance (as per Hughson et al. <sup>233</sup>) but the findings from this study indicated that the phase lead is likely a result of the upstream capacitance as the Windkessel model explained a substantial portion of the MCA variance (>80%) during both control and Ca<sup>2+</sup> blockade interventions

Thus it appears as though the phase lead is present in the cerebrovasculature mainly as a result of the upstream capacitance of the intra and extracranial vessels, with an additional influence of the cerebrovascular resistance lag. This buffering is likely present as a protective mechanism to minimize the acute affects of sudden posture changes on cerebral blood flow in order to prevent under perfusion (upon standing) and over perfusion (during a squat or Valsalva inducing maneuver).

### 2.2.5. Gain

The amplitude modulation (gain) between the blood pressure and CBV were also assessed to determine how the blood pressure waveforms were being regulated by the cerebrovasculature. The gain measure  $|H(f)|$ : [Figure 2.8 – bottom right panel] can be presented in either absolute (cm/s/mmHg), normalized to CBV (%/mmHg) or normalized to both CBV and blood pressure (%/%).<sup>125</sup> Normalizing gain to the CBV helps control for possible differences in the middle (or posterior) cerebral artery diameter between subjects and subject conditions (hypo or hypercapnia).<sup>125</sup> If the blood pressure response is changing within the study intervention then gain should be normalized to both % CBV and % mean arterial pressure changes. Gain is calculated from the real and imaginary components of the complex transfer function (Equation 2.4.) as follows:

**Equation 2.4.**

$$|H(f)| = \text{square root of } (|H(f)_I|^2 + |H(f)_R|^2)$$

Where:  $|H(f)|$  is the absolute magnitude of the transfer function;  $|H(f)_I|$  is the imaginary component of the transfer function; and  $|H(f)_R|$  is the real component of the transfer function.

### **Chapter Three: Comparison of squat-stand and oscillatory lower body negative pressure methodologies**

This study was approved by the clinical ethical committees of the Universities of British Columbia (H14-01951), and adhered to the principles of the Declaration of Helinski. All volunteers provided written informed consent and procedures were followed in accordance to institutional guidelines.

A version of this study was selected for an oral presentation at the CARNet 2015 (annual scientific meeting of the cerebral autoregulation research network). Methodological comparison of active and passive driven oscillations in blood pressure; implications for the assessment of cerebral-pressure flow relationships. Jonathan D. Smirl, Keegan Hoffman, Yu-Chieh Tzeng, Alex Hansen and Philip N. Ainslie. (2015) Jonathan Smirl was responsible for the data collection, data analysis, writing, and formatting of the abstract.

A version of this manuscript has been submitted to the *Journal of Applied Physiology* and has been resubmitted with the revisions suggested by the expert reviewers. Methodological comparison of active and passive driven oscillations in blood pressure; implications for the assessment of cerebral-pressure flow relationships. Jonathan D. Smirl, Keegan Hoffman, Yu-Chieh Tzeng, Alex Hansen and Philip N. Ainslie. (2015) Jonathan Smirl was responsible for the data collection, data analysis, writing, and formatting of the manuscript.

### **3.1. Aims and Hypotheses**

#### **Aims:**

- 1) To compare the two most common methods (active via squat-stand maneuvers; and passive via OLBNP) for increasing blood pressure variability and how they impact TFA metrics.
- 2) To compare the within subject reproducibility of the TFA metrics for both methodologies, in younger and older adults, over two measurement days separated by a minimum of 48 hours.

#### **Hypotheses:**

- 1) Squat-stand maneuvers and OLBNP will induce similar increases in TFA coherence, and thus lead to more mathematical interpretable phase and gain metrics.
- 2) The TFA phase and gain metrics associated with the squat-stand and OLBNP maneuvers will have less day-to-day variability than spontaneous measures.
- 3) Despite the decrease in CBF in the older adults, both younger and older adults will have comparable cerebral pressure-flow responses.

### 3.2. Rationale

The relationship between arterial blood pressure and cerebral blood flow (CBF) is a frequency dependent process that functions as a high-pass filter.<sup>18,125,190</sup> Higher frequency oscillations (>0.20 Hz) in blood pressure are passed along through the cerebrovasculature relatively unimpeded, whereas slower oscillations (<0.20 Hz) are adjusted and dampened by the cerebral vessels.<sup>18,125,176,190</sup> The most common method to assess this dynamic relationship is through the use of the linear mathematical approach of transfer function analysis (TFA)<sup>18,125,187,189</sup>.

Transfer function analysis provides information on metrics such as the timing of waveforms (phase)<sup>18,125,176,189,190,233</sup> and amplitude modulation (gain)<sup>18,125,187,189,190</sup> between the input (blood pressure) and output (cerebral blood velocity: CBV) signals. The coherence metric gives an indication on the reliability of the TFA and is of utmost importance when interpreting the phase and gain metrics.<sup>184</sup> For example, a high coherence (e.g. close to 1.00) indicates that the system is linear and thus the changes to phase and gain are interpretable, whereas a low coherence (<0.50) could be a result of a multitude of factors.<sup>18,125,184</sup> Namely, the low coherence could occur due to a poor signal-to-noise ratio, the system is non-linear, multiple inputs that regulate the output variable; or there is just no relationship present between the input and output variables.<sup>18</sup> As such, phase and gain values are typically not reported when coherence is below 0.50.<sup>18,125,184,190,200</sup> Although it has been noted that coherence values above 0.20 (for a specific frequency point-estimate) during a 5 minute sample can provide mathematically interpretable results,<sup>227</sup> this still means that more than 80% of input and output signals power spectra at this point-estimate are possibly unrelated due to noise in the signals or non-linearities in the relationship between blood pressure and CBV.

To address this concern, numerous methodologies to drive blood pressure (and thus improve coherence by maximizing the signal-to-noise ratio) have been proposed and include: deep breathing; <sup>196,200</sup>; oscillatory lower body negative pressure (OLBNP); <sup>185,203,228,229</sup>; squat-stand maneuvers; <sup>1-3,189,190</sup> and passive leg raises. <sup>204</sup>

Of these proposed driven methodologies, the squat-stand maneuvers<sup>1-3,189,190</sup> and OLBNP<sup>185,203,228,229</sup> elicited the greatest oscillations in blood pressure within the high-pass filter frequency range (<0.20 Hz) of the cerebrovasculature. These large swings in blood pressure not only could be used to increase the statistical reliability of the phase and gain metrics but also do so in a physiologically relevant manner i.e., the amplitude of these swings represent challenges that the cerebrovasculature endures on a daily basis – e.g. coughing, posture changes, exercise, defecation, etc.

During the squat-stand maneuvers, the squat phase engages the muscles of the legs, which increases the skeletal muscle pump and results in a large transient increase in venous return and blood pressure within 2-3 seconds (see Figure 3.1. for typical trace). Upon standing the muscles of the leg are relaxed, decreasing the pressure applied to the veins, enabling venous pooling to increase and results in a subsequent decrease in blood pressure. These large swings in mean arterial pressure (up to 40-45 mmHg) <sup>1-3</sup> are performed at frequencies within the high-pass filter range (0.05 and 0.10 Hz) and are transmitted to the cerebrovasculature. The squat-stand maneuvers elicit this response whether active or passive maneuvers are performed. <sup>234</sup> These large oscillations result in greatly increased coherence values at the frequency of interest (e.g., >0.98), which is believed to occur as a result of an improved signal-to-noise ratio. <sup>1-3,189,190</sup> During the OLBNP maneuvers, a large negative pressure (typically between -30 and -120 mmHg, depending on the size of the negative pressure box) <sup>203,228,229</sup> is rapidly

applied to the lower half of the torso and legs which increases venous pooling, thus reducing blood pressure. When the negative pressure is cycled off, the pooled venous blood returns to the heart and blood pressure is increased in a passive manner. Although the swings in blood pressure induced with oscillatory lower body negative pressure (up to 25 mmHg) <sup>228,229</sup> are not as large as those during the squat-stand maneuvers, they still can elicit large increases in coherence values (e.g., >0.90: see Figure 3.2. for typical trace). <sup>228,229</sup>

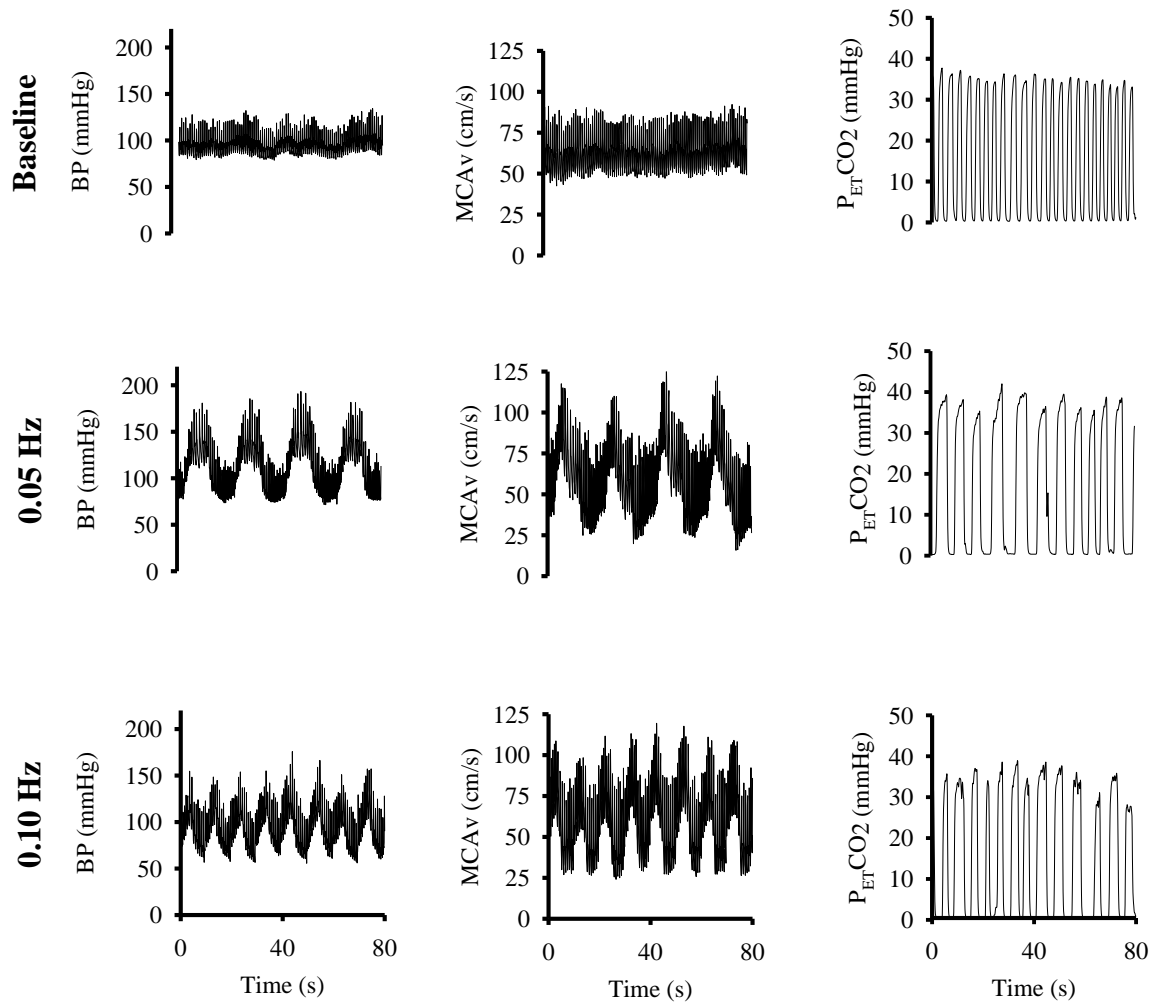


**Figure 3.1.** Typical trace for blood pressure (BP), middle cerebral artery velocity (MCAv) and end-tidal CO<sub>2</sub> (P<sub>ET</sub>CO<sub>2</sub>) during spontaneous (top), 0.05 Hz (middle) and 0.10 Hz (bottom) squat-stand maneuvers. The data are representative of one of the younger adults in the study.

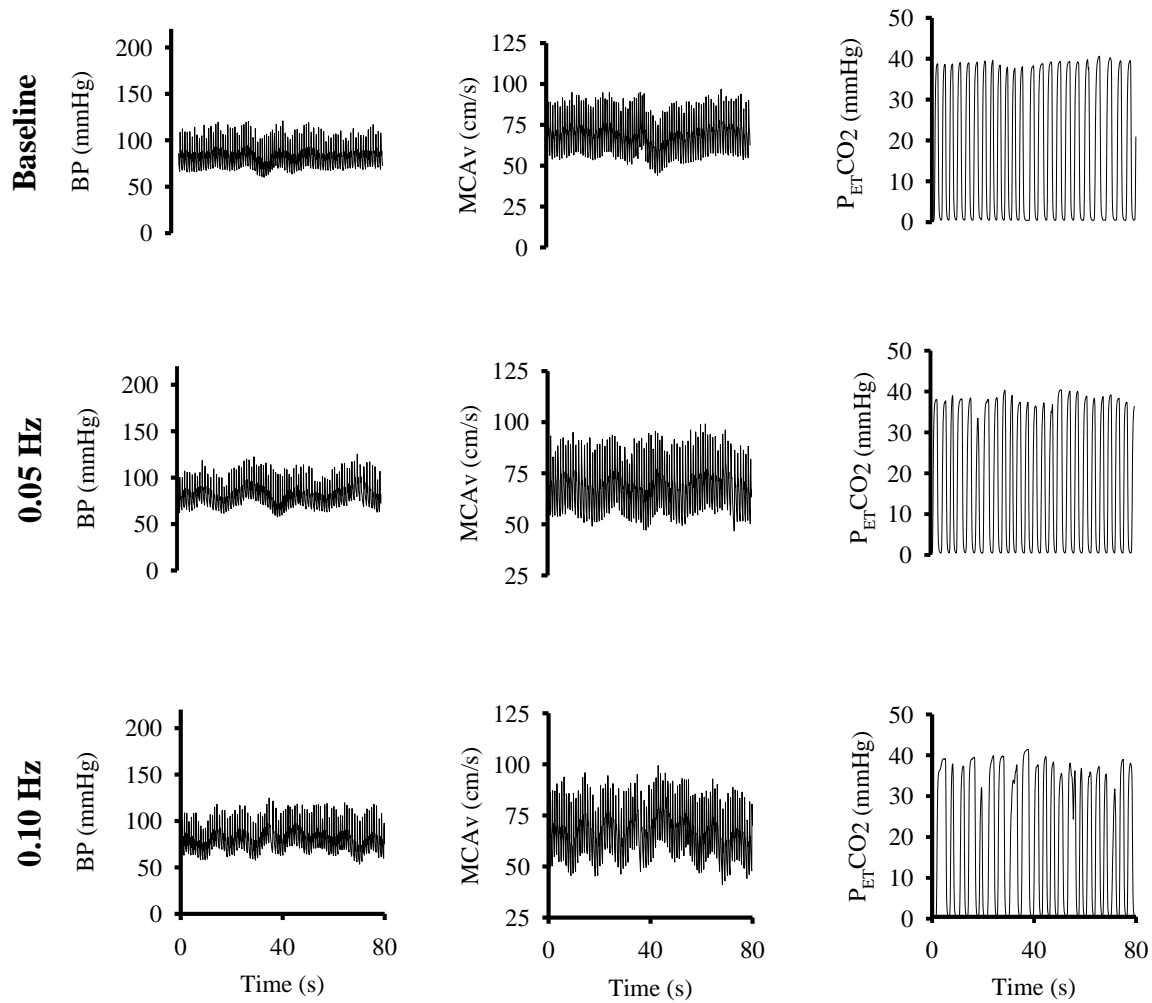


**Figure 3.2.** Typical trace for blood pressure (BP), middle cerebral artery velocity (MCAv) and end-tidal CO<sub>2</sub> (P<sub>ET</sub>CO<sub>2</sub>) during spontaneous (top), 0.05 Hz (middle) and 0.10 Hz (bottom) oscillatory lower body negative pressure maneuvers. The data are representative of one of the younger adults in the study.

To date, no study has directly compared these two driven methods within the same subjects to ensure that the reported changes in TFA metrics are comparable in the broader literature in both younger and older adult populations. This study is the first to quantifiably compare the active (squat-stand) with the passive (OLBNP) maneuvers and the first to report the repeatability of these driven measures by providing assessment across two different testing visitations. The hemodynamic challenges were induced to occur at 0.05 Hz and 0.10 Hz as these are representative of the frequency bands where cerebral autoregulation is thought to have the greatest influence on cerebral pressure-flow dynamics and are most prevalent within the literature.<sup>1-3,189,190,203,228,229</sup>

The hypotheses for this study are three-fold: 1) squat-stand and OLBNP maneuvers will induce increases in TFA coherence (as compared with spontaneous data); 2) the phase and gain metrics associated with the squat-stand and OLBNP maneuvers will have less day-to-day variability than spontaneous measures; and 3) despite the decrease in CBF within the older adult populations,<sup>51,235-237</sup> both younger and older adults will have comparable cerebral pressure-flow responses.

### **3.3. Methods**

#### *Ethical approval*

This study was approved by the clinical ethical committee of the University of British Columbia, and adhered to the principles of the Declaration of Helinski. All volunteers provided written informed consent and procedures were followed in accordance to institutional guidelines.

### *Subjects*

Ten healthy younger adult (10 male,  $24.8 \pm 2.7$  years, BMI:  $23.6 \pm 2.4$  kg/m<sup>2</sup>) and ten healthy older adult (8 male,  $66.4 \pm 3.7$  years, BMI:  $25.6 \pm 2.7$  kg/m<sup>2</sup>) subjects were recruited for this study. All subjects had a clear history of cardiorespiratory and cerebrovascular diseases and were not taking any form of medication. All older adult subjects were screened for any evidence of carotid stenosis; however, after completion of the screening process one older male adult was excluded from the study and therefore the older adult data are based on n=9. All subjects abstained from exercise, caffeine and alcoholic beverages for a period of 12 hours prior to the study. Each subject underwent a familiarization of the laboratory and testing protocols before the initiation of the protocols.

### *Experimental Protocols*

The subjects were required to visit the laboratory twice with a minimum of 48 hours to a maximum of 144 hours between visits (younger adults  $67.2 \pm 27.2$  hours; older adults  $72.0 \pm 31.7$  hours). Both visitations were performed at the same time of day and involved two hemodynamic challenge protocols (Squat-Stand and OLBNP). Prior to collecting the driven oscillatory blood pressure data the subjects began with a 5 minute seated resting period in order to obtain spontaneous baseline data. For the squat-stand maneuvers the subject began in a standing position, the subject then squatted down until the back of their legs obtained a ~90 degree angle, this position was held for a set period of time, after which they stood back up. The squat-stand cycle was performed at 2 different frequencies for 5 minutes each. The first frequency was 0.10 Hz (5 seconds squatting followed by 5 seconds standing). The second frequency was at 0.05 Hz (10 seconds squatting followed by 10 seconds standing). These

frequencies were selected as they are within the range where cerebral autoregulation is thought to have its greatest influence on the cerebral pressure-flow dynamics<sup>18</sup>. During the OLBNP maneuvers, the subject was in a supine position in industrially designed pressure boxes that sealed at their waist and were held in place via a mounted bicycle seat to prevent movement into the OLBNP box. The straps used to seal the participants in the OLBNP box did not interfere with their breathing patterns. Prior to initiating the OLBNP, a 5 minute resting period at 0 mmHg was performed to collect baseline data. The pressure in the box was then oscillated between -50 mmHg and 0 mmHg at 0.10 Hz (5 seconds at -50 mmHg followed by 5 seconds at 0 mmHg). This process was then repeated at a frequency of 0.05 Hz (10 seconds at -50 mmHg followed by 10 seconds at 0 mmHg). The -50 mmHg pressure change occurred within 1.5 seconds. The -50 mmHg pressure was selected to match the pressure generated in the steady-state findings of Formes *et al.*,<sup>238</sup> who tested a similarly aged population ( $68 \pm 1$  year) at a negative pressure of -50 mmHg. The results from this study revealed that this level of negative pressure is well tolerated in older individuals. The order of the 0.05 Hz and 0.10 Hz trials were randomly selected for both the squat-stand and OLBNP maneuvers.

### *Instrumentation*

In this study both the right and left middle cerebral arteries were insonated. Blood pressure was monitored with finger photoplethysmography. 3-lead electrocardiography was utilized to monitor R-R intervals. End-tidal gases were monitored with a gas analyzer. Please refer to sections 2.1. for more detail about these instruments.

### *Data Processing*

Please refer to section 2.2. (signal processing)

### *Power spectrum and transfer function analysis*

Please refer to section 2.2.1. (Fourier transform); 2.2.2. (transfer function analysis); 2.2.3. (coherence); 2.2.4. (phase); and 2.2.5. (gain) for more detail about these measures.

### *Within-subject coefficient of variation*

The relationship between arterial blood pressure and CBV is bound to be variable as there are many other physiological variables that can influence CBV.<sup>239</sup> This can confound the interpretation of the relationship between arterial blood pressure and CBV in terms of cerebral autoregulation, as the separation of random error from true physiological variability is difficult.<sup>239</sup> As such, this study was not designed to examine the intricacies of cerebral autoregulation *per se*, but is merely designed to determine the level of reproducibility via the within-subject coefficient of variation (CoV) for linear TFA metrics. In other fields, many authors have utilized the within-subject CoV as an indication of *good* reproducibility (<10%) and *reasonable variability* for reproducibility (<20%).<sup>240-242</sup> These cut-off points were applied to the findings in this study as a way to indicate which method had the least variability between measurement days, and thus the highest level of reproducibility within the findings. It has also been shown that the within-subject CoV has been shown to be a useful index for the reliability of very small sample sizes (N = 5)<sup>243,244</sup> and for comparisons between metrics with different scales.<sup>245</sup>

### *Statistical Analysis*

Statistical analyses were performed using SPSS version 20.0. The within-subject CoV was calculated to determine testing day-to-day reproducibility of the mean arterial pressure, left and right middle cerebral artery velocities,  $P_{ET}CO_2$ , and heart rate. Additionally, the Fourier transform power spectrums for mean arterial pressure and CBV, and TFA coherence, phase, gain, and normalized gain metrics CoV were also used to determine day-to-day reproducibility. Bland-Altman plots were constructed to demonstrate the bias in significant differences between squat-stand and oscillatory lower body negative pressure maneuvers.<sup>246</sup> A paired t-test was performed to determine the effect of CoV on modality (upright vs supine; or OLBNP vs squat-stand). A multivariate two-way ANOVA was conducted to examine the effect of age, and day on the cerebral pressure-flow relationship. Bivariate correlations were performed between cerebrovascular resistance index and driven TFA metrics. Data are presented as mean  $\pm$  SD. Significance was set a priori at  $P < 0.05$ .

### 3.4. Results

#### *Hemodynamic and cerebrovascular responses (Table 3.1.)*

The older adults had a significantly higher resting heart rate and mean arterial pressure, and lower  $P_{ET}CO_2$  and middle cerebral artery velocity as compared to the younger adults. There were no significantly different hemodynamic or cerebrovascular responses from day 1 to day 2 in either younger or older adult populations and all assessed measures revealed good CoV reproducibility (<10%). However, after the posture change from upright to supine,  $P_{ET}CO_2$  universally rose by ~2 mmHg ( $P<0.05$ ) which resulted in an increase in middle cerebral artery velocity of ~10% ( $P<0.005$ ) and a ~9% reduction in CVRi ( $P<0.05$ ).

**Table 3.1.** Hemodynamic and cerebrovascular responses during spontaneous baselines

	Day1	Day 2	Between-Day CoV (%)
<b>Upright – Younger Adults</b>			
Mean Arterial Pressure (mmHg)	85.4 ± 14.1	82.7 ± 10.1	5.5 ± 4.4
Left MCAv (cm/s)	58.9 ± 2.7	59.4 ± 2.6	1.9 ± 1.6
Right MCAv (cm/s)	58.4 ± 5.9	57.4 ± 5.9	3.5 ± 3.1
Heart Rate (bpm)	67.4 ± 13.3	67.4 ± 13.1	4.7 ± 3.5
End-Tidal PCO <sub>2</sub> (mmHg)	37.9 ± 2.0	38.2 ± 2.3	1.8 ± 1.9
<b>Supine – Younger Adults</b>			
Mean Arterial Pressure (mmHg)	83.9 ± 9.9	82.5 ± 9.9	5.7 ± 4.3
Left MCAv (cm/s)	66.9 ± 6.4*	66.6 ± 4.7*	3.3 ± 2.1
Right MCAv (cm/s)	64.1 ± 9.2*	63.2 ± 9.2*	4.3 ± 2.6
Heart Rate (bpm)	61.5 ± 13.2	59.2 ± 11.5	4.4 ± 5.3
End-Tidal PCO <sub>2</sub> (mmHg)	39.7 ± 2.6*	39.5 ± 2.6*	1.4 ± 1.1
<b>Upright – Older Adults</b>			
Mean Arterial Pressure (mmHg)	99.5 ± 13.4†	100.7 ± 10.0†	2.6 ± 1.6
Left MCAv (cm/s)	50.0 ± 9.9†	48.4 ± 9.3†	6.0 ± 3.3
Right MCAv (cm/s)	52.2 ± 6.6†	52.1 ± 6.7†	5.4 ± 3.7
Heart Rate (bpm)	70.5 ± 14.0	67.6 ± 12.4	6.4 ± 6.0
End-Tidal PCO <sub>2</sub> (mmHg)	34.3 ± 3.1†	35.6 ± 3.0†	3.0 ± 2.4
<b>Supine – Older Adults</b>			
Mean Arterial Pressure (mmHg)	107.5 ± 17.1†	106.9 ± 14.6†	4.3 ± 2.4
Left MCAv (cm/s)	52.1 ± 8.5*†	47.4 ± 4.8*†	7.2 ± 5.3
Right MCAv (cm/s)	55.3 ± 7.6*†	56.4 ± 5.7*†	4.3 ± 2.4
Heart Rate (bpm)	69.1 ± 13.3	73.8 ± 17.1	4.2 ± 4.2
End-Tidal PCO <sub>2</sub> (mmHg)	37.1 ± 2.5*†	37.0 ± 3.0*†	2.1 ± 1.3

Values are means ± SD. Coefficient of variation (CoV); middle cerebral artery velocity (MCAv). Good reproducibility (<10%); reasonable reproducibility (10-20%).<sup>240</sup> Statistical significance was set at  $P < 0.05$ . Note: there were no significant differences from day 1 to day 2. \*denotes different from upright condition; †denotes different from younger adults.

### *Fourier and Transfer Function Analysis*

*Power Spectrum:* Under spontaneous conditions there were relatively low average power spectrums in the VLF and LF ranges for both the mean arterial pressure ( $<12.00$  mmHg<sup>2</sup>) and middle cerebral artery velocity ( $<11.00$  cm<sup>2</sup>/s<sup>2</sup>) throughout aging (Table 3.2. and 3.3.). These reduced input levels were enhanced dramatically when the oscillations in blood pressure were induced. The power spectrum of mean arterial pressure was increased ~100-500 fold in the squat-stand maneuvers, and ~15-80 fold during the oscillatory lower body negative pressure maneuvers (Figures 3.3. and 3.4.). These increases in the input signal of the cerebral pressure-flow response are reflected in the output signal (middle cerebral artery power spectrum) with a ~100-300 fold increase during squat-stand maneuvers and ~5-35 fold increase with oscillations in lower body negative pressure (Figures 3.3. and 3.4.).

*Coherence:* During the spontaneous conditions, there was a relatively low average coherence values in the VLF (younger:  $0.44 \pm 0.16$ ; older:  $0.45 \pm 0.15$ ) and LF (younger:  $0.69 \pm 0.15$ ; older:  $0.65 \pm 0.17$ ) ranges (Tables 3.2. and 3.3.). However, these relatively low coherence values were dramatically increased with the increase in input and output signal strength during driven oscillations in blood pressure. During squat-stand maneuvers, both frequencies resulted in a coherence of 0.99-1.00 regardless of age. The oscillatory lower body negative pressure maneuvers increased coherence values to ~0.89 (younger) and ~0.94 (older) at 0.05 Hz and  $>0.95$  at 0.10 Hz (regardless of age: Tables 3.4. and 3.5.). The proportional biases between the two modalities in both frequencies are illustrated in Figures 3.5. and 3.6.

**Table 3.2.** Transfer function analysis of spontaneous data between MAP and MCAv under upright and supine conditions in younger adults measured on Day 1 and Day 2. Reproducibility is calculated for between-day within subject coefficient of variations.

	Day1	Day 2	Between-Day CoV (%)
<b>Spontaneous Upright</b>			
VLF MAP Power (mmHg <sup>2</sup> )	11.47 ± 8.67	8.78 ± 4.44	39.5 ± 24.9
LF MAP Power (mmHg <sup>2</sup> )	7.25 ± 5.89	7.20 ± 3.55	44.0 ± 29.9
VLF MCAv Power (cm/s) <sup>2</sup>	10.75 ± 6.92	7.92 ± 6.40	37.7 ± 20.3
LF MCAv Power (cm/s) <sup>2</sup>	7.08 ± 3.91	6.83 ± 3.50	30.2 ± 30.8
VLF Coherence	0.47 ± 0.15	0.52 ± 0.13	16.2 ± 12.5
LF Coherence	0.74 ± 0.14	0.78 ± 0.12	8.4 ± 8.4
VLF Phase (radians)	0.89 ± 0.37	0.92 ± 0.47	24.5 ± 24.2
LF Phase (radians)	0.53 ± 0.25	0.64 ± 0.26	30.3 ± 24.6
VLF Gain (cm/s/mm Hg)	0.85 ± 0.33	0.78 ± 0.22	26.5 ± 13.7
LF Gain (cm/s/mm Hg)	1.07 ± 0.18	0.99 ± 0.17	17.6 ± 9.6
VLF Gain (%/%)	1.21 ± 0.44	1.08 ± 0.42	30.2 ± 14.6
LF Gain (%/%)	1.55 ± 0.34	1.38 ± 0.43	22.2 ± 11.7
<b>Spontaneous Supine</b>			
VLF MAP Power (mmHg <sup>2</sup> )	8.78 ± 5.21	5.90 ± 3.00	47.7 ± 30.6
LF MAP Power (mmHg <sup>2</sup> )	2.96 ± 2.34*	2.93 ± 1.35*	43.3 ± 28.6
VLF MCAv Power (cm/s) <sup>2</sup>	10.49 ± 7.13	7.43 ± 4.15	38.3 ± 23.3
LF MCAv Power (cm/s) <sup>2</sup>	4.44 ± 2.94*	4.30 ± 1.98*	29.0 ± 20.4
VLF Coherence	0.44 ± 0.17	0.35 ± 0.16	30.4 ± 24.3*
LF Coherence	0.62 ± 0.14*	0.65 ± 0.14*	17.2 ± 9.2*
VLF Phase (radians)	1.07 ± 0.60	0.76 ± 0.60	26.4 ± 22.1
LF Phase (radians)	0.50 ± 0.30	0.54 ± 0.29	31.9 ± 24.9
VLF Gain (cm/s/mmHg)	0.94 ± 0.25*	1.14 ± 0.36*	21.5 ± 18.8
LF Gain (cm/s/mmHg)	1.31 ± 0.40*	1.32 ± 0.32*	13.7 ± 9.0
VLF Gain (%/%)	1.15 ± 0.27	1.45 ± 0.78	21.9 ± 25.9
LF Gain (%/%)	1.68 ± 0.65	1.67 ± 0.54	16.6 ± 12.9

Values are means ± SD. Coefficient of variation (CoV); mean arterial pressure (MAP); middle cerebral artery velocity (MCAv); low frequency (LF); very low frequency (VLF). Good reproducibility (<10%); reasonable reproducibility (10-20%).<sup>240</sup> Statistical significance was set at  $P < 0.05$ . Note there were no significant differences from day 1 to day 2. \*denotes significantly different from upright condition.

**Table 3.3.** Transfer function analysis of spontaneous data between MAP and MCAv under upright and supine conditions in older adults measured on Day 1 and Day 2. Reproducibility is calculated for between-day within subject coefficient of variations.

	Day1	Day 2	Between-Day CoV (%)
<b>Spontaneous Upright</b>			
VLF MAP Power (mmHg <sup>2</sup> )	7.81 ± 6.76	5.26 ± 3.83	54.5 ± 29.0
LF MAP Power (mmHg <sup>2</sup> )	4.59 ± 7.77	4.01 ± 3.22	42.8 ± 41.6
VLF MCAv Power (cm/s) <sup>2</sup>	5.91 ± 2.38	4.72 ± 1.16	24.2 ± 20.8
LF MCAv Power (cm/s) <sup>2</sup>	3.78 ± 4.62	4.65 ± 3.61	40.4 ± 33.2
VLF Coherence	0.55 ± 0.13	0.47 ± 0.07	19.2 ± 11.6
LF Coherence	0.66 ± 0.21	0.74 ± 0.21	17.9 ± 16.9
VLF Phase (radians)	1.04 ± 0.50	0.87 ± 0.35	31.6 ± 22.7
LF Phase (radians)	0.73 ± 0.43	0.47 ± 0.13	35.6 ± 26.5
VLF Gain (cm/s/mm Hg)	0.81 ± 0.31	0.84 ± 0.23	24.4 ± 14.9
LF Gain (cm/s/mm Hg)	0.97 ± 0.21	1.12 ± 0.31	15.3 ± 8.8
VLF Gain (%/%)	1.45 ± 0.56	1.59 ± 0.36	22.3 ± 15.1
LF Gain (%/%)	1.76 ± 0.40	2.11 ± 0.38	17.8 ± 7.9
<b>Spontaneous Supine</b>			
VLF MAP Power (mmHg <sup>2</sup> )	4.34 ± 3.10	4.86 ± 3.16	39.8 ± 25.4
LF MAP Power (mmHg <sup>2</sup> )	1.47 ± 0.67*	1.98 ± 1.04*	27.8 ± 16.6
VLF MCAv Power (cm/s) <sup>2</sup>	6.22 ± 3.50	7.95 ± 6.36	30.0 ± 26.1
LF MCAv Power (cm/s) <sup>2</sup>	1.83 ± 0.82	1.83 ± 0.72	25.8 ± 16.3
VLF Coherence	0.40 ± 0.18	0.37 ± 0.13	28.6 ± 14.0
LF Coherence	0.58 ± 0.16	0.61 ± 0.18	17.2 ± 12.3
VLF Phase (radians)	0.88 ± 0.38	1.03 ± 0.45	47.7 ± 33.0*
LF Phase (radians)	0.58 ± 0.28	0.62 ± 0.24	26.7 ± 19.3
VLF Gain (cm/s/mmHg)	0.98 ± 0.26	1.05 ± 0.54	27.0 ± 13.0
LF Gain (cm/s/mmHg)	1.14 ± 0.31	1.08 ± 0.35	16.6 ± 10.4
VLF Gain (%/%)	1.61 ± 0.50	1.90 ± 1.08	28.7 ± 9.7
LF Gain (%/%)	1.95 ± 0.37	1.92 ± 0.49	17.1 ± 10.9

Values are means ± SD. Coefficient of variation (CoV); mean arterial pressure (MAP); middle cerebral artery velocity (MCAv); low frequency (LF); very low frequency (VLF). Good reproducibility (<10%); reasonable reproducibility (10-20%).<sup>240</sup> Statistical significance was set at  $P < 0.05$ . \*denotes significantly different from upright condition.

**Table 3.4.** Transfer function analysis of driven data between MAP and MCAv under upright and supine conditions in younger adults measured on Day 1 and Day 2. Reproducibility is calculated for between-day within subject coefficient of variations.

	Day1	Day 2	Between-Day CoV (%)
<b>Squat-Stand maneuvers</b>			
0.05 Hz MAP Power (mmHg <sup>2</sup> )/Hz	20252 ± 11679	17186 ± 7995	23.8 ± 21.1
0.10 Hz MAP Power (mmHg <sup>2</sup> )/Hz	17036 ± 7300	13847 ± 7520	42.8 ± 32.4
0.05 Hz MCAv Power (cm/s) <sup>2</sup> /Hz	12110 ± 7954	9447 ± 4956	31.8 ± 20.7
0.10 Hz MCAv Power (cm/s) <sup>2</sup> /Hz	16892 ± 7261	14691 ± 8481	33.0 ± 17.7
0.05 Hz Coherence	0.99 ± 0.01	0.99 ± 0.00	0.5 ± 0.5
0.10 Hz Coherence	1.00 ± 0.00	1.00 ± 0.00	0.1 ± 0.1
0.05 Hz Phase (radians)	0.62 ± 0.23	0.64 ± 0.24	15.2 ± 12.5
0.10 Hz Phase (radians)	0.31 ± 0.14	0.35 ± 0.23	15.3 ± 10.8
0.05 Hz Gain (cm/s/mm Hg)	0.78 ± 0.17	0.74 ± 0.12	16.9 ± 9.0
0.10 Hz Gain (cm/s/mm Hg)	1.01 ± 0.17	1.01 ± 0.15	14.4 ± 11.8
0.05 Hz Gain (%/%)	1.16 ± 0.22	1.06 ± 0.12	15.1 ± 11.1
0.10 Hz Gain (%/%)	1.49 ± 0.28	1.51 ± 0.38	16.9 ± 12.7
<b>Oscillatory Lower Body Negative Pressure</b>			
0.05 Hz MAP Power (mmHg <sup>2</sup> )/Hz	934 ± 616*	944 ± 649*	53.2 ± 41.7
0.10 Hz MAP Power (mmHg <sup>2</sup> )/Hz	804 ± 486*	727 ± 480*	42.8 ± 32.4
0.05 Hz MCAv Power (cm/s) <sup>2</sup> /Hz	412 ± 300*	412 ± 247*	36.3 ± 28.1
0.10 Hz MCAv Power (cm/s) <sup>2</sup> /Hz	671 ± 576*	501 ± 332*	33.0 ± 17.7
0.05 Hz Coherence	0.85 ± 0.12*	0.74 ± 0.17*	16.5 ± 18.4*
0.10 Hz Coherence	0.97 ± 0.03*	0.90 ± 0.19*	2.6 ± 2.8*
0.05 Hz Phase (radians)	1.54 ± 0.57*	1.66 ± 0.69*	34.1 ± 22.8*
0.10 Hz Phase (radians)	0.65 ± 0.34*	0.64 ± 0.43*	36.2 ± 28.3*
0.05 Hz Gain (cm/s/mmHg)	0.67 ± 0.29*	0.58 ± 0.22*	22.7 ± 19.5
0.10 Hz Gain (cm/s/mmHg)	0.87 ± 0.29*	0.82 ± 0.22*	19.5 ± 13.9
0.05 Hz Gain (%/%)	0.90 ± 0.41*	0.70 ± 0.23*	24.6 ± 19.6
0.10 Hz Gain (%/%)	1.13 ± 0.29*	1.10 ± 0.34*	23.1 ± 15.1

Values are means ± SD. Coefficient of variation (CoV); mean arterial pressure (MAP); middle cerebral artery velocity (MCAv). Good reproducibility (<10%); reasonable reproducibility (10-20%).<sup>240</sup> Statistical significance was set at  $P < 0.05$ . Note: there were no significant differences from day 1 to day 2, nor between younger and older adults. \*denotes significantly different from squat-stand maneuvers.

**Table 3.5.** Transfer function analysis of driven data between MAP and MCAv under upright and supine conditions in older adults measured on Day 1 and Day 2. Reproducibility is calculated for between-day within subject coefficient of variations.

	Day1	Day 2	Between-Day CoV (%)
<b>Squat-Stand maneuvers</b>			
0.05 Hz MAP Power (mmHg <sup>2</sup> )/Hz	16801 ± 13821	13329 ± 12044	35.6 ± 22.3
0.10 Hz MAP Power (mmHg <sup>2</sup> )/Hz	5173 ± 3225	8067 ± 6983	32.8 ± 36.2
0.05 Hz MCAv Power (cm/s) <sup>2</sup> /Hz	5572 ± 4813	8029 ± 7354	50.0 ± 30.1
0.10 Hz MCAv Power (cm/s) <sup>2</sup> /Hz	3549 ± 1898	6547 ± 4989	37.2 ± 38.4
0.05 Hz Coherence	0.99 ± 0.01	0.99 ± 0.00	0.7 ± 0.6
0.10 Hz Coherence	0.99 ± 0.01	1.00 ± 0.00	0.5 ± 0.6
0.05 Hz Phase (radians)	0.75 ± 0.21	0.70 ± 0.13	7.5 ± 4.9
0.10 Hz Phase (radians)	0.39 ± 0.17	0.35 ± 0.12	19.4 ± 11.0
0.05 Hz Gain (cm/s/mm Hg)	0.69 ± 0.22	0.85 ± 0.23	17.9 ± 15.7
0.10 Hz Gain (cm/s/mm Hg)	0.87 ± 0.24	0.98 ± 0.23	10.0 ± 10.9
0.05 Hz Gain (%/%)	1.28 ± 0.38	1.67 ± 0.48	18.4 ± 10.8
0.10 Hz Gain (%/%)	1.69 ± 0.38	2.00 ± 0.47	14.4 ± 9.2
<b>Oscillatory Lower Body Negative Pressure</b>			
0.05 Hz MAP Power (mmHg <sup>2</sup> )/Hz	1567 ± 2289*	1845 ± 2178*	31.5 ± 28.3
0.10 Hz MAP Power (mmHg <sup>2</sup> )/Hz	661 ± 492*	1311 ± 2087*	49.2 ± 45.2
0.05 Hz MCAv Power (cm/s) <sup>2</sup> /Hz	403 ± 409*	722 ± 1070*	45.5 ± 35.3
0.10 Hz MCAv Power (cm/s) <sup>2</sup> /Hz	209 ± 240*	786 ± 1370*	62.9 ± 40.4
0.05 Hz Coherence	0.89 ± 0.11*	0.90 ± 0.10*	7.1 ± 8.5*
0.10 Hz Coherence	0.90 ± 0.10*	0.89 ± 0.13*	7.1 ± 10.8*
0.05 Hz Phase (radians)	1.31 ± 0.41*	1.09 ± 0.50*	28.1 ± 15.1*
0.10 Hz Phase (radians)	0.57 ± 0.41*	0.65 ± 0.41*	47.6 ± 38.7*
0.05 Hz Gain (cm/s/mmHg)	0.52 ± 0.13*	0.61 ± 0.15*	22.8 ± 19.0
0.10 Hz Gain (cm/s/mmHg)	0.66 ± 0.33*	0.76 ± 0.45*	51.3 ± 28.4*
0.05 Hz Gain (%/%)	0.93 ± 0.29*	1.07 ± 0.32*	22.0 ± 26.2
0.10 Hz Gain (%/%)	1.14 ± 0.55*	1.32 ± 0.75*	48.7 ± 34.8*

Values are means ± SD. Coefficient of variation (CoV); mean arterial pressure (MAP); middle cerebral artery velocity (MCAv). Good reproducibility (<10%); reasonable reproducibility (10-20%).<sup>240</sup> Statistical significance was set at  $P < 0.05$ . Note: there were no differences in between-day results, nor between younger and older adults. \*denotes significantly different from squat-stand maneuvers.

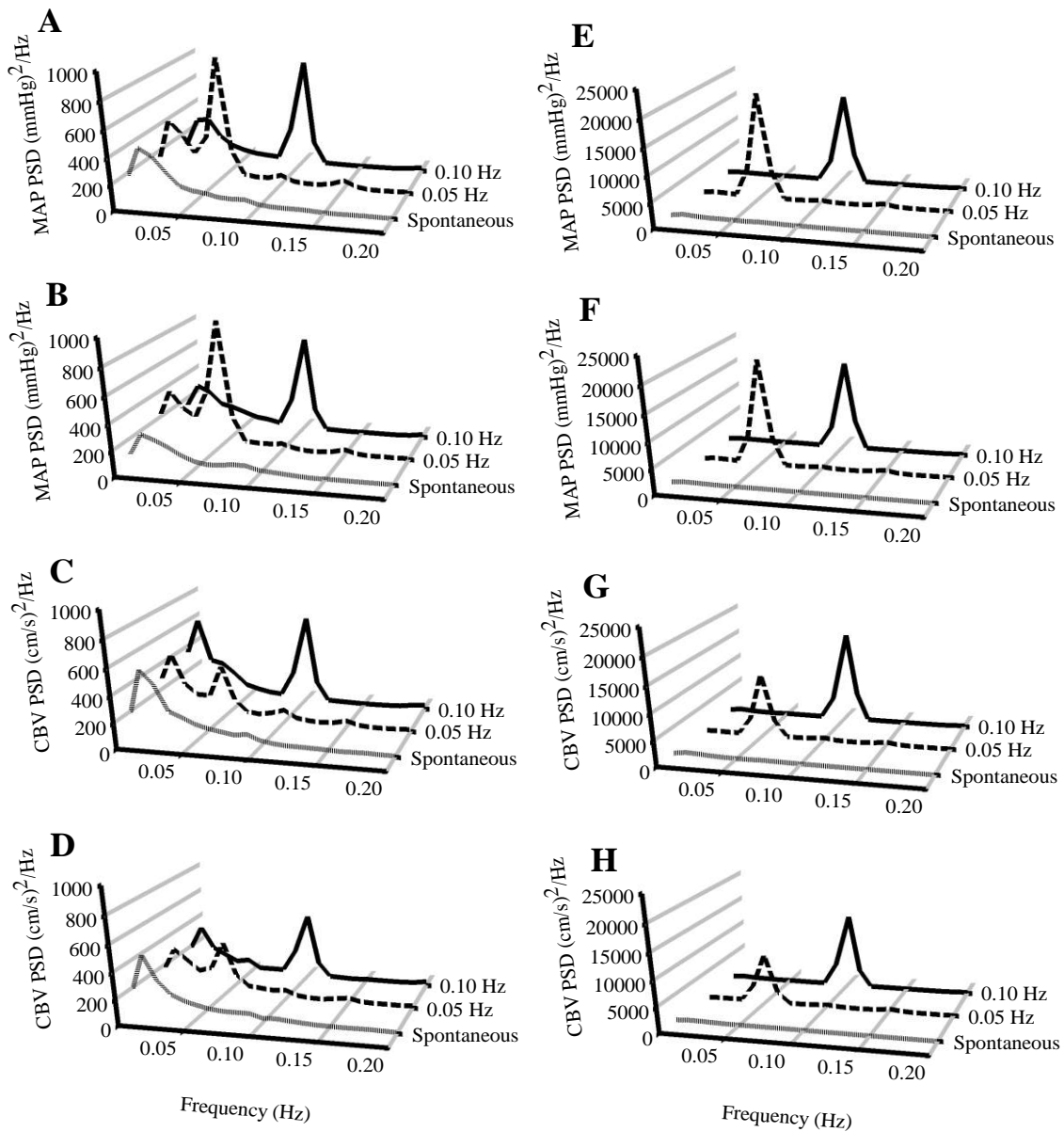


**Figure 3.3.** Absolute values of the power spectrum densities (PSD) for the mean arterial pressure (MAP) and cerebral blood velocity (CBV) in younger adults under spontaneous (grey), 0.05 Hz (dashed) and 0.10 Hz (black) conditions. The PSD during the oscillatory lower body negative pressure maneuvers are represented on the left side (A-D) and squat-stand maneuvers are on the right side (E-H). The PSD for the Day 1 measures are represented in traces A, C, E and G), with Day 2 measures represented in traces (B, D, F and H). Note there were no significant differences between Day 1 and Day 2, for standard deviation values refer to tables 3.2. and 3.4.

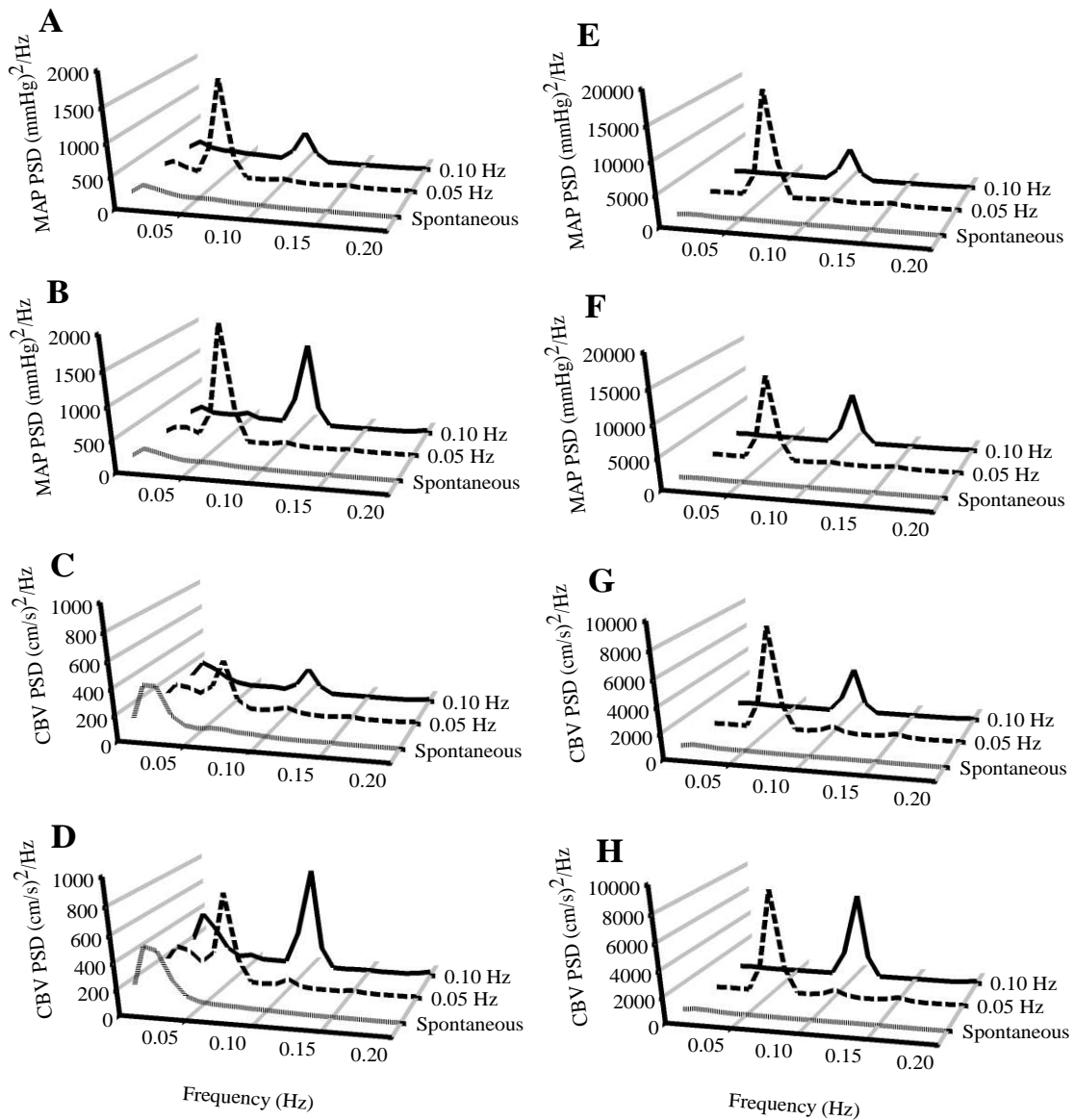


**Figure 3.4.** Absolute values of the power spectrum densities (PSD) for the mean arterial pressure (MAP) and cerebral blood velocity (CBV) in older adults under spontaneous (grey), 0.05 Hz (dashed) and 0.10 Hz (black) conditions. The PSD during the oscillatory lower body negative pressure maneuvers are represented on the left side (A-D) and squat-stand maneuvers are on the right side (E-H). The PSD for the Day 1 measures are represented in traces A, C, E and G), with Day 2 measures represented in traces (B, D, F and H). Note there were no significant differences between Day 1 and Day 2, for standard deviation values refer to tables 3.3. and 3.5.

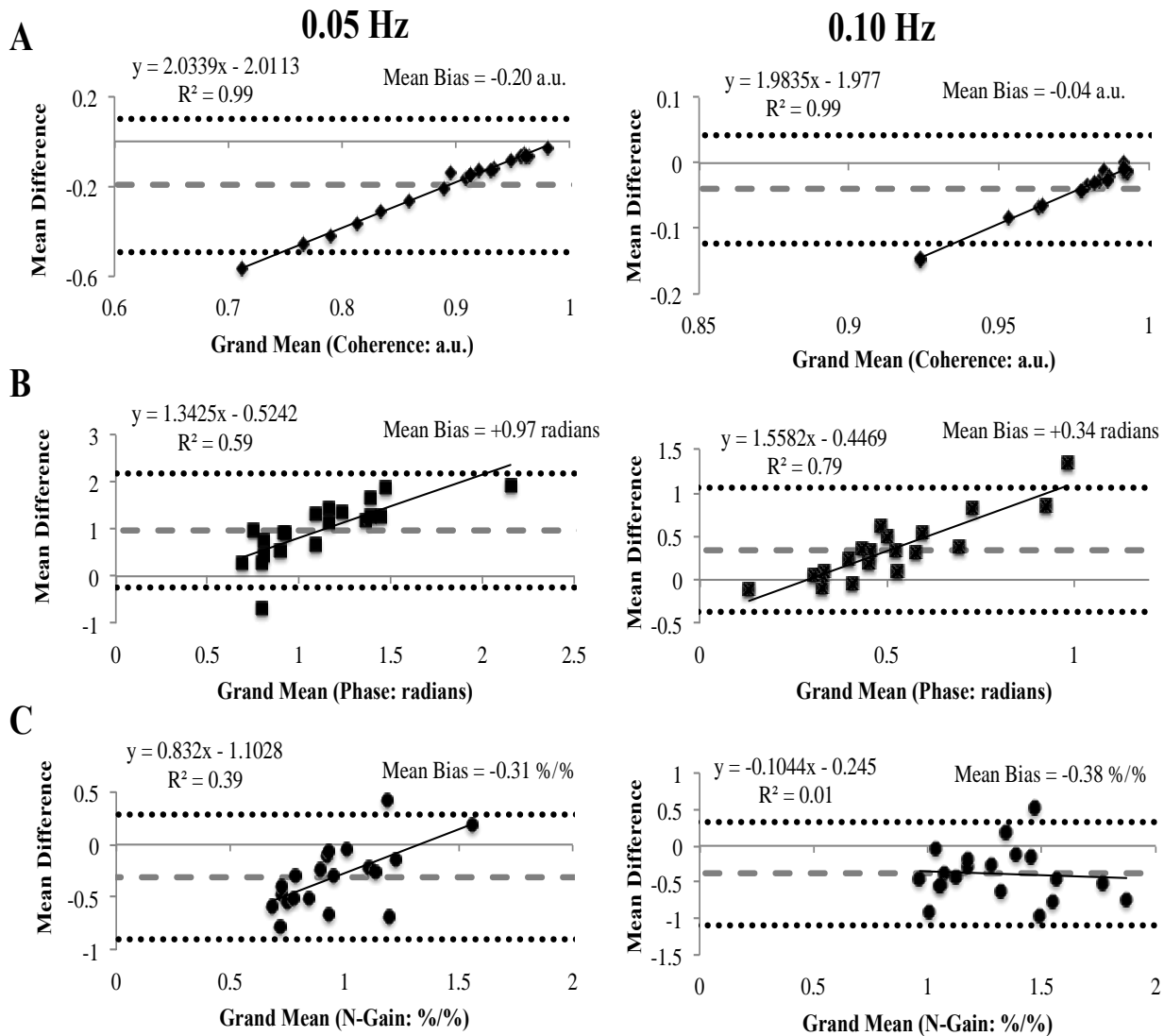


**Figure 3.5.** Bland-Altman plots of the significant differences between squat-stand and oscillatory lower body negative pressure maneuvers in younger adults. The left and right hand figures represent differences at 0.05 Hz and 0.10 Hz, respectively. The top traces demonstrates the proportional and mean bias in arbitrary units (a.u.) for coherence (A), middle trace demonstrates the proportional and mean bias in radians for phase (B) and bottom trace demonstrates the proportional and mean bias in %/% for normalized gain (N-Gain). The dashed middle horizontal line denotes the mean difference between the two modalities, the dotted lines represent the upper and lower 95% limits of agreement, and the solid line represents the regression line indicating the proportional bias.

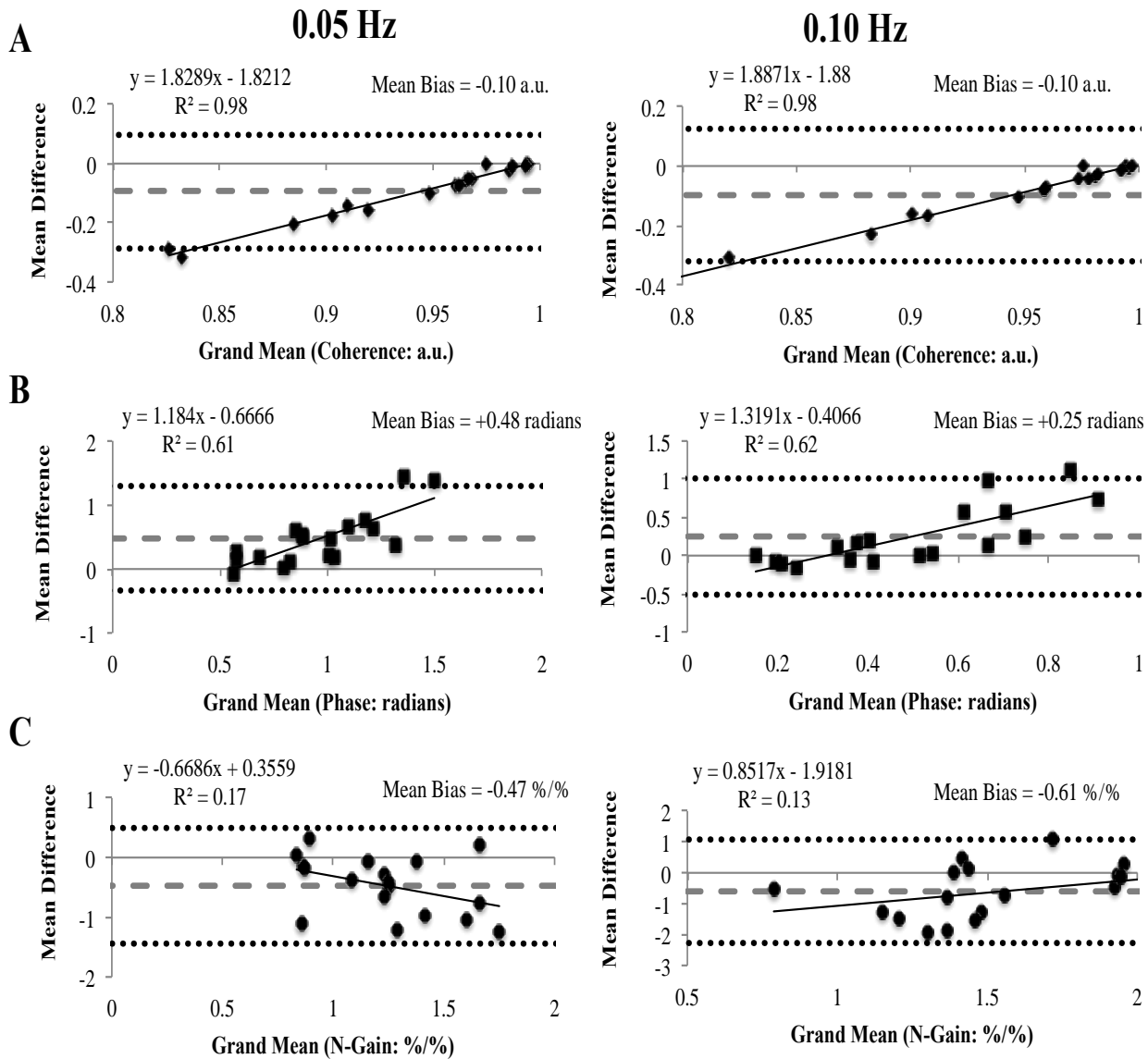


**Figure 3.6.** Bland-Altman plots of the significant differences between squat-stand and oscillatory lower body negative pressure maneuvers in older adults. The left and right hand figures represent differences at 0.05 Hz and 0.10 Hz, respectively. The top traces demonstrates the proportional and mean bias in arbitrary units (a.u.) for coherence (A), middle trace demonstrates the proportional and mean bias in radians for phase (B) and bottom trace demonstrates the proportional and mean bias in %/ % for normalized gain (N-Gain). The dashed middle horizontal line denotes the mean difference between the two modalities, the dotted lines represent the upper and lower 95% limits of agreement, and the solid line represents the regression line indicating the proportional bias.

*Transfer function phase and gain:* Both spontaneous and driven TFA phase and gain metrics are consistent with the high-pass filter model, with phase decreasing and gain increasing as frequency increases from 0.02 Hz to 0.20 Hz. However, there was a relatively large variation in values during spontaneous and driven conditions. Under spontaneous conditions the absolute gain measures in younger adults showed significant increases when the subject was supine ( $P<0.05$ ).

During the driven metrics, although all Fourier transform and TFA metrics were significantly different between the OLBNP and squat-stand maneuvers, there were no differences between the younger and older adults (Tables 3.4. and 3.5.). The OLBNP maneuvers resulted in an average bias in the younger adults of +0.97 radians (phase) and -0.31 %/% (normalized gain) at 0.05 Hz and +0.34 radians (phase) and -0.38 %/% (normalized gain) at 0.10 Hz ( $P<0.001$ ; Figure 3.3.). Similar findings for OLBNP bias were observed in the older adults, +0.48 radians (phase) and -0.47 %/% (normalized gain) at 0.05 Hz and +0.25 radians (phase) and -0.61 %/% (normalized gain) at 0.10 Hz ( $P<0.001$ ; Figure 3.4.).

#### *Comparison of between-day reproducibility of TFA metrics (Figure 3.7.)*

*Spontaneous data (Tables 3.2. and 3.3.):* Between-day reproducibility of the spontaneous upright and supine TFA metrics demonstrate that although the mean data for each measurement was not significantly different from day 1 to day 2, there were few metrics that showed reasonable level of between-day CoV (<20%). Across the aging spectrum only the LF coherence ( $15.1 \pm 12.2\%$ ), and LF absolute gain ( $15.1 \pm 12.2\%$ ) and LF normalized gain ( $18.5 \pm 10.9\%$ ) values met this criterion.

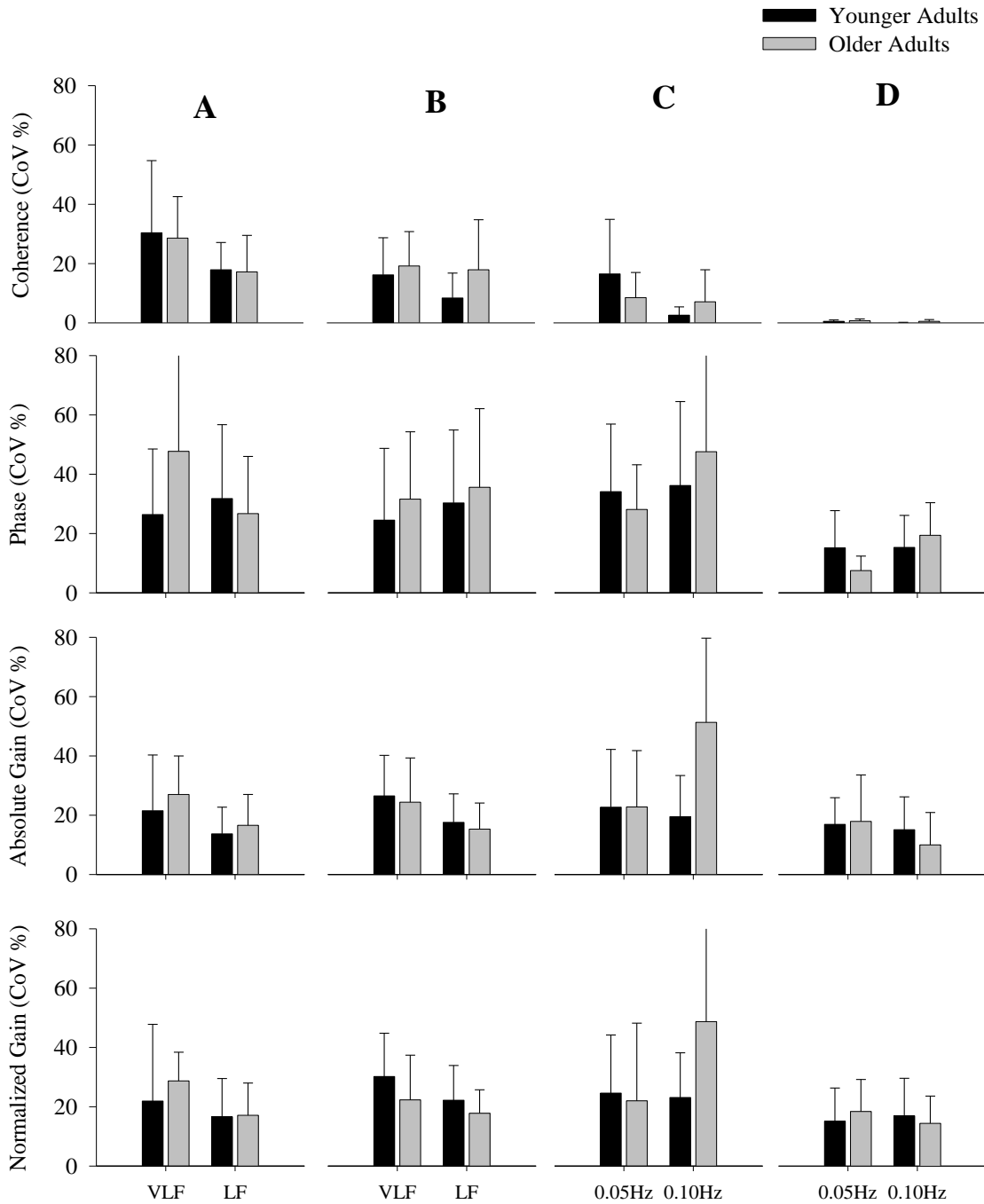


**Figure 3.7.** Within-subject coefficient of variance (CoV) expressed as percentages for coherence (top row), phase (2<sup>nd</sup> row), absolute gain (3<sup>rd</sup> row) and normalized gain (bottom row) during spontaneous supine (A), spontaneous upright (B), oscillatory lower body negative pressure (C) and squat-stand maneuvers (D). The younger adults are represented in the black bars, the older adults in the grey bars. Note: The only condition that had all CoV meet the criteria for reasonable reproducibility (<20%)<sup>240</sup> regardless of age were the squat-stand maneuvers (D).

*Oscillatory lower body negative pressure data (Tables 3.4. and 3.5.):* The findings from the spontaneous data were reflected in the between-day reproducibility of the OLBNP maneuvers. The mean data for all metrics were once again not significantly different from day 1 to day 2; however, the only metrics that met the reasonable variability value for CoV (<20%) were the 0.05 Hz ( $12.1 \pm 15\%$ ), and 0.10 Hz coherence ( $4.7 \pm 7.8\%$ ) values.

*Squat-stand data (Tables 3.4. and 3.5.):* In contrast, to the above-mentioned findings, the squat-stand maneuvers reproducibility revealed that all TFA metrics (gain, phase and coherence in both 0.05 and 0.10 Hz) were considered on average to have reasonable variability. In particular, the 0.05 Hz ( $0.5 \pm 0.5\%$ ;  $0.6 \pm 0.5\%$ ) and 0.10 Hz ( $0.1 \pm 0.1\%$ ;  $0.3 \pm 0.5\%$ ) coherence values in the younger and older adult population, respectively, were the most robust of all findings in the study. The reported TFA coherence ( $P < 0.01$  at both 0.05 and 0.10Hz) and phase ( $P = 0.01$  at 0.05 Hz and  $P = 0.03$  at 0.10Hz) during squat-stand maneuvers had generally better reproducibility than that assessed using OLBNP (Figure 3.7.).

### 3.5. Discussion

Utilizing day-to-day repeatability comparisons between squat-stand maneuvers and oscillatory lower body negative pressure maneuvers, the main findings of the study as they pertain to the linear relationship between arterial blood pressure and CBV were: 1) Although coherence is improved during both driven protocols, squat-stand maneuvers elicited the highest coherence values; 2) the squat-stand maneuvers resulted in more reproducibility across all TFA metrics; and 3) the cerebral pressure-flow responses during the driven oscillations are comparable in younger and older adults. Collectively, at least in the healthy populations studied these findings demonstrate that the optimal protocol for creating oscillations in blood pressure to increase the input power and enhance the linear interpretability of the TFA metrics in both younger and older adult populations is through the use of squat-stand maneuvers. These findings have methodological implications for the reliable assessment and interpretation of the linear aspect of the cerebral-pressure flow relationship in humans.

#### *Comparison with previous studies:*

To our knowledge, there have been seven studies to date <sup>1-3,190,230-232,247</sup> that have utilized repeated squat-stand or sit-to-stand maneuvers to elicit oscillations in blood pressure to enhance the signal-to-noise ratio and thus interpretability of the TFA metrics. Collectively, these studies have demonstrated significant improvements in coherence in both the VLF [ $0.53 \pm 0.13$  (spontaneous) to  $0.78 \pm 0.07$  (driven)] and LF [ $0.69 \pm 0.13$  (spontaneous) to  $0.88 \pm 0.08$  (driven)] ranges. However, comparisons between these studies are difficult as the studies either utilized a point-estimate approach <sup>1-3</sup> or narrow frequency bands (0.02-0.06 Hz; 0.08-0.14 Hz) <sup>190,230,231,247</sup> to sample the TFA metrics. The use of narrow frequency bands leads to general

reduction in coherence values as the peak input power (and thus signal-to-noise ratio) occurs at the driven frequency and is rapidly diminished the further away sampling occurs from this driven point.<sup>1</sup> As a result, the point estimate studies reported coherence in the range of 0.92-1.00<sup>1-3</sup>, where as the narrow frequency band studies reported coherence in the range of 0.60-0.90.<sup>190,230-232,247</sup> Contradictory to the current findings (where coherence = 0.99-1.00 at both 0.05 and 0.10 Hz) and previous findings from our research group,<sup>1-3</sup> are the reports that the 0.10 Hz driven frequencies result in minimal increases in mean arterial pressure power which result in reductions in coherence.<sup>230-232,247</sup> It was speculated that these reductions were due to a higher signal-to-noise ratio at this frequency and should be avoided due to their limited reliability.<sup>230-232,247</sup> However, such speculation contravenes the reproducibility findings by van Beek *et al.*,<sup>230</sup> which showed the only frequency from sit-to-stand maneuvers that revealed acceptable reproducibility of TFA metrics was 0.10Hz. Even with the discrepancy in coherence values between these sampling methods, the phase (0.05 Hz: ~0.70 radians; 0.10 Hz: ~0.45 radians) and normalized gain (0.05 Hz: ~0.90 %/mmHg; 0.10 Hz: ~1.20 %/mmHg) values are relatively consistent,<sup>1-3,190,230-232,247</sup> and are comparable to the present findings (Tables 3.4. and 3.5.). It is also noted that although utilizing a method – such as the squat-stand maneuvers – that results in greater reproducibility of the coherence (and associated phase and gain metrics), does not necessarily distinguish between healthy and pathological cerebral autoregulation. This latter potential difference should be examined in future studies.

The OLBNP methodology has been utilized with pressure ranges from -30 mmHg to -120 mmHg,<sup>185,203,228,229,248,249</sup> with larger negative pressures (in excess of -70 mmHg) generating greater increases in coherence values (-30 to -40 mmHg: 0.60-0.80; -70 to -120 mmHg: 0.90-0.95).<sup>203,228,229,249</sup> Although the -50 mmHg negative pressure within this study

was not as severe as some of the previous literature (-70 and -120 mmHg),<sup>228,229</sup> these studies were performed in a younger adult population (mean age of  $37 \pm 12$  years at -70 mmHg).<sup>228</sup> Instead, our study was designed to match the pressure generated in the steady-state findings of Formes *et al.*,<sup>238</sup> who tested a similarly aged population ( $68 \pm 1$  year) at a negative pressure of -50 mmHg, as this pressure has been shown to be tolerant for both sedentary and active older individuals. The spontaneous LF findings for coherence ( $0.63 \pm 0.06$ ), phase ( $0.65 \pm 0.15$  radians), and gain ( $1.41 \pm 0.18$  cm/s/mmHg) presented by Formes *et al.*,<sup>238</sup> are comparable to those reported in this study (Table 3.3.). The phase and gain findings in the current study (Tables 3.4. and 3.5.) are consistent with the previous literature at both 0.05 Hz and 0.10 Hz.  
203,228,229

#### *Day-to-day reproducibility*

To date there have been numerous studies that reported on the reproducibility of the cerebral pressure-flow relationship with a wide assortment of measurement techniques including: the autoregulatory index (ARI),<sup>204,227,250-255</sup> autoregressive moving average model<sup>256</sup> mean flow index,<sup>217,257,258</sup> near infrared spectroscopy (NIRS),<sup>259,260</sup> rate of regulation,<sup>211</sup> TFA,<sup>204,217,227,230,250,257,258,261</sup> and vector autoregressive model.<sup>256</sup> These 20 studies have been summarized in Table 3.6.

**Table 3.6.** Summary of previous literature assessing the reproducibility of the cerebral pressure-flow relationship.

	<b>N (cohort)</b>	<b>Age (years)</b>	<b>Pressure-flow metric</b>	<b>Time between measures</b>	<b>Reproducibility Findings</b>
Birch et al. <sup>261</sup>	5 (healthy)	40 ± 5	TFA at 0.083 Hz	8 sessions spread over 3 months	With OLBNP, there was a high degree of reproducibility in TFA phase and reproducibility improved with increased negative pressure
Brodie et al. <sup>250</sup>	10 (healthy)	38 ± 9	ARI under spontaneous oscillations	4 measures with 3-4 days between each	ARI measures had low ICC in both the right (0.51) and left (0.43) hemispheres across the measures
Brodie et al. <sup>251</sup>	10 (healthy)	35 ± 9	ARI and spontaneous TFA at 0.05 Hz	10 years	ARI fell on average by 16% in the 10 year follow-up, TFA phase and gain metrics were unchanged
Chacon et al. <sup>252</sup>	16 (healthy)	32 ± 9	Traditional and model free ARI	6 thigh cuff maneuvers separated by 8 minutes	Traditional ARI had a much higher within subject CoV (39 ± 42%) as compared with the model free ARI (16 ± 8%), indicating the model free ARI was a superior measure
Elting et al. <sup>204</sup>	16 (healthy)	33 ± 10	ARI and TFA sampled at 0.10 Hz	2 leg raise measures separated by 5 minutes	ICC was low in both hemispheres for ARI (~0.65) and 0.10 Hz phase (~0.45), but was better of 0.10 Hz normalized gain (~0.75)
Georgiadis et al. <sup>262</sup>	5 (moderate hypothermia with acute stroke)	58 ± 11	Static CA	2 hours	The 5 subjects had a within-subject CoV of 11 ± 7%

	<b>N (cohort)</b>	<b>Age (years)</b>	<b>Pressure-flow metric</b>	<b>Time between measures</b>	<b>Reproducibility Findings</b>
Gommer et al. <sup>227</sup>	19 (healthy)	Range 18-53	TFA in the 0.04-0.16 Hz range and ARI	1 morning session and 1 afternoon session 7 days apart	Under spontaneous conditions, mean ICC values for both TFA metrics and ARI were low in morning (0.36-0.61) and afternoon (0.37-0.55). Similar results were shown for paced breathing (ICC morning: 0.34-0.73; afternoon: 0.17-0.59)
Houtman et al. <sup>260</sup>	10 (healthy)	Range 23-51	NIRS	Time between measures not reported	Circulatory measures (stroke volume, heart rate and blood pressure) had low variance between days, cerebral oxygenation values however had a high level of random error and were not reproducible
Hu et al. <sup>253</sup>	30 (brain injury)	Range 17-69	Phase shift and ARI	4 times within a 5 minute recording	ICC was 0.58 for phase shift and was 0.08 for ARI, indicating both methods have poor reproducibility
Jachan et al. <sup>256</sup>	44 (severe carotid stenosis)	71 ± 10	Transfer function estimate, ARMAX and VAR models	2.5 - 6 months	Kendall's rank correlations revealed significant between measure correlations for all three pressure-flow estimates, despite a high level of variability in the data
Lorenz et al. <sup>257</sup>	30 (poor temporal windows)	68 ± 10	TFA phase and Mx	Measures repeated within 30 minutes	Although the phase difference and Mx reproducibility values were not shown, the authors stated this was done because they were 'poor'

	<b>N (cohort)</b>	<b>Age (years)</b>	<b>Pressure-flow metric</b>	<b>Time between measures</b>	<b>Reproducibility Findings</b>
Mahony et al. <sup>254</sup>	16 (healthy)	32 ± 9	ARI	6 thigh cuff maneuvers separated by 8 minutes	Within subject CoV was 42 ± 48% and within subject ARI score ranges were 3.3 ± 2.1, indicating poor reproducibility. The authors concluded that a minimum of 3 ARI scores should be averaged for a physiologically relevant value.
Mehagnoul-Schipper et al. <sup>259</sup>	27 (healthy)	75 ± 8	NIRS	Minimum of 2 days	Although no between day mean differences were noted for NIRS measures, all NIRS measures showed a low reliability coefficient (0.14 – 0.43)
Ortega-Guiterrez et al. <sup>217</sup>	19 (healthy)	Range 21-74	TFA phase and gain, and Mx	17 days Range (5-27)	All measures were performed under spontaneous conditions. The ICC for TFA phase was ~0.60, TFA gain was ~0.59, and Mx was ~0.43.
Panerai et al. <sup>191</sup>	39 (healthy)	40 ± 15	Coherent averages	8-16 blood pressure transients per subject over 10 minutes	33 of the 39 subjects reported weak, moderate and strong coherent averages in the right MCA and 29 of 39, in the left MCA indicating a large amount of within subject variability.
Reinhard et al. <sup>258</sup>	34 (healthy)	65 ± 8	TFA phase and Dx	2 ± 1 months	With deep breathing at 0.10 Hz the ICC for TFA phase was 0.790 and for Dx was 0.377

	<b>N (cohort)</b>	<b>Age (years)</b>	<b>Pressure-flow metric</b>	<b>Time between measures</b>	<b>Reproducibility Findings</b>
Saeed et al. <sup>255</sup>	11 (healthy)	37 ± 7	ARI	6 days Range (5-9)	The quality of the CBV signals was determined with a TFA coherence cut-off of 0.50. When CBV signals met this criterion, they were passed back into the time domain for ARI analysis. The ICC for ARI was 0.39 with frame-held TCD probes and 0.48 for hand-held TCD probes.
Smielewski et al. <sup>211</sup>	11 (healthy)	Range 20-30	Carotid artery compression and RoR	All tests performed on same day	RoR and Compression were performed twice under hypo-, normo- and hypercapnia. The CoV for RoR was dependent upon CO <sub>2</sub> levels: ~47% for hypo-, ~28% for normo-, and ~63% for hypercapnia. The compression test CoV results were ~13% under all conditions.
Tan <sup>186</sup>	5 (healthy)	Range 21-40	Projection pursuit regression	2 separate experimental days	Autoregulatory gain at 0.03 and 0.08 Hz did not change across days based on Lin's concordance coefficient (0.96 and 0.98 respectively)

	<b>N (cohort)</b>	<b>Age (years)</b>	<b>Pressure-flow metric</b>	<b>Time between measures</b>	<b>Reproducibility Findings</b>
van Beek et al. <sup>230</sup>	11 (healthy)	77 ± 5	TFA	3-4 months	Spontaneous and Sit-to-stand maneuvers at 0.05 Hz and 0.10 Hz. The CoV for spontaneous VLF phase (70%) and gain (38%), were higher than LF phase (23%) and gain (17%). A similar trend for CoV was observed in the sit-to-stand maneuvers: 0.05 Hz phase (85%) and gain (39%) were higher than the 0.10 Hz phase (14%) and gain (22%). The authors concluded that the LF and 0.10 Hz ranges were the only ones with acceptable reproducibility

Values are means ± SD. Autoregulatory index (ARI); autoregressive moving average model (ARMAX); cerebral autoregulation (CA); cerebral blood velocity (CBV); coefficient of variation (CoV); dynamic correlation index (Dx); hertz (Hz); intraclass correlation (ICC); low frequency (LF: 0.07-0.20Hz); mean flow index (Mx); near infrared spectroscopy (NIRS); oscillatory lower body negative pressure (OLBNP); rate of regulation (RoR); transcranial Doppler ultrasound (TCD); transfer function analysis (TFA); vector autoregressive model (VAR); and very low frequency (VLF: 0.02-0.07 Hz).

The collective findings from these studies indicate that although the reproducibility of the pressure-flow relationship has been assessed across a wide range of both age (17 - 80+ years) <sup>230,253,256,259</sup> and time between measures (minutes to a 10 year follow-up). <sup>250,252,254</sup> The bulk of these studies have revealed that majority of the research in this area has utilized measurement tools that have relatively low reproducibility (as indexed with an intraclass correlation (ICC) <0.80 and/or a within-subject CoV >20%). For example, every study that indexed the pressure-flow relationship with either the traditional ARI or NIRS had an ICC <0.70 regardless of the measurements occurred within minutes, <sup>252-254</sup> days, <sup>255,259,262</sup> or years. <sup>250</sup> Similar to the findings for ARI and NIRS, are those studies that assessed TFA metrics during spontaneous oscillations in blood pressure <sup>217,227,230,257</sup> which revealed low values for the reproducibility of both phase and gain metrics. Consistent with these findings are those presented in the current study. The presented findings for pressure-flow relationship during spontaneous upright and supine conditions (Tables 3.2. and 3.3.) reveal a similar outcome as the previous reproducibility studies (Table 3.6.). While the mean values of all spontaneously assessed metrics were not significantly different from day-to-day, there were very few metrics (only LF coherence and gain) that revealed reasonable between day CoV values (<20%). <sup>240-242</sup> These findings were also consistent with those reported for the OLBNP maneuvers, which revealed that once again the only reproducible day-to-day TFA metrics are the coherence measures (Tables 3.4. and 3.5.). Contrary to the aforementioned findings, are those of the findings of the squat-stand maneuvers (Tables 3.4. and 3.5.). These data revealed consistent and reproducible data for all TFA metrics (coherence, phase, gain, and normalized gain) at both 0.05 and 0.10 Hz (Figure 3.7.).

*Squat-stand maneuvers as the 'gold-standard' for linear TFA metric interpretation*

As noted by Bland and Altman in their seminal work published in 1986,<sup>246</sup> examining the reproducibility of a measurement tool across repeat measurements within the same subject group is the best way to ensure the repeatability of that measurement tool. There should be a minimal difference (close to 0) in the metrics associated with measurement tool if it is indeed measuring the same metric over time.<sup>246</sup> In the current study, the only method that met this criterion was the squat-stand maneuvers (Figure 3.7.). When multiple measurement tools are being employed during a study (in this case: spontaneous supine and upright oscillation data; OLBNP maneuvers; squat-stand maneuvers) the level of repeatability of the methods will greatly impact the agreement between trials.<sup>246</sup> When one measurement tool has poor reproducibility, the level of agreement between methods will likely be reduced, a problem that is exacerbated when both methods employed have poor reproducibility.<sup>246</sup>

The quantification and interpretation of the linear aspect of the relationship between arterial blood pressure and CBV in the current study was assessed via TFA. A common test of the linearity of this relationship is the coherence metric, with a value close to 1.00 indicating that the system is linear and thus acceptable to be assessed with TFA.<sup>18</sup> In the current study, it was determined that the squat-stand maneuvers resulted in coherences of 0.99-1.00 for both age-groups (Tables 3.4. and 3.5.). The most robust between-day CoV data reported are associated with the coherence values at 0.05 Hz (0.5-0.7%) and 0.10 Hz (0.1-0.5%), for the younger and older adults, respectively, during the squat-stand maneuvers. This method (squat-stand maneuvers) also resulted in significantly larger increases to the power spectra for both mean arterial pressure and middle cerebral artery

velocity (Figures 3.3. and 3.4.) which contributed to the enhanced linearity of the system and significantly higher coherence. Since TFA employs a linear mathematical approach to the quantification and interpretation of the cerebral pressure-flow relationship, the gold-standard for the quantification of this relationship with this assessment tool should be the method that results in coherence values that are  $\sim 1.00$ . The only method to date that has been proposed that meets this criterion is the squat-stand maneuvers; as such, we suggest that for this method should be considered the gold-standard. With this notion in mind, we performed comparisons between the two driven methods (OLBNP and squat-stand maneuvers) to determine the bias present between these measures at both 0.05 and 0.10 Hz (Figures 3.5. and 3.6.). It was observed that the OLBNP maneuvers resulted in a general overestimation (i.e., positive bias) of phase (0.05 Hz:  $\sim 0.50$ -1.00 radians; 0.10 Hz  $\sim 0.25$ -0.35 radians) and an underestimation (i.e., negative bias) of normalized gain (0.05 Hz: 0.30-0.50 %/%; 0.10 Hz 0.35-0.60 %/%; Figures 3.5. and 3.6.). Collectively, the reproducibility (Figure 3.7.) and Bland-Altman data from this study reveals that the squat-stand and OLBNP maneuvers have major differences in the associated TFA outcome measures and likely can not be used interchangeably. Most notable of these differences is the augmented level of reproducibility present in both age-groups for the squat-stand maneuvers for all TFA metrics at all frequencies (Figure 3.7.). This notion, indicates that even a small amount of noise in the signal (such as during the spontaneous oscillations and OLBNP maneuvers: Tables 3.2.-3.6.) can result in less reproducible TFA metrics. However, when the signal-to-noise ratio is maximized (as noted in the 100-300+ fold increase in the autospectra of the squat-stand maneuvers: Figures 3.3. and 3.4.), there is a significant decrease in the CoV for all TFA metrics and age-groups (Figure 3.7.). This

finding highlights the fact that the signal-to-noise ratio does indeed play a role in the linear interpretation of TFA metrics as demonstrated by the higher CoV values associated with the metrics that had lower coherence values.

Thus the collective findings from the current study indicate that when assessing TFA metrics associated with cerebral pressure-flow relationship in otherwise healthy populations, squat-stand maneuvers provide the most reproducible outcome measures. However, under conditions where squat-stand maneuvers are not feasible (e.g. people with mobility issues, incapacitated individuals, during cycling interventions) applying the OLBNP maneuvers (or possibly even deep breathing<sup>227,258</sup> or passive leg raises<sup>204</sup>) would be appropriate to elicit augmented coherence provided there was a sufficient magnitude of negative pressure applied.<sup>228,229,261</sup> *The critical next point to establish is to examine the ability of these squat-stand maneuvers to distinguish between healthy and pathological autoregulation.* However, it should also be noted that within the confines of the current study, the presented findings focus on the reproducibility (and linear interpretation) of the TFA metrics as they pertain *solely* to the relationship between mean arterial pressure and middle cerebral artery velocity and are not necessarily reflective of cerebral autoregulation as a whole entity.

#### *Effects of posture changes on CBF regulation:*

An important consideration is that we have compared the pressure-flow responses in the supine and upright positions. Movement from a supine to standing position can result in a reduction of ~1.5 litres of central blood volume.<sup>63,143</sup> Initially (within the first 15 seconds) there is an initial increase in cardiac output (+30%) and a reduction in mean

arterial pressure (-45%) before baroreflex adjustments occur.<sup>144</sup> Initially when a subject moves from the supine to upright position, there is reduced ventilation/perfusion matching within the lung and consequently PaCO<sub>2</sub> can decrease by ~1-4 mmHg which results in a decrease in CBV of ~10%.<sup>150,151</sup> Consistent with these changes, the results from this study showed that after the posture change from upright to supine, P<sub>ET</sub>CO<sub>2</sub> universally rose by ~2 mmHg which resulted in an increase in CBV of ~10% (Table 3.1.).

The change in posture and P<sub>ET</sub>CO<sub>2</sub> could be a contributing factor to the TFA metrics alterations during driven oscillations in blood pressure (Tables 3.4. and 3.5.; Figures 3.5. and 3.6.). Part of the alterations to the TFA metrics may also be explained by the acute ~9% *decrease* in CVRi, as this was positively correlated to the normalized gain in both the younger ( $r = 0.24; 0.38; P < 0.05$ ) and older ( $r = 0.47; 0.31; P < 0.03$ ) adults at 0.05 Hz and 0.10 Hz, respectively. The acutely reduced CVRi was also negatively correlated to phase in the older adults at both 0.05 Hz ( $r = -0.42; P = 0.005$ ) and 0.10 Hz ( $r = -0.48; P = 0.002$ ). These findings confirm those presented in our previous study, which induced a 40% *increase* in CVRi via both pharmacological (Indomethacin) and physiological (hypocapnia) interventions.<sup>1</sup> The acute *increase* in CVRi in the Indomethacin and hypocapnia trials of the previous study were positively correlated to increases in phase and negatively correlated with decreases in gain.<sup>1</sup> Thus collectively, the findings from these two studies indicate that changes in CVRi can impact the cerebral pressure-flow response and acute changes to CVRi should be considered when interpretations of TFA metrics are made.

*Implications for the assessment and interpretation of pressure-flow relationships:*

The current findings for the TFA metrics match well with the previous literature for both driven methods: squat-stand maneuvers<sup>1-3,190,230-232,247</sup> and OLBNP maneuvers.<sup>185,203,228,229</sup> The reproducibility metrics for spontaneous and OLBNP maneuvers also correspond well to the previous literature in the area (Table 3.6.). However, a surprising limitation of the previous literature is that no study has reported on the day-to-day reproducibility of TFA metrics either during squat-stand maneuvers or in reference to younger and older adult populations within the same study. As indicated by the previous findings on the ARI and TFA metrics during spontaneous blood pressure oscillations, even though findings from a study can be comparable to previous literature in the field, without knowing the reproducibility metrics of the employed methodology caution needs to be applied to the interpretation of single punctual measurements.

This study was designed to be the first study to present reproducibility metrics for both younger and older adults, during spontaneous and driven oscillations in blood pressure. Collectively, the findings reported in the current study emphasize notion that comparable findings in mean data between days, do not necessarily tell the entire story. Although there were no between-day differences for either the younger or older adults under any of the conditions (spontaneous upright, spontaneous supine, OLBNP, squat-stand maneuvers), there were vast differences in the underlying reproducibility and standard deviations of the between-day measures. Consequently the findings presented in this study have important implications on the design of future studies where between-day comparisons are needed. While the spontaneous and OLBNP data compare well to the previous literature in the area, there are few metrics with biologically acceptable between-

day reproducibility, (only the coherence and gain in the LF/0.10 Hz range) which indicate that caution should be applied to single-day measurements with these methods. The implications of the level of variability associated with these methods are likely important for ensuring the planning of effective sample sizes for interventional and clinical orientated studies. In contrast, all of the TFA metrics associated with the squat-stand maneuvers revealed reasonable levels of between-day CoV and had lower between-day variation in coherence, and thus more repeatable system linearity (Tables 3.4. and 3.5.). These findings indicate that the OLBNP and squat-stand maneuvers likely are not interchangeable. They also highlight the notion that when a small sample size is used for a single-day assessment of the relationship between mean arterial pressure and cerebral blood flow via linear TFA, a method should be employed that has a minimal CoV (higher reproducibility) and thus enables a more accurate assessment of the linear TFA metrics.

*Methodological Considerations:*

*Cerebral Autoregulation:* The interpretation of the presented findings focused on the reproducibility of the TFA metrics as they pertain *solely* to the relationship between mean arterial pressure and middle cerebral artery velocity and are not necessarily reflective of cerebral autoregulation as a whole entity. This was performed as there has yet to be a defined gold-standard assessment tool for cerebral autoregulation quantification.<sup>125</sup> The complexities associated with cerebral autoregulation are likely not entirely linear in nature. However as the presented findings clearly demonstrate, the relationship underlying arterial blood pressure and CBV can be approximated in a linear fashion (coherence 0.99-1.00) if

the appropriate method is applied (squat-stand maneuvers) which enhances the reproducibility and interpretability of the associated linear TFA metrics.

*Flow vs velocity:* Transcranial Doppler is utilized to provide an index of cerebral blood flow, under the assumption that velocity approximates flow values when the diameter of a vessel is constant. Recent high resolution magnetic resonance imaging studies<sup>65,66</sup> have revealed that when  $P_{ETCO_2}$  values are held within 8 mmHg of eucapnia (reviewed in:<sup>67</sup>) the diameter of the middle cerebral artery is relatively constant. In the current study,  $P_{ETCO_2}$  was  $\pm 2$  mmHg of eucapnia, which indicates that the velocity data is likely representative of cerebral blood flow and can be utilized to assess the cerebral pressure-flow relationship.

### **3.6. Key finding**

The use of squat-stand maneuvers provide a reproducible and physiological relevant protocol for creating oscillations in blood pressure to increase the input power and enhance the linear interpretability of the TFA metrics in both younger and older adult populations. These findings have methodological implications for the assessment and interpretation of the linear aspect of the relationship between arterial blood pressure and CBV in humans.

#### **Chapter Four: Influence of increased cerebrovascular resistance**

This study was approved by the clinical ethical committees of the Universities of British Columbia (H11-03287), and adhered to the principles of the Declaration of Helinski and Title 45, U.S. Code of Federal Regulations, Part 46, Protection of Human Subjects. All volunteers provided written informed consent and procedures were followed in accordance to institutional guidelines.

A version of this study was accepted and presented as an oral presentation at the CARNet 2012 (annual scientific meeting of the cerebral autoregulation research network). Jonathan D. Smirl, and Philip N. Ainslie. (2012) Influence of Cerebrovascular Resistance on Dynamic Cerebral Autoregulation in Humans. Jonathan Smirl was responsible for the data collection, data analysis, writing, and formatting of the abstract.

A version of this manuscript has been accepted and published in the *Journal of Applied Physiology* and has been reproduced with permission. <sup>1</sup> Influence of cerebrovascular resistance on dynamic pressure-flow relationships in humans. Jonathan D. Smirl, Yu-Chieh Tzeng, Brad Monteleone, and Philip N. Ainslie. Jonathan Smirl was responsible for the data collection, data analysis, writing, and formatting of the manuscript.

#### **4.1. Aims and Hypotheses**

##### **Aims:**

- 1) To investigate the influence of increases to cerebrovascular resistance on the relationship between arterial blood pressure and cerebral blood flow, via pharmacological (Indomethacin) and non-pharmacological (Hypocapnia) interventions.
- 2) To determine if there are any changes in the regulatory properties within the anterior and posterior regions of the cerebrovasculature.

##### **Hypotheses:**

- 1) Increases to cerebrovascular resistance, independent of changes to arterial carbon dioxide and blood pressure, will lead to increases in TFA phase and decreases in TFA gain.
- 2) There would be comparable TFA phase and gain metrics in both the anterior and posterior regions of the brain.

## 4.2. Rationale

One common method to assess the dynamic relationship between arterial blood pressure and CBV is through the use of TFA.<sup>18,263</sup> TFA utilizes Fourier transforms to quantify the linear relationship between blood pressure and CBV and provides information on the statistical dependence between the input (blood pressure) and output (CBV) variables (coherence), the time-lead (phase), and signal amplitude modulation (gain).<sup>18,125</sup> To date, TFA has been used to examine the influence of the CVRi on the dynamic cerebral pressure-flow relations under physiological (altered  $P_aCO_2$  levels)<sup>18,125,263,264</sup> or pharmacological interventions (e.g., via Phenylephrine infusion).<sup>18,29,125,264</sup> However, the way in which CVRi is manipulated under both of these conditions is fundamentally different and it is unclear if the changes in CVRi alone result in similar changes to those induced via hypocapnia.

Alterations to CVRi via  $P_aCO_2$  changes occur independent of changes to arterial blood pressure by either increasing or decreasing the diameter of downstream cerebral arterioles.<sup>29,264</sup> In contrast, phenylephrine increases CVRi via an entirely different mechanism.<sup>264,265</sup> Phenylephrine is a  $\alpha_1$ -adrenergic receptor agonist and likely does not cross the blood-brain barrier.<sup>265,266</sup> Instead it acts as a systemic vasopressor to increase arterial blood pressure, which in turn results in an increased CVRi. How a pharmacologically induced increase in CVRi, independent of alterations to  $P_aCO_2$  and arterial blood pressure, may influence the dynamic cerebral pressure-flow relationship has yet to be experimentally examined.

The purpose of our study was to investigate the influence of CVRi on the cerebral pressure-flow relationships in healthy humans independent of alterations to  $P_aCO_2$  and

arterial blood pressure. To address this question, we administered a clinical dose of Indomethacin - a potent and reversible cyclooxygenase inhibitor that is able to cross the blood brain barrier. Indomethacin has been shown to lower CBF by 20-35%<sup>120-122</sup> and elevate CVRi without altering metabolic rate,<sup>120,123</sup> plasma catecholamines,<sup>123,124</sup> or P<sub>a</sub>CO<sub>2</sub>.<sup>18,124,125</sup> We also induced hypocapnia by voluntary hyperventilation to effectively 'match' the elevations in CVRi that were present in the Indomethacin trial, to confirm that the alterations in the TFA metrics were a result of the increased CVRi. The dynamic relationship between blood pressure and CBV was quantified during exogenously driven changes in blood pressure in the very low (0.05 Hz) and low (0.10 Hz) frequency ranges.<sup>18,125,267</sup> We hypothesized that increases in CVRi, independent of alterations to P<sub>a</sub>CO<sub>2</sub> or arterial blood pressure, should lead to an increased phase and decreased gain metric in both the anterior and posterior regions of the brain.

### **4.3. Methods**

#### *Ethical approval*

The study was approved and complied with the standards set by the clinical ethical review board of the University of British Columbia. All volunteers provided written informed consent.

#### *Subjects*

Sixteen healthy subjects (12 male, 27.2 ± 7.2 years, BMI: 25.6 ± 2.9 kg/m<sup>2</sup>) were recruited for this study. None had a history of cardiorespiratory or cerebrovascular disease and none were taken any form of medication. All subjects abstained from exercise, caffeine

and alcoholic beverages for a period of 12 hours prior to the study. Each subject underwent a familiarization of the laboratory and testing protocols before the initiation of the protocols.

### *Experimental Conditions*

The subjects were required to visit the laboratory on two occasions. The subjects underwent three experimental trials: no intervention (control), oral Indomethacin (1.2mg/kg) and hypocapnia. The first two trials were performed on day 1 in the following order: control measures, oral Indomethacin administration (dose: 1.2mg/kg body weight), 90-minute rest, Indomethacin measures. On day 2 (minimum 2 day washout period) the subjects were instructed to hyperventilate (leading to an increase in CVR<sub>i</sub> resulting in a decrease in CBV) until the reduction in the MCA<sub>v</sub> matched the reduction of the Indomethacin trial. The matched level of P<sub>ET</sub>CO<sub>2</sub> during the hypocapnia trials was projected onto a screen and the subject was coached on their rate and depth of breathing. This was performed in order to maintain a stable P<sub>ET</sub>CO<sub>2</sub> throughout each hypocapnic experimental condition (seated baseline, and both squat-stand frequencies).

Resting spontaneous baseline data were recorded in a seated position. These data were used for the baseline measures of blood pressure, breathing frequency, P<sub>ET</sub>CO<sub>2</sub> and CBV in the anterior (MCA<sub>v</sub>) and posterior (PCA<sub>v</sub>) cerebral circulatory regions. In order to try to maximize the signal-to-noise ratio that is commonly associated with lower coherence values present in spontaneous cerebral autoregulation measures,<sup>125,267-269</sup> we had the subjects also perform the repeated squat-stand maneuvers. The subjects mimicked the experimenter in the performing of these maneuvers to ensure all subjects performed the

maneuvers at a similar depth. The subjects were randomly selected to perform either a 0.05 Hz (10 second squat–10 second stand) or 0.10 Hz (5 second squat–5 second stand) for 5-minutes each or vice-versa, with a 3-minute rest period to return to baseline levels in between trials. These data were used for the spectral analysis of the driven oscillations in blood pressure and CBV in the middle and posterior cerebral arteries, as representative vessels of the anterior and posterior cerebral circulatory regions at the driven frequency. The driven data were selected from the point estimate where we drove the blood pressure (either 0.05 Hz or 0.10 Hz) as this point had the highest signal-to-noise ratio, highest PSD value and thus the highest coherence value (refer to Figure 4.1. for absolute power spectrum density units and Figure 4.2. for normalized power spectrum density units; the variance [standard deviations] for Figures 4.1. and 4.2. is shown in Table 4.1.). The frequency where the power spectrum density reached peak amplitude (either 0.05 Hz or 0.10 Hz) was used as a basis for sampling the point estimates for coherence, phase and gain. The increased coherence indicates increased linearity within the blood pressure and CBV relationship, and enables a stronger statistical interpretation of the TFA phase and gain metrics. This practice has been used by our lab<sup>3,125</sup> and others.<sup>204</sup> During all trials, end tidal gases were monitored to ensure that normal breathing occurred and Valsalva-like maneuvers were avoided.

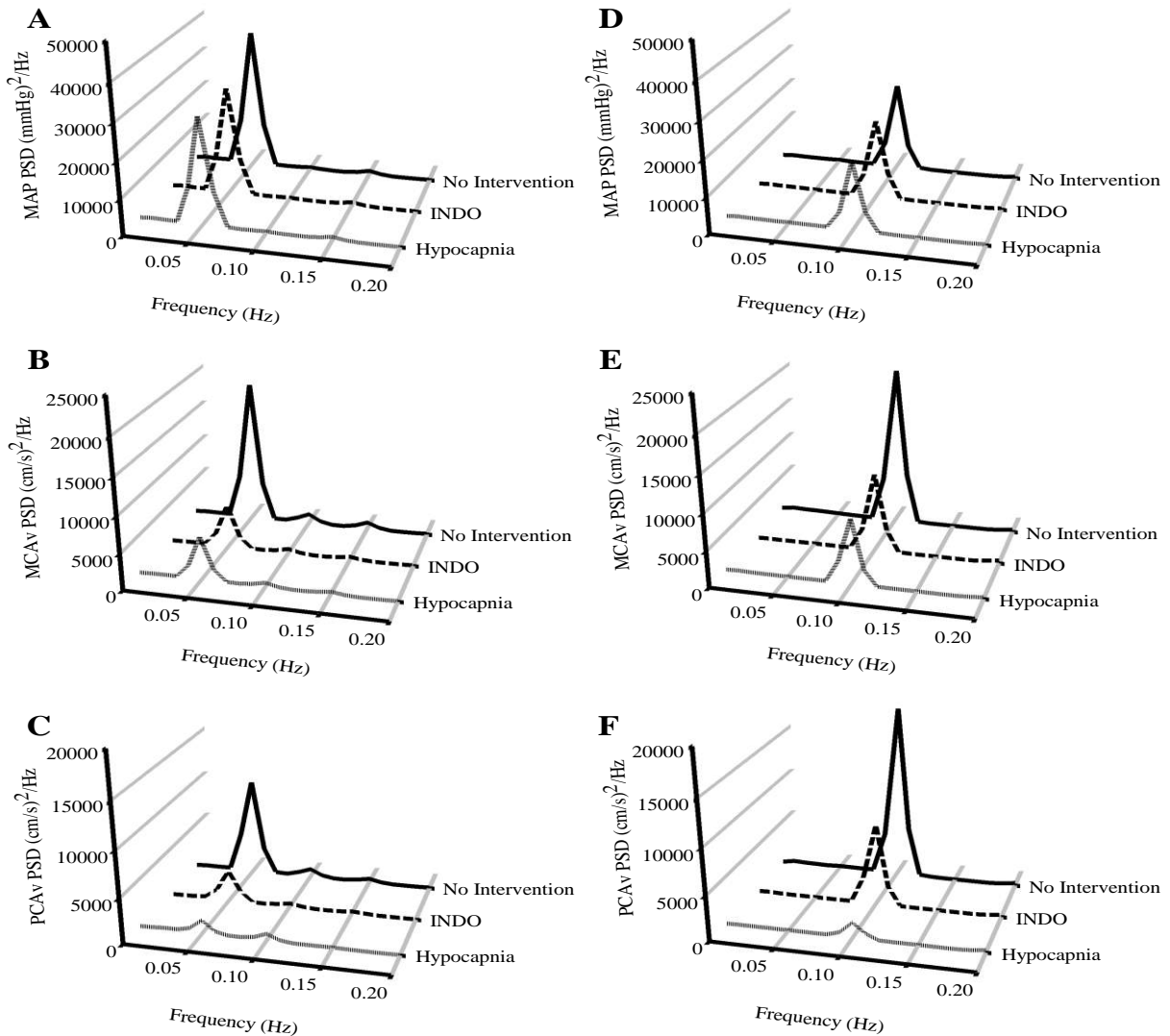


**Figure 4.1.** Absolute values of the power spectrum densities (PSD) for the mean arterial pressure [MAP: 0.05 Hz (A), 0.10 Hz (D)]; middle cerebral artery velocity [MCAv: 0.05 Hz (B), 0.10 Hz (E)]; and posterior cerebral artery velocity (PCAv: 0.05 Hz (C), 0.10 Hz (F)) during the squat-stand maneuvers for the three interventions. The frequency where the PSD reached peak amplitude (either 0.05 Hz or 0.10 Hz) was used as a basis for sampling the point estimates for Coherence, Phase and Gain. At 0.05 Hz MCAv and PCAv PSD during Indomethacin and hypocapnia interventions were reduced compared to the no intervention condition; at 0.10 Hz MCAv PSD during Indomethacin and hypocapnia interventions and PCAv PSD during the hypocapnia intervention were reduced compared to the no intervention condition (see Table 4.1. for details).

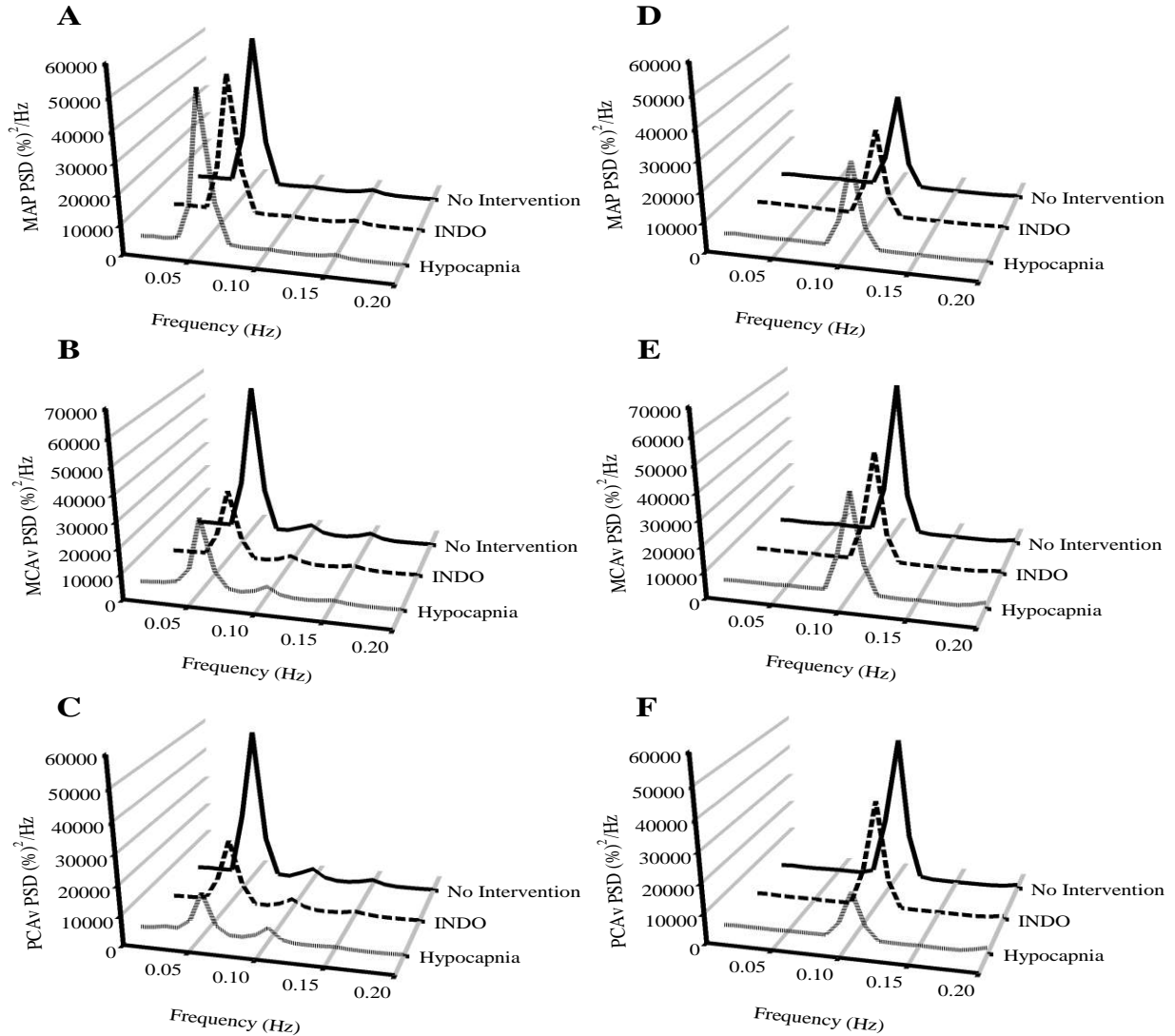


**Figure 4.2.** Normalized values of the power spectrum densities (PSD) for the mean arterial pressure [MAP: 0.05 Hz (A), 0.10 Hz (D)]; middle cerebral artery velocity [MCAv: 0.05 Hz (B), 0.10 Hz (E)]; and posterior cerebral artery velocity [PCAv: 0.05 Hz (C), 0.10 Hz (F)] during the squat-stand maneuvers for the three interventions. The frequency where the PSD reached peak amplitude (either 0.05 Hz or 0.10 Hz) was used as a basis for sampling the point estimates for Coherence, Phase and Gain. At 0.05 Hz MCAv and PCAv PSD during Indomethacin and hypocapnia interventions were reduced compared to the no intervention condition; at 0.10 Hz MCAv PSD during Indomethacin and hypocapnia interventions and PCAv PSD during the hypocapnia intervention were reduced compared to the no intervention condition (see Table 4.1. for details).

**Table 4.1.** Absolute and normalized point estimates of the power spectrum densities of MAP, MCAv, and PCAv during the squat-stand maneuvers for the three interventions.

	No Intervention	INDO	Hypocapnia
<b>Squat Stand (0.05 Hz)</b>			
MAP Power (mmHg) <sup>2</sup> /Hz	37884 ± 17586	29552 ± 14488	27741 ± 12256
MAP Power (%) <sup>2</sup> /Hz	51498 ± 30281	47176 ± 44840	50710 ± 34557
MCAv Power (cm/s) <sup>2</sup> /Hz	18617 ± 9625	5382 ± 4231*	5896 ± 4882*
MCAv Power (%) <sup>2</sup> /Hz	58312 ± 27093	27218 ± 18835*	28121 ± 20516*
PCAv Power (cm/s) <sup>2</sup> /Hz	10043 ± 5253	3518 ± 2661*	2244 ± 2979*
PCAv Power (%) <sup>2</sup> /Hz	50626 ± 23048	21982 ± 16680*	14478 ± 17027*
<b>Squat-Stand (0.10 Hz)</b>			
MAP Power (mmHg) <sup>2</sup> /Hz	24005 ± 9999	21161 ± 12534	18916 ± 10554
MAP Power (%) <sup>2</sup> /Hz	32417 ± 22947	29684 ± 28311	29080 ± 22642
MCAv Power (cm/s) <sup>2</sup> /Hz	21247 ± 11263	11339 ± 7820*	7860 ± 4567*
MCAv Power (%) <sup>2</sup> /Hz	60262 ± 22152	43819 ± 21599*	39642 ± 27029*
PCAv Power (cm/s) <sup>2</sup> /Hz	10989 ± 5357	5651 ± 3838	2637 ± 2098*
PCAv Power (%) <sup>2</sup> /Hz	48473 ± 20166	36269 ± 21913	16229 ± 13078*

Values are means ± SD. Indomethacin (INDO); mean arterial pressure (MAP); middle cerebral artery velocity (MCAv); posterior cerebral artery velocity (PCAv). Statistical significance was set at  $P < 0.05$ , \*denotes significance from No Intervention, †denotes significance from INDO intervention.

### *Instrumentation*

In this study both the middle and posterior cerebral arteries were insonated. Blood pressure was monitored with finger photoplethysmography. 3-lead electrocardiography was utilized to monitor R-R intervals. End-tidal gases were monitored with a gas analyzer. Please refer to sections 2.1. for more detail about these instruments.

### *Data Processing*

Please refer to section 2.2. (signal processing)

### *Power spectrum and transfer function analysis*

Please refer to section 2.2.1. (Fourier transform); 2.2.2. (transfer function analysis); 2.2.3. (coherence); 2.2.4. (phase); and 2.2.5. (gain) for more detail about these measures.

### *Statistical Analysis*

Statistical analyses were performed using PASW version 18.0 for Windows (PASW, Inc. Chicago, Illinois). The effects of trial (control, Indomethacin, hypocapnia) on MCA<sub>v</sub>, PCA<sub>v</sub>, heart rate, breathing frequency, blood pressure, P<sub>ET</sub>CO<sub>2</sub>, CVR<sub>i</sub> and TFA coherence, gain (absolute and normalized) and phase were assessed using a one-way repeated measures ANOVA with a Bonferroni correction for main effects and were run for each driven condition (0.05 Hz and 0.10 Hz). Comparisons between the anterior and posterior cerebral vessels were performed using paired T-tests with Bonferroni correction. Data are presented as mean ± SD for each 5-minute experimental condition, and  $P < 0.05$  are considered statistically significant.

#### 4.4. Results

There were no differences in  $P_{ET}CO_2$  ( $41.4 \pm 3.6$  vs  $40.3 \pm 2.3$  mmHg); MCAv ( $67.7 \pm 10.6$  vs  $66.4 \pm 10.4$  cm/s); PCAv ( $48.8 \pm 10.2$  vs  $47.3 \pm 9.7$  cm/s); blood pressure ( $84.1 \pm 11.6$  vs  $84.7 \pm 11.3$  mmHg) or HR ( $61.3 \pm 9.8$  vs  $63.2 \pm 10.4$  bpm) between baseline periods on either Day 1 and Day 2 of the experimental protocols.

##### *Cerebrovascular Responses (Table 4.2.)*

During the seated baseline trials there was a -32% and -31% reduction ( $P<0.001$ ) in MCAv and PCAv, respectively, during the Indomethacin intervention and a similar -34% and -37% reduction ( $P<0.001$ ) during the hypocapnia intervention. There were no changes in blood pressure across either of the interventions which, in conjunction with the reduced MCAv/PCAv, resulted in an increase in CVRi of  $\sim+50\%$  in both the anterior and posterior regions of the brain ( $P<0.001$ ). These alterations to the CBV occurred with (hypocapnia; 25.5 mmHg) and without (Indomethacin; 39.9 mmHg) a reduction in  $P_{ET}CO_2$ . There were no significant differences between breathing frequency between the control ( $13.8 \pm 4.4$  breaths / min) and Indomethacin ( $14.0 \pm 3.8$  breaths / min) baseline measures ( $P=0.990$ ), the hypocapnia breathing frequency ( $26.4 \pm 6.3$  breaths / min) was significantly higher than both the control intervention and Indomethacin trials by study design ( $P<0.001$ ). Although not significantly different, heart rate trended towards a reduction in the Indomethacin trial as compared with the control intervention condition ( $P=0.057$ ). Heart rate during the hypocapnia condition was higher than the Indomethacin trial ( $P<0.001$ ).

During the driven oscillations (representative trace shown in Figure 4.3.), compared to rest at 0.05 and 0.10 Hz, there was a reduction in both MCAv and PCAv of ~-20-30% ( $P<0.01$ ) during both experimental interventions that were independent of any alteration to blood pressure. The resulting increase in CVRi was similar in both the Indomethacin and hypocapnia interventions (~+20% in the MCAv and ~+30% in the PCAv;  $P<0.05$ ). There were no differences in heart rate during any of the experimental conditions at either 0.05 Hz ( $P>0.22$ ) or 0.10 Hz ( $P>0.23$ ). Breathing frequency was not different between the control and Indomethacin trials at either 0.05 Hz ( $P=0.797$ ) and 0.10 Hz ( $P=0.868$ ). By study design, the hypocapnia trials at both 0.05 Hz and 0.10 Hz had higher breathing frequency than both the control and Indomethacin trials ( $P<0.001$ ).

**Table 4.2.** Hemodynamic and cerebrovascular responses during squat-stand maneuvers.

	No Intervention	INDO	Hypocapnia
<b>Baseline (Sitting)</b>			
Blood Pressure (mmHg)	84.1 ± 11.6	85.4 ± 13.5	81.3 ± 9.2
MCAv (cm/s)	67.7 ± 10.6	45.5 ± 8.4*	44.7 ± 7.1*
MCA CVRi (mmHg/cm/s)	1.3 ± 0.3	1.9 ± 0.4*	1.9 ± 0.3*
PCAv (cm/s)	48.8 ± 10.2	33.6 ± 7.6*	30.5 ± 9.6*
PCA CVRi (mmHg/cm/s)	1.8 ± 0.5	2.6 ± 0.7*	2.9 ± 0.8*
End-Tidal PCO <sub>2</sub> (mmHg)	41.4 ± 3.6	39.9 ± 3.7	25.5 ± 4.7*†
Breathing frequency (per min)	13.8 ± 4.4	14.0 ± 3.8	26.4 ± 6.3*†
Heart Rate (bpm)	61.2 ± 9.8	52.6 ± 8.3	69.0 ± 12.5†
<b>Squat Stand (0.05 Hz)</b>			
Blood Pressure (mmHg)	92.4 ± 13.0	91.4 ± 16.3	89.7 ± 11.9
MCAv (cm/s)	59.9 ± 12.9	48.9 ± 9.7*	48.3 ± 7.5*
MCA CVRi (mmHg/cm/s)	1.6 ± 0.4	1.9 ± 0.4*	1.9 ± 0.3*
PCAv (cm/s)	45.4 ± 8.2	35.9 ± 8.1*	32.4 ± 7.5*
PCA CVRi (mmHg/cm/s)	2.1 ± 0.4	2.6 ± 0.7*	2.8 ± 0.7*
End-Tidal PCO <sub>2</sub> (mmHg)	38.9 ± 3.2	37.7 ± 3.5	25.8 ± 4.3*†
Breathing frequency (per min)	16.2 ± 4.5	17.5 ± 4.6	27.0 ± 7.0*†
Heart Rate (bpm)	86.3 ± 14.2	78.7 ± 12.5	84.5 ± 11.2
<b>Squat-Stand (0.10 Hz)</b>			
Blood Pressure (mmHg)	93.3 ± 15.4	91.2 ± 12.1	89.7 ± 11.1
MCAv (cm/s)	60.5 ± 13.8	50.0 ± 9.3*	48.1 ± 7.4*
MCA CVRi (mmHg/cm/s)	1.6 ± 0.4	1.9 ± 0.3*	1.9 ± 0.3*
PCAv (cm/s)	44.9 ± 8.5	36.2 ± 7.0*	33.1 ± 7.5*
PCA CVRi (mmHg/cm/s)	2.1 ± 0.5	2.6 ± 0.6*	2.7 ± 0.6*
End-Tidal PCO <sub>2</sub> (mmHg)	39.6 ± 4.4	38.0 ± 4.3	25.5 ± 4.2*†
Breathing frequency (per min)	17.0 ± 4.0	18.1 ± 5.0	28.7 ± 7.8*†
Heart Rate (bpm)	86.0 ± 12.9	79.0 ± 11.6	85.9 ± 11.2

Values are means ± SD. Middle cerebral artery velocity (MCAv); posterior cerebral artery velocity (PCAv); cerebrovascular resistance index (CVRi); beats per minute (bpm). Statistical significance was set at  $P < 0.05$ , \*denotes significance from No Intervention, †denotes significance from INDO intervention.

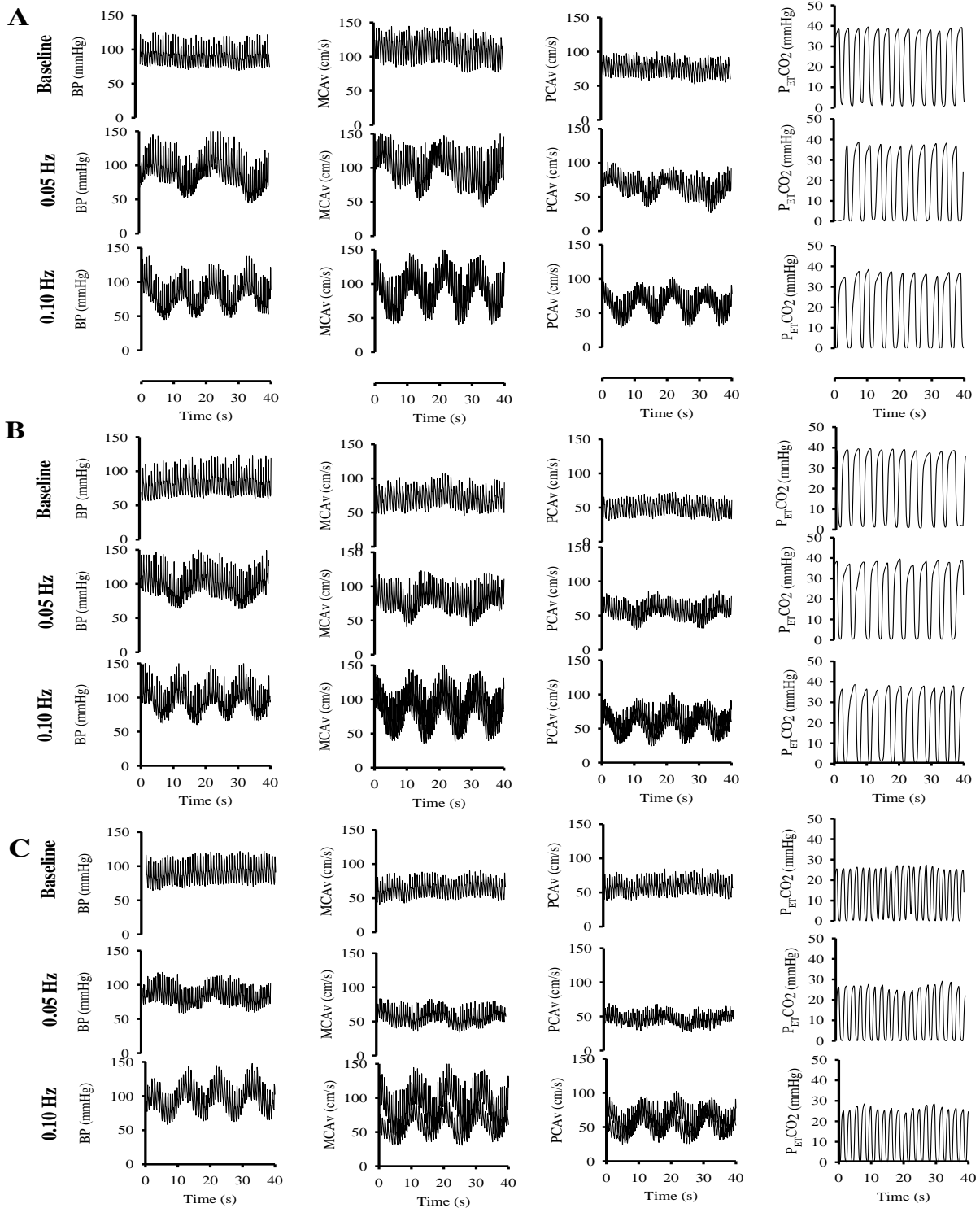


**Figure 4.3.** Representative individual data of the raw wave form highlighting the effects of the squat-stand maneuvers on blood pressure (BP), middle cerebral artery velocity (MCAv), posterior cerebral artery velocity (PCAv) and end-tidal CO<sub>2</sub> levels (P<sub>ET</sub>CO<sub>2</sub>). The data are presented under the no intervention (A), Indomethacin (B) and hypocapnia (C) experimental conditions.

*Transfer Function Analysis (MCA - Figure 4.4.A; PCA – Figure 4.4.B)*

When blood pressure was driven with the squat-stand maneuvers, coherence was increased at both frequencies (0.05 Hz and 0.10Hz) under all conditions to  $>0.92$  ( $P<0.001$ ). In the middle cerebral artery, gain was reduced  $\sim$ -40% at 0.05 Hz and  $\sim$ -20% at 0.10 Hz during the Indomethacin and hypocapnia interventions, as compared to baseline respectively. These reductions were also present in the posterior circulation as the posterior cerebral artery had reductions in absolute gain of -32% Indomethacin, -52% hypocapnia and -20% Indomethacin, -35% hypocapnia at 0.05 Hz and 0.10 Hz, respectively. When gain was normalized to % CBV, it was reduced in the Indomethacin and hypocapnia interventions at 0.05 Hz ( $P<0.001$ ), but not at 0.10 Hz ( $P>0.05$ ). At the point estimate of 0.05 Hz, phase was comparable (0.60 and 0.54 radians) for the anterior and posterior regions when there was no intervention ( $P>0.05$ ). Phase within both regions increased  $\sim$ +50% with the increased CVRi during the Indomethacin and hypocapnia interventions ( $P<0.001$ ). At 0.10 Hz, phase was once again comparable in both the anterior (0.33 radians) and posterior (0.29 radians) cerebral circulatory systems ( $P>0.05$ ). However, increased CVRi resulted in a greater phase lead in the middle cerebral artery (+72% Indomethacin, +85% hypocapnia) and posterior cerebral artery (+67% Indomethacin, +111% hypocapnia;  $P<0.001$ ).

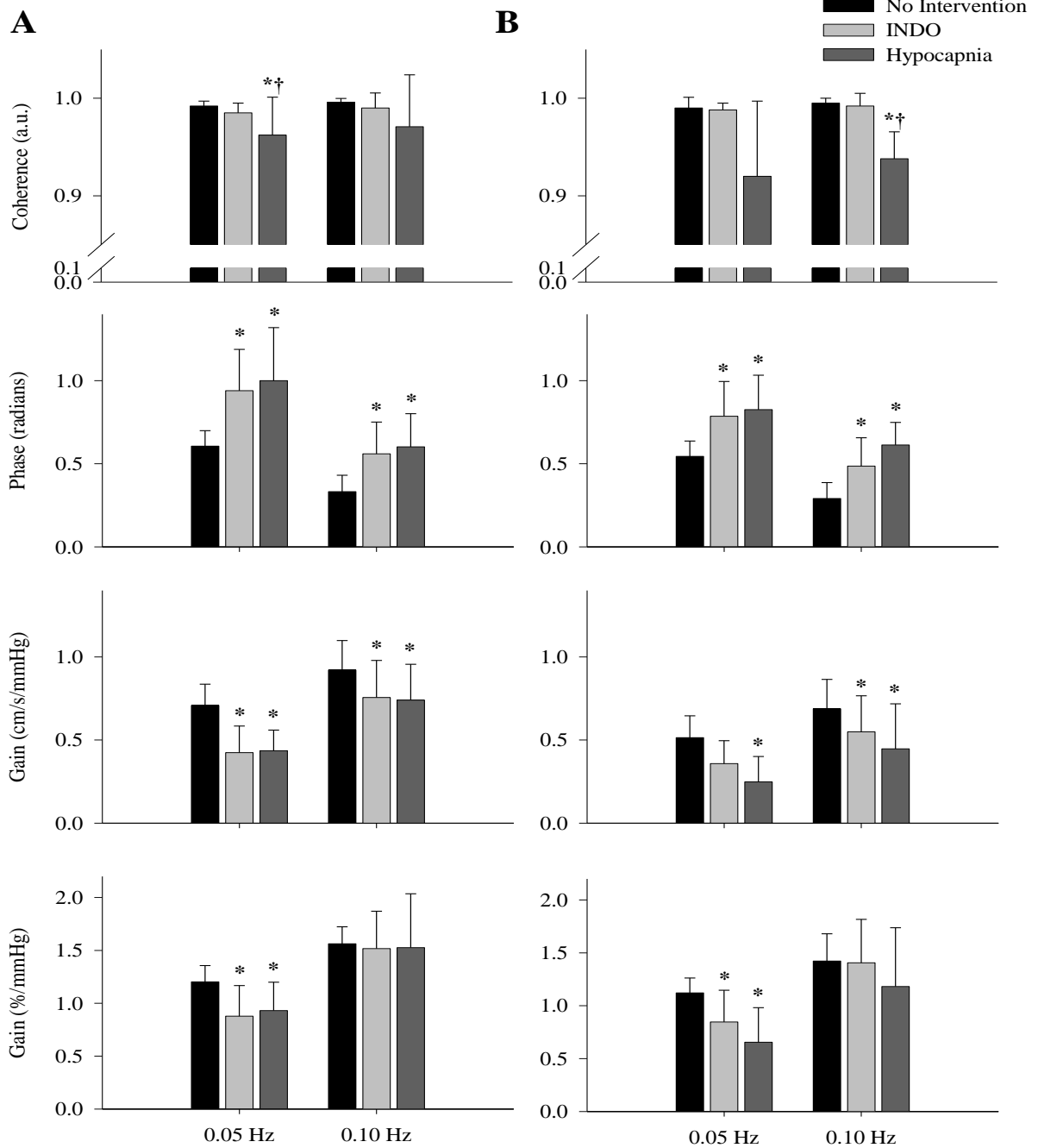


**Figure 4.4.** Transfer function analysis of coherence (top), phase (middle) and gain (bottom) for the group means of the middle cerebral artery (A) and posterior cerebral artery (B) driven oscillations during the three experimental conditions: No Intervention (black), Indomethacin (INDO: light grey), Hypocapnia (dark grey). \*denotes significance from No Intervention.

#### 4.5. Discussion

Using a novel approach to alter CVRi without changes to arterial blood pressure via pharmacological (Indomethacin) and physiological (Hyperventilation) interventions, the main findings of the study were: 1) that increases in CVRi, independent of alterations to  $P_{ET}CO_2$ , lead to increased TFA phase and decreased absolute gain at 0.05 and 0.10 Hz, and 2) the anterior and posterior cerebral regions had similar cerebral pressure-flow relationships. Collectively, these findings support our hypothesis and demonstrate that increases in CVRi affects dynamic cerebral pressure-flow relations in both the anterior and posterior regions of the brain; thus, CVRi is a factor that should be considered in the correct interpretation of cerebral pressure-flow dynamics as indexed using TFA metrics.

##### *Implications for the assessment and interpretation of pressure-flow relationships:*

The findings from this study are important for the understanding of how alterations to CVRi affect cerebral pressure-flow dynamics. For example, the impact of  $P_aCO_2$  is directly due to the changes in CVRi rather than an indirect influence of  $P_aCO_2$  per se. Thus, in situations where changes in CVRi occur naturally (e.g., CVRi increases with the development of hypertension)<sup>235,267</sup> it has been suggested that the increased cerebrovascular tone associated with the increased CVRi leads to altered TFA metrics (decreased absolute gain). Also, our data are consistent with the current literature<sup>267</sup> that when mathematically interpreting TFA metrics, it is important to maximize the blood pressure variability, thus increasing coherence and mitigating the confusion in interpreting TFA gain and phase metrics associated with lower coherence values. When input from the blood pressure variability was enhanced with the squat-stand maneuvers (Figures 4.1. and

4.2.), we observed uniform increases in phase and reductions in gain at both 0.05 Hz and 0.10 Hz point estimates. This indicates that there appears to be an altered cerebral pressure-flow response with increased CVRi (Figure 4.4.). Thus applying a methodology that employs increasing the blood pressure variability leads to an enhancement of the input signal (blood pressure), resulting in a more mathematically interpretable output values (phase, gain).<sup>267,270,271</sup> Our study also provides evidence that the anterior and posterior regions of the brain have similar pressure-flow relationships during changes in CVRi. These findings are considered further below in light of previous studies, potential mechanisms of action and relevant methodological considerations.

*Review of previous studies:*

Hypocapnia has been shown to affect the cerebral pressure-flow relationship in numerous studies under both steady-state<sup>176,189,270-275</sup> and dynamic<sup>176,189,272-275</sup> conditions. These studies took place within both healthy<sup>176,189,272,273</sup> and clinical populations (e.g., traumatic brain injury;<sup>270,272,273</sup> intracranial aneurism;<sup>37,38,268-271</sup> acute liver failure;<sup>271,274</sup> and during isoflurane anaesthesia<sup>274,276,277</sup>). The overall findings from these studies have demonstrated that cerebral vascular tone is an important protective mechanism in the regulation of CBF. In contrast to this hypocapnia literature, no studies have examined the dynamic cerebral pressure-flow response with Indomethacin. There have only been two studies<sup>276,277</sup> that have investigated the effects of Indomethacin via high dose intravenous infusion on the steady-state cerebrovascular response. Both of the steady-state studies involved clinical populations [e.g., very low birth weight preterm infants;<sup>276</sup> and severe head injured patients<sup>277</sup>]. However, unlike hypocapnia, the proposed mechanisms in the

two later studies were suggested to be due to the cerebral microvessels maintaining their ability to further vasodilate or constrict in response to other stimuli, in spite of the constrictive action of the drug. The commonality of all of these studies was that during periods of either hypocapnia ( $P_{ET}CO_2$  ~25-35 mmHg) and during Indomethacin treatment there were subsequent “improvements” in related cerebral pressure-flow responses.

The current study is the first to examine the effects of both hypocapnia and Indomethacin on pressure-flow relationships within the same population. To provide more interpretability to our TFA metrics, we induced large oscillations in blood pressure, thus increasing blood pressure variability (Figure 4.1. and 4.2.; Table 4.1.). With the increased blood pressure variability, coherence rose to a minimum of 0.92 during the squat-stand maneuvers (Figure 4.4.). Subsequently, the increased interpretability provided by the driven data within our study showed agreement with the previous studies;<sup>264,273,278</sup> specifically, that there were universal increases in phase lead and reductions in absolute gain (Figure 4.4.). There was a reduction in normalized gain at 0.05 Hz for the hypocapnia and Indomethacin interventions, but they were not significantly different than the control intervention group at 0.10 Hz (Figure 4.4.). A possible explanation for the apparent discrepancy in these findings is that there appears to be a frequency dependent normalized gain response to hypocapnia,<sup>125,279</sup> with reductions occurring around 0.05 Hz and no further alterations present with hypocapnia at 0.10 Hz. Our findings further emphasize those of Tzeng *et al.*,<sup>125</sup> as these alterations to normalized gain do not appear to be specific to hypocapnia, but are linked with increased CVRi as shown by the comparable findings within the Indomethacin intervention. This provides further confirmation that reporting

TFA gain in absolute vs normalized units can alter the interpretation of the findings.  
18,125,263

The findings within the pharmacological portion of the current study were not entirely consistent with the findings by Zhang *et al.*<sup>264</sup>. The conflicts between the two studies could be a result of the different mechanisms by which phenylephrine ( $\alpha_1$ -adrenoreceptor agonist), and Indomethacin (a non-selective cyclooxygenase 1 and 2 inhibitor) and hypocapnia (cerebral vasoconstriction) increase CVRi. Phenylephrine likely does not cross the blood-brain barrier, and thereby does not *directly alter* the cerebral arterioles.<sup>18,29,125,264-266,280</sup> Phenylephrine instead increases the CVRi indirectly through mechanoregulation<sup>29,264,281</sup> via constriction of the smooth muscle in the peripheral vasculature, which in turn increases systemic blood pressure. In contrast, Indomethacin and hypocapnia both alter CVRi *directly* via constriction of the cerebrovascular arterioles,<sup>265,272,275,281</sup> thus reducing CBV without altering systemic blood pressure. It is the similar manner by which both Indomethacin and hypocapnia influence CVRi which make them ideal to explore the mechanism(s) by which CVRi is able to influence cerebral pressure-flow dynamics.

*Mechanisms by which CVRi may influence the cerebral pressure-flow relationship:*

The results from this study indicate that the changes in the pressure-flow regulation (and possibly CA) are likely related to changes in CVRi rather than the previously reported hypocapnia<sup>229,264-266,272,275</sup> (Table 4.1.). Thus, we propose that the most likely cause for the alterations in the TFA metrics are due to the enhanced arteriolar tone in the cerebral vasculature. These findings are broadly consistent with previous studies that have revealed

TFA gain and phase parameters are determined by cerebrovascular properties such as vascular compliance and/or resistance.<sup>120-122,229,264,282</sup> However, we do also note that there is a possibility that both the hypocapnia and Indomethacin interventions could cause alterations to the cerebral pressure-flow dynamics independent of the alterations in CVRi. In this case, we acknowledge that alterations to CVRi would be without an existing physiological or physical causation mechanism that would link increased CVRi to the altered TFA metrics.

*Regional differences in cerebral pressure-flow regulation:*

To date the vast majority of the research on the regulation between blood pressure and CBV has focused solely on the middle cerebral artery and related anterior cerebral regions, whereas there has been relatively little research on the posterior cerebral circulation. Whilst one report indicated that pressure-flow relationships in the posterior cerebral artery are less efficient compared to the middle cerebral artery,<sup>120,123,282,283</sup> another revealed that alterations to the pressure-flow relationships within the posterior cerebral artery are likely the result of metabolic vasodilation and not an inherent difference in the autoregulatory characteristics of the posterior circulation.<sup>123,124,283,284</sup> Yet another study has shown that under general anaesthesia, the anterior and posterior regions of the brain have similar CO<sub>2</sub> reactivity and static cerebral autoregulation responses.<sup>18,124,125,284</sup> Our findings build upon these previous results and are the first to reveal that there are similar dynamic pressure-flow relationships present in the anterior and posterior cerebral circulatory systems (Figure 3.4.). This notion indicates that there are likely similar cerebral pressure-flow mechanisms present in both the anterior and posterior regions and highlights

the related importance of monitoring CVRi rather than just focusing on the effects of hypocapnia when reporting TFA metrics.

*Methodological Considerations:*

*Cerebral Autoregulation:* There has yet to be a firmly established gold standard for the evaluation of CA, <sup>18,125,190,267</sup> as such the discussion in this paper was not focused on interpreting our TFA findings as they relate to cerebral autoregulation. Instead the findings were focused solely on the relationship present between blood pressure and CBV. We chose to statistically quantify and assess this relationship via the linear analysis method of TFA. We feel that it is important to note that despite the widespread use of TFA to assess ‘dynamic’ cerebral autoregulation within the literature, it is extremely unlikely that the entire cerebral autoregulation response can be quantified through a linear model. There will be other co-contributing factors to the cerebral autoregulation response such as: cerebrovascular compliance, downstream capacitance, intracranial pressure, and venous outflow modulation. With the view that there are likely non-linear complexities that can confound the spontaneous cerebral autoregulation metrics, one may wonder why we chose to utilize TFA to assess this relationship and our rationale is explained next.

*Transfer Function Analysis:* Interpretation of TFA output metrics (phase and gain) are related to the overall coherence present within the analysis, as coherence represents the shared variance between the phase and gain metrics. In order to improve the mathematical interpretability and reliability of the TFA outputs within the VLF and LF, <sup>38,125,190,267-269</sup> we increased the input into the system (blood pressure variability) via squat-stand maneuvers

(Table 4.2. & 4.3.). Squat-stand maneuvers create very large swings in blood pressure (Figure 4.1.), which in turn enhance the input/output response within the cerebral pressure-flow relationship creating a nearly linear relationship (coherence values for the driven data in this study were  $>0.92$  a.u.). Through the application of this methodology we have increased the linearity of the cerebral pressure-flow relationship for mathematical interpretational purposes. Moreover, we view such blood pressure challenges as more realistic representation of daily activities (e.g., postural changes, coughing, exercise, etc.) and make our data set more physiologically meaningful. For the above reasons we have focused our discussion on the dynamic relationship between blood pressure and CBV instead of cerebral autoregulation. The data presented in this study, further confirms that the interpretation of the TFA gain findings can be altered based on reporting the results in absolute or normalized units.<sup>3,125</sup>

*Flow vs velocity:* The main assumption of transcranial Doppler is that the relative changes in MCAv (and PCAv) directly represent relative changes in the blood flow within this artery; however, at least during situations of normal blood pressure and arterial blood gases the majority of research suggests that transcranial Doppler provides a reliable index of CBF [reviewed in:<sup>38,204,285</sup>]. We also know of no evidence to suggest that Indomethacin may alter the diameter of the middle or posterior cerebral arteries. For example, previous studies using magnetic resonance imaging have demonstrated that Indomethacin causes a similar percentage change in global CBF and MCAv.<sup>235,267,285</sup>

#### **4.6. Key finding**

We have demonstrated for the first time that increases in CVRi, independent of alterations to  $P_a\text{CO}_2$  or systemic blood pressure, are associated with altered cerebral pressure-flow relationship as reflected by the universally increased phase and decreased absolute gain. There are similar autoregulatory mechanisms present in the anterior and posterior cerebral circulatory systems. Collectively, these findings indicate that changes in CVRi will result in changes to the TFA metrics associated cerebral pressure-flow relationships and as such CVRi should be considered in the correct interpretation of TFA metrics. These findings are important for our furthering our understanding of the mechanisms underlying the cerebral pressure-flow relationships in the human cerebral circulation and how these responses are commonly interpreted.

## **Chapter Five: Influence of long-term heart transplantation**

This study was approved by the clinical ethical committees of the Universities of British Columbia (H11-02576) and Alberta (Proooo11560), and adhered to the principles of the Declaration of Helinski and Title 45, U.S. Code of Federal Regulations, Part 46, Protection of Human Subjects. All volunteers provided written informed consent and procedures were followed in accordance to institutional guidelines.

A version of this study was accepted and presented as a poster at the CARNet 2014 (annual scientific meeting of the cerebral autoregulation research network). Jonathan D. Smirl, Mark J. Haykowsky, Michael D. Nelson, Yu-Chieh Tzeng, Katelyn R. Marsden, Helen Jones, and Philip N. Ainslie. (2014) The relationship between cerebral blood flow and blood pressure in long-term heart transplant recipients. Jonathan Smirl was responsible for the data collection, data analysis, writing, and formatting of the abstract.

A version of this manuscript has been accepted and published in *Hypertension* and has been reproduced with permission. <sup>2</sup> Relationship between cerebral blood flow and blood pressure in long-term heart transplant recipients. Jonathan D. Smirl, Mark J. Haykowsky, Michael D. Nelson, Yu-Chieh Tzeng, Katelyn R. Marsden, Helen Jones, and Philip N. Ainslie. Jonathan Smirl was responsible for the data collection, data analysis, writing, and formatting of the manuscript.

## **5.1. Aims and Hypotheses**

### **Aims:**

- 1) To investigate the cardiac baroreceptor sensitivity in long-term heart transplant patients to determine if this system has a role in the regulation of cerebral blood flow.
- 2) To investigate the relationship between arterial blood pressure and cerebral blood flow in long-term heart transplant recipients. In control for the effects of the cardiac allograft, we used a donor control population; to control for the influence of age, we used age-matched controls.

### **Hypotheses:**

- 1) The long-term heart transplant recipients would have reduced cardiac baroreceptor sensitivity due to the denervation of the allograft during surgery.
- 2) The long-term heart transplant recipients would have an altered cerebral pressure-flow response that is independent of the healthy human aging process.

## 5.2. Rationale

The longevity of heart transplant recipients has increased from 18 days following the first heart transplantation surgery<sup>167</sup> to a current mean survival expectancy of over 10.5 years.<sup>168</sup> The improved survival has led to alterations in the long-term functional outcomes post transplantation. For example, neurological impediments develop in approximately 60-80% of heart transplant recipients,<sup>169-171</sup> and have a 14-18% greater occurrence rate of cerebral hemorrhage or ischemic stroke.<sup>169,171,172</sup> The exact mechanism for these derangements however remains to be elucidated; however, adverse events may be the direct consequence of life-long immunosuppressant therapy,<sup>173</sup> or vascular remodelling secondary to chronic cerebral hypoperfusion associated with pre-transplant heart failure.<sup>170,171,174</sup>

We asked whether alterations in cerebral pressure-flow dynamics could also explain the increased risk. Indeed, because of cardiac allograft, there are marked reductions in heart rate variability<sup>286,287</sup> and baroreceptor sensitivity (BRS),<sup>286</sup> which could lead to unstable control of blood pressure in this clinical population. Evidence indicates that the responses of the cerebral vessels in some animals<sup>288</sup> and humans<sup>289</sup> are likely influenced by a coordinated reaction of the cardiovascular system as a whole especially when there are disturbances to the blood or oxygen supply to the brain.<sup>59</sup> Moreover, both animal<sup>290,291</sup> and human<sup>289</sup> studies have demonstrated the inverse relationship between cardiac BRS and dynamic cerebral autoregulation. In other words, at least in healthy young humans, dynamic cerebral autoregulation may compensate for reductions in cardiac BRS and vice-versa. These concepts have not been explored in a clinical model (e.g., the heart transplant recipient) where cardiac baroreceptor function is markedly reduced or abolished. Thus,

research is warranted in the long-term heart transplant recipient population to determine the impact of marked reductions in cardiac autonomic control on cerebral blood flow regulation.

Accordingly, we examined the dynamic relationship between beat-to-beat changes in blood pressure and cerebral blood flow in long-term heart transplant recipients under spontaneous conditions, as well as during frequency dependent squat-stand maneuvers. To control for the influence of heart transplantation *per se*, we compared patients with donor controls. To control for the influence of age, heart transplant recipients were also compared to a group of age-matched controls. We hypothesized that heart transplant recipients would have reduced BRS, and altered cerebral pressure-flow dynamics, independent of age.

### **5.3. Methods**

#### *Participants*

Eight male clinically stable heart transplant recipients ( $62 \pm 8$  years of age,  $9 \pm 7$  years post-transplant), 9 male age-matched controls ( $63 \pm 8$  years) and 10 male donor controls ( $27 \pm 5$  years), were recruited for this study (Table 4.1.). Seven of the eight heart transplant recipients were ischemic pre-surgery etiology. All subjects were extensively screened by the attending cardiologist for any clinical history of respiratory, cardiovascular or cerebrovascular diseases. Resting and exercise echocardiograms were performed by a cardiologist on all participants. In addition, we screened (via an transcranial Doppler examination) the anterior intra-cranial vessels for any signs intra-cranial stenosis; all subjects had normal examination results as indicated by normal intra-cranial velocity profiles.<sup>38</sup> All subjects were carefully screened for activity levels, withdrew from caffeine

and alcoholic beverages for a period of 12 hours prior to the study and all medications were maintained for the study. Each subject underwent a familiarization of the laboratory and testing protocols.

### *Experimental Protocols*

At least 5-minutes of resting spontaneous baseline data were recorded in the seated position. These data were used for spectral analysis of spontaneous oscillations in blood pressure and cerebral blood flow velocity. Next the subjects performed repeated squat-stand maneuvers. The subjects mimicked the experimenter in performing these maneuvers. In random order, subjects then performed squat-stand maneuvers at 0.05 Hz (10 second squat–10 second stand) and then 0.10 Hz (5 second squat–5 second stand) for 5 minutes, with a 5-minute rest period to return to baseline levels in between trials. These data were used for the spectral analysis of the driven oscillations in blood pressure and MCAv and were performed to increase the blood pressure variability, resulting in increased coherence (allowing for a more robust mathematical assessment of the phase and gain metrics).<sup>3</sup> End tidal gases were monitored to ensure that normal breathing occurred and Valsalva-like maneuvers were avoided.

**Table 5.1.** Participant characteristics

	<b>HTR (n=8)</b>	<b>AM (n=9)</b>	<b>DC (n=10)</b>
Age (years)	62 ± 8	63 ± 8	27 ± 5 †‡
Body Mass Index (kg/m <sup>2</sup> )	27 ± 4	26 ± 3	26 ± 5
Years after transplantation	9 ± 7		
Medications			
Corticosteroid	2		
Antiproliferative agent	4		
Calcinerurin inhibitor	4		
mTOR inhibitor	4		
Ca <sup>2+</sup> channel blocker (diltiazem)	5	2	
ACE inhibitor	4	1	
Diuretic	3	1	
Aspirin	6	2	
Lipid –lowering agent	4		

Values are means ± SD. Seven HTR subjects were ischemic pre-surgery etiology, one was non-ischemic etiology. Heart transplant recipient (HTR); age-matched (AM); donor control (DC); target of rapamycin (TOR); angiotensin-converting enzyme (ACE). Statistical significance was set at  $P < 0.05$ , †denotes significance between HTR vs. DC, ‡denotes significance between AM vs. DC.

### *Instrumentation*

In this study both the right and left middle cerebral arteries were insonated. Blood pressure was monitored with finger photoplethysmography. 3-lead electrocardiography was utilized to monitor R-R intervals. End-tidal gases were monitored with a gas analyzer. Please refer to sections 2.1. for more detail about these instruments.

### *Data Processing*

Please refer to section 2.2. (signal processing)

### *Power spectrum and transfer function analysis*

Please refer to section 2.2.1. (Fourier transform); 2.2.2. (transfer function analysis); 2.2.3. (coherence); 2.2.4. (phase); and 2.2.5. (gain) for more detail about these measures.

### *R-R Interval and Cardiac Baroreceptor Sensitivity Gain*

From the electrocardiogram and blood pressure waveform, the time of each R wave, and beat-to-beat values of systolic blood pressure are determined. The cardiac period (R-R interval) time series will be checked for the presence of artefacts, and spuriously detected or missed R waves are corrected by linear interpolation. Power spectral analysis is performed on the R-R interval and systolic blood pressure. Both the R-R interval and beat-to-beat systolic blood pressure are high pass filtered to remove fluctuations of  $<0.015$  Hz, low pass filtered to exclude components of  $>2$  Hz (Nyquist frequency), and re-sampled at 4 Hz. These series are then passed through a Hanning window and subject to discrete Fourier transform analysis. Spontaneous LF gain will be assessed in the range of 0.04-0.15 Hz and

driven cardiac BRS gain will be assessed from the 0.10 Hz squat-stand manoeuvre. This method has been previously validated against the modified Oxford method.<sup>278</sup>

#### *Critical Closing Pressure and Pulsatility Index Calculations*

Critical closing pressure was calculated by the linear extrapolation of the cerebral blood flow velocity and blood pressure relationship below the diastolic values to the zero-flow pressure.<sup>279</sup> Pulsatility index was calculated as:  $(\text{systolic MCAv} - \text{diastolic MCAv}) / \text{mean MCAv}$ .

#### *Statistical Analysis*

Statistical analyses were performed using SPSS version 20.0. The effects of condition (spontaneous resting, 0.05 Hz, 0.10 Hz) or Group (heart transplant recipients, age-matched, donor-controls) on cerebral blood flow velocity, Heart Rate, blood pressure (mean and systolic),  $P_{\text{ETCO}_2}$ , CVRi, critical closing pressure, pulsatility index and TFA coherence, normalized gain and phase were assessed using a one-way ANOVA with a post hoc Tukey comparison for group effects. Bivariate correlations between BRS gain and TFA coherence, normalized gain and phase were performed using Pearson Product Moment. Data are presented as mean  $\pm$  SD.

## 5.4. Results

### *Demographics (Table 5.1 and 5.2)*

There were no significant differences between groups for body mass index (Table 5.1). By study design, donor-controls were significantly younger than heart transplant recipients and age-matched controls. During the seated baseline testing and both driven frequencies (0.05 Hz and 0.10 Hz) mean arterial pressure, systolic blood pressure, pulse pressure and  $P_{ET}CO_2$  levels were comparable for all groups (Table 4.2). Critical closing pressures for all subjects were physiologically relevant values (all positive) and were comparable between all groups. Resting heart rate was reduced in the age-matched controls ( $68 \pm 13$  bpm) and donor-controls ( $63 \pm 8$  bpm) compared to heart transplant recipients ( $91 \pm 8$  bpm).  $MCA_v$  was reduced in both older populations (heart transplant recipients  $41 \pm 8$ ; age-matched  $42 \pm 8$  cm/s) compared to donor-controls ( $62 \pm 7$  cm/s). Pulsatility index (arbitrary units) at rest was reduced in the heart transplant recipients ( $0.83 \pm 0.12$ ) compared to both the age-matched ( $1.01 \pm 0.17$ ) and donor ( $1.02 \pm 0.11$ ) controls. During the driven protocols, heart rate was similarly elevated in the heart transplant recipients compared to age-matched and donor-controls and the  $MCA_v$  was reduced compared to the donor-controls, pulsatility index was comparable for all groups (Table 5.2). The older populations (2.2-2.3 mmHg/cm/s) had an elevated  $CVR_i$  compared to the younger group (1.4-1.5 mmHg/cm/s) across all testing protocols.

Representative data tracing – that was similar between groups – of blood pressure,  $MCA_v$  and  $P_{ET}CO_2$  for the seated baseline, 0.05 Hz and 0.10 Hz squat-stand manoeuvres from a heart transplant recipient are shown in Figure 5.1. As shown in Figure 5.1., the

squat-stand maneuvers evoked clear oscillations in both blood pressure and MCAv, whereas  $P_{ET}CO_2$  levels were well maintained in all groups (Table 5.2.).

*Cardiac Baroreceptor Sensitivity (Table 5.3.)*

The donor-controls had a significantly higher spontaneous BRS LF gain ( $10.8 \pm 5.1$  ms/mmHg) compared to both the heart transplant recipients ( $1.4 \pm 1.2$  ms/mmHg;  $p < 0.01$ ) and the age-matched controls ( $4.4 \pm 1.8$  ms/mmHg;  $p < 0.01$ ). The heart transplant recipients also had a significantly reduced BRS LF gain as compared to the age-matched controls (Table 5.3.). During the 0.10 Hz squat-stand manoeuvres, all groups were significantly different (heart transplant recipients  $0.2 \pm 0.1$  ms/mmHg; age-matched  $2.0 \pm 0.9$  ms/mmHg; donor-controls  $3.9 \pm 1.0$  ms/mmHg;  $p < 0.03$ , Table 5.3.). The donor-controls showed a marked elevation in their R-R interval power spectrum density when compared with both the heart transplant recipients ( $p < 0.01$ ) and age-matched controls ( $p < 0.05$ ) in the spontaneous and driven LF ranges (Table 5.3.). The R-R interval power spectrum density for the age-matched controls was also elevated when compared with the heart transplant recipients (Table 5.3.).

**Table 5.2.** Hemodynamic and Cerebrovascular Responses During Squat-Stand Maneuvers

	HTR	AM	DC
<b>Baseline (Sitting)</b>			
MAP (mmHg)	97 ± 8	99 ± 12	93 ± 5
Pulse Pressure (mmHg)	41 ± 16	55 ± 28	47 ± 17
MCAv (cm/s)	41 ± 8	42 ± 8	62 ± 7*†
Pulsatility Index (a.u.)	0.8 ± 0.1	1.0 ± 0.2*	1.0 ± 0.1*
CVRi (mmHg/cm/s)	2.3 ± 0.5	2.3 ± 0.5	1.4 ± 0.2*†
CrCP (mmHg)	47 ± 19	46 ± 16	48 ± 17
Heart Rate (bpm)	91 ± 8	68 ± 13*	63 ± 8*
End-Tidal PCO <sub>2</sub> (mmHg)	36 ± 7	36 ± 4	38 ± 2
<b>Squat Stand (0.05 Hz)</b>			
MAP - Squat (mmHg)	122 ± 17	122 ± 15	111 ± 10
MAP - Stand (mmHg)	78 ± 18	78 ± 15	78 ± 12
Systolic BP – Squat (mmHg)	202 ± 38	193 ± 28	174 ± 19
Systolic BP – Stand (mmHg)	141 ± 51	134 ± 30	132 ± 17
Pulse Pressure - Squat (mmHg)	122 ± 33	107 ± 25	94 ± 15
Pulse Pressure - Stand (mmHg)	94 ± 51	83 ± 26	80 ± 12
MCAv (cm/s)	43 ± 7	44 ± 8	62 ± 8*†
Pulsatility Index - Squat (a.u.)	0.9 ± 0.2	0.8 ± 0.2	0.8 ± 0.1
Pulsatility Index - Stand (a.u.)	1.6 ± 0.3	1.3 ± 0.4	1.5 ± 0.3
CVRi (mmHg/cm/s)	2.3 ± 0.4	2.2 ± 0.5	1.5 ± 0.2*†
Heart Rate (bpm)	105 ± 11	78 ± 14*	79 ± 8*
End-Tidal PCO <sub>2</sub> (mmHg)	37 ± 7	36 ± 3	40 ± 3
<b>Squat-Stand (0.10 Hz)</b>			
MAP - Squat (mmHg)	123 ± 20	128 ± 12	115 ± 10
MAP - Stand (mmHg)	78 ± 11	82 ± 10	75 ± 10
Systolic BP – Squat (mmHg)	204 ± 34	202 ± 26	181 ± 16
Systolic BP – Stand (mmHg)	150 ± 32	141 ± 20	132 ± 18
Pulse Pressure - Squat (mmHg)	120 ± 26	111 ± 26	98 ± 13
Pulse Pressure - Stand (mmHg)	107 ± 34	88 ± 19	84 ± 14
MCAv (cm/s)	43 ± 9	44 ± 7	62 ± 8*†
Pulsatility Index - Squat (a.u.)	0.9 ± 0.2	0.8 ± 0.2	0.8 ± 0.1
Pulsatility Index - Stand (a.u.)	1.6 ± 0.3	1.4 ± 0.4	1.6 ± 0.3
CVRi (mmHg/cm/s)	2.3 ± 0.3	2.3 ± 0.5	1.5 ± 0.2*†
Heart Rate (bpm)	106 ± 10	82 ± 14*	80 ± 8*
End-Tidal PCO <sub>2</sub> (mmHg)	37 ± 6	38 ± 4	40 ± 4

Values are means ± SD. Heart transplant recipient (HTR); age-matched (AM); donor control (DC); mean arterial pressure (MAP); blood pressure (BP); arbitrary units (a.u.); middle cerebral artery velocity (MCAv); cerebrovascular resistance index (CVRi). Statistical significance was set at  $P < 0.05$ , \*denotes significance from HTR, †denotes significance from AM.

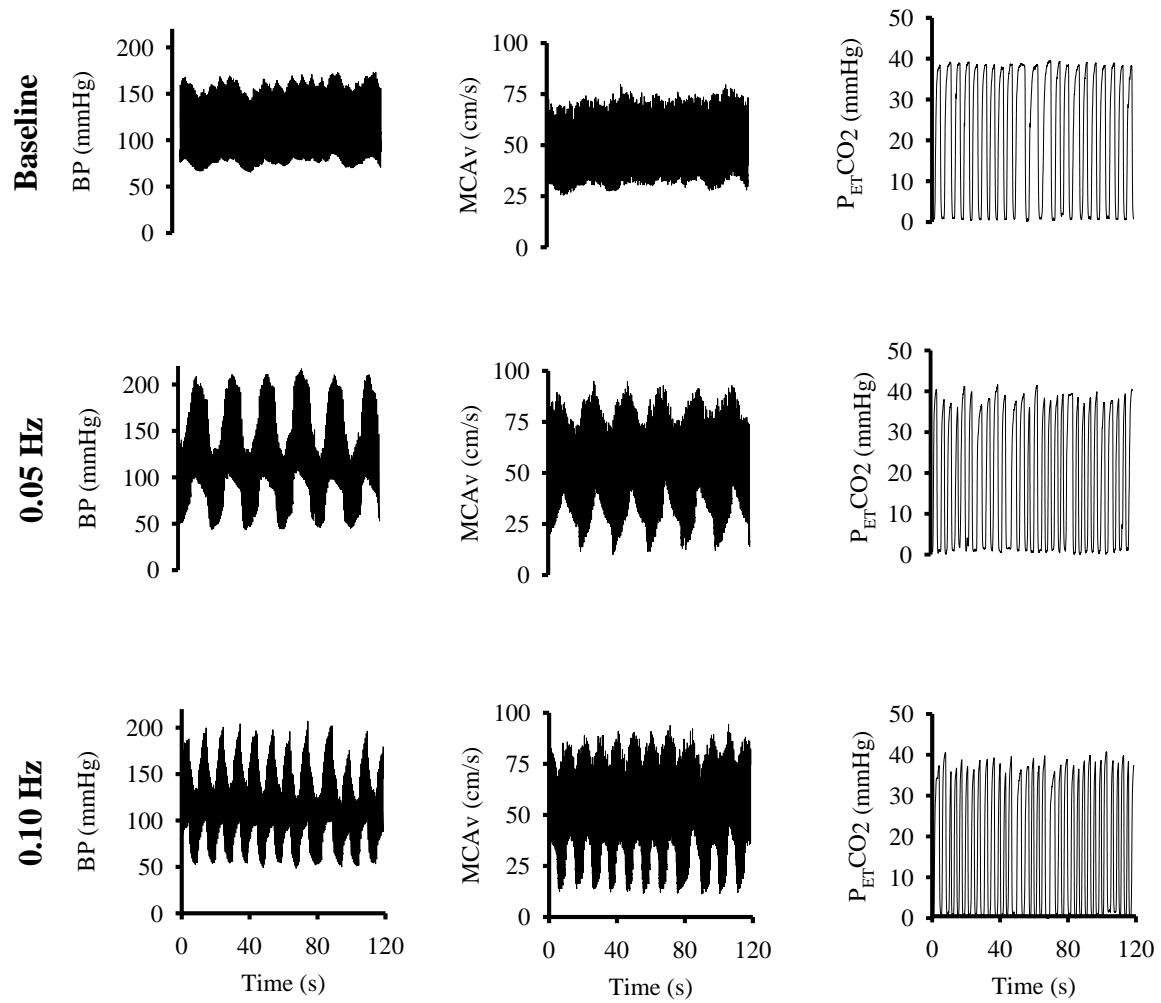


**Figure 5.1.** Typical trace for blood pressure (BP), middle cerebral artery velocity (MCAv) and end-tidal CO<sub>2</sub> (P<sub>ET</sub>CO<sub>2</sub>) during spontaneous (top), 0.05 Hz (middle) and 0.10 Hz (bottom) trials, in a long-term heart transplant recipient.

**Table 5.3.** Transfer function analysis for cardiac baroreceptor sensitivity.

	HTR	AM	DC
<b>Baseline (Sitting)</b>			
LF RRI Power (ms <sup>2</sup> )	23 ± 15	726 ± 665*	2842 ± 2920*†
BRS LF Gain (ms/mmHg)	1.4 ± 1.2	4.4 ± 1.8*	10.8 ± 5.1*†
<b>Squat-Stand (0.10 Hz)</b>			
RRI Power (ms <sup>2</sup> )/Hz	1255 ± 1155	97773 ± 91881*	420052 ± 266339*†
BRS Gain (ms/mmHg)	0.2 ± 0.1	2.0 ± 0.9*	3.9 ± 1.0*†

Values are means ± SD. Age-Match Control (AM); Baroreceptor Sensitivity (BRS); Donor-Control (DC); Heart Transplant Recipient (HTR); R-R Interval (RRI); middle cerebral artery velocity (MCAv); low frequency (LF; 0.04-0.15 Hz). Statistical significance was set at  $P < 0.05$ , \*denotes significance from HTR, †denotes significance from AM.

*Cerebral Pressure-Flow Dynamics (Table 5.4.)*

There were no differences between the groups (heart transplant recipients, age-matched and donor-controls) when comparing the power spectrums for mean arterial pressure or MCAv in either the VLF or LF ranges, during spontaneous (Figure 5.2.) and driven conditions (Figure 5.3.). The mean arterial pressure and MCAv power spectrum density was significantly increased during the squat-stand manoeuvres for all groups (Table 5.4.).

**Table 5.4.** Transfer function analysis between blood pressure and MCAv.

	HTR	AM	DC
<b>Baseline (Sitting)</b>			
VLF MAP Power (mmHg <sup>2</sup> )	8.26 ± 5.12	8.81 ± 7.62	8.55 ± 4.59
LF MAP Power (mmHg <sup>2</sup> )	6.75 ± 4.71	5.09 ± 5.42	5.94 ± 3.16
VLF MCAv Power (cm/s) <sup>2</sup>	3.07 ± 2.06	3.28 ± 3.81	5.32 ± 3.27
LF MCAv Power (cm/s) <sup>2</sup>	2.78 ± 2.54	3.45 ± 6.19	6.07 ± 4.38
VLF Coherence	0.60 ± 0.24	0.66 ± 0.18	0.55 ± 0.16
LF Coherence	0.79 ± 0.09	0.71 ± 0.16	0.83 ± 0.05
VLF Phase (radians)	0.83 ± 0.42	0.88 ± 0.35	0.92 ± 0.43
LF Phase (radians)	0.42 ± 0.19	0.47 ± 0.16	0.57 ± 0.17
VLF Gain (%/mmHg)	1.11 ± 0.37	1.14 ± 0.34	1.24 ± 0.29
LF Gain (%/mmHg)	1.50 ± 0.26	1.64 ± 0.45	1.63 ± 0.24
<b>Squat Stand (0.05 Hz)</b>			
MAP Power (mmHg <sup>2</sup> )/Hz	35423 ± 16637	32695 ± 15483	18639 ± 13019
MCAv Power (cm/s) <sup>2</sup> /Hz	6410 ± 3582	6525 ± 2950	8305 ± 4839
Coherence	0.99 ± 0.01	0.98 ± 0.02	0.98 ± 0.01
Phase (radians)	0.65 ± 0.19	0.49 ± 0.19	0.73 ± 0.21
Gain (%/mmHg)	1.05 ± 0.32	1.03 ± 0.20	1.16 ± 0.21
<b>Squat-Stand (0.10 Hz)</b>			
MAP Power (mmHg <sup>2</sup> )/Hz	21450 ± 7115	23389 ± 11799	14040 ± 7870
MCAv Power (cm/s) <sup>2</sup> /Hz	6534 ± 3426	8893 ± 5863	11549 ± 5285
Coherence	0.99 ± 0.01	0.99 ± 0.02	0.99 ± 0.01
Phase (radians)	0.38 ± 0.10	0.31 ± 0.18	0.41 ± 0.12
Gain (%/mmHg)	1.29 ± 0.24	1.34 ± 0.48	1.53 ± 0.25

Values are means ± SD. Age-Match Control (AM); Donor-Control (DC); Heart Transplant Recipient (HTR); mean arterial pressure (MAP); middle cerebral artery velocity (MCAv); very low frequency (VLF; 0.02-0.07 Hz); low frequency (LF; 0.07-0.20 Hz). Statistical significance was set at  $P < 0.05$ , \*denotes significance from HTR, †denotes significance from AM.

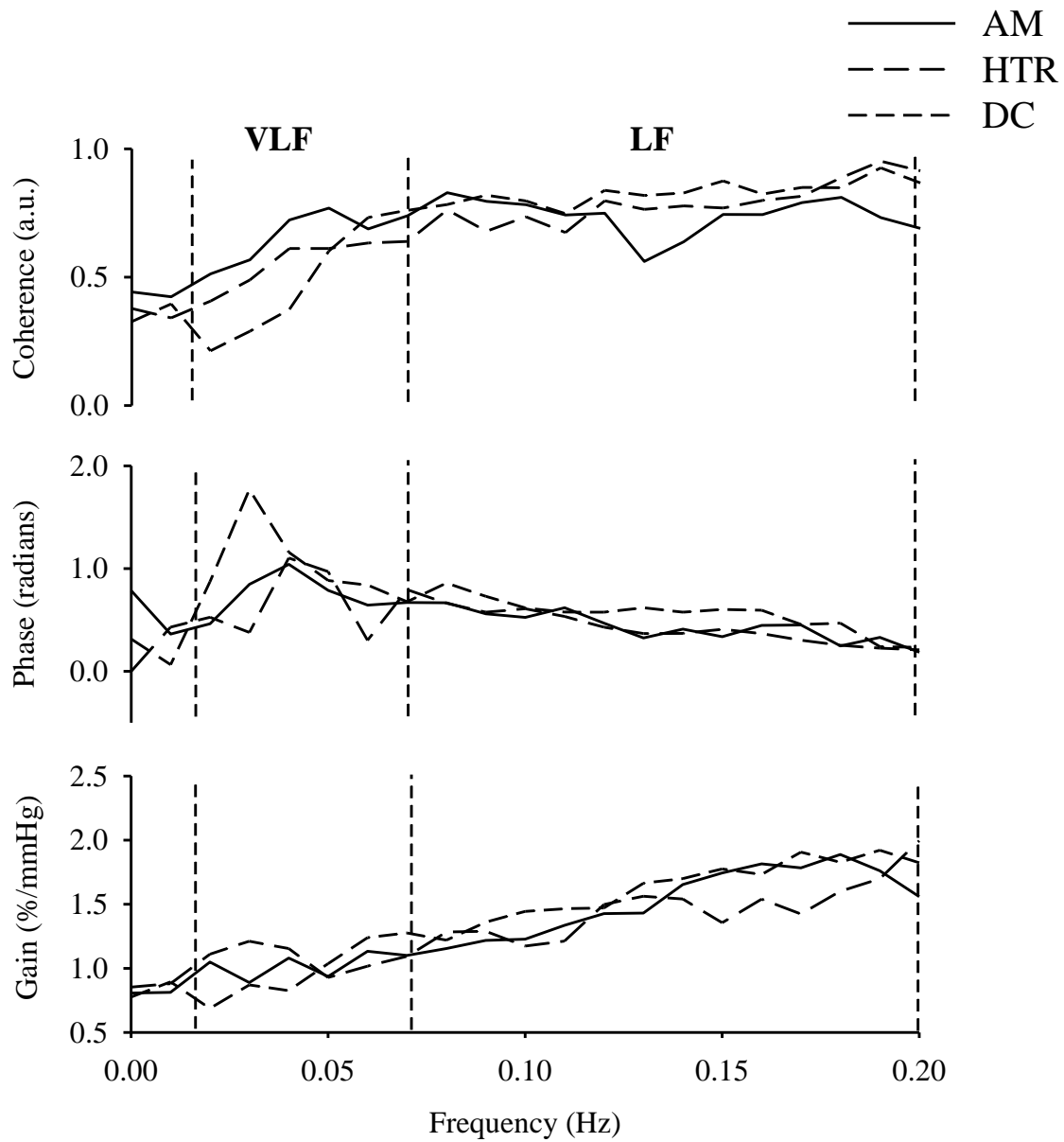


**Figure 5.2.** MCAv transfer function analysis of coherence, phase, and normalized gain in the very low frequency (VLF) and low frequency (LF) for the group means of the spontaneous data for the three group: AM (solid), HTR (long dash), DC (short dash).

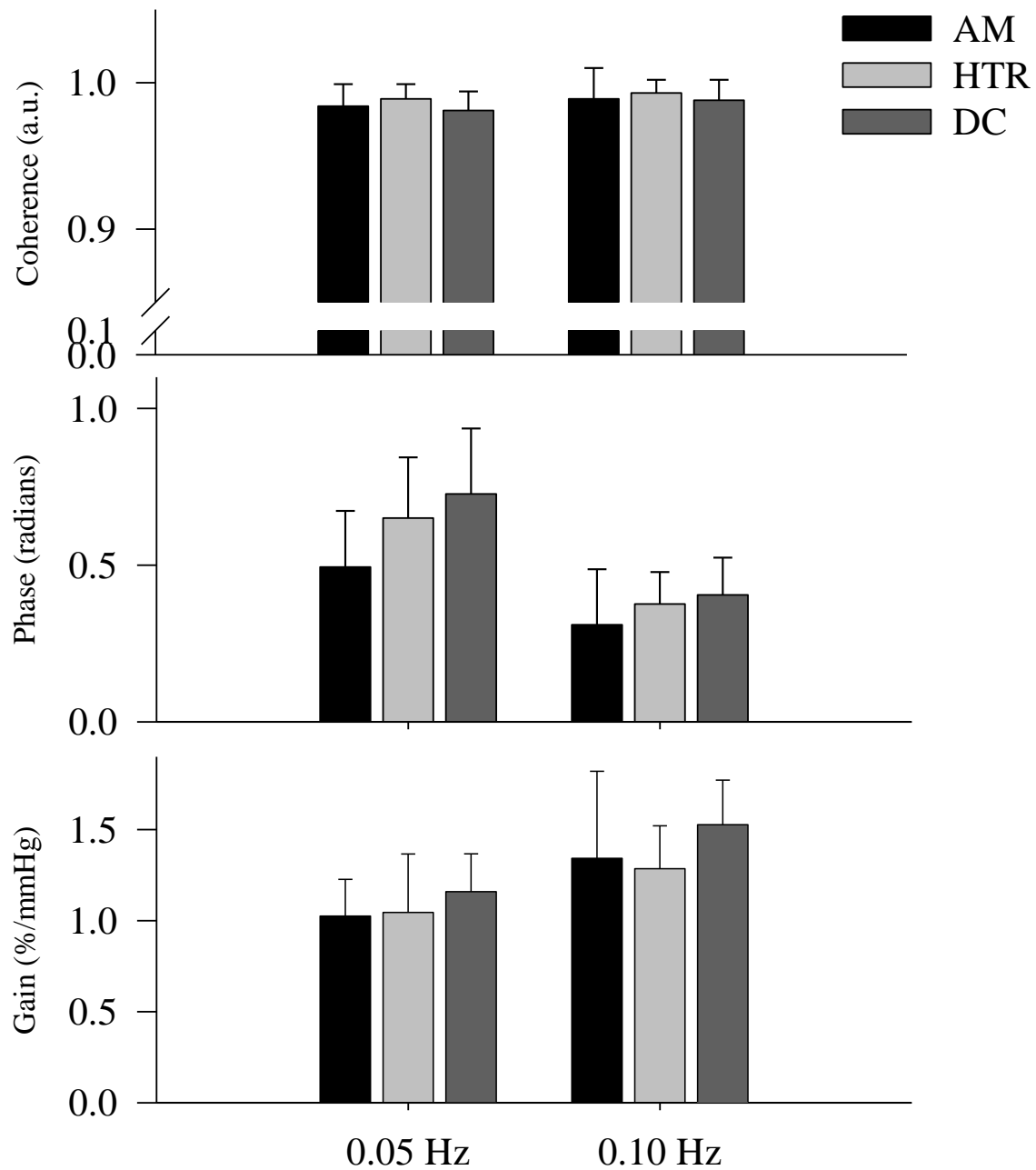


**Figure 5.3.** MCAv transfer function analysis of coherence, phase, and normalized gain at the driven frequencies of 0.05 Hz (left) and 0.10 Hz (right) for the three groups: AM (black), HTR (light grey), DC (dark grey). Note: the absolute gain in the DC were significantly higher than both the AM and HTR.

TFA phase and normalized gain were not significantly different between groups at either the 0.05 Hz or 0.10 Hz squat-stand frequencies (Figure 5.3.). There was also no relationship to the increased CVR<sub>i</sub> in the heart transplant recipients and age-matched as compared to the donor-controls and any TFA metrics (Table 5.4.). The reductions in BRS in both the heart transplant recipients and age-matched controls under conditions of spontaneous rest (Figure 5.2.), as well as both driven frequencies (Figure 4.3.) were unrelated to variability in the TFA metrics.

## **5.5. Discussion**

To our knowledge, this is the first study to assess cerebral pressure-flow relationship in long-term heart transplant recipients. Our findings show that despite marked reductions in cardiac BRS in heart transplant recipients, cerebral pressure-flow dynamics remain intact. Moreover, reductions in BRS were not correlated to inter-individual variability in TFA metrics in the heart transplant recipients.

### *Cardiac Baroreceptor Sensitivity in Heart Transplant Recipients*

Following heart transplantation, the sympathetic and parasympathetic nerves that normally regulate heart rate are severed, leaving the heart denervated. Our findings are consistent with prior studies showing reduced cardiac BRS in short-term (<24 months) heart transplant recipients.<sup>292,293</sup> In the longer-term (mean 5 years) heart transplant recipients, there is some evidence that partial sympathetic re-innervation may occur,<sup>287</sup> as reflected in an increase in the R-R interval power spectrum at 0.10 Hz. In this study, we observed a marked reduction in R-R interval power in the heart transplant recipients

(reduced by >95% as compared to age-matched and >99% compared with donor-controls; Table 3), which was positively correlated with BRS gain under both spontaneous ( $R^2 = 0.38, p < 0.01$ ) and driven ( $R^2 = 0.60, p < 0.01$ ) conditions. There was also an increase in the R-R interval power spectrum at 0.10 Hz in the heart transplant recipients, indicating some re-innervation of the sympathetic nervous system.<sup>287,293</sup>

### *Cerebral Pressure-Flow Dynamics*

Although the long-term heart transplant recipients had marked reductions in R-R interval and BRS gain (Table 5.3.), these alterations did not impact their cerebral pressure flow dynamics (Figure 5.2.; Figure 5.3.; Table 5.4.). We show that long-term heart transplant recipients have comparable reductions in MCAv and increases in CVRi compared to their age-matched counterparts (Table 5.2.). Moreover, the increase in CVRi with age does not appear to influence the TFA phase or normalized gain metrics studied in the present investigation – findings consistent with reports that cerebral pressure-flow dynamics are unaltered by age, at least up to the age of 75 [reviewed in:<sup>294</sup>]. We now extend these findings to include long-term heart transplant recipients (Figure 5.3.; Table 5.4.).

That long-term heart transplant recipients have comparable cerebral-pressure flow dynamics compared to both age-matched and donor-controls is clinically significant. We interpret these results to indicate that despite possible cerebrovascular remodeling during pre-transplant antecedent heart failure<sup>170,171,174</sup>, and reductions in resting pulsatility index (Table 5.2.) and cardiac BRS (Table 5.3.), the cerebrovasculature is able to adapt to acute and marked (i.e., 40-45 mmHg) changes in arterial blood pressure (Figure 5.1.; Table 5.2.).

### *Relationship between cardiac baroreflex and transfer function metrics*

The reduction in cardiac BRS in heart transplant recipients was not correlated with TFA metrics during either spontaneous or driven conditions. These findings are consistent with a recent study<sup>232</sup> in healthy older adults, which showed that increases in BRS was not related to dynamic cerebral autoregulation metrics. The findings of these studies in older adults and in heart transplant recipients, contrast with those in young healthy adults which demonstrated that there was an inverse relationship between BRS and markers of dynamic cerebral autoregulation.<sup>289</sup> Thus, reductions in cardiac BRS in aging and heart transplantation seem to play a diminished role in the integrated regulation of CBF.

### *Limitations:*

#### *Transcranial Doppler ultrasonography:*

The main assumption of transcranial Doppler is that the velocity recorded in the middle cerebral artery is directly representative of changes in cerebral blood flow. Throughout situations where there are normal arterial blood gas levels and blood pressure ranges the majority of research provides evidence that transcranial Doppler provides a reliable index of cerebral blood flow [reviewed in:<sup>38</sup>].

#### *Transfer Function Analysis:*

TFA applies a linear mathematical approach to interpret the relationship between the input blood pressure and the output cerebral blood flow. The work by Zhang et al.<sup>18</sup> has suggested that the cerebral autoregulatory system may be: linear, non-linear, have multiple inputs, or merely be two unrelated phenomena. Hence during this study we did not discuss

cerebral autoregulation *per se*, but merely presented data regarding to the relationship that exists between blood pressure and CBF. The coherence present within the analysis will affect the mathematical interpretability of the TFA (phase and gain) <sup>125</sup>. We employed the squat-stand maneuvers to non-pharmacologically increase blood pressure variability, enhancing the coherence (driven coherence was >0.98 a.u.) and allowing for more mathematically interpretable TFA and gain metrics. <sup>3</sup> In addition, we view the driven blood pressure challenges to be a realistic representation of natural oscillations that can occur to blood pressure activities of daily living (e.g., postural changes, coughing, exercise, etc.) and thus makes our data set physiologically relevant. This method induced oscillations that were 40-45 mmHg (Table 5.2.). Nevertheless, although the maximum myogenic regulatory control mechanism may not have been challenged enough to truly assess the risk factor for a cerebral haemorrhage or ischemic stroke, this would seem unlikely giving the physiological realistic changes in blood pressure.

#### *Arteriosclerosis:*

The long-term heart transplant recipient patients were not screened invasively in for arthrosclerosis in this study, as this is not a routine procedure for this population. The heart transplant recipients were more than five years post-transplant and did not have accompanying risk factors such as hypertension under resting conditions. Although the subjects within the current study did not undergo MRI, the normal intra-cranial velocities and dynamic pressure-flow relationships would indicate an absence of global cerebral arthrosclerosis. However, we cannot rule out the possibility of localized and regional arthrosclerosis.

### *Cross-Sectional Design:*

As this study is drawing conclusions from a cross-section of the population it is not possible to make a causal inference in the relationship between BRS and cerebral blood flow regulation. It would be nearly impossible to perform a longitudinal study where the same population was followed from young healthy adults to older adults and had a subset of this population undergo heart transplant surgery. We would also like to acknowledge that the heart transplant recipients within this study were otherwise very healthy individuals and our findings may not relate to heart transplant recipients with greater co-morbidities.

### **5.6. Key finding**

To our knowledge, this is the first study to date that has assessed the cerebral pressure-flow relationship in long-term heart transplant recipients. We have revealed 1) that in spite of reductions to BRS, long-term heart transplant recipients have comparable cerebral-pressure flow dynamics compared to both age-matched and donor-controls; and 2) the reductions in BRS in long-term heart transplant recipients were not related to any TFA metrics. Together these data indicate that the cerebrovasculature in long-term heart transplant recipients is able to normally regulate the cerebral pressure-flow dynamics, and is unlikely to explain the increased occurrence of severe cerebrovascular complications documented in the population.

## **Chapter Six: Influence of aging during supine cycling exercise**

This study was approved by the clinical ethical committees of the Universities of British Columbia (H14-01951). All volunteers provided written informed consent and procedures were followed in accordance to institutional guidelines.

A version of this study was selected for a poster presentation at Physoc 2015 (annual scientific meeting of the Physiological Society). The relationship between blood pressure and cerebral blood flow during supine cycling: Influence of aging. Jonathan D. Smirl, Keegan Hoffman, Yu-Chieh Tzeng, Alex Hansen and Philip N. Ainslie. Jonathan Smirl was responsible for the data collection, data analysis, writing, and formatting of the abstract.

A version of this manuscript has been submitted to the *Journal of Physiology* and it has been resubmitted with the revisions suggested by the expert reviewers. The relationship between blood pressure and cerebral blood flow during supine cycling: Influence of aging. Jonathan D. Smirl, Keegan Hoffman, Yu-Chieh Tzeng, Alex Hansen and Philip N. Ainslie. Jonathan Smirl was responsible for the data collection, data analysis, writing, and formatting of the manuscript.

## **6.1. Aims and Hypotheses**

### **Aims:**

- 1) To investigate and quantify the relationship between arterial blood pressure and cerebral blood flow during moderate intensity cycling in both younger (20-30 years old) and older (62-72 years old) healthy adults
- 2) To employ the novel approach of OLBNP to enhance blood pressure variability *during* moderate intensity cycling exercise, which will augment coherence and thus interpretability of the TFA metrics.

### **Hypotheses:**

- 1) OLBNP will elicit swings in blood pressure during exercise, which will increase coherence to nearly 1.00 and thus interpretability of the phase and gain metrics.
- 2) Despite the decrease in CBV within the older adult population, the high-pass filter model of the cerebral pressure-flow relationship will be intact during moderate exercise in both younger and older adults.

## 6.2. Rationale

Maintenance of the blood supply to the heart and brain is of critical importance for the cardiovascular system, both at rest and during exercise. The brain is especially susceptible to alterations in blood flow, as it is unable to store large amounts of substrates and has a high metabolic rate<sup>295</sup>. In order to maintain blood flow, the brain has developed the ability to regulate its blood flow somewhat independently of alterations to the rest of the body<sup>16,17,176,215,296</sup>. An excellent example of this is the can be observed by examining the relationship between arterial blood pressure and cerebral blood flow during exercise [reviewed in: <sup>160</sup>]. The global cerebral blood velocity (CBV) response during mild-moderate (40-60% of maximal intensity) bilateral cycling exercise has shown a similar increase in CBV (~20-25%), while mean arterial pressure only increased ~5-10% in both younger and older adults <sup>48</sup>. As exercise intensity proceeds to exhaustion, there is a further elevation in mean arterial pressure (~25-35%), while CBV can return to levels comparable to those at baseline likely due to exercise induced hypocapnia <sup>48</sup>.

Over the course of normal healthy human aging, physiological changes occur that result in the structural and functional alterations of the cerebrovascular system, such as loss of white matter <sup>155</sup>; hormonal changes in the brain <sup>156</sup>; loss of brain mass<sup>155</sup>; and a progressive loss of cortical neurons <sup>157,158</sup>. As a result of these alterations there is an observed reduction in resting cerebral blood flow and CBV. <sup>51</sup> Cross sectional studies have revealed that with healthy aging, cerebral blood flow declines approximately 25-40% between 30 and 89 years of age. <sup>51,156,159</sup> Similar findings were reported in a longitudinal study by Fotenos *et al.*; <sup>155</sup> namely, there is a reduction in whole-brain volume of 0.45% per year after 30 years of age.

The relationship between arterial blood pressure and cerebral blood flow is a frequency dependent process that functions as a high-pass filter, where the cerebral arterioles are able to adjust blood pressure changes at frequencies below 0.20 Hz (oscillations ~5 seconds in duration) and subsequently regulate cerebral blood flow.<sup>18,125,176,190</sup> One common method to assess this dynamic relationship is through linear transfer function analysis (TFA)<sup>18,190</sup>. Through TFA, the high-pass filter model has revealed that phase decreases and gain increases from 0.02-0.20 Hz<sup>18,190</sup> and under *resting conditions* has been shown to be unaltered in individuals up to ~70 years old.<sup>232,294,297,298</sup> However this notion has yet to be assessed in older adults *during exercise*.

While conditions at rest are useful for understanding the intricacies of the frequency dependent nature underlying this relationship, they might not inform how the brain deals with more profound changes in blood pressure such as those encountered during everyday life and exercise. To date, there have been seven studies that have attempted to examine the cerebral pressure-flow relationship in the middle cerebral artery during exercise (Table 6.1.)<sup>237,299-304</sup>. All of these studies were performed in young [mean age: 25 years] healthy individuals and one study also included a middle-aged adult cohort [mean age: 57 years]<sup>237</sup>. The collective findings of these studies are paradoxical as they demonstrate that the TFA phase response does not follow the high-pass filter model (i.e., it increases, rather than decreases, as frequency increases from 0.02-0.20 Hz), whereas gain does follow the expected trends (i.e., increased gain as frequency increases from 0.02-0.20 Hz). However, within these studies there was a relatively low coherence (~0.44) in both the very low frequency (VLF: 0.02-0.07 Hz) and low frequency (0.07-0.20 Hz) bands during the moderate exercise intensity (~50% heart rate reserve) – a factor that makes the

interpretation of phase and gain less reliable<sup>18,125</sup>. A possible way to counteract these reductions in coherence – and improve the reliability of TFA - is to induce oscillations in blood pressure<sup>1,3,190,305</sup>. When oscillations in blood pressure are induced, they enhance the signal-to-noise ratio by increasing the power of the input signal (blood pressure) which is reflected in increased power of the output signal (CBV), thus increasing coherence and the mathematical interpretability of the phase and gain metrics<sup>1-3,267</sup>. Although this approach has been well defined at rest,<sup>203,228,229</sup> it has never been applied *during* exercise.

**Table 6.1.** Summary of previous literature assessing the cerebral pressure-flow relationship during moderate intensity exercise (~50% of heart rate reserve)

	<b>HR (bpm)</b>	<b>Coherence</b>		<b>Phase (radians)</b>		<b>Gain (cm/s/mmHg)</b>	
		<b>VLF</b>	<b>LF</b>	<b>VLF</b>	<b>LF</b>	<b>VLF</b>	<b>LF</b>
Brys et al. <sup>299</sup> N = 40; 28 ± 5 years	~130		0.50 ± 0.10		0.78 ± 0.10		0.94 ± 0.07
Ogoh et al. <sup>301</sup> N = 7; 26 ± 1 year	~115		0.70 ± 0.05		0.63 ± 0.13		0.82 ± 0.10
Ogoh et al. <sup>300</sup> N = 7; 25 ± 1 year	~120		0.65 ± 0.03		0.20 ± 0.20		1.10 ± 0.20
Ogoh et al. <sup>304</sup> N = 8; 22 ± 2 years	~130	0.38 ± 0.05	0.63 ± 0.04	0.31 ± 0.22	0.41 ± 0.05	0.62 ± 0.05	0.97 ± 0.08
Ainslie et al. <sup>302</sup> N = 14; 25 ± 4 years	~130		0.60 ± 0.05		0.90 ± 0.50		0.85 ± 0.45
Ainslie et al. <sup>303</sup> N = 28; 26 ± 5 years	~130		0.58 ± 0.06		0.83 ± 0.55		0.90 ± 0.50
Fisher et al. <sup>237</sup> N = 9; 24 ± 3 years	~130	0.45 ± 0.15	0.52 ± 0.10	0.60 ± 0.52	0.85 ± 0.34	0.55 ± 0.25	0.85 ± 0.13
N = 10; 57 ± 7 years	~110	0.50 ± 0.12	0.56 ± 0.12	0.35 ± 0.44	0.75 ± 0.20	0.45 ± 0.20	0.75 ± 0.15

Values are means ± SD. Heart rate (HR); very low frequency (VLF: 0.02-0.07 Hz); low frequency (LF: 0.07-0.20 Hz).

This study was designed to examine the cerebral pressure-flow relationship during moderate intensity exercise to determine if the previously reported paradoxical findings (altered phase or intact gain) accurately represent this relationship. For the first time, an experimental approach was devised using non-pharmacological manipulations of blood pressure variability (via oscillatory lower body negative pressure – OLBNP) that were induced *during* moderate intensity supine exercise and related frequencies of interest (0.05 Hz and 0.10Hz). This approach was designed to enhance the signal-to-noise and thus provide a more accurate representation of the TFA metrics during exercise. The hypotheses were two-fold: 1) OLBNP will elicit swings in blood pressure during exercise which will enhance the coherence and thus interpretability of the phase and gain metrics; and 2) despite the decrease in CBV and alterations to the cerebrovasculature that occur within the older adult population<sup>51,235-237</sup>, the high-pass filter model of the cerebral pressure-flow relationship will be intact during moderate exercise in both younger and older adults.

### **6.3. Methods**

#### *Ethical approval*

This study was approved by the clinical ethical committee of the University of British Columbia, and adhered to the principles of the Declaration of Helinski. All volunteers provided written informed consent and procedures were followed in accordance to institutional guidelines.

#### *Subjects*

Ten healthy younger adults (10 male,  $24.8 \pm 2.7$  years, BMI:  $23.6 \pm 2.4$  kg/m<sup>2</sup>) and ten healthy older adults (8 male,  $66.4 \pm 3.7$  years, BMI:  $25.6 \pm 2.7$  kg/m<sup>2</sup>) subjects were recruited for this study. All of the subjects had a clear history of cardiorespiratory and cerebrovascular diseases and were not taking any form of medication. All older adult subjects were screened for any evidence of carotid stenosis, after completion of the screening process one older male adult was excluded from the study; therefore the older adults results are based on n=9. All subjects abstained from exercise, caffeine and alcoholic beverages for a period of 12 hours prior to the study. Each subject underwent a familiarization of the laboratory and testing protocols before the initiation of the protocols.

#### *Experimental Protocols*

The subjects were required to visit the laboratory on two occasions, separated by at least 48 hours. The first testing visitation determined the workload for the supine cycling exercise protocol (which was completed on the second visit). A maximal exercise test was implemented and consisted of participants performing a 5-minute warm-up at a self-

selected pace on the supine cycle ergometer. The initial workload was the equivalent of their self-selected warm-up pace and workload was increased by 25 watts (20 watts for older adults) every 2 minutes until a predetermined heart rate was achieved (130 beats/min for younger adults; 100 beats/min for older adults). After the predetermined heart rate level was achieved the workloads were increased every minute until the subject was no longer able to continue. The end of the test was determined by: the subject reaching age-predicted maximal heart rate; a perceived exertion of 9-10 on a 1-10 Borg Scale; volitional exhaustion has occurred; and/or the subject was no longer able to sustain a pedal cadence of 60 rpm. The peak workload obtained during this session was used to determine the workload for the moderate exercise challenge on the second testing day.

On the second testing visitation, the subjects were examined with OLBNP maneuvers both at rest and during moderate exercise. In both cases, the subject was placed in a supine position in industrially designed pressure chamber that sealed at their waist and were held in place via a mounted bicycle seat to prevent movement into the OLBNP chamber. The straps used to seal the participants in the OLBNP chamber did not interfere with the subjects breathing patterns. For the resting data, a 5 minute period at 0 mmHg was performed to collect baseline data. The pressure in the box was then oscillated between -50 mmHg and 0 mmHg at 0.10 Hz (5 seconds at -50 mmHg followed by 5 seconds at 0 mmHg). This process was then repeated at a frequency of 0.05 Hz (10 seconds at -50 mmHg followed by 10 seconds at 0 mmHg). The -50 mmHg pressure change occurred within 1.5 seconds. The -50 mmHg pressure was selected to match the pressure generated in the steady-state findings of Formes *et al.*<sup>238</sup>, who tested a similarly aged population (68 ± 1 year) at a sustained negative pressure of -50 mmHg. The results from this study

revealed that this level of negative pressure is well tolerated in older individuals. For the exercise data, the subject workload was set at  $46 \pm 4$  % of their previous day's peak wattage and was performed until steady-state was achieved. The moderate exercise intensity was selected based on previous research <sup>48</sup>, which has demonstrated that this intensity is associated with the greatest elevation in CBV and coincides with the minimal change to end-tidal CO<sub>2</sub> (P<sub>ET</sub>CO<sub>2</sub>). After the subject was at steady-state the testing protocol of the cycling exercise was initiated in the OLBNP chamber. The first trial consisted of 5-minutes at 0 Hz of steady-state exercise with the vacuum turned on to simulate the experience of the negative pressure but provide a comparable environment to the previously performed studies. The second and third trials consisted of steady-state cycling bouts while the OLBNP chamber was cycled between 0 and -50 mmHg, with pressure changes occurring within 1.5 seconds (typical trace presented in Figure 1.). A >5-minute rest break was provided between frequencies to allow for the subject to partially recover from the previous exercise bout. The order of the 0.05 Hz and 0.10 Hz trials were randomly selected for OLBNP maneuvers, both at rest and during exercise.

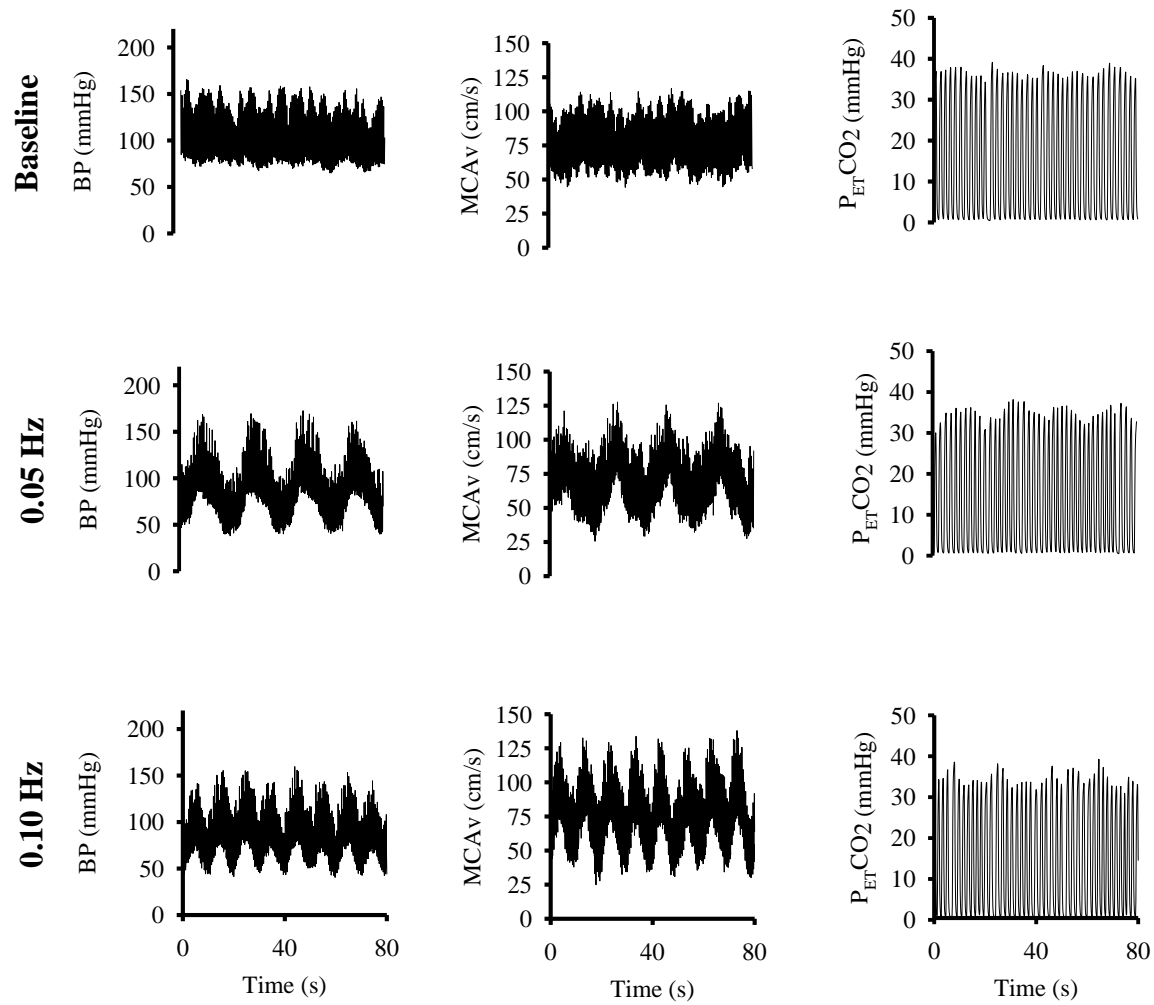


**Figure 6.1.** Typical trace for blood pressure (BP), middle cerebral artery velocity (MCAv) and end-tidal CO<sub>2</sub> (P<sub>ET</sub>CO<sub>2</sub>) during spontaneous (top), 0.05 Hz (middle) and 0.10 Hz (bottom) oscillatory negative pressure trials during a moderate supine cycling intensity.

### *Instrumentation*

In this study both the right and left middle cerebral arteries were insonated. Blood pressure was monitored with finger photoplethysmography. 3-lead electrocardiography was utilized to monitor R-R intervals. End-tidal gases were monitored with a gas analyzer. Please refer to sections 2.1. for more detail about these instruments.

### *Data Processing*

Please refer to section 2.2. (signal processing)

### *Power spectrum and transfer function analysis*

Please refer to section 2.2.1. (Fourier transform); 2.2.2. (transfer function analysis); 2.2.3. (coherence); 2.2.4. (phase); and 2.2.5. (gain) for more detail about these measures.

### *Statistical Analysis*

Statistical analyses were performed using SPSS version 20.0. A multivariate two-way ANOVA was conducted to examine the effect of modality (resting or moderate exercise) and frequency of oscillation (either 0.00 Hz, 0.05 Hz and 0.10 Hz) on the hemodynamic and cerebrovascular responses (mean arterial pressure, middle cerebral artery velocity, heart rate and  $P_{ET}CO_2$ ) within each age group. A multivariate two-way ANOVA was also used to determine the effects of modality (resting or moderate exercise) and frequency band (spontaneous or driven) on the Fourier transform (mean arterial pressure and middle cerebral artery power spectra) and transfer function metrics (coherence, phase, gain and normalized gain). Comparisons between age-groups were

performed with paired t-tests. Data are presented as mean  $\pm$  SD. Significance was set a priori at  $P < 0.05$ .

#### **6.4. Results**

##### *Respiratory, Cardiovascular, and Cerebrovascular Responses (Tables 6.2. and 6.3.)*

Under both resting and exercise conditions there was no main effect between the different oscillation frequencies (spontaneous, 0.05 or 0.10 Hz) in either age group. At rest there were no significant differences between the age-groups in  $P_{ET}CO_2$ . Mean arterial pressure was elevated ~15-25% in the older adults during both resting and exercise conditions. The CBV for younger adults was elevated by ~20-35% compared to older adults throughout the interventions which resulted in the older adult CVR<sub>i</sub> being elevated ~45% ( $P < 0.001$ ). By study design, exercise heart rate was elevated in the younger adults ( $123.6 \pm 13.1$  bpm;  $47.4 \pm 7.9\%$  heart rate reserve) as compared to the older adults ( $103.0 \pm 12.4$  bpm;  $47.3 \pm 4.8\%$  heart rate reserve;  $P < 0.01$ ). This was performed to ensure that both groups were while exercising at the same moderate exercise intensity as based on their individual heart rate reserves.

**Table 6.2.** Hemodynamic and cerebrovascular responses in younger adults at rest and during exercise with spontaneous and driven blood pressure (0.05 and 0.10 Hz) oscillations.

	Rest	Exercise
<b>Spontaneous LBNP</b>		
Mean Arterial Pressure (mmHg)	82.5 ± 9.9	97.7 ± 17.6*
Left MCAv (cm/s)	66.6 ± 4.7	72.2 ± 7.3*
Right MCAv (cm/s)	63.2 ± 9.2	69.8 ± 10.1*
Cerebrovascular Resistance index (mmHg/cm/s)	1.3 ± 0.2	1.4 ± 0.3
Heart Rate (bpm)	59.2 ± 11.5	120.6 ± 11.6*
End Tidal CO <sub>2</sub> (mmHg)	39.5 ± 2.6	39.8 ± 1.9
<b>0.05 Hz LBNP</b>		
Mean Arterial Pressure (mmHg)	82.4 ± 12.0	93.2 ± 16.8*
Left MCAv (cm/s)	64.5 ± 4.5	66.6 ± 6.8*
Right MCAv (cm/s)	60.3 ± 7.8	65.4 ± 9.8*
Cerebrovascular Resistance index (mmHg/cm/s)	1.3 ± 0.3	1.4 ± 0.3
Heart Rate (bpm)	60.0 ± 12.2	125.9 ± 14.4*
End Tidal CO <sub>2</sub> (mmHg)	38.4 ± 2.1	38.6 ± 2.4
<b>0.10 Hz LBNP</b>		
Mean Arterial Pressure (mmHg)	83.4 ± 13.3	92.8 ± 16.8*
Left MCAv (cm/s)	62.7 ± 4.7	68.3 ± 7.7*
Right MCAv (cm/s)	58.9 ± 7.2	66.8 ± 10.1*
Cerebrovascular Resistance index (mmHg/cm/s)	1.4 ± 0.3	1.4 ± 0.4
Heart Rate (bpm)	60.8 ± 12.1	124.4 ± 13.5*
End Tidal CO <sub>2</sub> (mmHg)	37.9 ± 2.4	38.6 ± 2.6

Values are means ± SD. Lower body negative pressure (LBNP); middle cerebral artery velocity (MCAv). Statistical significance was set at  $P < 0.05$ . Note: there was a main effect for modality but there were no main effect between frequencies for younger adults.

\*denotes different from rest within frequency.

**Table 6.3.** Hemodynamic and cerebrovascular responses in older adults at rest and during exercise with spontaneous and driven blood pressure (0.05 and 0.10 Hz) oscillations.

	Rest	Exercise
<b>Spontaneous LBNP</b>		
Mean Arterial Pressure (mmHg)	103.5 ± 11.2	113.1 ± 13.3*
Left MCAv (cm/s)	53.6 ± 9.7	57.9 ± 7.4
Right MCAv (cm/s)	53.1 ± 6.8	59.0 ± 8.4
Cerebrovascular Resistance index (mmHg/cm/s)	1.9 ± 0.4	2.0 ± 0.4
Heart Rate (bpm)	63.8 ± 14.5	101.7 ± 13.6*
End Tidal CO <sub>2</sub> (mmHg)	37.5 ± 3.1	39.3 ± 3.5
<b>0.05 Hz LBNP</b>		
Mean Arterial Pressure (mmHg)	102.4 ± 12.1	108.3 ± 14.1*
Left MCAv (cm/s)	54.0 ± 9.8	56.5 ± 6.4
Right MCAv (cm/s)	53.3 ± 6.4	56.0 ± 6.7
Cerebrovascular Resistance index (mmHg/cm/s)	1.9 ± 0.4	2.1 ± 0.3
Heart Rate (bpm)	63.6 ± 13.0	103.3 ± 13.1*
End Tidal CO <sub>2</sub> (mmHg)	37.5 ± 2.7	37.8 ± 3.2
<b>0.10 Hz LBNP</b>		
Mean Arterial Pressure (mmHg)	102.3 ± 12.7	109.6 ± 17.0*
Left MCAv (cm/s)	53.4 ± 11.8	57.0 ± 6.9
Right MCAv (cm/s)	53.9 ± 8.2	56.3 ± 5.9
Cerebrovascular Resistance index (mmHg/cm/s)	1.9 ± 0.4	2.0 ± 0.3
Heart Rate (bpm)	63.5 ± 14.5	103.8 ± 10.9*
End Tidal CO <sub>2</sub> (mmHg)	37.8 ± 2.6	38.3 ± 3.0

Values are means ± SD. Lower body negative pressure (LBNP); middle cerebral artery velocity (MCAv). Statistical significance was set at  $P < 0.05$ . Note: there was a main effect for modality but there were no main effect between frequencies for older adults. \*denotes different from rest within frequency.

*Transfer Function Analysis (Tables 6.4. and 6.5.)*

*Power spectrum and coherence:* Under resting spontaneous and driven oscillations, the younger and older adults had comparable autospectra power for all indices except the LF middle cerebral artery velocity power. Conversely, during the exercise intervention, the older adults had reduced absolute autospectra for all indices except the VLF mean arterial pressure power.

As compared to the spontaneous oscillations, the enhanced blood pressure variability as a result of the OLBNP maneuvers during moderate exercise resulted in a 500+ fold increase in the mean arterial pressure power and a 200+ fold increase in the middle cerebral artery velocity power in both the younger and older adults (Figure 6.2.). The enhanced input and output signals at both rest and during moderate exercise were reflected in improvements in coherence (rest: ~0.75-0.90,  $P < 0.001$ ; exercise: >0.97,  $P < 0.001$ ; Figure 6.3.). This is reflected in an average within-subject coherence elevation of ~5-30% during exercise (as compared to the same frequency at rest) in both younger and older adults.

**Table 6.4.** Transfer function analysis metrics in younger adults for the relationship between mean arterial pressure and cerebral blood flow at rest and during moderate exercise.

	Rest	Exercise
<b>Spontaneous Oscillations</b>		
VLF MAP Power (mmHg <sup>2</sup> )	5.90 ± 3.00	7.47 ± 7.50
LF MAP Power (mmHg <sup>2</sup> )	2.93 ± 1.35	5.27 ± 3.28
VLF MCAv Power (cm/s) <sup>2</sup>	7.43 ± 4.15	9.52 ± 2.81
LF MCAv Power (cm/s) <sup>2</sup>	4.30 ± 1.98	6.36 ± 2.68
VLF Coherence	0.35 ± 0.16	0.28 ± 0.11
LF Coherence	0.65 ± 0.14	0.48 ± 0.16
VLF Phase (radians)	0.76 ± 0.60	1.56 ± 0.61‡
LF Phase (radians)	0.54 ± 0.29	1.01 ± 0.54‡
VLF Gain (cm/s/mm Hg)	1.14 ± 0.36	0.95 ± 0.32
LF Gain (cm/s/mm Hg)	1.32 ± 0.32	1.09 ± 0.18
VLF Gain (%/%)	1.45 ± 0.78	1.34 ± 0.55
LF Gain (%/%)	1.67 ± 0.54	1.50 ± 0.42
<b>Driven Oscillations</b>		
0.05 Hz MAP Power (mmHg <sup>2</sup> )/Hz	944 ± 649*	15799 ± 7441*‡
0.10 Hz MAP Power (mmHg <sup>2</sup> )/Hz	727 ± 480†	8406 ± 3287†‡
0.05 Hz MCAv Power (cm/s) <sup>2</sup> /Hz	412 ± 247*	3552 ± 2492*‡
0.10 Hz MCAv Power (cm/s) <sup>2</sup> /Hz	501 ± 332†	9001 ± 4649†‡
0.05 Hz Coherence	0.84 ± 0.11*	0.97 ± 0.02*‡
0.10 Hz Coherence	0.96 ± 0.04†	1.00 ± 0.00†‡
0.05 Hz Phase (radians)	1.61 ± 0.52	1.23 ± 0.49‡
0.10 Hz Phase (radians)	0.61 ± 0.25	0.73 ± 0.18†‡
0.05 Hz Gain (cm/s/mm Hg)	0.67 ± 0.29*	0.48 ± 0.17*
0.10 Hz Gain (cm/s/mm Hg)	0.82 ± 0.22†	1.02 ± 0.16
0.05 Hz Gain (%/%)	0.69 ± 0.21*	0.65 ± 0.28*
0.10 Hz Gain (%/%)	1.10 ± 0.34	1.34 ± 0.37

Values are means ± SD. Mean arterial pressure (MAP); middle cerebral artery velocity (MCAv); low frequency (LF); very low frequency (VLF). Statistical significance was set at  $P < 0.05$ . \*denotes significance from VLF; †denotes significance from LF; ‡denotes significance from rest.

**Table 6.5.** Transfer function analysis metrics in older adults for the relationship between mean arterial pressure and cerebral blood flow at rest and during moderate exercise.

	Rest	Exercise
<b>Spontaneous Oscillations</b>		
VLF MAP Power (mmHg <sup>2</sup> )	4.86 ± 3.16	8.58 ± 17.30
LF MAP Power (mmHg <sup>2</sup> )	1.98 ± 1.04	2.31 ± 1.76
VLF MCAv Power (cm/s) <sup>2</sup>	7.95 ± 6.36	4.54 ± 2.76
LF MCAv Power (cm/s) <sup>2</sup>	1.83 ± 0.72	2.11 ± 1.53
VLF Coherence	0.37 ± 0.13	0.40 ± 0.11
LF Coherence	0.61 ± 0.18	0.48 ± 0.19
VLF Phase (radians)	1.03 ± 0.45	1.47 ± 0.48
LF Phase (radians)	0.62 ± 0.24	0.70 ± 0.19
VLF Gain (cm/s/mm Hg)	1.05 ± 0.54	0.95 ± 0.54
LF Gain (cm/s/mm Hg)	1.08 ± 0.35	0.99 ± 0.47
VLF Gain (%/%)	1.90 ± 1.08	1.89 ± 1.44
LF Gain (%/%)	1.92 ± 0.49	1.74 ± 0.74
<b>Driven Oscillations</b>		
0.05 Hz MAP Power (mmHg <sup>2</sup> )/Hz	1845 ± 2178*	7685 ± 7247*‡
0.10 Hz MAP Power (mmHg <sup>2</sup> )/Hz	1311 ± 2087†	4616 ± 3169†‡
0.05 Hz MCAv Power (cm/s) <sup>2</sup> /Hz	722 ± 1070*	1668 ± 1114*‡
0.10 Hz MCAv Power (cm/s) <sup>2</sup> /Hz	786 ± 1370†	3665 ± 2501†‡
0.05 Hz Coherence	0.90 ± 0.10*	0.98 ± 0.02*‡
0.10 Hz Coherence	0.89 ± 0.13†	0.98 ± 0.02†‡
0.05 Hz Phase (radians)	0.99 ± 0.35	1.35 ± 0.32‡
0.10 Hz Phase (radians)	0.68 ± 0.41	0.46 ± 0.27†‡
0.05 Hz Gain (cm/s/mm Hg)	0.61 ± 0.15*	0.59 ± 0.24*
0.10 Hz Gain (cm/s/mm Hg)	0.76 ± 0.45	0.91 ± 0.27
0.05 Hz Gain (%/%)	1.07 ± 0.32*	1.11 ± 0.44*
0.10 Hz Gain (%/%)	1.32 ± 0.75	1.64 ± 0.54

Values are means ± SD. Mean arterial pressure (MAP); middle cerebral artery velocity (MCAv); low frequency (LF); very low frequency (VLF). Statistical significance was set at  $P < 0.05$ . \*denotes significance from VLF; †denotes significance from LF; ‡denotes significance from rest.

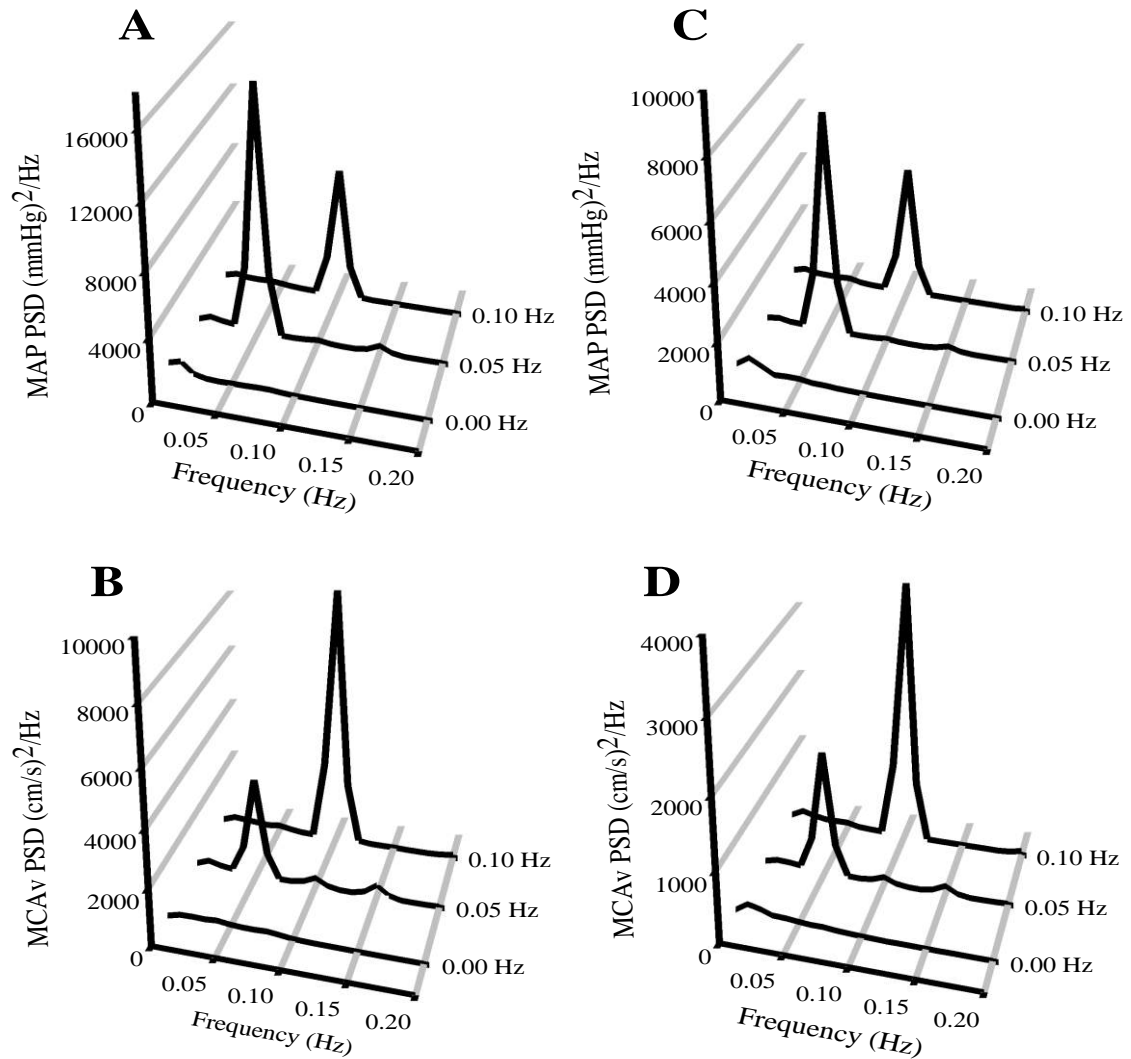


**Figure 6.2.** Absolute values of the power spectrum densities (PSD) for the mean arterial pressure [MAP: younger adults (A), older adults (C)]; and middle cerebral artery velocity [MCAv: younger adults (B), older adults (D)] with spontaneous and driven oscillations in blood pressure during moderate exercise. The frequency where the PSD reached peak amplitude (either 0.05 Hz or 0.10 Hz) was used as a basis for sampling the point estimates for Coherence, Phase and Gain values. Note the minimum 200+ fold increase in PSD for the driven (0.05 and 0.10 Hz) as compared with the spontaneous oscillations at 0.00 Hz.

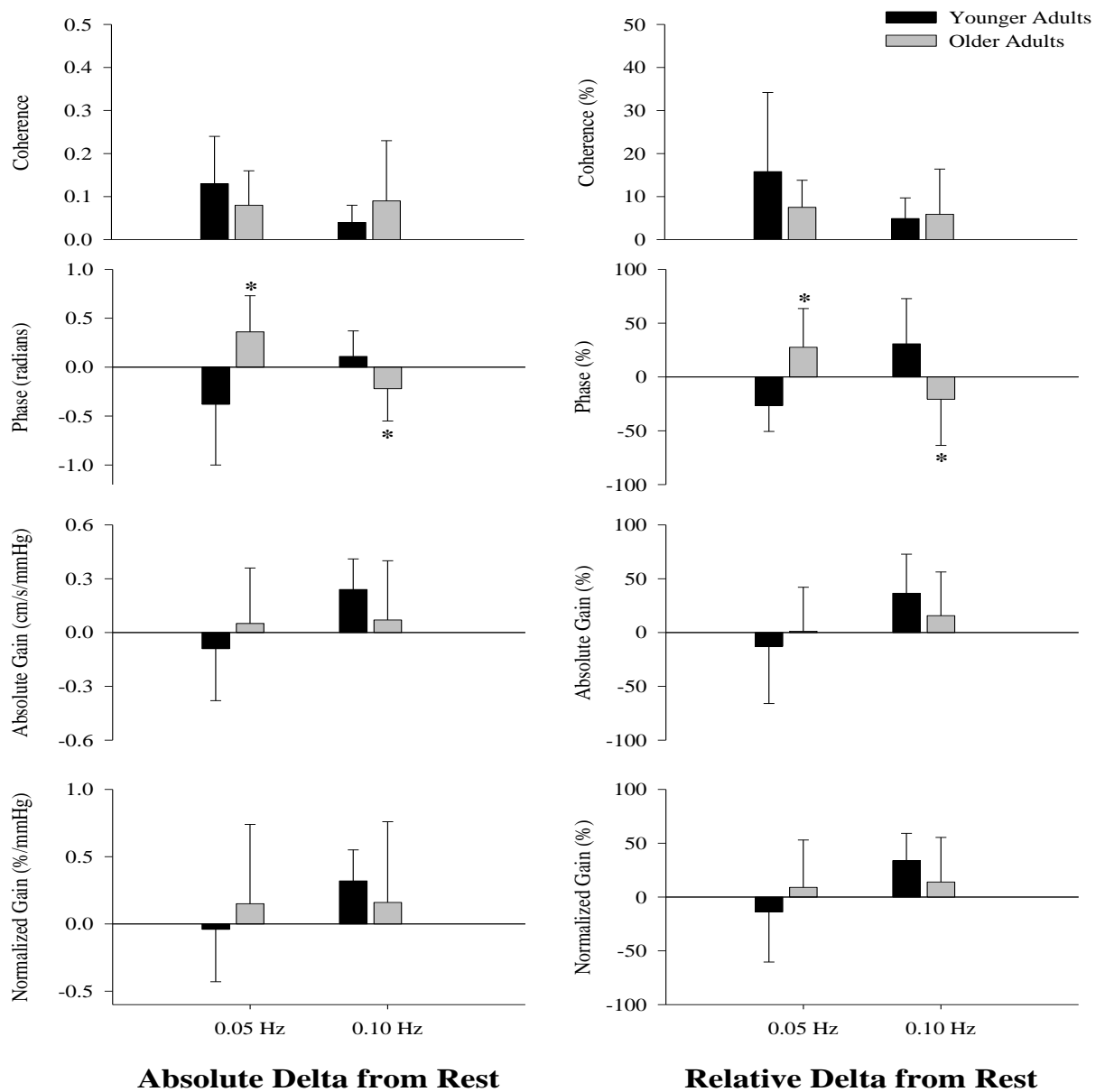


**Figure 6.3.** The absolute (left) and relative (right) delta changes from resting to exercise conditions in coherence (top row), phase (second row), absolute gain (third row) and normalized gain (bottom row) during driven oscillations in younger (black) and older adults (grey). Note: there was a consistent elevation in coherence and 0.10 Hz gain metrics in all individuals with driven oscillations during exercise. There were age-related differences in the expression of the phase metric at both 0.05 and 0.10 Hz. \*denotes differences younger and older adults.

*Phase and gain:* During spontaneous oscillations where coherence was generally low ( $<0.50$ ), the phase and gain metrics in the younger adults followed the expected high-pass filter model of the cerebrovasculature. Whereas the older adults had a paradoxical response - the phase response followed the expected trend of a decreasing lead as frequency approached 0.20 Hz; however, the gain and normalized gain were maintained or slightly decreased in magnitude (instead of increasing as expected) with increasing frequency. These findings were consistent under both resting and exercise conditions as assessed with spontaneous oscillations.

The increased coherence values for the driven oscillations (vs. spontaneous oscillations) during exercise (Figure 6.4.) reflect an increase in the linearity of the system and thus result in the phase and gain values being more mathematically interpretable<sup>1-3,267</sup>. With the improved linearity of the cerebral pressure-flow relationship during the OLBNP maneuvers during the exercise trials, the phase and gain metrics were revealed to follow the expected trends of the high-pass filter model in both younger and older adults (Figure 6.5.).

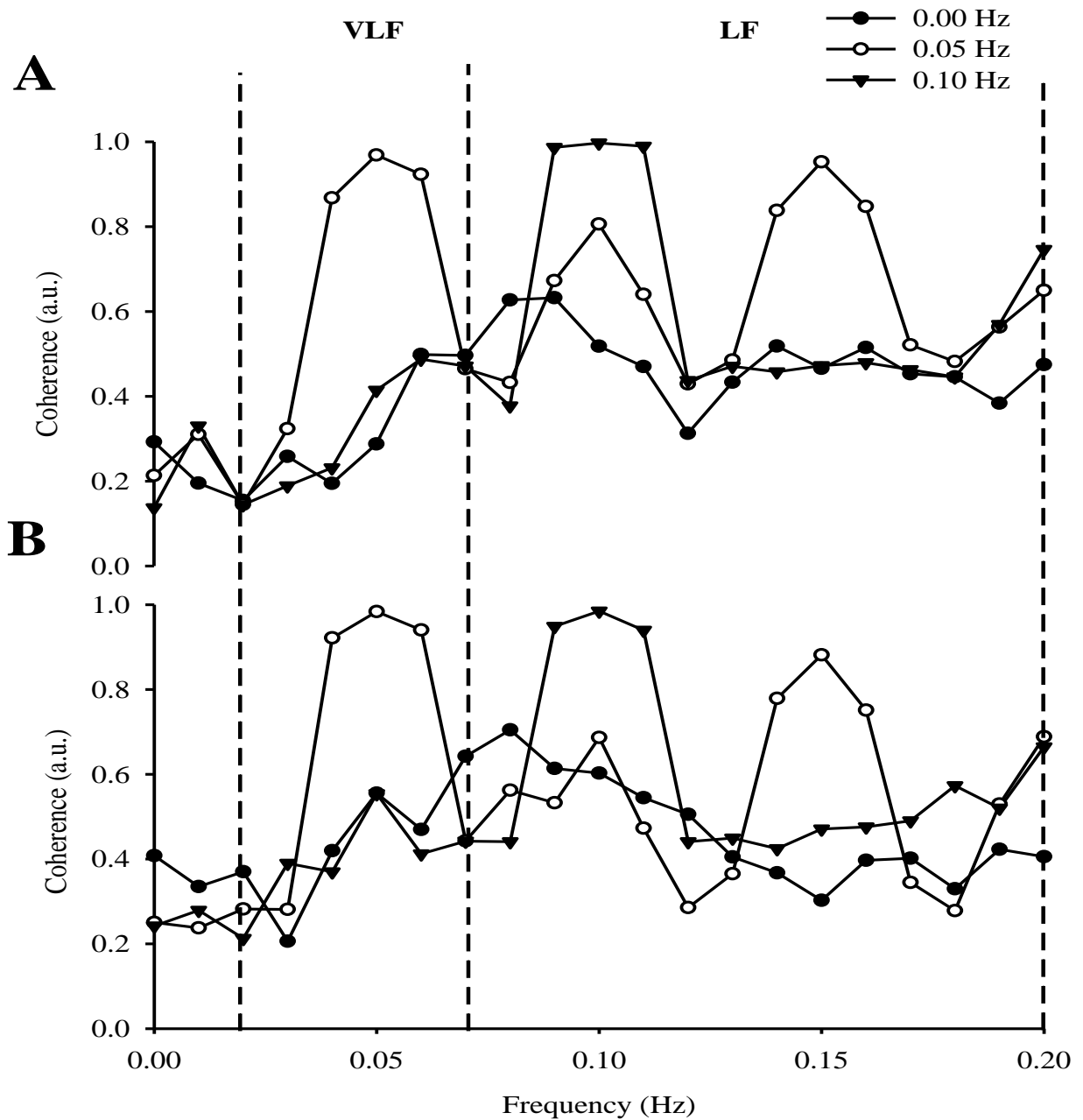


**Figure 6.4.** The augmentation in coherence to  $\sim 1.00$  during the driven oscillations in blood pressure during moderate exercise in younger (A) and older (B) adults. Note: the relatively low coherence ( $<0.60$ ) in the spontaneous data (filled circles) for both the younger and older adults. Regardless of age, the coherence point estimate of the driven oscillations (0.05 Hz: open circles; 0.10 Hz: filled triangles) was approximately 1.00 indicating that the cerebral pressure-flow relationship can be approximated in a linear fashion at the frequencies of interest, which greatly enhances the interpretation of the associated transfer function metrics.

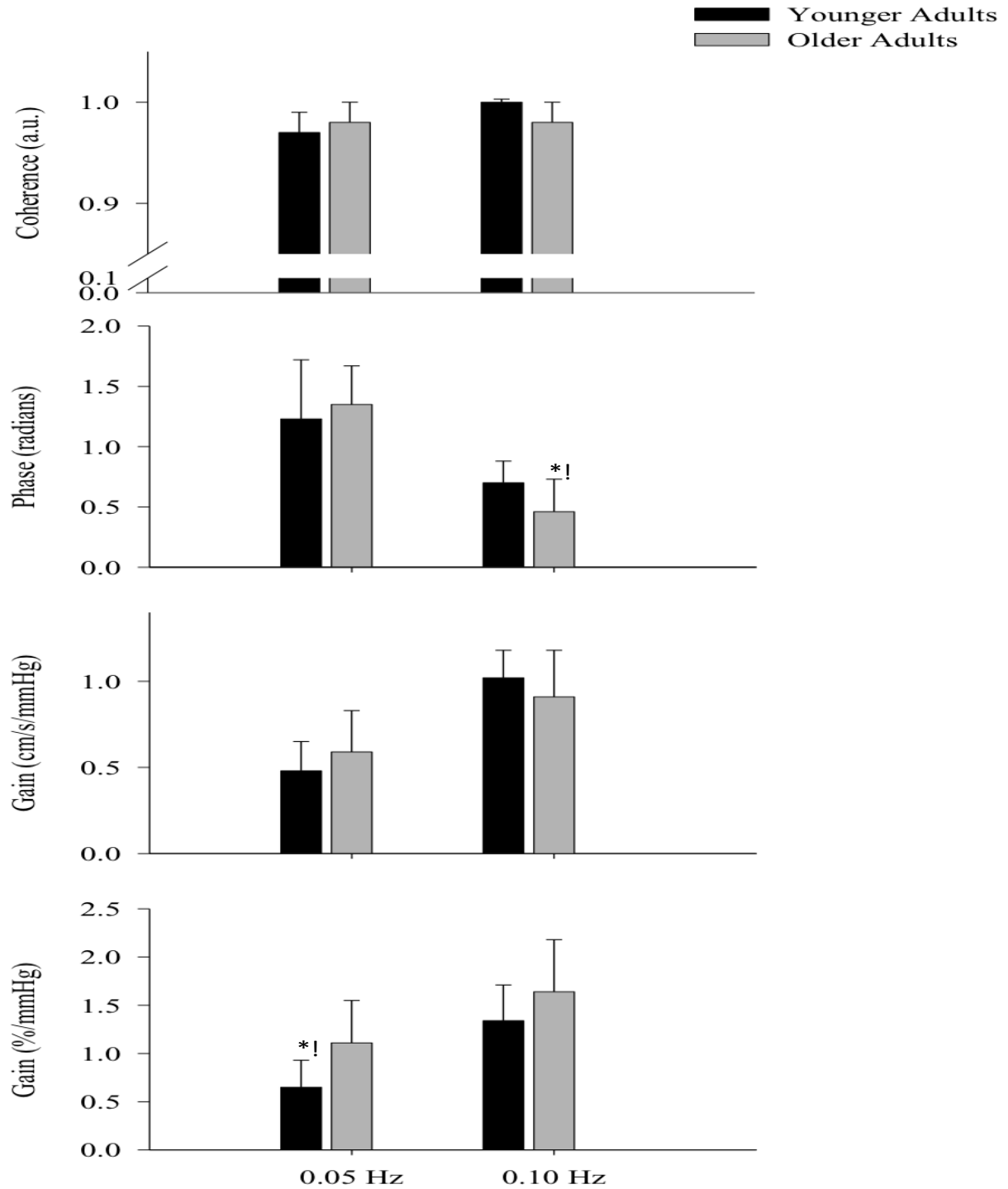


**Figure 6.5.** The transfer function analysis of coherence (top), phase (second row), absolute gain (third row) and normalized gain (bottom row) at the driven frequencies of 0.05 Hz (left) and 0.10 Hz (right) for the younger (black) and older (light grey), adults during moderate exercise. Note: the high-pass filter nature of the phase and gain responses for the younger and older adults. \*denotes differences younger and older adults.

As compared to the driven oscillations at rest, the exercise data during the OLBNP maneuvers revealed subtle within-subject changes to the TFA phase metric that appear to be age-related (Figure 6.3.). During exercise the younger adults phase was  $-26.5 \pm 24.1\%$  lower than resting data at 0.05 Hz, whereas the older adults had an elevated phase by  $27.6 \pm 36.1\%$  ( $P < 0.001$ ). In contrast at 0.10 Hz, the younger adults phase was  $35.1 \pm 49.7\%$  higher during exercise, while the older adults had a reduced phase of  $-20.7 \pm 42.9\%$  ( $P < 0.01$ ). Despite the absolute and normalized gain metrics being elevated in all subjects at 0.10 Hz during exercise, there were no within-subject age-related changes in the absolute or normalized gain metrics between rest and exercise OLBNP trials (Figure 6.3.).

*Effects of aging on TFA metrics (Tables 6.4. and 6.5.):*

Under resting conditions with spontaneous oscillations, there were no differences in TFA metrics between the younger and older adults. During the driven oscillations without exercise, the coherence ( $P = 0.02$ ) and normalized gain ( $P < 0.01$ ) reduced in the younger adults at 0.05 Hz. During the exercise trial with spontaneous oscillations there were no differences in TFA metrics between the younger and older adults. However, the augmented coherence during the OLBNP protocol revealed the older adults had a normalized gain +71% elevated at 0.05 Hz ( $+0.46 \pm 0.36\ %/\%$ ) and phase reduced -31% at 0.10 Hz ( $-0.24 \pm 0.22$  radians: Figure 6.4.). At all frequencies (both spontaneous and driven), normalized gain was positively correlated with CVRi ( $r = 0.51$  to  $0.61$ :  $P < 0.03$ ). Paradoxically, when the age groups were pooled, phase was both positively correlated with CVRi in the spontaneous LF data ( $r = 0.40$ :  $P = 0.04$ ) and negatively correlated in the 0.10 Hz driven data ( $r = -0.40$ :  $P = 0.04$ ), likely due to a poor signal-to-noise ratio in the spontaneous data.

## 6.5. Discussion

Using the novel approach to drive blood pressure during a supine cycling intervention, the main findings of the study were: 1) oscillating blood pressure during moderate exercise resulted in coherence values approaching 1.00; 2) the paradoxical nature of the cerebral-pressure flow response in older adults under spontaneous oscillations was normalized with improvements to coherence; 3) during the driven blood pressure oscillations the older adults had slightly elevated normalized gain at 0.05 Hz and reduced phase at 0.10 Hz compared with the younger adults; and 4) the comparison between resting and exercise OLBNP maneuvers revealed subtle changes to the TFA phase metric. Collectively, these findings support our hypothesis and for the first time conclusively demonstrate that despite the decrease in CBV within the older adult population, the high-pass filter model of the cerebrovasculature is present during moderate supine cycling exercise. Despite the intact nature of the high-pass filter model, these findings also reveal subtle age-related changes in the TFA phase metric and how it is expressed during moderate exercise.

### *Comparison to previous studies:*

The previous studies that have examined the relationship between arterial blood pressure and CBV speculated that their findings were representative of an *intact* response<sup>237,299,301-304</sup>. Only two of these studies reported both the VLF and LF data for phase and gain<sup>237,304</sup>, while the other studies based their interpretation upon phase and gain values in the LF range<sup>299,301-303</sup>. The two studies that did report both frequency ranges of interest noted paradoxical findings in both younger and middle-aged adults (Table 6.1.).

For example: the phase and gain values both responded in a similar direction with increasing frequency, which is counter to the high-pass filter nature of the cerebrovasculature. The findings from these studies are similar to the spontaneous data of the older adults within the current study (Table 6.3.). These supposedly *impaired* cerebral autoregulatory results during moderate exercise were speculated in an earlier study by Ogoh *et al.* <sup>164</sup>, to occur as a result of an increase in systemic metabolites and/or excess ammonia released from the skeletal muscles crossing the blood-brain barrier and disrupting the regulatory properties of the cerebrovasculature. A second explanation was presented by Ainslie *et al.* <sup>303</sup>, who noted that an elevated LF gain response may be due to capillary over-perfusion occurring during exercise. A final explanation for these findings was presented by Fisher *et al.* <sup>237</sup>, who noted the low coherence values (as highlighted in Table 6.1.) associated with the cerebral-pressure flow response may impact the interpretation of these findings. Our current study largely validates this latter concept <sup>237</sup>, as the spontaneous coherence values associated with moderate steady-state exercise were on average below 0.50 in both the VLF and LF ranges regardless of age. When the OLBNP was applied during exercise, the relationship between arterial blood pressure and cerebral blood flow was nearly linear in nature (coherence above 0.97 for all ages and frequencies: Tables 6.4. and 6.5.). With this novel methodological approach, examination of the cerebral pressure-flow relationship during moderate exercise revealed that the cerebrovasculature is indeed functioning as a high-pass filter with gain increasing and phase decreasing as frequency increases from 0.02-0.20 Hz. Thus, although some of the previous research in this field speculated the regulatory properties of the cerebrovascular were intact during moderate exercise, this is the first study to conclusively demonstrate this notion.

*Effect of aging on the cerebrovasculature during exercise:*

There is a general reduction in cerebral blood flow of ~0.8% per year after the age of 20<sup>51</sup>. It has been proposed that this reduction occurs due to increases in CVRi<sup>235</sup> which could be a result of reductions in brain mass<sup>236</sup>. The current study observed similar alterations to CVRi and CBF as noted elsewhere<sup>2,51</sup>. There was an age range of ~35-40 years between the groups in the current study, with a 20-25% reduction in CBV in the middle cerebral artery and ~45% increase in CVRi noted in the older adults (Tables 6.2. and 6.3.). When OLBNP maneuvers were performed during moderate exercise, it was revealed that while both younger and older adults cerebrovasculature responded as a high-pass filter during moderate exercise, there were some phase and gain differences with aging. Namely, it was revealed that the older adults normalized gain at 0.05 Hz was elevated and phase was reduced at 0.10 Hz when compared with the younger adults (Figure 6.5.). These findings are in contrast to the spontaneous data within the current study and those reported by Fisher *et al.*<sup>237</sup>. Previous research has shown that under resting conditions<sup>232,294,297,298</sup> and during moderate exercise<sup>237</sup> with spontaneous oscillations it appeared as though there were no differences in TFA metrics across the aging spectrum in individuals up to ~70 years old.

However, the enhanced coherence in the current study has revealed the cerebrovasculature of younger and older adults may have slight differences in the TFA patterns despite maintaining the high-pass filter nature of CBF regulation. The findings from the current study demonstrated subtle age-related changes in the expression of the TFA phase metric between resting and moderate exercise conditions. In the exercise trials, the younger adults had a reduced phase at 0.05 Hz and elevated phase at 0.10 Hz as

compared to the same frequency at rest. In contrast the older adults had an augmented phase at 0.05 Hz and a decreased phase at 0.10 Hz (Figure 6.3.). It is unlikely the cardiac baroreflex is responsible for the difference in findings and expression of the TFA metrics between younger and older adults, as research under resting conditions has demonstrated that the baroreflex plays a minimal role in the cerebral pressure-flow response<sup>2,234</sup>. Instead it is more likely that the increase in CVRi with aging (Tables 6.2. and 6.3.) leads to alterations in either arteriolar tone<sup>1</sup>, sympathetic tone<sup>237,299</sup>, and/or changes within the mechanical buffering of the compliance vessels<sup>229</sup>. Any of these mechanisms could affect the cerebral pressure-flow response during moderate exercise (exacerbating the age-related differences). However, more research in this area is needed to confirm these possibilities.

It is also highly improbable that just a single mechanism (arteriolar tone, sympathetic tone, downstream capacitance) that is responsible for the age-related differences that were observed during exercise (Figures 6.3. and 6.5.). However, related to vascular compliance, it is possible that the previously mentioned mechanisms could be mediated by nitric oxide, as it has been shown to have differentiated effects across the aging spectrum.<sup>116</sup> For instance, in younger adults (mean age 25 years), infusion of a nitric oxide inhibitor (L-NMMA) has little-to-no impact on cerebral blood flow (but does increase mean arterial pressure), indicating that nitric oxide pathway is not vital in controlling cerebral blood flow in young adults<sup>116</sup>. Contrasting this finding, are results from an older population (mean age 78 years) where the same nitric oxide blockade reduced in a decrease cerebral blood flow by ~22% and elevations in cerebrovascular resistance of ~40%<sup>116</sup>. The authors speculated that these findings confirm that the nitric oxide pathway is important in the control of cerebral blood flow, but only in an elderly

population where endothelial dysfunction and/or atherosclerosis may be present <sup>116</sup>. Although animal studies indicate that exercise induces increases in nitric oxide levels (30-40%) in the medial prefrontal cortex and stria terminalis <sup>306</sup>, it is unknown if this occurs in humans or is altered with aging.

*Mechanisms for maintaining the cerebrovasculature high-pass filter during exercise:*

During moderate exercise there is a significant increase in mean arterial pressure that challenges the cerebrovasculature to effectively regulate against over-perfusion and increases to intracranial pressure. Since cerebral haemorrhages do not occur during routine exercise, the cerebrovasculature must have several regulatory protective mechanisms. In baboons, it has been shown that there is a smaller redistribution of cardiac output to the brain as compared with the skeletal muscle <sup>307</sup>, which helps partially protect the brain. Hohimer *et al.*, <sup>307</sup> concluded that the relatively constant level of cerebral blood flow at rest and during moderate exercise was due CVRi increasing ~20% during exercise. This increase in CVRi has been proposed to be due to enhanced sympathetic tone, which could partially explain the observed TFA metric changes with aging <sup>237,299</sup>. It has also been speculated that the cardiac baroreceptor mediated control of blood pressure variability may play a significant role in the regulation of arterial blood pressure during exercise and thus by extension regulate cerebral blood flow <sup>301</sup>. However, in more recent publications, it seems that the cardiac baroreceptors play a minimal role in the regulation of the cerebral pressure-flow relationship during healthy aging <sup>234</sup> or following long-term heart transplantation <sup>2</sup>. The role of the myogenic tone <sup>185,308</sup>, increased capacitance (via Windkessel modelling) <sup>229</sup> and enhanced sympathetic activity are likely the main

mechanisms responsible for the regulation of cerebral blood flow during exercise. These potential mechanisms could possibly be mediated by the exercise-induced release of nitric oxide, which may explain the differences observed between the younger and older adults in the current study (Figures 6.3. and 6.5.). More research in this area is needed to confirm these speculations.

*Implications for the assessment and interpretation of pressure-flow relationships:*

The previous findings on the relationship between mean arterial pressure and cerebral blood flow have highlighted the issue with using a linear assessment tool (TFA) to measure a system that is reliant upon coherence for interpretation<sup>1-3,267</sup>. A low coherence value can mean a number of things: 1) there is a poor signal-to-noise ratio; 2) there are multiple inputs to the system; 3) the system is inherently non-linear; and 4) there is simply no relationship between the input and output variables<sup>18</sup>. This study addressed the concern noted by Fisher *et al.*<sup>237</sup>, that the low coherence values during moderate exercise with spontaneous oscillations in blood pressure make interpretation of the findings difficult. Oscillating blood pressure during exercise, the novel design of this study, enhanced the Fourier transform power spectrums of both mean arterial pressure (~2000 mmHg<sup>2</sup>/Hz) and middle cerebral artery velocity (~500 (cm/s)<sup>2</sup>/Hz) above that which is typically observed during OLBNP<sup>228,229</sup> to levels typically observed during squat-stand maneuvers<sup>1-3</sup>. The enhanced autospectra input to the system is reflected by a greatly increased output autospectra (Figure 6.2.), which maximises the signal-to-noise ratio and results in a coherence approaching 1.00 (Figure 6.4.), producing much more interpretable phase and gain metrics in both younger and older adults alike (Figure 6.5.). Thus future studies

assessing the cerebral pressure-flow response during exercise should employ a methodology that enhances the coherence through oscillations in blood pressure.

*Methodological Considerations:*

*Flow vs velocity:* Cerebral blood flow was indexed in this study through the application of transcranial Doppler. This method utilizes the assumption that when the diameter of the insonated vessel is constant, the velocity of the red blood cells within the vessel approximates the flow within that vessel. This concept has been recently reviewed by Ainslie and Hoiland <sup>67</sup>, where they summarized the findings of two recent high resolution magnetic resonance imaging studies of the cerebrovasculature <sup>65,66</sup>. It was shown that the diameter of the middle cerebral artery is relatively constant when  $P_{ETCO_2}$  values are held within 8 mmHg of eucapnia. In the current study,  $P_{ETCO_2}$  had a range of 2-3 mmHg around eucapnia, which indicates that the velocity data is representative of cerebral blood flow and can be utilized to assess the cerebral pressure-flow relationship.

*Cerebral Autoregulation:* Due to the myriad of unknown variables that are suspected to be responsible for cerebral autoregulation, the focus of this paper was not to discuss the black-box concept of cerebral autoregulation but to present the findings as they concern the relationship between mean arterial pressure and CBV. The complexities associated with the all-encompassing concept of cerebral autoregulation are likely (at least to an extent) non-linear in nature. However, most non-linear systems can still be approximated within a linear model as is the case with the findings of the current study. The coherence within the current study (mean range of 0.97-1.00 a.u., clearly indicates that

when the appropriate methodology is applied during exercise (OLBNP), the interpretability of the associated transfer function metrics is greatly enhanced.

## **6.6. Key finding**

This is the first study to conclusively demonstrate that the high-pass filter regulatory properties of the cerebrovascular are intact during moderate exercise in healthy aging. This was demonstrated through the novel approach of oscillating blood pressure during a moderate steady-state exercise with lower body negative pressure. The cerebral pressure-flow system was nearly linear in nature as indicated by a coherence of  $\sim 1.00$ . The increased signal-to-noise ratio resulted in an enhanced interpretability of the phase and gain metrics. With this novel methodology, it was also revealed that despite maintaining the high-pass filter nature of the cerebrovasculature, the older adults had an elevated normalized gain at 0.05 Hz and reduced phase at 0.10 Hz when compared with the younger adults during exercise. A within-subject comparison from rest revealed age-related differences in the expression of the phase metric at both 0.05 and 0.10 Hz. It is speculated that these age-related changes to TFA metrics are due to either alterations in arteriolar tone, sympathetic tone or the mechanical buffering of the compliance vessels that are possibly influenced by the exercise induced release of nitric oxide. However, more research in this area is required to confirm these notions.

## **Chapter Seven: Influence of high altitude**

This study was approved by the clinical ethical committees of the Universities of British Columbia (H11-03287), and adhered to the principles of the Declaration of Helinski and Title 45, U.S. Code of Federal Regulations, Part 46, Protection of Human Subjects. All volunteers provided written informed consent and procedures were followed in accordance to institutional guidelines.

A version of this study was accepted and presented as an oral presentation at the CARNet 2013 (annual scientific meeting of the cerebral autoregulation research network). Jonathan D. Smirl, Nia C.S. Lewis, Samuel J.E. Lucas, Gregory R. duManoir, Kurt J. Smith, Nima Sherpa, Aperna S. Basnyat and Philip N. Ainslie. Cerebral Pressure-Flow Relationship in Lowlanders and Natives at High Altitude. Jonathan Smirl was responsible for the data collection, data analysis, writing, and formatting of the abstract.

A version of this manuscript has been accepted and published in the *Journal of Cerebral Blood Flow and Metabolism* and has been reproduced with permission.<sup>3</sup> Jonathan D. Smirl, Nia C.S. Lewis, Samuel J.E. Lucas, Gregory R. duManoir, Kurt J. Smith, Akke Bakker, Aperna S. Basnyat and Philip N. Ainslie. Cerebral Pressure-Flow Relationship in Lowlanders and Natives at High Altitude. Jonathan Smirl was responsible for the data collection, data analysis, writing, and formatting of the manuscript.

## **7.1. Aims and Hypotheses**

### **Aims:**

- 1) To perform a comprehensive examination of the cerebral pressure-flow relationship in lowlanders: prior to; upon initial arrival; after partial acclimatization; and return from high altitude.
- 2) To examine if acute mountain sickness symptoms are related to the regulation of cerebral blood flow.
- 3) To compare the relationship between arterial blood pressure and cerebral blood flow regulation in partially acclimatized lowlanders and high altitude Sherpa.

### **Hypotheses:**

- 1) Upon initial arrival and prolonged exposure to high altitude the cerebral pressure-flow relationship will be comparable to the sea-level values (both pre- and post-high altitude exposure).
- 2) The symptoms of acute mountain sickness will be unrelated to the cerebral pressure-flow relationship.
- 3) The high altitude Sherpa will have intrinsic differences in the pressure-flow coupling as compare to the partially acclimatized lowlanders.

## 7.2. Rationale

The dynamic relationship between blood pressure and CBF has been shown to function as a high-pass filter, where higher frequency oscillations ( $>0.20$  Hz) in perfusion pressure are passed along unimpeded while slower frequency oscillations ( $<0.20$  Hz) are dampened by the cerebral arterioles.<sup>18,125,190</sup> TFA is a common method to assess this pressure-flow relationship.<sup>18</sup> Using this approach, a number of studies have reported that the dynamic cerebral pressure-flow relationship is impaired in conditions of hypobaric hypoxia, and may<sup>309,310</sup> or may not<sup>311-313</sup> be an important underlying mechanism in the pathophysiology of acute mountain sickness. A limitation in the majority of these studies, however, is that this altered relationship upon initial exposure<sup>314,315</sup> or after acclimatization<sup>316,317</sup> has been inferred from TFA under spontaneous conditions (as reported by decreases in phase [i.e., the time lag] and/or increases in gain [i.e., the signal amplitude]). An alternative interpretation to the reported impairment in the dynamic cerebral pressure-flow relationship at high altitude is that these observations are influenced by poor blood pressure variability, a limitation of using TFA under spontaneous conditions.<sup>194,267</sup> Induced non-pharmacological elevations in blood pressure variability can be utilized to mitigate this limitation and improve the reliability and interpretation of the TFA metrics.

267

In contrast to lowlanders at high altitude, we know of only two studies that have examined the cerebral pressure-flow relationship in natives to high altitude.<sup>318,319</sup> In their first study, Jansen *et al.*<sup>318</sup> assessed the pressure-flow relationship during steady-state hypertensive changes in blood pressure (i.e., 0 Hz), induced by pharmacological (i.e., phenylephrine) intervention. Findings showed that high altitude Sherpa, and most

lowlanders arriving to high altitude, had impaired cerebral pressure-flow responses at 4243m, as reflected in a more pressure-passive response to acute hypertension compared to a sea-level group in their cross-sectional study.<sup>318</sup> In their follow-up study,<sup>319</sup> it was reported that Sherpa who resided below 4000m had an intact pressure-flow response; however, in those residing above 4000m the chronic exposure to hypoxia led to more pressure-passive responses, indicative of impaired cerebral autoregulation.<sup>319</sup> In addition, the impairment in steady-state (i.e., static) cerebral autoregulation in this Sherpa group was improved following exposure to supplemental oxygen, a finding the authors speculated resulted from the vasoconstrictive effect of hyperoxia ( $F_{iO_2} = 1.0$ ) on the cerebral vessels, either directly or via the measured reduction in  $P_{ET}CO_2$ .<sup>319</sup>

To date, however, there has not been a comprehensive examination of the dynamic pressure-flow relationship (using TFA) under spontaneous and driven conditions upon initial arrival and after acclimatization within the same subject population, or comparisons made to high altitude natives (e.g., Sherpa). As mentioned, Jansen *et al.* has applied supplemental oxygen (100%) to Sherpa,<sup>318</sup> while another study has applied supplemental  $O_2$  (100%) to lowlanders after initial arrival to high altitude.<sup>314</sup> Such hyperoxia, however, is known to have a direct vasoconstrictive influence on the cerebrovasculature,<sup>320</sup> and it is unknown how normalizing end-tidal  $PO_2$  ( $P_{ET}O_2$ ) in partially acclimatized lowlanders affects the cerebral pressure-flow response. Vascular remodelling could theoretically occur at high altitude (over the course of ~1-week or more) due to changes in capillary density and blood volume which result in angiogenesis (reviewed in:<sup>321</sup>). While this remodelling is occurring, there is a period of uncompensated hypoxia which could influence the cerebral pressure-flow relationship<sup>321</sup>. Answering these questions would provide insight into

whether observed changes in pressure-flow relationships are caused simply by the hypoxia<sup>310,314-319</sup> or some additional influence of possible vascular remodelling<sup>321</sup> associated with high altitude exposure. We therefore attempted to address the following main questions: 1) Is the dynamic cerebral pressure-flow relationship impaired at high altitude (5050m) during spontaneous and non-pharmacological induced elevations in blood pressure variability?; 2) Are the changes in the pressure-flow relationship upon initial arrival to 5050m related to symptoms of acute mountain sickness? and 3) Are there intrinsic differences in the pressure-flow relationship between high altitude natives and lowlanders partial acclimatized to 5050m?

We hypothesized that: 1) The dynamic cerebral pressure-flow relationship will be impaired at high altitude upon initial arrival and after acclimatization, as assessed using spontaneous TFA measures; however, when blood pressure variability is maximized via repeated squat-stand maneuvers, the pressure-flow relationship will remain intact; 2) As highlighted in well-controlled chamber studies,<sup>312,313,322</sup> there will be no correlation between changes in the pressure-flow relationship upon initial arrival to 5050m with symptoms of acute mountain sickness; 3) High altitude natives will have intrinsic differences in pressure-flow coupling compared with acclimatized lowlanders at 5050m.

### **7.3. Methods**

#### *Subjects*

Thirty-two healthy subjects (16 lowlanders, 16 Sherpa: Table 7.1.) were recruited for this study. None had a history of cardiorespiratory or cerebrovascular disease and none were taking any form of medication upon enrolment into the study. All subjects abstained

from exercise, caffeine and alcoholic beverages for a period of 12-hours prior to the testing. Each subject underwent a familiarization of the laboratory and testing protocols before the initiation of the protocols.

**Table 7.1.** Participant characteristics.

	SL	Day 2	Week 2	Sherpa	O <sub>2</sub> Reversal	Return
Sex (male/female)	13/3	12/2	10/2	16/0	6/2	5/1
Age (years)	28.4 ± 7.2	28.2 ± 6.0	30.6 ± 6.8	32.5 ± 14.5	30.1 ± 8.1	31.7 ± 3.7
Height (cm)	175.7 ± 6.5	175.5 ± 6.6	175.9 ± 7.2	169.1 ± 5.8	174.3 ± 7.5	177.8 ± 9.1
Weight (kg)	76.8 ± 12.8	73.0 ± 11.7	74.2 ± 12.9	69.1 ± 13.3	73.0 ± 14.1	81.3 ± 12.1
BMI (kg/m <sup>2</sup> )	24.8 ± 3.4	23.7 ± 3.4	23.9 ± 3.5	24.1 ± 3.8	24.0 ± 4.0	25.6 ± 2.9

Values are means ± SD. Sea-level (SL); Oxygen (O<sub>2</sub>); body mass index (BMI). Return, return to sea level

### *Experimental design and ascent Protocol*

Following a full familiarization of the experimental protocols (summarized below); the lowlanders performed experimental trials at SL (350m, Kelowna, BC, Canada; barometric pressure  $715 \pm 15$  mm Hg) and whilst residing at high altitude (5050m; the Ev-K2-CNR Pyramid Laboratory, Khumbu Valley, Nepal; barometric pressure  $413 \pm 4$  mmHg). The SL trials (n=16) were completed 2-months prior to departure for Kathmandu and a subset of the group (n=6) were re-tested 2-weeks after returning from high altitude. Participants spent 7 days in Kathmandu (~1400m) acclimatizing before flying to Lukla (2840m) and trekking to the Ev-K2-CNR Pyramid Laboratory (5050m) over a 9-day period (rest days: Namche Bazaar, 3440m; Pengbouche, 3995m; Pheriche, 4240m). The high altitude trials were completed upon initial arrival to high altitude (Day 2: n=14) and after an acclimatization period of 2-weeks (Week 2: n=12), with a subset of this group also performing the trials with oxygen normalization where end-tidal  $PO_2$  was returned to sea-level values (n=8; 38%  $O_2$ , 0.04%  $CO_2$ , 61.96%  $N_2$  for 10-minutes prior to baseline measures). The Sherpa performed one experimental trial consisting of the spontaneous baseline measures and both squat-stand protocols (without supplemental oxygen) at high altitude (n=16). All Sherpa were born, raised and resided between 3500-4300m. None had spent any time at elevations lower than 2500m in the last six months. See Figure 7.1. for a schematic of the experimental testing conditions.

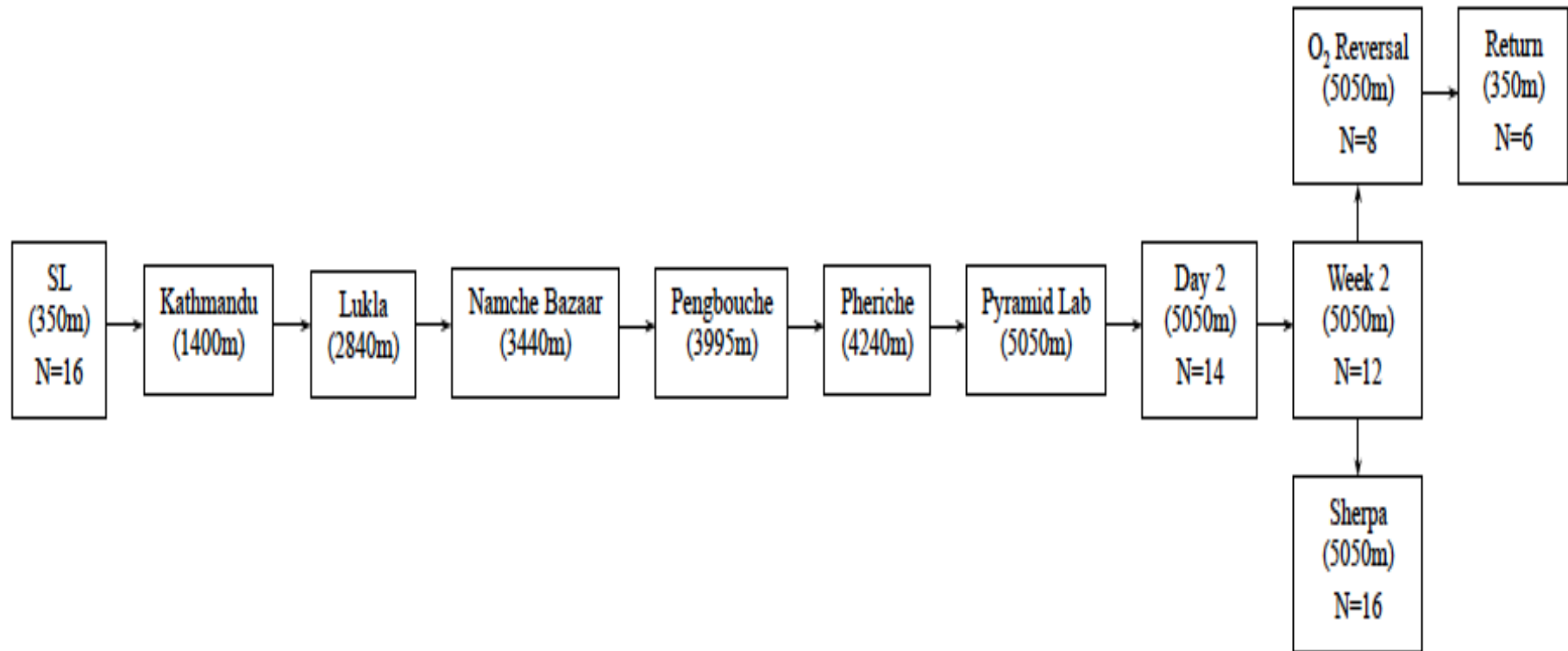


**Figure 7.1.** Schematic of the ascent protocol: the sea-level (SL) trials were completed 2 months prior to departure for Kathmandu. Lowlanders spent 7 days acclimatizing before flying to Lukla and trekking to the Ev-K2-CNR Pyramid Laboratory over a 9-day period (rest days: Namche Bazaar: 3440m; Pengbouche: 3995m; Pheriche: 4240m). Day 2 trials were conducted on the second day after arrival to the Pyramid Lab. After successful acclimatization to high altitude, the follow-up tests in the lowlanders (Week 2, O<sub>2</sub> Reversal) and Sherpa were performed. Two-weeks after returning to SL, a subset of the lowlanders were re-tested.

Upon arrival to the lab (either SL or 5050m), subjects underwent a familiarization of the experimental procedures and then performed the protocol. At least 5-minutes of resting spontaneous baseline data were recorded in a seated position. These data were used for the spectral analysis of spontaneous oscillations in blood pressure and CBV in the anterior (via MCAv) and posterior (via PCAv) cerebral circulatory regions. In order to increase the blood pressure variability, subjects performed repeated squat-stand maneuvers.<sup>190</sup> During the maneuvers, subjects mimicked the experimenter to ensure all subjects performed the maneuvers at a similar depth to induce blood pressure fluctuations. The subjects were randomly selected to perform maneuvers at 0.05 Hz (10-s squat–10-s stand – driving blood pressure in the VLF range) or 0.10 Hz (5-s squat–5-s stand – driving blood pressure in the LF range) first for 5-minutes each before performing the other frequency. A minimum 3-minute rest period was permitted in order to return to baseline levels in-between trials. These data were used for the spectral analysis of driven oscillations in blood pressure and both the MCAv and PCAv. During all trials, the end-tidal gases were monitored to ensure that normal breathing occurred and Valsalva-like maneuvers were avoided.

This study was part of a larger research expedition conducted in April-May in 2012; as such participants took part in a number of studies conducted during the 3-weeks at the Ev-K2-CNR Pyramid Laboratory. The recovery time between the various testing sessions was managed to prevent any potentially confounding results (e.g., >48-hours between all drug and/or exercise intervention studies). Additionally, during the first 8 days of the trek to the Pyramid Lab, sea-level participants were given low-dose acetazolamide (125 mg) twice a day as an acute mountain sickness prophylactic.<sup>323</sup>

Treatment of acetazolamide was discontinued on day 8 of the trek to allow sufficient time (e.g., > 48-hours) for the drug to clear participants' system prior to the first data collection session, as the half-life of acetazolamide is reported to be ~10-hours<sup>324</sup> and this low-dose is typically 90-100% passed through the system within 24-hours of administration.<sup>325</sup> This was done to minimize potential impacts of acute mountain sickness on cerebrovascular, cardiovascular and ventilatory responses,<sup>326</sup> but not result in acute mountain sickness severity great enough to prevent participants taking part in testing or require medical intervention (e.g., oxygen, dexamethasone injection).

The severity of acute mountain sickness was determined on an individual basis using the Environmental Symptoms Questionnaire Cerebral Symptoms (ESQ-C)<sup>327</sup> and Lake Louise (LL)<sup>328</sup> scoring protocols. Subjects deemed to be acute mountain sickness positive were determined from a LL score of  $\geq 3$  in the presence of a headache and/or an ESQ-C score  $\geq 0.7$ .<sup>329</sup>

### *Instrumentation*

In this study both the middle and posterior cerebral arteries were insonated. Blood pressure was monitored with finger photoplethysmography. 3-lead electrocardiography was utilized to monitor R-R intervals. End-tidal gases were monitored with a gas analyzer. Please refer to sections 2.1. for more detail about these instruments.

### *Data Processing*

Please refer to section 2.2. (signal processing)

### *Power spectrum and transfer function analysis*

Please refer to section 2.2.1. (Fourier transform); 2.2.2. (transfer function analysis); 2.2.3. (coherence); 2.2.4. (phase); and 2.2.5. (gain) for more detail about these measures.

### *Statistical Analysis*

Statistical analyses were performed using PASW version 18.0 for Windows (PASW, Inc. Chicago, Illinois). The effects of trial (sea-level, Day 2, Week 2) on MCA<sub>v</sub>, PCA<sub>v</sub>, blood pressure, P<sub>ET</sub>CO<sub>2</sub>, P<sub>ET</sub>O<sub>2</sub>, SaO<sub>2</sub>, CVR<sub>i</sub> and TFA coherence, gain and phase measures were assessed using a one-way ANOVA with a post-hoc Tukey comparison for group effects. An independent samples t-test was performed between the lowlanders at Week 2 and Sherpa data for MCA<sub>v</sub>, PCA<sub>v</sub>, blood pressure, P<sub>ET</sub>CO<sub>2</sub>, P<sub>ET</sub>O<sub>2</sub>, SaO<sub>2</sub>, CVR<sub>i</sub> and TFA coherence, gain and phase measures. Finally, a paired samples t-test was performed between the Week 2 and O<sub>2</sub> normalization, and the sea-level and return data on MCA<sub>v</sub>, PCA<sub>v</sub>, blood pressure, P<sub>ET</sub>CO<sub>2</sub>, P<sub>ET</sub>O<sub>2</sub>, SaO<sub>2</sub>, CVR<sub>i</sub> and TFA coherence, gain and phase measures. The paired samples t-test was performed on the subsets of individuals (n=6) that were involved in both sets of testing (i.e., only those subjects that were present for both the pre- and post- high altitude tests were part of the paired t-test). Data are presented as Mean ± SD, and statistical significance was set at  $P < 0.05$ .

#### 7.4. Results

All 16 subjects completed the full experimental protocol at sea-level; however, due to illness and time constraints only 14 and 12 subjects completed the protocol upon initial arrival to high altitude and after acclimatization, respectively. A subset of the acclimatized subjects performed the O<sub>2</sub> normalization (n=8) and the return to sea-level protocols (n=6; Figure 1). All 16 Sherpa subjects completed their experimental protocol. Estimates of middle cerebral artery diameter and flow were made in 10 lowlanders following acclimatization and in 6 Sherpa. Age and body mass index characteristics were similar between subject groups (Table 7.1.).

##### *Influence of squat-stand maneuvers*

During the spontaneous measures the blood pressure power was 2.55-13.70 mmHg<sup>2</sup> (Table 7.2.) which was increased to 12310-31271 mmHg<sup>2</sup> (Table 7.3.) during the driven protocol, representing a >500-fold increase in blood pressure variability. The TFA coherence values also increased from 0.48-0.81 a.u. (spontaneous data: Table 2) to >0.97 a.u. (squat-stand data: Table 7.3.).

**Table 7.2.** Transfer function analysis of spontaneous seated data between blood pressure and MCAv and PCAv.

	SL	Day 2	Week 2	Sherpa	O <sub>2</sub> Reversal	Return
<b>Spontaneous MCAv</b>						
VLF MAP Power (mmHg <sup>2</sup> )	7.00 ± 3.11	6.50 ± 5.00	10.35 ± 7.26	13.21 ± 9.27	6.31 ± 2.75	9.89 ± 6.20
LF MAP Power (mmHg <sup>2</sup> )	2.64 ± 1.63	5.54 ± 4.06	4.93 ± 4.71	3.66 ± 2.63	7.10 ± 5.01	7.12 ± 3.45*
VLF MCAv Power (cm/s) <sup>2</sup>	7.01 ± 3.86	7.90 ± 7.70	11.28 ± 8.97	7.30 ± 10.11	5.82 ± 8.86	5.33 ± 3.76
LF MCAv Power (cm/s) <sup>2</sup>	3.77 ± 2.27	7.85 ± 8.07	4.01 ± 3.78	2.65 ± 3.51	4.04 ± 2.94	6.15 ± 3.39
VLF Coherence	0.51 ± 0.18	0.52 ± 0.21	0.68 ± 0.18	0.67 ± 0.39	0.48 ± 0.16‡	0.62 ± 0.10
LF Coherence	0.69 ± 0.13	0.77 ± 0.11	0.81 ± 0.07*	0.75 ± 0.40	0.79 ± 0.10	0.80 ± 0.04
VLF Phase (radians)	1.02 ± 0.68	0.64 ± 0.38	0.41 ± 0.31*	0.55 ± 0.32	0.60 ± 0.35	0.72 ± 0.50
LF Phase (radians)	0.53 ± 0.17	0.50 ± 0.16	0.35 ± 0.10*	0.38 ± 0.23	0.27 ± 0.17	0.57 ± 0.18
VLF Gain (cm/s/mm Hg)	0.88 ± 0.40	1.01 ± 0.74	0.90 ± 0.43	0.67 ± 0.39	0.68 ± 0.36	0.66 ± 0.33
LF Gain (cm/s/mm Hg)	1.21 ± 0.37	1.02 ± 0.33	0.92 ± 0.23	0.75 ± 0.40	0.73 ± 0.24	0.93 ± 0.24
<b>Spontaneous PCAv</b>						
VLF MAP Power (mmHg <sup>2</sup> )	6.75 ± 2.98	6.47 ± 4.99	10.39 ± 7.22	13.70 ± 8.58	6.29 ± 2.76	9.88 ± 6.18
LF MAP Power (mm Hg <sup>2</sup> )	2.55 ± 1.63	5.49 ± 4.02	4.95 ± 4.65	3.76 ± 2.60	7.08 ± 4.99	7.14 ± 3.46*
VLF PCAv Power (cm/s) <sup>2</sup>	6.49 ± 5.15	4.23 ± 5.79	5.33 ± 3.13	2.95 ± 2.06	2.71 ± 2.13	2.48 ± 0.81
LF PCAv Power (cm/s) <sup>2</sup>	3.89 ± 4.67	2.66 ± 1.79	1.82 ± 1.17	1.28 ± 0.70	1.57 ± 0.57	3.26 ± 1.21
VLF Coherence	0.52 ± 0.14	0.44 ± 0.18	0.59 ± 0.21	0.59 ± 0.12	0.56 ± 0.23	0.46 ± 0.18
LF Coherence	0.65 ± 0.14	0.75 ± 0.10	0.73 ± 0.12	0.60 ± 0.19	0.72 ± 0.11	0.74 ± 0.11
VLF Phase (radians)	0.96 ± 0.62	0.73 ± 0.49	0.52 ± 0.24	0.43 ± 0.51	0.57 ± 0.21	1.08 ± 0.47
LF Phase (radians)	0.54 ± 0.21	0.52 ± 0.22	0.38 ± 0.09	0.47 ± 0.19	0.32 ± 0.15	0.53 ± 0.21
VLF Gain (cm/s/mm Hg)	0.85 ± 0.39	0.62 ± 0.57	0.69 ± 0.35	0.39 ± 0.17	0.56 ± 0.23	0.43 ± 0.24
LF Gain (cm/s/mm Hg)	1.13 ± 0.46	0.70 ± 0.22*	0.64 ± 0.19*	0.54 ± 0.19	0.49 ± 0.14	0.70 ± 0.17

Values are means ± SD. Sea-level (SL); Oxygen (O<sub>2</sub>); mean arterial pressure (MAP); middle cerebral artery velocity (MCAv); posterior cerebral artery velocity (PCAv); low frequency (LF); very low frequency (VLF). Statistical significance was set at  $P < 0.05$ , \*denotes significance from SL, †denotes significance from Day 2, ‡ denotes significance from Week 2.

**Table 7.3.** Transfer function analysis of driven data between blood pressure and MCAv or PCAv.

	SL	Day 2	Week 2	Sherpa	O <sub>2</sub> Reversal	Return
<b>MCAv</b>						
<b>Squat Stand (0.05 Hz)</b>						
MAP Power (mm Hg <sup>2</sup> )/Hz	29410 ± 16090	23807 ± 14145	17505 ± 11674	23020 ± 13003	25462 ± 10945	20294 ± 6264
MCAv Power (cm/s) <sup>2</sup> /Hz	13255 ± 7045	7932 ± 6697	6983 ± 5095*	8001 ± 5095	10513 ± 6865	9005 ± 2063
Coherence	0.99 ± 0.01	0.98 ± 0.02	0.97 ± 0.05	0.98 ± 0.03	0.99 ± 0.01	0.99 ± 0.01
Phase (radians)	0.63 ± 0.13	0.78 ± 0.36	0.81 ± 0.35	0.70 ± 0.27	0.68 ± 0.19	0.62 ± 0.13
Gain (cm/s/mm Hg)	0.70 ± 0.14	0.60 ± 0.25	0.65 ± 0.20	0.58 ± 0.19	0.63 ± 0.22	0.68 ± 0.09
<b>Squat-Stand (0.10 Hz)</b>						
MAP Power (mm Hg <sup>2</sup> )/Hz	19573 ± 9333	20200 ± 7279	14032 ± 5243*	13970 ± 6746	16906 ± 9062	12310 ± 5920
MCAv Power (cm/s) <sup>2</sup> /Hz	16994 ± 10981	17078 ± 9661	10600 ± 5801*	18657 ± 6634	10533 ± 2856	10866 ± 2856
Coherence	1.00 ± 0.00	1.00 ± 0.01	1.00 ± 0.00	1.00 ± 0.00	1.00 ± 0.01	0.99 ± 0.01
Phase (radians)	0.35 ± 0.12	0.41 ± 0.22	0.34 ± 0.12	0.32 ± 0.13	0.35 ± 0.10	0.43 ± 0.05
Gain (cm/s/mm Hg)	0.92 ± 0.18	0.91 ± 0.28	0.87 ± 0.19	0.77 ± 0.25	0.81 ± 0.22	0.99 ± 0.17
<b>PCAv</b>						
<b>Squat Stand (0.05 Hz)</b>						
MAP Power (mm Hg <sup>2</sup> )/Hz	31271 ± 15360	21395 ± 11579	17538 ± 11690	22804 ± 13771	25493 ± 10965	20316 ± 6281
MCAv Power (cm/s) <sup>2</sup> /Hz	8677 ± 5245	4497 ± 5457	3558 ± 3172*	3814 ± 2213	4128 ± 3332	4238 ± 2058
Coherence	0.99 ± 0.01	0.98 ± 0.03	0.97 ± 0.06	0.97 ± 0.07	0.99 ± 0.01	0.99 ± 0.01
Phase (radians)	0.59 ± 0.15	0.75 ± 0.33	0.76 ± 0.38	0.74 ± 0.26	0.68 ± 0.24	0.62 ± 0.12
Gain (cm/s/mm Hg)	0.51 ± 0.14	0.45 ± 0.26	0.43 ± 0.14	0.40 ± 0.13	0.38 ± 0.11	0.45 ± 0.09
<b>Squat-Stand (0.10 Hz)</b>						
MAP Power (mm Hg <sup>2</sup> )/Hz	20453 ± 9108	20234 ± 7270	14065 ± 5271	13296 ± 5761	16943 ± 9109	12340 ± 5942
MCAv Power (cm/s) <sup>2</sup> /Hz	11753 ± 8070	7272 ± 6555	5148 ± 3672	4393 ± 2749	4270 ± 3110	5293 ± 82582
Coherence	1.00 ± 0.00	0.99 ± 0.03	1.00 ± 0.00	1.00 ± 0.01	1.00 ± 0.00	0.99 ± 0.01
Phase (radians)	0.30 ± 0.12	0.42 ± 0.22	0.35 ± 0.12	0.35 ± 0.12	0.36 ± 0.10	0.49 ± 0.04*
Gain (cm/s/mm Hg)	0.73 ± 0.18	0.55 ± 0.21	0.56 ± 0.15	0.56 ± 0.17	0.49 ± 0.12	0.66 ± 0.13

Values are means ± SD. Sea-level (SL); Oxygen (O<sub>2</sub>); mean arterial pressure (MAP); middle cerebral artery velocity (MCAv); posterior cerebral artery velocity (PCAv). Statistical significance was set at  $P < 0.05$ , \*denotes significance from SL, †denotes significance from Day 2, ‡ denotes significance from Week 2.

*Initial Arrival (Day 2)*

Upon initial arrival to high altitude (5050m),  $P_{ET}O_2$  and  $P_{ET}CO_2$  were reduced by 47 mm Hg and 10 mm Hg, respectively, and there was a 17% reduction in arterial  $O_2$  saturation ( $P<0.001$ ). There were no changes in mean blood pressure, velocity or CVRi in the middle cerebral artery. In contrast, there was a 21% reduction in velocity ( $P<0.01$ ), coinciding with a 35% increase in CVRi ( $P<0.01$ ) in the posterior circulation (Table 7.4.).

**Table 7.4.** Hemodynamic and cerebrovascular responses during spontaneous baseline

	SL	Day 2	Week 2	Sherpa	O <sub>2</sub> Reversal	Return
<b>Baseline (Sitting)</b>						
Mean BP (mmHg)	87 ± 11	89 ± 8	93 ± 14*	89 ± 11	86 ± 15	89 ± 4
Mean MCAv (cm/s)	68 ± 11	67 ± 9	60 ± 9	46 ± 14‡	55 ± 13	55 ± 8*
MCA CVRi (mmHg/cm/s)	1.2 ± 0.2	1.4 ± 0.2	1.6 ± 0.4*	2.1 ± 0.6‡	1.7 ± 0.5	1.4 ± 0.3
Mean PCAv (cm/s)	49 ± 11	39 ± 7*	41 ± 7*	37 ± 8	35 ± 5‡	36 ± 8*
PCA CVRi (mmHg/cm/s)	1.7 ± 0.4	2.3 ± 0.4*	2.4 ± 0.6*	2.5 ± 0.5	2.7 ± 0.7	2.2 ± 0.7
End-Tidal PCO <sub>2</sub> (mmHg)	40 ± 7	30 ± 3*	29 ± 3*	33 ± 3‡	30 ± 4	36 ± 4
End-Tidal PO <sub>2</sub> (mmHg)	100 ± 8	53 ± 4*	55 ± 3*	53 ± 5	109 ± 6‡	107 ± 7
O <sub>2</sub> Saturation (%)	96 ± 2	80 ± 3*	83 ± 2*†	80 ± 5‡	97 ± 1‡	97 ± 2

Values are means ± SD. Sea-level (SL); Oxygen (O<sub>2</sub>); blood pressure (BP); middle cerebral artery velocity (MCAv); posterior cerebral artery velocity (PCAv); cerebrovascular resistance index (CVRi). Statistical significance was set at  $P < 0.05$ , \*denotes significance from SL, †denotes significance from Day 2, ‡ denotes significance from Week 2.

Compared to sea-level values, there were no statistically significant differences in the power spectrum of blood pressure, MCAv or PCAv with initial exposure to high altitude under either spontaneous (Table 7.2.) or driven (Table 7.3.) protocols. TFA revealed no statistical differences between sea-level and day 2 for either spontaneous or the driven values for each of coherence, phase and gain within the middle cerebral artery at both sea-level and day 2. Although, as expected, main effects between conditions were present (Tables 7.2. & 7.3.). Within the posterior cerebral circulation, LF gain was reduced by an average of 38% during spontaneous breathing ( $P<0.01$ ) and by 24% during the 0.10 Hz stand-squats ( $P=0.057$ ). All other day 2 TFA indices were not statistically different to sea-level values within the posterior cerebral artery (Tables 7.2. & 7.3.; Figures 7.2. & 7.3.). Taken together, these TFA metrics are indicative of an intact high-pass filter model for the middle cerebral artery circulation upon initial arrival to high altitude. Within the posterior cerebral circulation there appears to be a decrease in the amplitude modulation in the spontaneous LF gain metric (i.e., an ‘improved’ relationship), which is less evident with the increased blood pressure variability associated with the driven protocol.

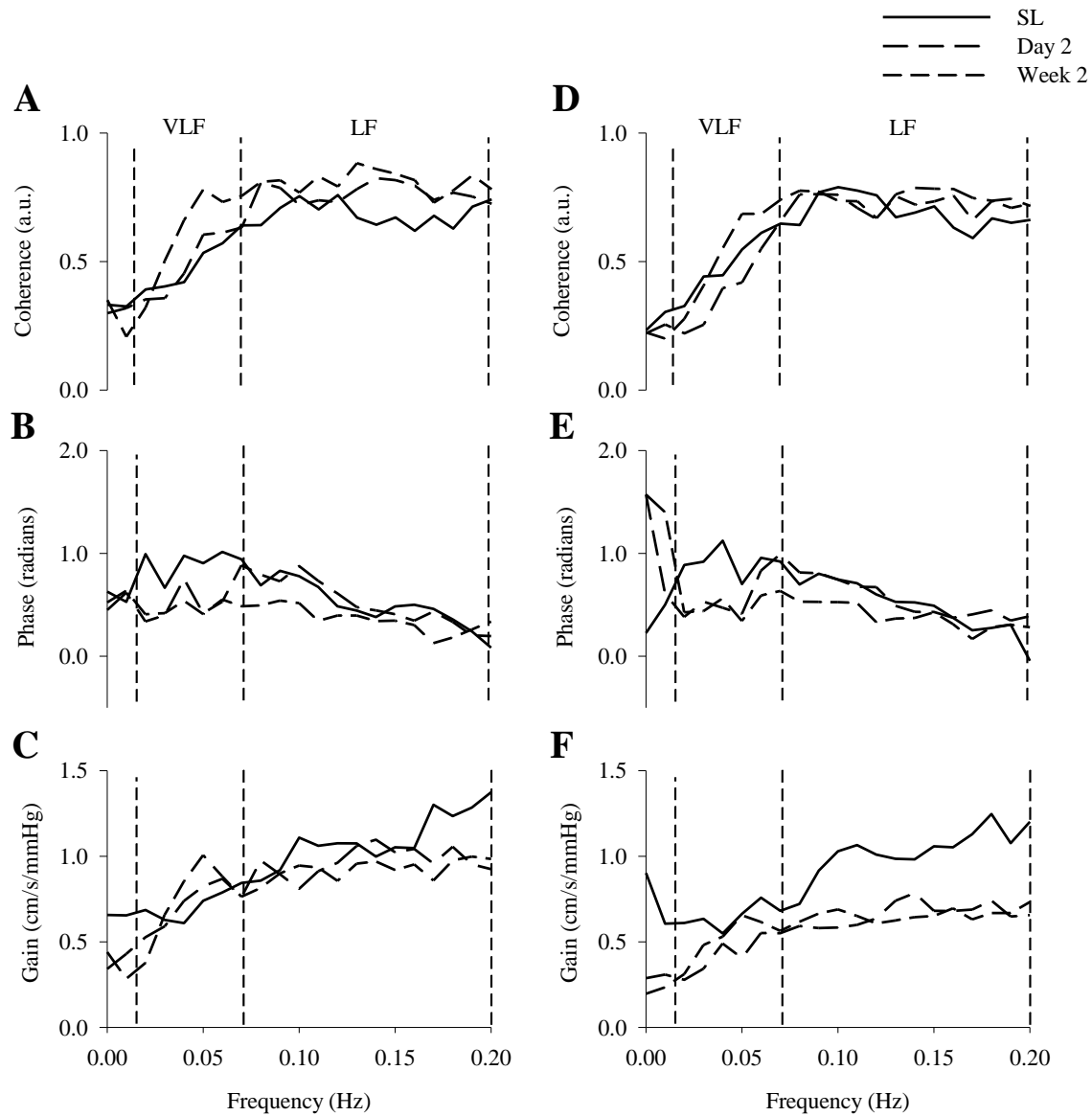


**Figure 7.2.** Transfer function analysis of the cerebral pressure-flow relationship during spontaneous oscillations in blood pressure and cerebral blood flow velocities at sea level (SL-solid), upon arrival (day 2, long dash) and following partial acclimatization to 5050m (week 2, short dash). Data are presented as group means for coherence, phase and gain within the middle cerebral artery (A, B, C) and the posterior cerebral artery (D, E, F) in the very low frequency (VLF) and low frequency (LF). Notes: In the anterior cerebral circulation Week 2 LF Coherence, VLF phase and LF phase were different from SL; in the posterior cerebral circulation day 2 and week 2 PCA LF gain was different from sea-level. There were no statistical differences between day 2 and week 2 in either cerebral hemisphere.

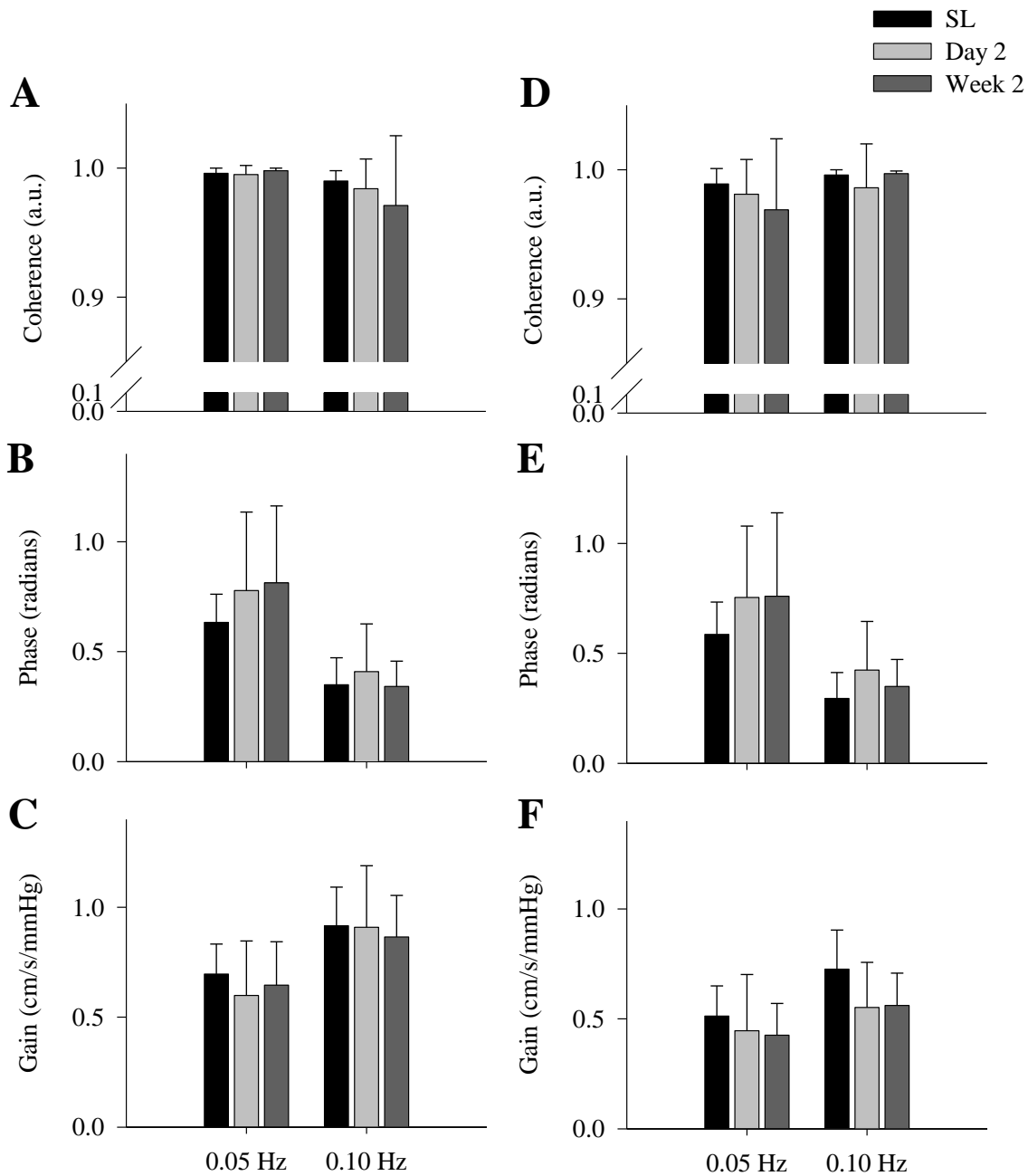


**Figure 7.3.** Transfer function analysis of the cerebral pressure-flow relationship during driven oscillations in blood pressure and cerebral blood flow velocities at sea-level (SL-black), upon arrival (Day 2, light grey) and following partial acclimatization to 5050m (Week 2, dark grey). Data are presented as group means  $\pm$  SD for coherence, phase and gain within the middle cerebral artery (A, B, C) and the posterior cerebral artery (D, E, F) at 0.05 Hz and 0.10 Hz. Note: There were no statistical differences at any time point in the 0.05 and 0.10 Hz range.

Although seven subjects had acute mountain sickness symptoms upon initial arrival to high altitude, there were no evident correlations between the ESQ-C ( $0.20 \pm 0.19$ ) or LL ( $3.2 \pm 1.6$ ) acute mountain sickness scores with either TFA metric (phase:  $R^2 < 0.04$ ; gain:  $R^2 < 0.02$ ) on Day 2 at 5050m. There were also no statistical differences in any TFA metric between those with and those without acute mountain sickness symptomology.

#### *Influence of Two-Weeks of Acclimatization (Week 2)*

After two-weeks of acclimatization to 5050m, all subjects were free of acute mountain sickness symptoms and there was a 4% increase in the O<sub>2</sub> saturation levels to ~83% ( $P < 0.001$ ). The MCAv trended to being reduced ( $P = 0.064$ ) compared with sea-level values, and CVRi was increased (by 33%;  $P < 0.01$ ). At the end of week 2 the PCAv and related CVRi were unchanged from day 2 and were significantly altered compared to sea-level ( $P < 0.01$ ; Table 7.4.).

Under spontaneous conditions, there were no statistical differences in the power spectrum of either: blood pressure, MCAv or PCAv after two-weeks at high altitude compared to either the initial exposure or sea-level values (Table 7.2.). Under driven conditions, MCAv and PACv power spectrums were reduced to ~50% of the sea-level values ( $P < 0.05$ ). TFA of the spontaneous data revealed the middle cerebral artery to have reduced phase measures in both the VLF and LF ranges ( $P < 0.05$ ). In contrast, the posterior cerebral artery had a 43% reduction in the LF gain during spontaneous baseline ( $P < 0.01$ ) as compared with sea-level values. These measures indicate that there appears to be an altered high-pass filter under spontaneous conditions within both the middle

cerebral artery and posterior cerebral artery after partial acclimatization to high altitude. With the increase in blood pressure variability associated with the squat-stands, the posterior cerebral artery gain index for 0.10 Hz was trending to being reduced as compared to sea level (-23%,  $P=0.061$ ; Table 7.3.). The remaining TFA metrics under driven conditions were all comparable to both sea level and day 2 values (Table 7.3.), which is indicative of an intact high-pass filter model within the cerebral circulatory system.

#### *Comparison with high altitude natives*

The high altitude natives had a 22% lower MCAv and correspondingly higher CVRi ( $P<0.01$ ) compared with the partially acclimatized lowlanders (week 2), whilst PCAv was comparable between the two groups (Table 7.4.). The Sherpa had higher  $P_{ET}CO_2$  levels (33 vs. 29 mmHg,  $P<0.01$ ) and lower  $O_2$  saturation levels (80% vs. 83%,  $P<0.05$ ) than the lowlanders. All other hemodynamic and cerebrovascular measures were comparable (Table 7.4.). Under spontaneous and driven conditions there were no statistically significant differences between the Sherpa and the acclimatized lowlanders for any of the TFA metrics (Tables 7.2. & 7.3.).

#### *Effects of $O_2$ Normalization ( $n=8$ )*

With the normalization of  $P_{ET}O_2$ ,  $P_{ET}CO_2$  increased by 3 mm Hg ( $P<0.05$ ), the  $O_2$  saturation levels returned to sea level values ( $97 \pm 1\%$ ) and PCAv reduced by 15% ( $P<0.05$ ). All other hemodynamic and cerebrovascular measures were comparable (Table 7.4.). Under spontaneous conditions, VLF Coherence in the MCAv was reduced by 30%

( $P < 0.05$ ; Table 7.2.). All other TFA metrics were not statistically different with normalization of  $P_{ET}O_2$  during either spontaneous or driven conditions (Tables 7.2. & 7.3.).

#### *Returning to sea level (n=6)*

Two-weeks after returning to sea level, MCAv and PCAv were ~14% lower than pre-high altitude values ( $P < 0.05$ ). All other hemodynamic and cardiovascular measures had returned to their pre-high altitude levels (Table 7.4.). Under spontaneous conditions, while there was two-fold increase in the arterial blood pressure LF power spectrum (3.4 to 7.1 mmHg<sup>2</sup>,  $P < 0.05$ ) all other spontaneous TFA metrics were not statistically different to initial SL measures (Table 7.2.). During the induced elevations in blood pressure variability, there was a 40% increase in 0.10 Hz phase in the posterior cerebral circulation ( $P < 0.05$ ), while all other TFA metrics were statistically unaltered from their initial SL values (Tables 7.2. & 7.3.).

## **7.5. Discussion**

The key findings from this study were: 1) Spontaneous VLF and LF phase was progressively reduced and coherence was elevated over time at high altitude compared with sea level, indicating impaired cerebral pressure-flow coupling for the anterior cerebral circulation. However, when blood pressure variability was increased in these frequency ranges via squat-stand maneuvers, such changes were not present in either the frequency or time domain; 2) The severity of acute mountain sickness was unrelated to any changes in the pressure-flow relationship upon initial arrival to 5050m; 3) There

appears to be no intrinsic differences in the cerebral pressure-flow relationship between high altitude natives and partially-acclimatised lowlanders at 5050m; 4) With normalization of  $P_{ET}O_2$ , the cerebral pressure-flow relationship at 5050m was unchanged in partially acclimatized lowlanders; and 5) Although there was a ~14% reduction in MCAv and PCAv present after returning to sea level for two-weeks compared to pre-expedition sea level values, the cerebral pressure-flow relationship was generally unaltered. Collectively our findings indicate that high altitude is likely to lead to some alterations in the spontaneous cerebral pressure-flow relationship in humans residing at 5050m, although would seem not to be linked to acute mountain sickness symptomology. However, this observation is dependent on the method of assessment, and may subtly differ between the anterior and posterior cerebral circulation. When blood pressure variability is increased via a squat-stand intervention the cerebral pressure-flow relationship (in both frequency- and time-domains) is unaltered at high altitude (5050m) in lowlanders and high altitude natives. Because of this observation we conclude that changes detected via the spontaneous TFA assessment of the pressure-flow relationship may not necessarily reflect a physiologically important alteration in the capacity of the brain to regulate blood pressure. Before these main findings are discussed in the context of previous literature, relative methodological considerations that underpin these findings are considered.

#### *Methodological Considerations:*

As there is no agreed-upon gold standard for the assessment of cerebral autoregulation,<sup>125</sup> we have chosen not to evaluate the mechanisms behind the influence

of HA on cerebral autoregulation per se; rather, we have focused purely on the relationship that exists between blood pressure and CBV. To quantify this pressure-flow relationship we utilized TFA, which defines the linear statistical relationship (coherence) between the input (blood pressure) and the output (MCAv or PCAv). Despite the widespread use of TFA to assess ‘dynamic’ autoregulation, it is important to note that the process of cerebral autoregulation is not likely a purely linear system between blood pressure and CBF. Other factors such as cerebrovascular compliance, cerebral blood volume, intracranial pressure and venous outflow acting as a Starling resistor are likely to also contribute to this form of CBF control. We utilized the squat-stand maneuvers to increase the blood pressure variability and thus improve the mathematical interpretability and reliability<sup>190</sup> of the TFA phase and gain metrics. The downside to performing these maneuvers is that by linearizing the pressure-flow response mechanism (coherence values for the driven data in this study were >0.97 a.u.) we may have ‘overwhelmed’ the autoregulatory mechanisms within the cerebrovasculature, which is a key reason for our discussion focusing on the cerebral pressure-flow relationship instead of cerebral autoregulation per se. Nevertheless, we view such blood pressure challenges as more physiological and realistic of daily activities (e.g., postural changes, coughing, exercise, defecation, etc.) than spontaneous measures alone. Moreover, in support of a maintained cerebrovascular capacity, even when we quantify the influence of the squat-stand maneuvers in the time domain (e.g., % changes in blood pressure vs. % changes in CBV over time) our conclusions persist (see Appendix: Supplementary Information – Time-Domain Analysis).

Although we did not measure CBF directly at all time points, we utilized transcranial Doppler ultrasound to provide an index of CBF that enables us to use the relative changes in MCAv or PCAv to directly represent relative changes in the CBF within these arteries (reviewed in: <sup>38</sup>). Further, given the known limitations of this technique and the possibility of dilation in the middle cerebral artery, <sup>330,331</sup> we did not place emphasis on absolute MCAv or PCAv values but only the relative changes. Importantly, the high temporal resolution provided by the transcranial Doppler ultrasound makes it an ideal tool to study the pressure-flow relationship. Nevertheless, to complement this measure and quantify potential changes in middle cerebral artery diameter and CBF, we also employed the novel approach of Transcranial color-coded Duplex <sup>331</sup> in a sub-group of our lowlanders and Sherpa. We found no evidence of between-group differences in middle cerebral artery diameter or flow (see Appendix: Supplementary Information – transcranial colour-coded duplex).

*Dynamic cerebral pressure-flow relationships at high altitude:*

Only five studies have assessed the dynamic cerebral pressure-flow relationship in lowlanders at high altitude. <sup>310,314-317</sup> These investigations were conducted at a range of elevations (4559-5400m) and generally in small samples of subjects. Out of these five, three studies assessed the dynamic cerebral pressure-flow relationship at one time point after arrival (between 1-10 days) to high altitude. <sup>310,314,315</sup> Upon initial arrival to high altitude, Van Osta *et al.* <sup>310</sup> reported that there was an altered cerebral autoregulatory response, as measured using the ARI, in proportion to the severity of acute mountain sickness symptomology in an individual. However, consistent with our initial arrival

findings (<20-hours), they did not note any overall subject differences for the blood pressure or MCAv at high altitude from sea level.<sup>310</sup> We have previously reported an increase in VLF gain (36%) and a decrease in VLF phase (29%) upon initial arrival to high altitude (1-2 days),<sup>314</sup> and saw similar changes in a follow-up study after ~1-week at 5050m<sup>315</sup> (VLF gain increased 71% and VLF phase decreased 67% compared to sea level). Interestingly, we did not observe any changes in the LF gain or LF phase metrics in either study.<sup>314,315</sup> These findings seem to contradict our current findings, as the VLF data is indicative of a general impairment in the pressure-flow response, whereas the LF data demonstrates an intact response. More likely these findings highlight that there is a frequency dependant response, where by the slower oscillations (VLF: >14-s per oscillation) are more affected by the initial arrival to high altitude than are the LF oscillations. The mechanism(s) underlying these frequency differences are unknown (see: *Methodological Considerations*).

Only one study, to our knowledge, has assessed the dynamic cerebral pressure-flow relationship following partial (more than 1-month) acclimatization.<sup>316</sup> That study did not report any data upon initial arrival to high altitude. Although some of the data from that acclimatization study was published in an earlier preliminary report,<sup>316</sup> a more recent analysis<sup>317</sup> revealed that after a one-month acclimatization period there was an increase in the VLF gain metric<sup>316</sup> and a decrease in VLF phase.<sup>317</sup> Their combined findings from both reports indicate that there is an altered pressure-flow response that is frequency-dependant after partial acclimatization to high altitude. In the recent analysis,<sup>317</sup> those researchers attempted to use deep breathing at 0.05 Hz to improve blood pressure variability and hence TFA mathematical reliability; however, the deep breathing

failed to affect either the VLF coherence ( $0.71 \pm 0.04$  spontaneous vs.  $0.76 \pm 0.04$  a.u. paced breathing) or the VLF gain ( $1.48 \pm 0.30$  spontaneous vs.  $1.36 \pm 0.16$  cm/s/mm Hg paced breathing). Therefore, it seems that their deep-breathing intervention did not adequately increase the blood pressure variability. Further, this deep-breathing intervention resulted in approximately an 8-10-fold increase in the blood pressure power spectrum,<sup>317</sup> whereas the squat-stand maneuvers used in our current study induced a >500-fold increase in the blood pressure power spectrum (Tables 7.2. & 7.3.), which were comparable to the increases shown in another sea level study.<sup>190</sup>

Our study, inclusive of both spontaneous and driven blood pressure changes in a larger sample size, did not support the general alteration in VLF pressure-flow relationships in the initial arrival data. However, our driven data did confirm the intact LF response upon initial arrival in the middle and posterior cerebral artery phase and gain metrics (Table 7.3.). In the partial acclimatization data, our spontaneous data findings do support the reduced VLF phase<sup>317</sup> in the middle cerebral artery, yet the reduction in VLF phase in the posterior cerebral artery did not reach statistical significance ( $P=0.108$ ; Table 7.3.). In contrast to Iwasaki *et al.*,<sup>317</sup> our driven data did show an improvement in the VLF (+45%) and LF (+23%) coherence and, in the context of the increased blood pressure variability, indicate that the pressure-flow relationship is maintained in the middle cerebral artery (Table 7.3.). Of note, however, is the altered pressure-flow response in the posterior circulation; as evidenced by LF gain measures in both the spontaneous (Table 7.2.) and driven (Table 7.3.) data. Consistent with a greater sensitivity of the posterior region of the brain to acute severe hypoxia,<sup>42</sup> this finding raises the possibility of subtle regional differences in pressure-flow regulation upon

prolonged exposure to high altitude. However, it should be noted that changes in TFA gain are likely the least robust metric in the assessment of the pressure-flow relationship during changes in arterial blood gases.<sup>125</sup>

To summarize, our findings indicated that high altitude is likely to lead to some alterations in the spontaneous cerebral pressure-flow relationship in humans residing at 5050m, although would seem not to be linked to acute mountain sickness symptomology. Moreover, these findings are not universal as the driven data reveal that the cerebral pressure-flow response is indeed intact when there is an increase in the blood pressure variability as induced by squat-stands. Because of these observations we conclude that the differences in spontaneous TFA observed do not necessarily reflect physiologically important alterations in the capacity of the brain to regulate blood pressure.

*Pressure-flow relationships and acute mountain sickness:*

A loss of cerebral autoregulation has been reported to be an important underlying mechanism in the pathophysiology of acute mountain sickness (reviewed in:<sup>311</sup>). However, a correlative relationship between changes in dynamic cerebral pressure-flow regulation and severity of acute mountain sickness<sup>309,310</sup> is not a universal finding.<sup>312,313</sup> Our study is the first to examine the relationship between acute mountain sickness and the dynamic cerebral pressure-flow relationship in the field rather than based on predictions from sea-level variability in cerebral autoregulation.<sup>309,312,313,322</sup> Our findings are consistent with well-controlled chamber studies<sup>312,313</sup> and demonstrate that alterations in the cerebral pressure-flow relationship do not appear to play a pivotal role in the development of acute mountain sickness. We do acknowledge, however, that these

findings are only in the context of the current study and relate to the mild-to-moderate symptoms of acute mountain sickness that we observed upon initial arrival to 5050m following prior prophylactic use of acetazolamide during a graded ascent to 5050m.

*Comparison with high altitude natives:*

An early study by Lahiri and Milledge<sup>332</sup> demonstrated that Sherpa ventilated less than acclimatized lowlanders and had a hypoxic ventilatory response that was one-third that of acclimatized lowlanders. Our findings of higher  $P_{ET}CO_2$  levels and lower  $P_{ET}O_2$  and  $SaO_2$  levels in the Sherpa are consistent with these findings (Table 7.4.). Although the elevated  $P_{ET}CO_2$  and reduced  $P_{ET}O_2$  would tend to increase CBF,<sup>42</sup> the slightly higher elevations in hematocrit in the high altitude natives<sup>333</sup> probably offset the vasodilatory influence of these changes in blood gases. Our finding of a comparable ‘intact’ pressure-flow response in Sherpa and partially acclimatized lowlanders at 5050m is seemingly in contrast to a previous report.<sup>318</sup> The conflicting outcomes between our findings and those of Jansen *et al.* may be a result of the differences in elevation (5050m vs. 4243m), acclimatization (14 vs. 5-7 days) and method to assess the cerebral pressure-flow response (TFA vs. % change of MCAv with phenylephrine injection).

The 22% lower MCAv in the high altitude natives compared with lowlanders in the present study is also different than this previous report,<sup>318</sup> where comparable MCAv was reported (Sherpa:  $61 \pm 11$ ; lowlanders:  $63 \pm 12$  cm/s). Early studies have established that natives with chronic mountain sickness and related polycythemia have reductions in CBF compared with chronic mountain sickness free natives and lowlanders<sup>334</sup>. However, in our study, the high altitude natives were free of chronic mountain sickness and

polycythemia, which may help explain their comparable middle cerebral artery diameter and flow at high altitude. Our finding of a lower MCAv is also inconsistent with the maintained middle cerebral artery diameter and flow in Sherpa when compared with the acclimatized lowlanders. Interestingly, the PCAv in the current study was comparable between groups (Table 7.4.) and consistent with this latter finding. Although small elevations in hematocrit in the high altitude natives may explain their reduced MCAv, it would not explain the discrepancy between a maintained MCAv and PCAv unless there were some regional differences. We cannot explain these differences on the basis of our current data.

*Normalization of end-tidal PO<sub>2</sub> at 5050m:*

Two studies to date have utilized the application of hyperoxia (FiO<sub>2</sub>=1.0) at high altitude to reverse the ‘impairment’ of the cerebral pressure-flow response.<sup>314,319</sup> In both Sherpa<sup>319</sup> and newly arrived lowlanders,<sup>314</sup> supplemental oxygen (FiO<sub>2</sub>=1.0) has been found to alleviate some of the altered cerebral pressure-flow responses which has been reported. In contrast to the previous studies, we applied hyperoxia (38% O<sub>2</sub>, 0.04% CO<sub>2</sub>, 61.96% N<sub>2</sub>) that was sufficient to return P<sub>ET</sub>O<sub>2</sub> and SaO<sub>2</sub> back to typical SL values. With this approach, we revealed comparable phase and gain metrics in both the spontaneous and driven data for the normalization of P<sub>ET</sub>O<sub>2</sub> as compared with the partially acclimatized subjects (Tables 7.2. & 7.3.). Our findings indicate that supplemental O<sub>2</sub>, despite elevations in P<sub>ET</sub>CO<sub>2</sub> due to hypoventilation, neither augments nor impairs the cerebral pressure-flow response at high altitude.

*Influence of high altitude exposure on MCAv and PCAv and pressure-flow coupling upon return to sea-level:*

Two-weeks after returning to sea level, we observed that all hemodynamic and cardiovascular measures returned to their pre-high altitude levels except for the absolute values of MCAv and PCAv (down 14% in both;  $P < 0.05$ ; Table 7.4.). Recent reports have shown that CBF (as assessed using arterial spin labeling MRI) is elevated 6-hours following return to sea level from 4350m<sup>335</sup> and within 8-hours of returning from 3800m.<sup>336</sup> The time course of recovery of CBF and cerebral metabolic rate of oxygen consumption following return from high altitude is not known and warrants future investigation. Nevertheless, the decreased MCAv and PCAv upon return did not alter the dynamic cerebral pressure-flow response, as indicated by the comparable findings in TFA metrics between pre- and post-high altitude.

## **7.6. Key finding**

We conclude that under spontaneous conditions there appears to be ‘alterations’ in the cerebral-pressure flow relationship after partial acclimatization that is not alleviated by the normalization of  $P_{ET}O_2$ . However, when the blood pressure variability is increased via squat-stand maneuvers, there appears to be little evidence of altered cerebral pressure-flow relationships (as evident in both the frequency and time domain) at high altitude in lowlanders either upon initial arrival or after partial acclimatization or in native populations with generations of exposure to high altitude. We interpret our findings to indicate that the spontaneous changes in TFA metrics do not necessarily reflect physiologically important alterations in the capacity of the brain to regulate blood pressure.

## **Chapter Eight: Overall Conclusions**

The following and final section outlines the overall significance and contributions of the presented research chapters as they pertain to the cerebral-pressure flow relationship field. The strengths and weakness of the presented research will be highlighted, and the broader application for the research findings will be considered. Potential future directions for this field of research will be finally discussed.

### **8.1. Overall significance and contribution of the thesis research**

Prior to this thesis, a major limitation of the human research examining the relationship between arterial blood pressure and CBF through the application of TFA is that it has been performed under spontaneous conditions.<sup>18,41,237,316,317</sup> The collective findings from the presented research chapters clearly highlight that under these resting and spontaneous circumstances, there is very little power in the input signal (blood pressure), which makes linear interpretation of the output (CBV) metrics underlying this relationship tenuous. Of the proposed methods within the literature to enhance the input power via oscillations in blood pressure variability (squat-stand maneuvers, OLBNP, deep-breathing and passive leg raises), the findings from Chapter 3 supported the notion that the squat-stand maneuvers are the most robust and reliable in both younger and older otherwise healthy adult populations. The study also demonstrated that changes in posture result in acute changes to CVRi may impact TFA metrics, a topic which was further explored in Chapter 4.

The aim of Chapter 4 was to determine how the cerebral-pressure flow relationship is affected when there are acute increases to CVRi in younger adults. To

address this question, a clinical dose of Indomethacin was administered as a novel means to lower CBF by 20-35%.<sup>120-122</sup> Hypocapnia was also induced by voluntary hyperventilation to effectively ‘match’ the elevations in CVRi that were present in the Indomethacin trial. This study also sought to determine if there are any changes in the regulatory properties within the anterior and posterior regions of the cerebrovasculature. Collectively, the findings from this chapter indicated that changes in CVRi in younger adults resulted in increases in phase lead and reductions to the amplitude modulation in both the anterior and posterior regions of the brain. Therefore, these results demonstrated that in situations where there are varying levels of CVRi (either between subjects or interventions), the impact needs to be considered for the parsimonious interpretation of TFA metrics.

In Chapter 5, the cerebral pressure-flow responses were examined in younger adults and in two populations where CVRi is altered through the course of human aging: older healthy adults and long-term heart transplant recipients. The long-term heart transplant recipients provide a unique model to address not only the role of increased CVRi but also the role of the cardiac baroreceptor in CBF regulation.<sup>286,287</sup> Previous studies in young, but not older adults, have shown relationships between the sensitivity of the cardiac baroreflexes and pressure-flow regulation as assessed via TFA.<sup>289</sup> The heart transplant recipients provided a further means to mechanistically examine this relationship because during the allograft surgery, all sympathetic and parasympathetic nerves are severed to (and from) the heart, therefore effectively eliminating the effects of the cardiac baroreceptors on the regulation of cardiac output. In this study it was found that long-term heart transplant recipients (and their age-matched counter parts) had

similar increases to CVRi as the younger adults in Chapter 4, but did not have the increased phase lead and decreased TFA gain. Instead, these two older adult populations had comparable cerebral pressure-flow responses as the younger adults (matched to the typical age of a North American donor heart). Moreover, it was found that despite a marked blunting of the cardiac baroreflex in the heart transplant recipients, cerebral pressure-flow responses were well maintained. Collectively, in these groups the findings indicate the cardiac baroreceptors play a minimal role in the regulation of CBV and chronic elevations in CVRi that occurs during human aging do not result in alterations in cerebral-pressure flow responses. Thus, it appears the acutely increased phase and decreased gain noted in Chapter 4 may not accurately reflect the chronic elevations in CVRi in older adults. The findings from Chapter 5 indicate that these alterations in CVRi throughout the aging spectrum likely maintain the pressure-flow response, potentially due to gradual changes in either arteriolar tone and/or the mechanical buffering of the compliance vessels.

While assessing the cerebral-pressure flow response under resting or external perturbed changes in blood pressure are useful (see Chapters 3-5, and 7), they might not inform how the brain deals with more profound changes in blood pressure such as those encountered during exercise (Chapter 6). All of the previous experiments on the cerebral-pressure flow relationship during moderate intensity exercise were assessed during spontaneous oscillations and either demonstrated paradoxical findings<sup>237,304</sup> (e.g., TFA phase and gain both increasing with as frequency increased from 0.02-0.20 Hz), or based their interpretations on a single frequency range.<sup>164,299,301-303</sup> During moderate exercise there is a low coherence under these conditions, which makes interpretation of the

relationship between arterial blood pressure and CBF less reliable. Chapter 5 utilized the novel approach of creating oscillations in blood pressure *during* exercise. This provided a means to enhance the input signal (blood pressure) to the brain, which in turn resulted in an enhanced output signal (CBV) at a level comparable to those normally only observed during stationary squat-stand maneuvers. Through the utilization of this unique approach, Chapter 6 was the first study to clearly demonstrate that the high-pass filter model of the cerebrovasculature is intact during moderate exercise in both younger and older adults, despite the increased mean arterial pressure and maintained CBV levels. This study also revealed that despite both groups having the cerebrovasculature function as a high pass-filter, there were some age differences in the TFA metrics during exercise. Namely, the older adults had an elevated normalized gain at 0.05 Hz and reduced phase at 0.10 Hz when compared with the younger adults. It is speculated that these age-related changes to TFA metrics are due to either: alterations in arteriolar tone or the mechanical buffering of the compliance vessels. However, more research in this area is required to confirm these notions.

A comprehensive field-based study at high altitude (Chapter 7) was used to explore the cerebral pressure-flow relationships prior to, during acclimatization to 5050m, and return from high altitude in both the anterior and posterior regions of the brain. The findings of this study revealed that acute mountain sickness symptoms are unrelated to the regulation of CBV or the cerebral pressure-flow relationships as assessed via TFA. Moreover, despite the desaturation of the arterial blood to ~80% due to this extreme hypoxic environment, there were no changes to the cerebral pressure-flow response in either the anterior or posterior regions of the brain across the entire range of

exposure acclimatization timelines. Such findings in lowlanders were generally comparable to lifelong residents to high altitude, Sherpa.

The collective findings from these five studies indicate that squat-stand maneuvers are an optimal method to examine the nature of the cerebral-pressure flow response in a linear fashion as coherence with this methodology can be  $\sim 1.00$ . The findings also indicate that there are likely protective mechanisms (via changes to arteriolar tone and/or mechanical buffering of the compliance vessels) that are developed within the cerebrovasculature throughout the aging process. Although the older adult populations in Chapters 3 and 5 demonstrated levels of CVRi that were similar to the acute increases in the younger adults (Chapter 4), under resting conditions they did not demonstrate the elevations to phase and reductions to gain that were acutely observed in the younger adults. Thus, it appears the acutely increased CVRi noted in Chapter 4 may not accurately reflect the chronic elevations in older adults under resting conditions. In Chapter 6 it was revealed that despite maintaining the high-pass filter nature of the cerebrovasculature, the older adults had an elevated normalized gain at 0.05 Hz and reduced phase at 0.10 Hz when compared with the younger adults during moderate exercise, a finding that indicates with aging the cerebral pressure-flow response is altered during moderate exercise. Consequently it was speculated that these protective alterations during aging occur despite alterations to arterial saturation levels and blunted cardiac baroreceptor responses and are likely due to alterations in the myogenic tone of the arterioles or the mechanical buffering of the compliance vessels, which assist in maintaining the high-pass filter nature of the cerebrovasculature during moderate exercise. Thus the collective findings from this thesis have described that the healthy

human brain has compensatory processes in order to maintain effective pressure-flow relationships during healthy aging and exercise, and persist despite blunting of cardiac baroreflexes and reductions in arterial oxygen saturation.

## **8.2. Strengths and limitations of the thesis research**

The greatest strengths of this thesis, by employing methods that enhance the signal-to-noise ratio, are that all of the research chapters have focused on the findings within linear aspects of the relationship between arterial blood pressure and CBV. By utilizing this approach to systematically investigate numerous aspects of the literature where there were previously paradoxical findings, the true nature of the linear cerebral pressure-flow relationship has been revealed. Throughout healthy human aging and a variety of stresses it appears as though the cerebrovasculature is able to adequately maintain the regulation of CBV in both the anterior and posterior regions of the brain.

The three greatest potential limitations of the research presented in this thesis are: 1) the use of transcranial Doppler ultrasonography, 2) the subject populations that were tested, and 3) the use of a linear assessment tool to quantify what is likely a non-linear system. The sole use of transcranial Doppler ultrasonography to index CBF instead of directly measuring flow itself is a major limitation, but this is due to the current state of the technological advancements. Today this technology provided the optimal method for assessing this relationship through the methodologies employed in the presented research. In the future, advancements to transcranial colour-coded duplex sonography and edge tracking software may supersede these methods. In order for this to occur, the transcranial colour-coded duplex probes will need to be able to be held fixed in place for

extended periods of time with reliable software that can accurately follow the subtle changes in vessel diameter. This will enable measures of beat-to-beat CBF to be available to truly assess the cerebral pressure-flow relationship. The second major limitation is that the vast majority of the research subjects in the presented studies were healthy males. This in turn means that the application of the collective findings can only be meaningfully extrapolated to this population. There are a growing number of research studies that have demonstrated that the underlying physiology in males and females are not always transferable (reviewed in: <sup>337-340</sup>) and more research in this area is needed within the field of cerebrovascular physiology. The second component of the presented studies focusing mainly in the investigation of healthy males is that the collective findings may not necessarily be applicable to many clinical populations. However, the findings from the current studies provide a ‘normative’ reference group for future comparative studies. Moreover, the methods employed in this thesis have applications within the clinical realm – an area of research that deserves future considerations. The final major limitation was reiterated in each research chapter, namely that this thesis was unable to discuss cerebral autoregulation as it is inherently a non-linear system with multiple inputs that affect the output measure of CBV. Due to the inherent and complex nature of cerebral autoregulation, the findings of this thesis conservatively focused on interpreting the results of each study as they pertain to the underlying relationship between arterial blood pressure and CBF. In order to interpret this findings in a meaningful manner, we applied methodologies that resulted in extremely high levels of coherence in order to maximize the signal-to-noise ratio as suggested by Katsogridakis and colleagues.<sup>267</sup>

There are other methods, however, that provide insight into the inherent non-linear nature of cerebral autoregulation. Two selected examples as approaches that can be used to gauge the non-linearity of cerebral autoregulation are the autoregressive-moving average ARI,<sup>191-194,341,342</sup> and Windkessel modelling.<sup>229,337-340,343,344</sup> In 2003, Panerai *et al.*<sup>191,267</sup> proposed the concept of an autoregressive-moving average ARI to estimate the appropriate model coefficients for dynamic cerebral autoregulation. In this initial study it was established that the autoregressive-moving average ARI provided greater stability and reduced variability as compared with the RoR;<sup>176,191-194,341,342</sup> as such, it could be utilized as an assessment tool for dynamic cerebral autoregulation in place of the traditional ARI and RoR models. Since the initial study,<sup>191</sup> this research group has utilized the autoregressive-moving average ARI to continuously estimate dynamic cerebral autoregulation and established findings similar to those reported in this thesis, namely: it is effectively able to track changes in  $P_aCO_2$ ;<sup>192,194,342</sup> and is unaltered with healthy aging.<sup>193,194</sup> The collective findings from these studies led this research group to propose that cerebral autoregulation is composed of a series of interlinked mechanisms involving myogenic tone and the autonomic nervous system, with a concurrent influence of  $P_aCO_2$ .<sup>341</sup> The Windkessel model of cerebral autoregulation examines how changes to peripheral compliance and resistance during changes in blood pressure affect CBF.<sup>229,343,344</sup> A two-element (arterial bed resistance and compliance of the entire vascular bed) Windkessel model (see Chapter one: Figure 1.13) has shown to be an important contributor to the dynamic regulation of CBF during pharmacological alterations to blood pressure.<sup>343</sup> A calcium channel blockade (nimodipine) intervention with Windkessel modelling revealed that when myogenic tone is reduced, there is an increase in

conductive gain (and TFA phase) but no change to capacitive gain (or TFA gain).<sup>229</sup> This implies that calcium blockade has a greater effect on the compliance of the entire cerebrovascular tree than just within the resistance of the cerebral arterial bed. A second study examined the effects of hypercapnia (inhalation of 5% CO<sub>2</sub>) on CBV regulation found a secondary effect to the dilation of the cerebral vessels; the increase in cerebral blood volume may be due to reductions in compliance of the cerebrovasculature.<sup>344</sup> The collective findings from these studies indicate that myogenic tone is a prominent regulator in arterial bed resistance within the cerebrovasculature and compliance is affected by hypercapnia. The implications of these findings suggest that interventions altering CBV may not be accurately assessing impaired cerebral autoregulation but merely observing the changes in the resistance and compliance of the cerebrovasculature.

229,344

### **8.3. Potential applications of research findings**

The potential application from the collective findings from these five studies indicate that squat-stand maneuvers are the useful method to examine the nature of the cerebral-pressure flow response in a linear fashion as coherence with this method can be ~1.00. Depending on the experimental question, this method could supersede the current notion that spontaneous measures should be employed when examining the cerebral pressure-flow relationship with linear TFA (See Chapter 3: Figure 3.5). This concept is clearly highlighted by the speculative findings of the previous research into the cerebral pressure-flow relationship during moderate intensity exercise<sup>237,304</sup> and at high-altitude,<sup>316,317</sup> as the spontaneous data within these areas of research demonstrated inconsistent

results. The inconsistencies in the literature were likely due to the poor signal-to-noise ratio, as indicated by the low coherence ( $<0.50$ ) values associated with spontaneous oscillations in blood pressure. When these oscillations are enhanced with the appropriate methodology, the linear nature of the cerebral pressure-flow response can be reliably and meaningfully interpreted in both younger and older adults. In the case of this thesis, employing this method revealed that the healthy human body develops methods to maintain the regulation of CBF throughout the aging spectrum.

#### **8.4. Future directions**

The future directions of this field of research likely will address the limitations of research presented in this chapter. Within 10-20 years, technological advancements may lead to transcranial Doppler ultrasonography being phased out in favour of the transcranial colour-coded duplex sonography with real-time edge tracking software. This advancement will enable measures of beat-to-beat flow, which will allow the assessment the true cerebral pressure-*flow* relationship. Likewise, over the next decade or so, the time resolution of MRI and blood pressure compatible devices, may improve to a level that could better assess dynamic pressure-flow relationships.

The second direction envisioned for this field, is that research should move away from being mainly based on healthy male subjects. Instead there should be a focus on the underlying physiological differences between males and females. There should also be more focus on the clinical populations where the cerebrovasculature is impacted such as patients with dementia, Alzheimer's disease, concussion, traumatic brain injury, end-

stage heart failure and stroke. Some of the methods employed in this thesis could be employed within these clinical realms.

Future research in this field should also begin to utilize more non-linear modelling techniques (such as the autoregressive-moving average ARI and Windkessel models) to assess cerebral autoregulation. The findings from the spontaneous data within this thesis clearly highlight that interpretation of this relationship is tenuous with TFA due to the poor signal-to-noise ratio and inherent non-linearity of this relationship. Driving blood pressure oscillations enhances the input/output of the cerebral pressure-flow relationship, but still only allows for more interpretable findings about the linear components of this response. To accurately identify the non-linear components of the cerebral autoregulation mechanisms, appropriately utilized methods (such as those previously described in this chapter) should be employed. Being able to accurately quantify cerebral autoregulation and its underlying mechanisms are important. Developing a more complete understanding of likely mechanisms and the root causes of impairments of cerebral autoregulation, will lead to advancements for the early diagnosis and treatment of a range of cerebrovascular diseases and injuries.

## Bibliography

1. Smirl JD, Tzeng YC, Monteleone BJ, Ainslie PN. Influence of cerebrovascular resistance on the dynamic relationship between blood pressure and cerebral blood flow in humans. *J Appl Physiol*. 2014;116:1614–1622.
2. Smirl JD, Haykowsky MJ, Nelson MD, Tzeng YC, Marsden KR, Jones H, Ainslie PN. Relationship Between Cerebral Blood Flow and Blood Pressure in Long-Term Heart Transplant Recipients. *Hypertension*. 2014;64:1314–1320.
3. Smirl JD, Lucas SJE, Lewis NCS, Dumanior GR, Smith KJ, Bakker A, Basnyat AS, Ainslie PN. Cerebral pressure-flow relationship in lowlanders and natives at high altitude. *J Cereb Blood Flow Metab*. 2013;34:248–257.
4. Williams LR, Leggett RW. Reference values for resting blood flow to organs of man. *Clin Phys Physiol Meas*. 1989;10:187–217.
5. Rowell LB. Human Cardiovascular Control. New York: Oxford University Press; 1993.
6. Monro A. Observations on the structure and functions of the nervous system. Edinburgh: 1783.
7. Peters A, Schweiger U, Pellerin L, Hubold C, Oltmanns KM, Conrad M, Schultes B, Born J, Fehm HL. The selfish brain: competition for energy resources. *Neurosci Biobehav Rev*. 2004;28:143–180.
8. Boyajian RA, Schwend RB, Wolfe MM, Bickerton RE, Otis SM. Measurement of anterior and posterior circulation flow contributions to cerebral blood flow. An ultrasound-derived volumetric flow analysis. *J Neuroimaging*. 1995;5:1–3.
9. Bain AR, Smith KJ, Lewis NC, Foster GE, Wildfong KW, Willie CK, Hartley GL, Cheung SS, Ainslie PN. Regional changes in brain blood flow during severe passive hyperthermia: effects of PaCO<sub>2</sub> and extracranial blood flow. *J Appl Physiol*. 2013;115:653–659.
10. Sato K, Ogoh S, Hirasawa A, Oue A, Sadamoto T. The distribution of blood flow in the carotid and vertebral arteries during dynamic exercise in humans. *J Physiol*. 2011;589:2847–2856.
11. Smith K, MacLeod D, Willie C, Lewis N, Hoiland R, Ikeda K, Tymko M, Donnelly J, Day T, MacLeod N, Lucas S, Ainslie P. Influence of high altitude on cerebral blood flow and fuel utilization during exercise and recovery. *J Physiol*. 2014;
12. Dumke PR, Schmidt CF. Quantitative measurements of cerebral blood flow in the macaque monkey. *Am J Physiol*. 1943;138:421–431.

13. Bradac GB. Cerebral Angiography. New York: Springer Berlin Heidelberg; 2011.
14. Bayliss WM, Hill L, Gulland GL. On Intra-Cranial Pressure and the Cerebral Circulation: Part I. Physiological; Part II. Histological. *J Physiol.* 1895;18:334–362.
15. Roy CS, Sherrington CS. On the regulation of blood-supply of the brain. *J Physiol.* 1890;11:85–108.
16. Lassen NA. Cerebral blood flow and oxygen consumption in man. *Physiol Rev.* 1959;39:183–238.
17. Paulson OB, Strandgaard S, Edvinsson L. Cerebral autoregulation. *Cerebrovasc Brain Metab Rev.* 1990;2:161–192.
18. Zhang R, Zuckerman JH, Giller CA, Levine BD. Transfer function analysis of dynamic cerebral autoregulation in humans. *Am J Physiol.* 1998;274:H233–41.
19. Kety SS, Schmidt CF. The determination of cerebral blood flow in man by the use of nitrous oxide in low concentrations. *Am J Physiol.* 1945;143:53–66.
20. Kety SS, Schmidt CF. The nitrous oxide method for the quantitative determination of cerebral blood flow in man: Theory, procedure and normal values. *J Clin Invest.* 1948;27:476–483.
21. Abercrombie J. Pathological and practical researches of diseases of the brain and spinal cord. 3rd ed. Edinburgh: John Carfrae and Son; 1836.
22. Sandrone S, Bacigaluppi M, Galloni MR, Cappa SF, Moro A, Catani M, Filippi M, Monti MM, Perani D, Martino G. Weighing brain activity with the balance: Angelo Mosso's original manuscripts come to light. *Brain.* 2014;137:621–633.
23. Harvey W. Anatomical studies on the motion of the heart and the blood. Terecentennial Edition. Mensha, Wisconsin: The Collegiate Press; 1928.
24. Krejza J, Arkuszewski M, Kasner SE, Weigele J, Ustymowicz A, Hurst RW, Cucchiara BL, Messe SR. Carotid artery diameter in men and women and the relation to body and neck size. *Stroke.* 2006;37:1103–1105.
25. Seidel E, Eicke BM, Tettenborn B, Krummenauer F. Reference values for vertebral artery flow volume by duplex sonography in young and elderly adults. *Stroke.* 1999;30:2692–2696.
26. Chami HA, Keyes MJ, Vita JA, Mitchell GF, Larson MG, Fan S, Vasan RS, O'Connor GT, Benjamin EJ, Gottlieb DJ. Brachial artery diameter, blood flow and flow-mediated dilation in sleep-disordered breathing. *Vasc Med.* 2009;14:351–360.

27. Kellie G. An account of the appearances observed in the dissection of two of three individuals presumed to have perished in the storm of the 3rd, and whose bodies were discovered in the vicinity of Leith on the morning of the 4th, November 1821: with some reflections on the pathology of the brain. *Transactions of the Medico-Chirurgical Society of Edinburgh*. 1824;:82–169.
28. Macintyre I. A hotbed of medical innovation: George Kellie (1770-1829), his colleagues at Leith and the Monro-Kellie doctrine. *J Med Biogr*. 2013;22:93–100.
29. Kety SS, Schmidt CF. The effects of altered arterial tensions of carbon dioxide and oxygen on cerebral blood flow and cerebral oxygen consumption of normal young men. *Journal of Clinical Investigation*. 1948;27:484–492.
30. Gibbs FA, Maxwell HP, Gibbs EL. Volume flow of blood through the brain of man at rest, during hyperventilation and while breathing high CO<sub>2</sub>. *Fed Proc*. 1946;5:33.
31. Gibbs FA, Maxwell HP, Gibbs EL. Volume flow of blood through the human brain. *Arch Neurol Psychiatry*. 1947;57:137–144.
32. Lassen NA, Munck O. The cerebral blood flow in man determined by the use of radioactive krypton. *Acta Physiol Scand*. 1955;33:30–49.
33. Hoedt-Rasmussen K, Sveinsdottir E, Lassen NA. Regional cerebral blood flow in man determined by intra-arterial injection of radioactive inert gas. *Circ Res*. 1966;18:237–247.
34. Ingvar DH, Lassen NA. Quantitative determination of regional cerebral blood-flow in man. *The Lancet*. 1961;278:806–807.
35. Ingvar DH, Cronqvist S, Ekberg R, Risberg J, Hoedt-Rasmussen K. Normal values of regional cerebral blood flow in man, including flow and weight estimates of gray and white matter. A preliminary summary. *Acta Neurol Scand Suppl*. 1965;14:72–78.
36. Olesen J, Paulson OB, Lassen NA. Regional cerebral blood flow in man determined by the initial slope of the clearance of intra-arterially injected <sup>133</sup>Xe. *Stroke*. 1971;2:519–540.
37. Aaslid R, Markwalder TM, Nornes H. Noninvasive transcranial Doppler ultrasound recording of flow velocity in basal cerebral arteries. *J Neurosurg*. 1982;57:769–774.

38. Willie CK, Colino FL, Bailey DM, Tzeng YC, Binsted G, Jones LW, Haykowsky MJ, Bellapart J, Ogoh S, Smith KJ, Smirl JD, Day TA, Lucas SJ, Eller LK, Ainslie PN. Utility of transcranial Doppler ultrasound for the integrative assessment of cerebrovascular function. *J Neurosci Methods*. 2011;196:221–237.
39. Beaudin AE, Brugniaux JV, Vohringer M, Flewitt J, Green JD, Friedrich MG, Poulin MJ. Cerebral and myocardial blood flow responses to hypercapnia and hypoxia in humans. *Am J Physiol Heart Circ Physiol*. 2011;301:H1678–86.
40. Vovk A, Cunningham DA, Kowalchuk JM, Paterson DH, Duffin J. Cerebral blood flow responses to changes in oxygen and carbon dioxide in humans. *Can J Physiol Pharmacol*. 2002;80:819–827.
41. Ainslie PN, Burgess K, Subedi P, Burgess KR. Alterations in cerebral dynamics at high altitude following partial acclimatization in humans: wakefulness and sleep. *J Appl Physiol*. 2007;102:658–664.
42. Willie CK, Macleod DB, Shaw AD, Smith KJ, Tzeng YC, Eves ND, Ikeda K, Graham J, Lewis NC, Day TA, Ainslie PN. Regional brain blood flow in man during acute changes in arterial blood gases. *J Physiol*. 2012;590:3261–3275.
43. Skow RJ, MacKay CM, Tymko MM, Willie CK, Smith KJ, Ainslie PN, Day TA. Differential cerebrovascular CO<sub>2</sub> reactivity in anterior and posterior cerebral circulations. *Respir Physiol Neurobiol*. 2013;189:76–86.
44. Moreno JA, Mesalles E, Gener J, Tomasa A, Ley A, Roca J, Fernandez-Llamazares J. Evaluating the outcome of severe head injury with transcranial Doppler ultrasonography. *Neurosurg Focus*. 2000;8:e8.
45. Willie CK, Cowan EC, Ainslie PN, Taylor CE, Smith KJ, Sin PYW, Tzeng YC. Neurovascular coupling and distribution of cerebral blood flow during exercise. *J Neurosci Methods*. 2011;198:270–273.
46. Geinas JC, Marsden KR, Tzeng YC, Smirl JD, Smith KJ, Willie CK, Lewis NC, Binsted G, Bailey DM, Bakker A, Day TA, Ainslie PN. Influence of posture on the regulation of cerebral perfusion. *Aviat Space Environ Med*. 2012;83:751–757.
47. Smith KJ, Wong LE, Eves ND, Koelwyn GJ, Smirl JD, Willie CK, Ainslie PN. Regional cerebral blood flow distribution during exercise: influence of oxygen. *Respir Physiol Neurobiol*. 2012;184:97–105.
48. Smirl JD, Haykowsky MJ, Nelson MD, Altamirano-Diaz LA, Ainslie PN. Resting and exercise cerebral blood flow in long-term heart transplant recipients. *J Heart Lung Transplant*. 2012;31:906–908.

49. Marsden KR, Haykowsky MJ, Smirl JD, Jones H, Nelson MD, Altamirano-Diaz LA, Gelinas JC, Tzeng YC, Smith KJ, Willie CK, Bailey DM, Ainslie PN. Aging blunts hyperventilation-induced hypocapnia and reduction in cerebral blood flow velocity during maximal exercise. *Age*. 2012;34:725–735.
50. Bailey DM, Marley CJ, Brugniaux JV, Hodson D, New KJ, Ogoh S, Ainslie PN. Elevated aerobic fitness sustained throughout the adult lifespan is associated with improved cerebral hemodynamics. *Stroke*. 2013;44:3235–3238.
51. Ainslie PN, Cotter JD, George KP, Lucas S, Murrell C, Shave R, Thomas KN, Williams MJA, Atkinson G. Elevation in cerebral blood flow velocity with aerobic fitness throughout healthy human ageing. *J Physiol*. 2008;586:4005–4010.
52. Gruhn N, Larsen FS, Boesgaard S, Knudsen GM, Mortensen SA, Thomsen G, Aldershvile J. Cerebral blood flow in patients with chronic heart failure before and after heart transplantation. *Stroke*. 2001;32:2530–2533.
53. Massaro AR, Dutra AP, Almeida DR, Diniz RVZ, Malheiros SMF. Transcranial Doppler assessment of cerebral blood flow: effect of cardiac transplantation. *Neurology*. 2006;66:124–126.
54. Choi B-R, Kim JS, Yang YJ, Park K-M, Lee CW, Kim Y-H, Hong M-K, Song J-K, Park S-W, Park S-J, Kim J-J. Factors associated with decreased cerebral blood flow in congestive heart failure secondary to idiopathic dilated cardiomyopathy. *Am J Cardiol*. 2006;97:1365–1369.
55. Madsen PL, Secher NH. Near-infrared oximetry of the brain. *Prog Neurobiol*. 1999;58:541–560.
56. Wintermark M, Sesay M, Barbier E, Borbely K, Dillon WP, Eastwood JD, Glenn TC, Grandin CB, Pedraza S, Soustiel J-F, Nariai T, Zaharchuk G, Caille J-M, Dousset V, Yonas H. Comparative overview of brain perfusion imaging techniques. *Stroke*. 2005;36:e83–99.
57. Carroll TJ, Teneggi V, Jobin M, Squassante L, Treyer V, Hany TF, Burger C, Wang L, Bye A, Schulthess Von GK, Buck A. Absolute quantification of cerebral blood flow with magnetic resonance, reproducibility of the method, and comparison with H<sub>2</sub>(<sup>15</sup>O) positron emission tomography. *J Cereb Blood Flow Metab*. 2002;22:1149–1156.
58. Mintun MA, Fox PT, Raichle ME. A highly accurate method of localizing regions of neuronal activation in the human brain with positron emission tomography. *J Cereb Blood Flow Metab*. 1989;9:96–103.
59. Willie CK, Tzeng YC, Fisher JA, Ainslie PN. Integrative regulation of human brain blood flow. *J Physiol*. 2014;592:841–859.

60. Querido JS, Sheel AW. Regulation of cerebral blood flow during exercise. *Sports Med.* 2007;37:765–782.
61. Kumano H, Furuya H, Yomosa H, Nagahata T, Okuda T, Sakaki T. Response of pial vessel diameter and regional cerebral blood flow to CO<sub>2</sub> during midazolam administration in cats. *Acta Anaesthesiol Scand.* 1994;38:729–733.
62. Muizelaar JP, van der Poel HG, Li ZC, Kontos HA, Levasseur JE. Pial arteriolar vessel diameter and CO<sub>2</sub> reactivity during prolonged hyperventilation in the rabbit. *J Neurosurg.* 1988;69:923–927.
63. Serrador JM, Picot PA, Rutt BK, Shoemaker JK, Bondar RL. MRI measures of middle cerebral artery diameter in conscious humans during simulated orthostasis. *Stroke.* 2000;31:1672–1678.
64. Valdueza JM, Balzer JO, Villringer A, Vogl TJ, Kutter R, Einhaupl KM. Changes in blood flow velocity and diameter of the middle cerebral artery during hyperventilation: assessment with MR and transcranial Doppler sonography. *AJNR Am J Neuroradiol.* 1997;18:1929–1934.
65. Coverdale NS, Gati JS, Opalevych O, Perrotta A, Shoemaker JK. Cerebral blood flow velocity underestimates cerebral blood flow during modest hypercapnia and hypocapnia. *J Appl Physiol.* 2014;117:1090–1096.
66. Verbree J, Bronzwaer A-SGT, Ghariq E, Versluis MJ, Daemen MJAP, van Buchem MA, Dahan A, van Lieshout JJ, van Osch MJP. Assessment of middle cerebral artery diameter during hypocapnia and hypercapnia in humans using ultra-high-field MRI. *J Appl Physiol.* 2014;117:1084–1089.
67. Ainslie PN, Hoiland RL. Transcranial Doppler ultrasound: valid, invalid, or both? *J Appl Physiol.* 2014;117:1081–1083.
68. Faraci FM, Heistad DD, Mayhan WG. Role of large arteries in regulation of blood flow to brain stem in cats. *J Physiol.* 1987;387:115–123.
69. Knudsen HL, Frangos JA. Role of cytoskeleton in shear stress-induced endothelial nitric oxide production. *Am J Physiol.* 1997;273:H347–55.
70. Resnick N, Yahav H, Shay-Salit A, Shushy M, Schubert S, Zilberman LCM, Wofovitz E. Fluid shear stress and the vascular endothelium: for better and for worse. *Prog Biophys Mol Biol.* 2003;81:177–199.
71. Peebles KC, Richards AM, Celi L, McGrattan K, Murrell CJ, Ainslie PN. Human cerebral arteriovenous vasoactive exchange during alterations in arterial blood gases. *J Appl Physiol.* 2008;105:1060–1068.

72. Ho Y-CL, Vidyasagar R, Shen Y, Balanos GM, Golay X, Kauppinen RA. The BOLD response and vascular reactivity during visual stimulation in the presence of hypoxic hypoxia. *Neuroimage*. 2008;41:179–188.
73. Rostrup E, Larsson HBW, Born AP, Knudsen GM, Paulson OB. Changes in BOLD and ADC weighted imaging in acute hypoxia during sea-level and altitude adapted states. *Neuroimage*. 2005;28:947–955.
74. Willie CK, Ainslie PN, Drvis I, Macleod DB, Bain AR, Madden D, Maslov PZ, Dujic Z. Regulation of brain blood flow and oxygen delivery in elite breath-hold divers. *J Cereb Blood Flow Metab*. 2015;35:66–73.
75. Noble KA. Traumatic brain injury and increased intracranial pressure. *J Perianesth Nurs*. 2010;25:242–8– quiz 248–50.
76. Strandgaard S, Olesen J, Skinhoj E, Lassen NA. Autoregulation of brain circulation in severe arterial hypertension. *Br Med J*. 1973;1:507–510.
77. Kontos HA, Wei EP, Navari RM, Levasseur JE, Rosenblum WI, Patterson JJJ. Responses of cerebral arteries and arterioles to acute hypotension and hypertension. *Am J Physiol*. 1978;234:H371–83.
78. Donnelly J, Aries MJ, Czosnyka M. Further understanding of cerebral autoregulation at the bedside: possible implications for future therapy. *Expert Rev Neurother*. 2015;15:169–185.
79. Ling GSF, Neal CJ. Maintaining cerebral perfusion pressure is a worthy clinical goal. *Neurocrit Care*. 2005;2:75–81.
80. White H, Venkatesh B. Cerebral perfusion pressure in neurotrauma: a review. *Anesth Analg*. 2008;107:979–988.
81. Numan T, Bain AR, Hoiland RL, Smirl JD, Lewis NC, Ainslie PN. Static autoregulation in humans: a review and reanalysis. *Med Eng Phys*. 2014;36:1487–1495.
82. Hamel E. Perivascular nerves and the regulation of cerebrovascular tone. *J Appl Physiol*. 2006;100:1059–1064.
83. Peterson EC, Wang Z, Britz G. Regulation of cerebral blood flow. *Int J Vasc Med*. 2011;2011:823525.
84. Suzuki J, Iwabuchi T, Hori S. Cervical sympathectomy for cerebral vasospasm after aneurysm rupture. *Neurol Med Chir (Tokyo)*. 1975;15 pt 1:41–50.
85. Shenkin HA. Cervical sympathectomy on patients with occlusive cerebrovascular disease. *Arch Surg*. 1969;98:317–320.

86. Shenkin HA, Cabieses F, van den Noordt G. The effect of bilateral stellectomy upon the cerebral circulation of man. *J Clin Invest.* 1951;30:90–93.
87. Jeng JS, Yip PK, Huang SJ, Kao MC. Changes in hemodynamics of the carotid and middle cerebral arteries before and after endoscopic sympathectomy in patients with palmar hyperhidrosis: preliminary results. *J Neurosurg.* 1999;90:463–467.
88. Sobey CG, Faraci FM. Novel mechanisms contributing to cerebral vascular dysfunction during chronic hypertension. *Curr Hypertens Rep.* 2001;3:517–523.
89. Nielsen KC, Owman C. Contractile response and amine receptor mechanisms in isolated middle cerebral artery of the cat. *Brain Res.* 1971;27:33–42.
90. Dyrna F, Hanske S, Krueger M, Bechmann I. The blood-brain barrier. *J Neuroimmune Pharmacol.* 2013;8:763–773.
91. Wong AD, Ye M, Levy AF, Rothstein JD, Bergles DE, Searson PC. The blood-brain barrier: an engineering perspective. *Front Neuroeng.* 2013;6:7.
92. Reese TS, Karnovsky MJ. Fine structural localization of a blood-brain barrier to exogenous peroxidase. *J Cell Biol.* 1967;34:207–217.
93. Schoknecht K, David Y, Heinemann U. The blood-brain barrier-Gatekeeper to neuronal homeostasis: Clinical implications in the setting of stroke. *Semin Cell Dev Biol.* 2014;
94. Abbott NJ, Ronnback L, Hansson E. Astrocyte-endothelial interactions at the blood-brain barrier. *Nat Rev Neurosci.* 2006;7:41–53.
95. Janzer RC, Raff MC. Astrocytes induce blood-brain barrier properties in endothelial cells. *Nature.* 1987;325:253–257.
96. Stewart PA, Wiley MJ. Developing nervous tissue induces formation of blood-brain barrier characteristics in invading endothelial cells: a study using quail--chick transplantation chimeras. *Dev Biol.* 1981;84:183–192.
97. Arthur FE, Shivers RR, Bowman PD. Astrocyte-mediated induction of tight junctions in brain capillary endothelium: an efficient in vitro model. *Brain Res.* 1987;433:155–159.
98. Armulik A, Genove G, Mae M, Nisancioglu MH, Wallgard E, Niaudet C, He L, Norlin J, Lindblom P, Strittmatter K, Johansson BR, Betsholtz C. Pericytes regulate the blood-brain barrier. *Nature.* 2010;468:557–561.
99. Persidsky Y, Ramirez SH, Haorah J, Kanmogne GD. Blood-brain barrier: structural components and function under physiologic and pathologic conditions. *J Neuroimmune Pharmacol.* 2006;1:223–236.

100. del Zoppo GJ. Aging and the neurovascular unit. *Ann N Y Acad Sci.* 2012;1268:127–133.
101. Itoh Y, Suzuki N. Control of brain capillary blood flow. *J Cereb Blood Flow Metab.* 2012;32:1167–1176.
102. Muoio V, Persson PB, Sendeski MM. The neurovascular unit - concept review. *Acta Physiol (Oxf).* 2014;210:790–798.
103. Jespersen SN, Ostergaard L. The roles of cerebral blood flow, capillary transit time heterogeneity, and oxygen tension in brain oxygenation and metabolism. *J Cereb Blood Flow Metab.* 2012;32:264–277.
104. Fergus A, Lee KS. Regulation of cerebral microvessels by glutamatergic mechanisms. *Brain Res.* 1997;754:35–45.
105. Howarth C. The contribution of astrocytes to the regulation of cerebral blood flow. *Frontiers in neuroscience.* 2014;8:1–9.
106. Hamner JW, Tan CO, Tzeng YC, Taylor JA. Cholinergic control of the cerebral vasculature in humans. *J Physiol.* 2012;590:6343–6352.
107. Wiedensohler R, Kuchta J, Aschoff A, Harders A, Klug N. Visually evoked changes of blood flow velocity and pulsatility index in the posterior cerebral arteries: a transcranial Doppler study. *Zentralbl Neurochir.* 2004;65:13–17.
108. Azevedo E, Rosengarten B, Santos R, Freitas J, Kaps M. Interplay of cerebral autoregulation and neurovascular coupling evaluated by functional TCD in different orthostatic conditions. *J Neurol.* 2007;254:236–241.
109. Koehler RC, Roman RJ, Harder DR. Astrocytes and the regulation of cerebral blood flow. *Trends Neurosci.* 2009;32:160–169.
110. Kusano Y, Echeverry G, Miekisiak G, Kulik TB, Aronhime SN, Chen JF, Winn HR. Role of adenosine A2 receptors in regulation of cerebral blood flow during induced hypotension. *J Cereb Blood Flow Metab.* 2010;30:808–815.
111. O'Regan M. Adenosine and the regulation of cerebral blood flow. *Neurol Res.* 2005;27:175–181.
112. Fredholm BB, Battig K, Holmen J, Nehlig A, Zvartau EE. Actions of caffeine in the brain with special reference to factors that contribute to its widespread use. *Pharmacol Rev.* 1999;51:83–133.
113. Furchgott RF, Zawadzki JV. The obligatory role of endothelial cells in the relaxation of arterial smooth muscle by acetylcholine. *Nature.* 1980;288:373–376.

114. Furchgott RF. Endothelium-derived relaxing factor: discovery, early studies, and identification as nitric oxide. *Biosci Rep.* 1999;19:235–251.
115. Toda N, Ayajiki K, Okamura T. Cerebral blood flow regulation by nitric oxide: recent advances. *Pharmacol Rev.* 2009;61:62–97.
116. Kamper AM, Spilt A, de Craen AJM, van Buchem MA, Westendorp RGJ, Blauw GJ. Basal cerebral blood flow is dependent on the nitric oxide pathway in elderly but not in young healthy men. *Exp Gerontol.* 2004;39:1245–1248.
117. Pickard JD. Role of prostaglandins and arachidonic acid derivatives in the coupling of cerebral blood flow to cerebral metabolism. *J Cereb Blood Flow Metab.* 1981;1:361–384.
118. Attwell D, Buchan AM, Charpak S, Lauritzen M, Macvicar BA, Newman EA. Glial and neuronal control of brain blood flow. *Nature.* 2010;468:232–243.
119. Szabo K, Rosengarten B, Juhasz T, Lako E, Csiba L, Olah L. Effect of non-steroid anti-inflammatory drugs on neurovascular coupling in humans. *J Neurol Sci.* 2014;336:227–231.
120. Hohimer AR, Richardson BS, Bissonnette JM, Machida CM. The effect of indomethacin on breathing movements and cerebral blood flow and metabolism in the fetal sheep. *J Dev Physiol.* 1985;7:217–228.
121. St Lawrence KS, Ye FQ, Lewis BK, Weinberger DR, Frank JA, McLaughlin AC. Effects of indomethacin on cerebral blood flow at rest and during hypercapnia: an arterial spin tagging study in humans. *J Magn Reson Imaging.* 2002;15:628–635.
122. Wennmalm A, Eriksson S, Hagenfeldt L, Law D, Patrono C, Pinca E. Effect of prostaglandin synthesis inhibitors on basal and carbon dioxide-stimulated cerebral blood flow in man. *Adv Prostaglandin Thromboxane Leukot Res.* 1983;12:351–355.
123. Wennmalm A, Carlsson I, Edlund A, Eriksson S, Kaijser L, Nowak J. Central and peripheral haemodynamic effects of non-steroidal anti-inflammatory drugs in man. *Arch Toxicol Suppl.* 1984;7:350–359.
124. Fan J-L, Burgess KR, Thomas KN, Peebles KC, Lucas SJE, Lucas RAI, Cotter JD, Ainslie PN. Influence of indomethacin on the ventilatory and cerebrovascular responsiveness to hypoxia. *Eur J Appl Physiol.* 2011;111:601–610.
125. Tzeng YC, Ainslie PN, Cooke WH, Peebles KC, Willie CK, MacRae BA, Smirl JD, Horsman HM, Rickards CA. Assessment of cerebral autoregulation: the quandary of quantification. *Am J Physiol Heart Circ Physiol.* 2012;303:H658–71.

126. Pellicer A, Aparicio M, Cabanas F, Valverde E, Quero J, Stiris TA. Effect of the cyclo-oxygenase blocker ibuprofen on cerebral blood volume and cerebral blood flow during normocarbica and hypercarbia in newborn piglets. *Acta Paediatr.* 1999;88:82–88.
127. Parepally JMR, Mandula H, Smith QR. Brain uptake of nonsteroidal anti-inflammatory drugs: ibuprofen, flurbiprofen, and indomethacin. *Pharm Res.* 2006;23:873–881.
128. Kantor HS, Hampton M. Indomethacin in submicromolar concentrations inhibits cyclic AMP-dependent protein kinase. *Nature.* 1978;276:841–842.
129. Goueli SA, Ahmed K. Indomethacin and inhibition of protein kinase reactions. *Nature.* 1980;287:171–172.
130. Henze D, Menzel M, Soukup J, Scharf A, Holz C, Nemeth N, Hanisch F, Clausen T. Endothelin-1 and cerebral blood flow in a porcine model. *J Clin Neurosci.* 2007;14:650–657.
131. Yoshizumi M, Kurihara H, Sugiyama T, Takaku F, Yanagisawa M, Masaki T, Yazaki Y. Hemodynamic shear stress stimulates endothelin production by cultured endothelial cells. *Biochem Biophys Res Commun.* 1989;161:859–864.
132. Robinson MJ, Macrae IM, Todd M, Reid JL, McCulloch J. Reduction of local cerebral blood flow to pathological levels by endothelin-1 applied to the middle cerebral artery in the rat. *Neurosci Lett.* 1990;118:269–272.
133. Fuxe K, Kurosawa N, Cintra A, Hallstrom A, Goiny M, Rosen L, Agnati LF, Ungerstedt U. Involvement of local ischemia in endothelin-1 induced lesions of the neostriatum of the anaesthetized rat. *Exp Brain Res.* 1992;88:131–139.
134. Sharkey J, Ritchie IM, Kelly PA. Perivascular microapplication of endothelin-1: a new model of focal cerebral ischaemia in the rat. *J Cereb Blood Flow Metab.* 1993;13:865–871.
135. Macrae IM, Robinson MJ, Graham DI, Reid JL, McCulloch J. Endothelin-1-induced reductions in cerebral blood flow: dose dependency, time course, and neuropathological consequences. *J Cereb Blood Flow Metab.* 1993;13:276–284.
136. Zhang Y, Belayev L, Zhao W, Irving EA, Busto R, Ginsberg MD. A selective endothelin ET(A) receptor antagonist, SB 234551, improves cerebral perfusion following permanent focal cerebral ischemia in rats. *Brain Res.* 2005;1045:150–156.
137. Kreipke CW, Rafols JA, Reynolds CA, Schafer S, Marinica A, Bedford C, Fronczak M, Kuhn D, Armstead WM. Clazosentan, a novel endothelin A antagonist, improves cerebral blood flow and behavior after traumatic brain injury. *Neurol Res.* 2011;33:208–213.

138. Patel TR, Galbraith S, Graham DI, Hallak H, Doherty AM, McCulloch J. Endothelin receptor antagonist increases cerebral perfusion and reduces ischaemic damage in feline focal cerebral ischaemia. *J Cereb Blood Flow Metab.* 1996;16:950–958.
139. Wahl M, Kuschinsky W, Bosse O, Olesen J, Lassen NA, Ingvar DH, Michaelis J, Thureau K. Effect of 1-norepinephrine on the diameter of pial arterioles and arteries in the cat. *Circ Res.* 1972;31:248–256.
140. Mitchell DA, Lambert G, Secher NH, Raven PB, van Lieshout J, Esler MD. Jugular venous overflow of noradrenaline from the brain: a neurochemical indicator of cerebrovascular sympathetic nerve activity in humans. *J Physiol.* 2009;587:2589–2597.
141. Trangmar SJ, Chiesa ST, Stock CG, Kalsi KK, Secher NH, Gonzalez-Alonso J. Dehydration affects cerebral blood flow but not its metabolic rate for oxygen during maximal exercise in trained humans. *J Physiol.* 2014;592:3143–3160.
142. Bain AR, Ainslie PN. On the limits of cerebral oxygen extraction. *J Physiol.* 2014;592:2917–2918.
143. Self DA, White CD, Shaffstall RM, Mtinangi BL, Croft JS, Hainsworth R. Differences between syncope resulting from rapid onset acceleration and orthostatic stress. *Aviat Space Environ Med.* 1996;67:547–554.
144. Thomas KN, Cotter JD, Galvin SD, Williams MJA, Willie CK, Ainslie PN. Initial orthostatic hypotension is unrelated to orthostatic tolerance in healthy young subjects. *J Appl Physiol.* 2009;107:506–517.
145. Bundgaard-Nielsen M, Sorensen H, Dalsgaard M, Rasmussen P, Secher NH. Relationship between stroke volume, cardiac output and filling of the heart during tilt. *Acta Anaesthesiol Scand.* 2009;53:1324–1328.
146. Savin E, Bailliart O, Checoury A, Bonnin P, Grossin C, Martineaud JP. Influence of posture on middle cerebral artery mean flow velocity in humans. *Eur J Appl Physiol Occup Physiol.* 1995;71:161–165.
147. Alperin N, Hushek SG, Lee SH, Sivaramakrishnan A, Lichtor T. MRI study of cerebral blood flow and CSF flow dynamics in an upright posture: the effect of posture on the intracranial compliance and pressure. *Acta Neurochir Suppl (Wien).* 2005;95:177–181.
148. Deegan BM, Geraghty MC, Hodgeman RM, Reisner AA, O’Laighin G, Serrador JM. Assessment of techniques used to evaluate the effect of posture and cardiac output on cerebral autoregulation. *Conf Proc IEEE Eng Med Biol Soc.* 2008;2008:1992–1995.

149. Kung DK, Chalouhi N, Jabbour PM, Starke RM, Dumont AS, Winn HR, Howard MA3, Hasan DM. Cerebral blood flow dynamics and head-of-bed changes in the setting of subarachnoid hemorrhage. *Biomed Res Int*. 2013;2013:640638.
150. Serrador JM, Hughson RL, Kowalchuk JM, Bondar RL, Gelb AW. Cerebral blood flow during orthostasis: role of arterial CO<sub>2</sub>. *Am J Physiol Regul Integr Comp Physiol*. 2006;290:R1087–93.
151. Immink RV, Secher NH, Roos CM, Pott F, Madsen PL, van Lieshout JJ. The postural reduction in middle cerebral artery blood velocity is not explained by PaCO<sub>2</sub>. *Eur J Appl Physiol*. 2006;96:609–614.
152. Alperin N, Lee SH, Sivaramakrishnan A, Hushek SG. Quantifying the effect of posture on intracranial physiology in humans by MRI flow studies. *J Magn Reson Imaging*. 2005;22:591–596.
153. Thomas BP, Yezhuvath US, Tseng BY, Liu P, Levine BD, Zhang R, Lu H. Life-long aerobic exercise preserved baseline cerebral blood flow but reduced vascular reactivity to CO<sub>2</sub>. *J Magn Reson Imaging*. 2013;38:1177–1183.
154. Gisolf J, van Lieshout JJ, van Heusden K, Pott F, Stok WJ, Karemaker JM. Human cerebral venous outflow pathway depends on posture and central venous pressure. *J Physiol*. 2004;560:317–327.
155. Fotenos AF, Snyder AZ, Girton LE, Morris JC, Buckner RL. Normative estimates of cross-sectional and longitudinal brain volume decline in aging and AD. *Neurology*. 2005;64:1032–1039.
156. Matteis M, Troisi E, Monaldo BC, Caltagirone C, Silvestrini M. Age and sex differences in cerebral hemodynamics: a transcranial Doppler study. *Stroke*. 1998;29:963–967.
157. Pantano P, Baron JC, Lebrun-Grandie P, Duquesnoy N, Boussier MG, Comar D. Effects of normal aging on regional CBF and CMRO<sub>2</sub> in humans. *Monogr Neural Sci*. 1984;11:123–130.
158. Pantano P, Baron JC, Lebrun-Grandie P, Duquesnoy N, Boussier MG, Comar D. Regional cerebral blood flow and oxygen consumption in human aging. *Stroke*. 1984;15:635–641.
159. Buijs PC, Krabbe-Hartkamp MJ, Bakker CJ, de Lange EE, Ramos LM, Breteler MM, Mali WP. Effect of age on cerebral blood flow: measurement with ungated two-dimensional phase-contrast MR angiography in 250 adults. *Radiology*. 1998;209:667–674.
160. Ogoh S, Ainslie PN. Cerebral blood flow during exercise: mechanisms of regulation. *J Appl Physiol*. 2009;107:1370–1380.

161. Secher NH, Seifert T, van Lieshout JJ. Cerebral blood flow and metabolism during exercise: implications for fatigue. *J Appl Physiol*. 2008;104:306–314.
162. Moraine JJ, Lamotte M, Berre J, Niset G, Leduc A, Naeije R. Relationship of middle cerebral artery blood flow velocity to intensity during dynamic exercise in normal subjects. *Eur J Appl Physiol Occup Physiol*. 1993;67:35–38.
163. Hellstrom G, Fischer-Colbrie W, Wahlgren NG, Jogestrand T. Carotid artery blood flow and middle cerebral artery blood flow velocity during physical exercise. *J Appl Physiol*. 1996;81:413–418.
164. Ogoh S, Dalsgaard MK, Yoshiga CC, Dawson EA, Keller DM, Raven PB, Secher NH. Dynamic cerebral autoregulation during exhaustive exercise in humans. *Am J Physiol Heart Circ Physiol*. 2005;288:H1461–7.
165. Colcombe SJ, Erickson KI, Raz N, Webb AG, Cohen NJ, McAuley E, Kramer AF. Aerobic fitness reduces brain tissue loss in aging humans. *J Gerontol A Biol Sci Med Sci*. 2003;58:176–180.
166. Marks BL, Katz LM, Styner M, Smith JK. Aerobic fitness and obesity: relationship to cerebral white matter integrity in the brain of active and sedentary older adults. *Br J Sports Med*. 2011;45:1208–1215.
167. Toledo-Pereyra LH. Heart transplantation. *J Invest Surg*. 2010;23:1–5.
168. Stehlik J, Edwards LB, Kucheryavaya AY, Aurora P, Christie JD, Kirk R, Dobbels F, Rahmel AO, Hertz MI. The Registry of the International Society for Heart and Lung Transplantation: twenty-seventh official adult heart transplant report--2010. *J Heart Lung Transplant*. 2010;29:1089–1103.
169. van de Beek D, Kremers W, Daly RC, Edwards BS, Clavell AL, McGregor CGA, Wijdicks EFM. Effect of neurologic complications on outcome after heart transplant. *Arch Neurol*. 2008;65:226–231.
170. Montero CG, Martinez AJ. Neuropathology of heart transplantation: 23 cases. *Neurology*. 1986;36:1149–1154.
171. Mayer TO, Biller J, O'Donnell J, Meschia JF, Sokol DK. Contrasting the neurologic complications of cardiac transplantation in adults and children. *J Child Neurol*. 2002;17:195–199.
172. Belvis R, Marti-Fabregas J, Cocho D, Garcia-Bargo MD, Franquet E, Agudo R, Brosa V, Camprecios M, Puig M, Marti-Vilalta JL. Cerebrovascular disease as a complication of cardiac transplantation. *Cerebrovasc Dis*. 2005;19:267–271.
173. Tung H-H, Chen H-L, Wei J, Tsay S-L. Predictors of quality of life in heart-transplant recipients in Taiwan. *Heart Lung*. 2011;40:320–330.

174. Zierer A, Melby SJ, Voeller RK, Guthrie TJ, Al-Dadah AS, Meyers BF, Pasque MK, Ewald GA, Moon MR, Moazami N. Significance of neurologic complications in the modern era of cardiac transplantation. *Ann Thorac Surg.* 2007;83:1684–1690.
175. Baufreton C, Pinaud F, Corbeau JJ, Chevailler A, Jolivot D, Minassian Ter A, Henrion D, de Bruux JL. Increased cerebral blood flow velocities assessed by transcranial Doppler examination is associated with complement activation after cardiopulmonary bypass. *Perfusion.* 2011;26:91–98.
176. Aaslid R, Lindegaard KF, Sorteberg W, Nornes H. Cerebral autoregulation dynamics in humans. *Stroke.* 1989;20:45–52.
177. Meng L, Gelb AW. Regulation of Cerebral Autoregulation by Carbon Dioxide. *Anesthesiology.* 2014;
178. Dabertrand F, Nelson MT, Brayden JE. Ryanodine receptors, calcium signaling, and regulation of vascular tone in the cerebral parenchymal microcirculation. *Microcirculation.* 2013;20:307–316.
179. Eriksen VR, Hahn GH, Greisen G. Dopamine therapy is associated with impaired cerebral autoregulation in preterm infants. *Acta Paediatr.* 2014;103:1221–1226.
180. Hori D, Brown C, Ono M, Rappold T, Sieber F, Gottschalk A, Neufeld KJ, Gottesman R, Adachi H, Hogue CW. Arterial pressure above the upper cerebral autoregulation limit during cardiopulmonary bypass is associated with postoperative delirium. *Br J Anaesth.* 2014;113:1009–1017.
181. Czosnyka M, Miller C. Monitoring of Cerebral Autoregulation. *Neurocrit Care.* 2014;
182. Ma L, Roberts JS, Pihoker C, Richards TL, Shaw DWW, Marro KI, Vavilala MS. Transcranial Doppler-based assessment of cerebral autoregulation in critically ill children during diabetic ketoacidosis treatment. *Pediatr Crit Care Med.* 2014;15:742–749.
183. Heistad DD, Kontos HA. Section 2: The cardiovascular system volume III, peripheral circulation and organ blood flow, part I. In: Shepherd JT, Abboud FM, editors. *Handbook of Physiology.* American Physiology Society; 1983. p. 137–182.
184. Tzeng YC, Ainslie PN. Blood pressure regulation IX: cerebral autoregulation under blood pressure challenges. *Eur J Appl Physiol.* 2014;114:545–559.
185. Tan CO, Hamner JW, Taylor JA. The role of myogenic mechanisms in human cerebrovascular regulation. *J Physiol.* 2013;591:5095–5105.

186. Tan CO. Defining the characteristic relationship between arterial pressure and cerebral flow. *J Appl Physiol*. 2012;113:1194–1200.
187. Giller CA. The frequency-dependent behavior of cerebral autoregulation. *Neurosurgery*. 1990;27:362–368.
188. Tiecks FP, Lam AM, Aaslid R, Newell DW. Comparison of static and dynamic cerebral autoregulation measurements. *Stroke*. 1995;26:1014–1019.
189. Birch AA, Dirnhuber MJ, Hartley-Davies R, Iannotti F, Neil-Dwyer G. Assessment of autoregulation by means of periodic changes in blood pressure. *Stroke*. 1995;26:834–837.
190. Claassen JAHR, Levine BD, Zhang R. Dynamic cerebral autoregulation during repeated squat-stand maneuvers. *J Appl Physiol*. 2009;106:153–160.
191. Panerai RB, Eames PJ, Potter JF. Variability of time-domain indices of dynamic cerebral autoregulation. *Physiol Meas*. 2003;24:367–381.
192. Dineen NE, Brodie FG, Robinson TG, Panerai RB. Continuous estimates of dynamic cerebral autoregulation during transient hypocapnia and hypercapnia. *J Appl Physiol*. 2010;108:604–613.
193. Dineen NE, Panerai RB, Brodie F, Robinson TG. Effects of ageing on cerebral haemodynamics assessed during respiratory manoeuvres. *Age Ageing*. 2011;40:199–204.
194. Panerai RB, Dineen NE, Brodie FG, Robinson TG. Spontaneous fluctuations in cerebral blood flow regulation: contribution of PaCO<sub>2</sub>. *J Appl Physiol*. 2010;109:1860–1868.
195. Julien C. The enigma of Mayer waves: Facts and models. *Cardiovasc Res*. 2006;70:12–21.
196. Diehl RR, Linden D, Lucke D, Berlit P. Phase relationship between cerebral blood flow velocity and blood pressure. A clinical test of autoregulation. *Stroke*. 1995;26:1801–1804.
197. Brown CM, Marthol H, Zikeli U, Ziegler D, Hilz MJ. A simple deep breathing test reveals altered cerebral autoregulation in type 2 diabetic patients. *Diabetologia*. 2008;51:756–761.
198. Panerai RB, Rennie JM, Kelsall AW, Evans DH. Frequency-domain analysis of cerebral autoregulation from spontaneous fluctuations in arterial blood pressure. *Med Biol Eng Comput*. 1998;36:315–322.

199. Zhang R, Zuckerman JH, Iwasaki K, Wilson TE, Crandall CG, Levine BD. Autonomic neural control of dynamic cerebral autoregulation in humans. *Circulation*. 2002;106:1814–1820.
200. Reinhard M, Muller T, Guschlbauer B, Timmer J, Hetzel A. Transfer function analysis for clinical evaluation of dynamic cerebral autoregulation--a comparison between spontaneous and respiratory-induced oscillations. *Physiol Meas*. 2003;24:27–43.
201. Ogawa Y, Iwasaki K-I, Aoki K, Gokan D, Hirose N, Kato J, Ogawa S. The different effects of midazolam and propofol sedation on dynamic cerebral autoregulation. *Anesth Analg*. 2010;111:1279–1284.
202. Purkayastha S, Saxena A, Eubank WL, Hoxha B, Raven PB. alpha1-Adrenergic receptor control of the cerebral vasculature in humans at rest and during exercise. *Exp Physiol*. 2013;98:451–461.
203. Hamner JW, Cohen MA, Mukai S, Lipsitz LA, Taylor JA. Spectral indices of human cerebral blood flow control: responses to augmented blood pressure oscillations. *J Physiol*. 2004;559:965–973.
204. Elting JW, Aries MJH, van der Hoeven JH, Vroomen PCAJ, Maurits NM. Reproducibility and variability of dynamic cerebral autoregulation during passive cyclic leg raising. *Med Eng Phys*. 2013;36:585–591.
205. Lang EW, Mehdorn HM, Dorsch NWC, Czosnyka M. Continuous monitoring of cerebrovascular autoregulation: a validation study. *J Neurol Neurosurg Psychiatry*. 2002;72:583–586.
206. Czosnyka M, Brady K, Reinhard M, Smielewski P, Steiner LA. Monitoring of cerebrovascular autoregulation: facts, myths, and missing links. *Neurocrit Care*. 2009;10:373–386.
207. Liu X, Czosnyka M, Donnelly J, Budohoski KP, Varsos GV, Nasr N, Brady KM, Reinhard M, Hutchinson PJ, Smielewski P. Comparison of frequency and time domain methods of assessment of cerebral autoregulation in traumatic brain injury. *J Cereb Blood Flow Metab*. 2014;35:248–256.
208. Czosnyka M, Smielewski P, Kirkpatrick P, Menon DK, Pickard JD. Monitoring of cerebral autoregulation in head-injured patients. *Stroke*. 1996;27:1829–1834.
209. Sorrentino E, Budohoski KP, Kasprovicz M, Smielewski P, Matta B, Pickard JD, Czosnyka M. Critical thresholds for transcranial Doppler indices of cerebral autoregulation in traumatic brain injury. *Neurocrit Care*. 2011;14:188–193.
210. Friedman JH, Stuetzle W. Projection pursuit regression. *Journal of the American statistical Association*. 1981;76:817–823.

211. Smielewski P, Czosnyka M, Kirkpatrick P, McEroy H, Rutkowska H, Pickard JD. Assessment of cerebral autoregulation using carotid artery compression. *Stroke*. 1996;27:2197–2203.
212. Panerai RB. Cerebral autoregulation: from models to clinical applications. *Cardiovasc Eng*. 2008;8:42–59.
213. Meel-van den Abeelen ASS, Simpson DM, Wang LJY, Slump CH, Zhang R, Tarumi T, Rickards CA, Payne S, Mitsis GD, Kostoglou K, Marmarelis V, Shin D, Tzeng YC, Ainslie PN, Gommer E, Muller M, Dorado AC, Smielewski P, Yelicich B, Puppo C, Liu X, Czosnyka M, Wang C-Y, Novak V, Panerai RB, Claassen JAHR. Between-centre variability in transfer function analysis, a widely used method for linear quantification of the dynamic pressure-flow relation: the CARNet study. *Med Eng Phys*. 2014;36:620–627.
214. Taylor JA, Tan CO, Hamner JW. Assessing Cerebral Autoregulation via Oscillatory Lower Body Negative Pressure and Projection Pursuit Regression. *J Vis Exp*. 2014;
215. Panerai RB. Complexity of the human cerebral circulation. *Philos Transact A Math Phys Eng Sci*. 2009;367:1319–1336.
216. Meel-van den Abeelen ASS, van Beek AHEA, Slump CH, Panerai RB, Claassen JAHR. Transfer function analysis for the assessment of cerebral autoregulation using spontaneous oscillations in blood pressure and cerebral blood flow. *Med Eng Phys*. 2014;36:563–575.
217. Ortega-Gutierrez S, Petersen N, Masurkar A, Reccius A, Huang A, Li M, Choi JH, Marshall RS. Reliability, asymmetry, and age influence on dynamic cerebral autoregulation measured by spontaneous fluctuations of blood pressure and cerebral blood flow velocities in healthy individuals. *J Neuroimaging*. 2014;24:379–386.
218. Alexandrov AV, Sloan MA, Wong LKS, Douville C, Razumovsky AY, Koroshetz WJ, Kaps M, Tegeler CH. Practice standards for transcranial Doppler ultrasound: part I--test performance. *J Neuroimaging*. 2007;17:11–18.
219. Nuttall GA, Cook DJ, Fulgham JR, Oliver WCJ, Proper JA. The relationship between cerebral blood flow and transcranial Doppler blood flow velocity during hypothermic cardiopulmonary bypass in adults. *Anesth Analg*. 1996;82:1146–1151.
220. Nijboer JA, Dorlas JC, Mahieu HF. Photoelectric plethysmography--some fundamental aspects of the reflection and transmission method. *Clin Phys Physiol Meas*. 1981;2:205–215.

221. Guelen I, Westerhof BE, van der Sar GL, van Montfrans GA, Kiemeneij F, Wesseling KH, Bos WJ. Finometer, finger pressure measurements with the possibility to reconstruct brachial pressure. *Blood Press Monit.* 2003;8:27–30.
222. Guelen I, Westerhof BE, van der Sar GL, van Montfrans GA, Kiemeneij F, Wesseling KH, Bos WJW. Validation of brachial artery pressure reconstruction from finger arterial pressure. *J Hypertens.* 2008;26:1321–1327.
223. Elvan-Taspinar A, Uiterkamp LA, Sikkema JM, Bots ML, Koomans HA, Bruinse HW, Franx A. Validation and use of the Finometer for blood pressure measurement in normal, hypertensive and pre-eclamptic pregnancy. *J Hypertens.* 2003;21:2053–2060.
224. Oppenheim AV, Willsky AS, Nawab SH. Discrete-Time Signal Processing. 2nd ed. Englewood Cliffs, NJ: Prentice Hall; 1996.
225. Smith SW. The scientist and engineer's guide to digital signal processing. San Diego, CA: California Technical Publishing; 1997.
226. Welch PD. The use of fast Fourier transform for the estimation of power spectra: a method based on time averaging over short, modified periodograms. *IEEE transactions on Audio and Electroacoustics.* 1967;15:70–73.
227. Gommer ED, Shijaku E, Mess WH, Reulen JPH. Dynamic cerebral autoregulation: different signal processing methods without influence on results and reproducibility. *Med Biol Eng Comput.* 2010;48:1243–1250.
228. Brothers RM, Zhang R, Wingo JE, Hubing KA, Crandall CG. Effects of heat stress on dynamic cerebral autoregulation during large fluctuations in arterial blood pressure. *J Appl Physiol.* 2009;107:1722–1729.
229. Tzeng YC, Chan GSH, Willie CK, Ainslie PN. Determinants of human cerebral pressure-flow velocity relationships: new insights from vascular modelling and Ca(2)(+) channel blockade. *J Physiol.* 2011;589:3263–3274.
230. van Beek AHEA, Olde Rikkert MGM, Pasman JW, Hopman MTE, Claassen JAHR. Dynamic cerebral autoregulation in the old using a repeated sit-stand maneuver. *Ultrasound Med Biol.* 2010;36:192–201.
231. Oudegeest-Sander MH, van Beek AHEA, Abbink K, Olde Rikkert MGM, Hopman MTE, Claassen JAHR. Assessment of dynamic cerebral autoregulation and cerebrovascular CO<sub>2</sub> reactivity in ageing by measurements of cerebral blood flow and cortical oxygenation. *Exp Physiol.* 2014;99:586–598.
232. Aengevaeren VL, Claassen JAHR, Levine BD, Zhang R. Cardiac baroreflex function and dynamic cerebral autoregulation in elderly Masters athletes. *J Appl Physiol.* 2013;114:195–202.

233. Hughson RL, Edwards MR, O'Leary DD, Shoemaker JK. Critical analysis of cerebrovascular autoregulation during repeated head-up tilt. *Stroke*. 2001;32:2403–2408.
234. Zhang R, Claassen JAHR, Shibata S, Kilic S, Martin-Cook K, Diaz-Arrastia R, Levine BD. Arterial-cardiac baroreflex function: insights from repeated squat-stand maneuvers. *Am J Physiol Regul Integr Comp Physiol*. 2009;297:R116–23.
235. Serrador JM, Sorond FA, Vyas M, Gagnon M, Iloputaife ID, Lipsitz LA. Cerebral pressure-flow relations in hypertensive elderly humans: transfer gain in different frequency domains. *J Appl Physiol*. 2005;98:151–159.
236. Pfefferbaum A, Mathalon DH, Sullivan EV, Rawles JM, Zipursky RB, Lim KO. A quantitative magnetic resonance imaging study of changes in brain morphology from infancy to late adulthood. *Arch Neurol*. 1994;51:874–887.
237. Fisher JP, Ogoh S, Young CN, Raven PB, Fadel PJ. Regulation of middle cerebral artery blood velocity during dynamic exercise in humans: influence of aging. *J Appl Physiol*. 2008;105:266–273.
238. Formes K, Zhang P, Tierney N, Schaller F, Shi X. Chronic physical activity mitigates cerebral hypoperfusion during central hypovolemia in elderly humans. *Am J Physiol Heart Circ Physiol*. 2010;298:H1029–37.
239. Panerai RB, Carey BJ, Potter JF. Short-term variability of cerebral blood flow velocity responses to arterial blood pressure transients. *Ultrasound Med Biol*. 2003;29:31–38.
240. Quan H, Shih WJ. Assessing reproducibility by the within-subject coefficient of variation with random effects models. *Biometrics*. 1996;52:1195–1203.
241. Scott MJ, Randolph PH, Leier CV. Reproducibility of systolic and diastolic time intervals in normal humans: an important issue in clinical cardiovascular pharmacology. *J Cardiovasc Pharmacol*. 1989;13:125–130.
242. Dawson EA, Low DA, Meeuwis IHM, Kerstens FG, Atkinson CL, Cable NT, Green DJ, Thijssen DHJ. Reproducibility of cutaneous vascular conductance responses to slow local heating assessed using 7-laser array probes. *Microcirculation*. 2015;
243. Tian L. Inferences on the common coefficient of variation. *Stat Med*. 2005;24:2213–2220.
244. Tian L. Inferences on the within-subject coefficient of variation. *Stat Med*. 2006;25:2008–2017.

245. Shoukri MM, Elkum N, Walter SD. Interval estimation and optimal design for the within-subject coefficient of variation for continuous and binary variables. *BMC Med Res Methodol.* 2006;6:24.
246. Bland JM, Altman DG. Statistical methods for assessing agreement between two methods of clinical measurement. *Lancet.* 1986;1:307–310.
247. van Beek AHEA, Lagro J, Olde Rikkert MGM, Zhang R, Claassen JAHR. Oscillations in cerebral blood flow and cortical oxygenation in Alzheimer's disease. *Neurobiol Aging.* 2012;33:428.e21–31.
248. Tan CO, Taylor JA. On the judicious use of metrics for cerebral autoregulation. *Eur J Appl Physiol.* 2013;113:2867–2868.
249. Hamner JW, Tan CO, Lee K, Cohen MA, Taylor JA. Sympathetic control of the cerebral vasculature in humans. *Stroke.* 2010;41:102–109.
250. Brodie FG, Panerai RB, Foster S, Evans DH, Robinson TG. Long-term changes in dynamic cerebral autoregulation: a 10 years follow up study. *Clin Physiol Funct Imaging.* 2009;29:366–371.
251. Brodie FG, Atkins ER, Robinson TG, Panerai RB. Reliability of dynamic cerebral autoregulation measurement using spontaneous fluctuations in blood pressure. *Clin Sci.* 2009;116:513–520.
252. Chacon M, Jara JL, Panerai RB. A new model-free index of dynamic cerebral blood flow autoregulation. *PLoS One.* 2014;9:e108281.
253. Hu K, Peng CK, Czosnyka M, Zhao P, Novak V. Nonlinear assessment of cerebral autoregulation from spontaneous blood pressure and cerebral blood flow fluctuations. *Cardiovasc Eng.* 2008;8:60–71.
254. Mahony PJ, Panerai RB, Deverson ST, Hayes PD, Evans DH. Assessment of the thigh cuff technique for measurement of dynamic cerebral autoregulation. *Stroke.* 2000;31:476–480.
255. Saeed NP, Panerai RB, Robinson TG. Are hand-held TCD measurements acceptable for estimates of CBFv? *Ultrasound Med Biol.* 2012;38:1839–1844.
256. Jachan M, Reinhard M, Spindeler L, Hetzel A, Schelter B, Timmer J. Parametric versus nonparametric transfer function estimation of cerebral autoregulation from spontaneous blood-pressure oscillations. *Cardiovasc Eng.* 2009;9:72–82.
257. Lorenz MW, Loesel N, Thoelen N, Gonzalez M, Lienerth C, Dvorak F, Rolz W, Humpich M, Sitzer M. Effects of poor bone window on the assessment of cerebral autoregulation with transcranial Doppler sonography - a source of systematic bias and strategies to avoid it. *J Neurol Sci.* 2009;283:49–56.

258. Reinhard M, Roth M, Guschlbauer B, Czosnyka M, Timmer J, Weiller C, Hetzel A. The course of dynamic cerebral autoregulation during cervical internal carotid artery occlusion. *Neurol Res.* 2011;33:921–926.
259. Mehagnoul-Schipper DJ, Colier WN, Jansen RW. Reproducibility of orthostatic changes in cerebral oxygenation in healthy subjects aged 70 years or older. *Clin Physiol.* 2001;21:77–84.
260. Houtman S, Colier WN, Hopman MT, Oeseburg B. Reproducibility of the alterations in circulation and cerebral oxygenation from supine rest to head-up tilt. *Clin Physiol.* 1999;19:169–177.
261. Birch AA, Neil-Dwyer G, Murrills AJ. The repeatability of cerebral autoregulation assessment using sinusoidal lower body negative pressure. *Physiol Meas.* 2002;23:73–83.
262. Gommer ED, Staals J, van Oostenbrugge RJ, Lodder J, Mess WH, Reulen JPH. Dynamic cerebral autoregulation and cerebrovascular reactivity: a comparative study in lacunar infarct patients. *Physiol Meas.* 2008;29:1293–1303.
263. Ainslie PN, Duffin J. Integration of cerebrovascular CO<sub>2</sub> reactivity and chemoreflex control of breathing: mechanisms of regulation, measurement, and interpretation. *Am J Physiol Regul Integr Comp Physiol.* 2009;296:R1473–95.
264. Zhang R, Behbehani K, Levine BD. Dynamic pressure-flow relationship of the cerebral circulation during acute increase in arterial pressure. *J Physiol.* 2009;587:2567–2577.
265. Miller RD, Pardo M. Basics of Anesthesia: Expert Consult. 2011;
266. Olesen J. The effect of intracarotid epinephrine, norepinephrine, and angiotensin on the regional cerebral blood flow in man. *Neurology.* 1972;22:978–987.
267. Katsogridakis E, Bush G, Fan L, Birch AA, Simpson DM, Allen R, Potter JF, Panerai RB. Detection of impaired cerebral autoregulation improves by increasing arterial blood pressure variability. *J Cereb Blood Flow Metab.* 2012;33:519–523.
268. Omboni S, Parati G, Frattola A, Mutti E, Di Rienzo M, Castiglioni P, Mancia G. Spectral and sequence analysis of finger blood pressure variability. Comparison with analysis of intra-arterial recordings. *Hypertension.* 1993;22:26–33.
269. Sammons EL, Samani NJ, Smith SM, Rathbone WE, Bentley S, Potter JF, Panerai RB. Influence of noninvasive peripheral arterial blood pressure measurements on assessment of dynamic cerebral autoregulation. *J Appl Physiol.* 2007;103:369–375.

270. Voldby B, Enevoldsen EM, Jensen FT. Cerebrovascular reactivity in patients with ruptured intracranial aneurysms. *J Neurosurg.* 1985;62:59–67.
271. Strauss G, Hansen BA, Knudsen GM, Larsen FS. Hyperventilation restores cerebral blood flow autoregulation in patients with acute liver failure. *J Hepatol.* 1998;28:199–203.
272. Haubrich C, Steiner L, Kim DJ, Kasprovicz M, Smielewski P, Diehl RR, Pickard JD, Czosnyka M. How does moderate hypocapnia affect cerebral autoregulation in response to changes in perfusion pressure in TBI patients? *Acta Neurochir Suppl (Wien).* 2012;114:153–156.
273. Muller M, Bianchi O, Erulku S, Stock C, Schwerdtfeger K. Brain lesion size and phase shift as an index of cerebral autoregulation in patients with severe head injury. *Acta Neurochir (Wien).* 2003;145:643–7– discussion 647–8.
274. McCulloch TJ, Boesel TW, Lam AM. The effect of hypocapnia on the autoregulation of cerebral blood flow during administration of isoflurane. *Anesth Analg.* 2005;100:1463–7– table of contents.
275. Ogoh S, Nakahara H, Ainslie PN, Miyamoto T. The effect of oxygen on dynamic cerebral autoregulation: critical role of hypocapnia. *J Appl Physiol.* 2010;108:538–543.
276. Chock VY, Ramamoorthy C, Van Meurs KP. Cerebral autoregulation in neonates with a hemodynamically significant patent ductus arteriosus. *J Pediatr.* 2012;160:936–942.
277. Puppo C, Lopez L, Farina G, Caragna E, Moraes L, Iturralde A, Biestro A. Indomethacin and cerebral autoregulation in severe head injured patients: a transcranial Doppler study. *Acta Neurochir (Wien).* 2007;149:139–49– discussion 149.
278. Horsman HM, Peebles KC, Galletly DC, Tzeng YC. Cardiac baroreflex gain is frequency dependent: insights from repeated sit-to-stand maneuvers and the modified Oxford method. *Appl Physiol Nutr Metab.* 2013;38:753–759.
279. Panerai RB. The critical closing pressure of the cerebral circulation. *Med Eng Phys.* 2003;25:621–632.
280. Stewart JM, Medow MS, DelPozzi A, Messer ZR, Terilli C, Schwartz CE. Middle cerebral O<sub>2</sub> delivery during the modified Oxford maneuver increases with sodium nitroprusside and decreases during phenylephrine. *Am J Physiol Heart Circ Physiol.* 2013;304:H1576–83.
281. Lavi S, Egbarya R, Lavi R, Jacob G. Role of nitric oxide in the regulation of cerebral blood flow in humans: chemoregulation versus mechanoregulation. *Circulation.* 2003;107:1901–1905.

282. Haubrich C, Wendt A, Diehl RR, Klotzsch C. Dynamic autoregulation testing in the posterior cerebral artery. *Stroke*. 2004;35:848–852.
283. Nakagawa K, Serrador JM, Larose SL, Moslehi F, Lipsitz LA, Sorond FA. Autoregulation in the posterior circulation is altered by the metabolic state of the visual cortex. *Stroke*. 2009;40:2062–2067.
284. Rozet I, Vavilala MS, Lindley AM, Visco E, Treggiari M, Lam AM. Cerebral autoregulation and CO<sub>2</sub> reactivity in anterior and posterior cerebral circulation during sevoflurane anesthesia. *Anesth Analg*. 2006;102:560–564.
285. Bruhn H, Fransson P, Frahm J. Modulation of cerebral blood oxygenation by indomethacin: MRI at rest and functional brain activation. *J Magn Reson Imaging*. 2001;13:325–334.
286. Hughson RL, Maillet A, Dureau G, Yamamoto Y, Gharib C. Spectral analysis of blood pressure variability in heart transplant patients. *Hypertension*. 1995;25:643–650.
287. Uberfuhr P, Frey AW, Reichart B. Vagal reinnervation in the long term after orthotopic heart transplantation. *J Heart Lung Transplant*. 2000;19:946–950.
288. Ponte J, Purves MJ. The role of the carotid body chemoreceptors and carotid sinus baroreceptors in the control of cerebral blood vessels. *J Physiol*. 1974;237:315–340.
289. Tzeng YC, Lucas SJE, Atkinson G, Willie CK, Ainslie PN. Fundamental relationships between arterial baroreflex sensitivity and dynamic cerebral autoregulation in humans. *J Appl Physiol*. 2010;108:1162–1168.
290. Ishitsuka T, Iadecola C, Underwood MD, Reis DJ. Lesions of nucleus tractus solitarius globally impair cerebrovascular autoregulation. *Am J Physiol*. 1986;251:H269–81.
291. Yoshida K, Meyer JS, Sakamoto K, Handa J. Autoregulation of cerebral blood flow. Electromagnetic flow measurements during acute hypertension in the monkey. *Circ Res*. 1966;19:726–738.
292. Raczak G, La Rovere MT, Mortara A, Assandri J, Prpa A, Pinna GD, Maestri R, D'Armini AM, Vigano M, Cobelli F. Arterial baroreflex modulation of heart rate in patients early after heart transplantation: lack of parasympathetic reinnervation. *J Heart Lung Transplant*. 1999;18:399–406.
293. Bernardi L, Bianchini B, Spadacini G, Leuzzi S, Valle F, Marchesi E, Passino C, Calciati A, Vigano M, Rinaldi M. Demonstrable cardiac reinnervation after human heart transplantation by carotid baroreflex modulation of RR interval. *Circulation*. 1995;92:2895–2903.

294. van Beek AH, Claassen JA, Rikkert MGO, Jansen RW. Cerebral autoregulation: an overview of current concepts and methodology with special focus on the elderly. *J Cereb Blood Flow Metab.* 2008;28:1071–1085.
295. Ainslie PN, Shaw AD, Smith KJ, Willie CK, Ikeda K, Graham J, Macleod DB. Stability of cerebral metabolism and substrate availability in humans during hypoxia and hyperoxia. *Clin Sci.* 2014;126:661–670.
296. Lucas SJE, Tzeng YC, Galvin SD, Thomas KN, Ogoh S, Ainslie PN. Influence of changes in blood pressure on cerebral perfusion and oxygenation. *Hypertension.* 2010;55:698–705.
297. Lipsitz LA, Mukai S, Hamner J, Gagnon M, Babikian V. Dynamic regulation of middle cerebral artery blood flow velocity in aging and hypertension. *Stroke.* 2000;31:1897–1903.
298. Sorond FA, Khavari R, Serrador JM, Lipsitz LA. Regional cerebral autoregulation during orthostatic stress: age-related differences. *J Gerontol A Biol Sci Med Sci.* 2005;60:1484–1487.
299. Brys M, Brown CM, Marthol H, Franta R, Hilz MJ. Dynamic cerebral autoregulation remains stable during physical challenge in healthy persons. *Am J Physiol Heart Circ Physiol.* 2003;285:H1048–54.
300. Ogoh S, Brothers RM, Barnes Q, Eubank WL, Hawkins MN, Purkayastha S, O-Yurvati A, Raven PB. The effect of changes in cardiac output on middle cerebral artery mean blood velocity at rest and during exercise. *J Physiol.* 2005;569:697–704.
301. Ogoh S, Fadel PJ, Zhang R, Selmer C, Jans O, Secher NH, Raven PB. Middle cerebral artery flow velocity and pulse pressure during dynamic exercise in humans. *Am J Physiol Heart Circ Physiol.* 2005;288:H1526–31.
302. Ainslie PN, Barach A, Murrell C, Hamlin M, Hellemans J, Ogoh S. Alterations in cerebral autoregulation and cerebral blood flow velocity during acute hypoxia: rest and exercise. *Am J Physiol Heart Circ Physiol.* 2007;292:H976–83.
303. Ainslie PN, Hamlin M, Hellemans J, Rasmussen P, Ogoh S. Cerebral hypoperfusion during hypoxic exercise following two different hypoxic exposures: independence from changes in dynamic autoregulation and reactivity. *Am J Physiol Regul Integr Comp Physiol.* 2008;295:R1613–22.
304. Ogoh S, Dalsgaard MK, Secher NH, Raven PB. Dynamic blood pressure control and middle cerebral artery mean blood velocity variability at rest and during exercise in humans. *Acta Physiol (Oxf).* 2007;191:3–14.

305. Rickards CA, Ryan KL, Cooke WH, Convertino VA. Tolerance to central hypovolemia: the influence of oscillations in arterial pressure and cerebral blood velocity. *J Appl Physiol*. 2011;111:1048–1058.
306. Camargo LHA, Alves FHF, Biojone C, Correa FMA, Resstel LBM, Crestani CC. Involvement of N-methyl-D-aspartate glutamate receptor and nitric oxide in cardiovascular responses to dynamic exercise in rats. *Eur J Pharmacol*. 2013;713:16–24.
307. Hohimer AR, Hales JR, Rowell LB, Smith OA. Regional distribution of blood flow during mild dynamic leg exercise in the baboon. *J Appl Physiol*. 1983;55:1173–1177.
308. Tzeng YC, Willie CK, Atkinson G, Lucas SJE, Wong A, Ainslie PN. Cerebrovascular regulation during transient hypotension and hypertension in humans. *Hypertension*. 2010;56:268–273.
309. Cochand NJ, Wild M, Brugniaux JV, Davies PJ, Evans KA, Wise RG, Bailey DM. Sea-level assessment of dynamic cerebral autoregulation predicts susceptibility to acute mountain sickness at high altitude. *Stroke*. 2011;42:3628–3630.
310. Van Osta A, Moraine J-J, Melot C, Mairbaurl H, Maggiorini M, Naeije R. Effects of high altitude exposure on cerebral hemodynamics in normal subjects. *Stroke*. 2005;36:557–560.
311. Bailey DM, Bartsch P, Knauth M, Baumgartner RW. Emerging concepts in acute mountain sickness and high-altitude cerebral edema: from the molecular to the morphological. *Cell Mol Life Sci*. 2009;66:3583–3594.
312. Subudhi AW, Dimmen AC, Julian CG, Wilson MJ, Panerai RB, Roach RC. Effects of acetazolamide and dexamethasone on cerebral hemodynamics in hypoxia. *J Appl Physiol*. 2011;110:1219–1225.
313. Subudhi AW, Panerai RB, Roach RC. Effects of hypobaric hypoxia on cerebral autoregulation. *Stroke*. 2010;41:641–646.
314. Ainslie PN, Ogoh S, Burgess K, Celi L, McGrattan K, Peebles K, Murrell C, Subedi P, Burgess KR. Differential effects of acute hypoxia and high altitude on cerebral blood flow velocity and dynamic cerebral autoregulation: alterations with hyperoxia. *J Appl Physiol*. 2008;104:490–498.
315. Ainslie PN, Lucas SJE, Fan J-L, Thomas KN, Cotter JD, Tzeng YC, Burgess KR. Influence of sympathoexcitation at high altitude on cerebrovascular function and ventilatory control in humans. *J Appl Physiol*. 2012;113:1058–1067.
316. Levine BD, Zhang R, Roach RC. Dynamic cerebral autoregulation at high altitude. *Adv Exp Med Biol*. 1999;474:319–322.

317. Iwasaki K-I, Zhang R, Zuckerman JH, Ogawa Y, Hansen LH, Levine BD. Impaired dynamic cerebral autoregulation at extreme high altitude even after acclimatization. *J Cereb Blood Flow Metab.* 2011;31:283–292.
318. Jansen GF, Krins A, Basnyat B, Bosch A, Odoom JA. Cerebral autoregulation in subjects adapted and not adapted to high altitude. *Stroke.* 2000;31:2314–2318.
319. Jansen GFA, Krins A, Basnyat B, Odoom JA, Ince C. Role of the altitude level on cerebral autoregulation in residents at high altitude. *J Appl Physiol.* 2007;103:518–523.
320. Watson NA, Beards SC, Altaf N, Kassner A, Jackson A. The effect of hyperoxia on cerebral blood flow: a study in healthy volunteers using magnetic resonance phase-contrast angiography. *Eur J Anaesthesiol.* 2000;17:152–159.
321. Xu K, Lamanna JC. Chronic hypoxia and the cerebral circulation. *J Appl Physiol.* 2006;100:725–730.
322. Bailey DM, Evans KA, James PE, McEneny J, Young IS, Fall L, Gutowski M, Kewley E, McCord JM, Moller K, Ainslie PN. Altered free radical metabolism in acute mountain sickness: implications for dynamic cerebral autoregulation and blood-brain barrier function. *J Physiol.* 2009;587:73–85.
323. Basnyat B, Gertsch JH, Holck PS, Johnson EW, Luks AM, Donham BP, Fleischman RJ, Gowder DW, Hawksworth JS, Jensen BT, Kleiman RJ, Loveridge AH, Lundeen EB, Newman SL, Noboa JA, Miegs DP, O'Beirne KA, Philpot KB, Schultz MN, Valente MC, Wiebers MR, Swenson ER. Acetazolamide 125 mg BD is not significantly different from 375 mg BD in the prevention of acute mountain sickness: the prophylactic acetazolamide dosage comparison for efficacy (PACE) trial. *High Alt Med Biol.* 2006;7:17–27.
324. Ritschel WA, Paulos C, Arancibia A, Agrawal MA, Wetzelsberger KM, Lucker PW. Urinary excretion of acetazolamide in healthy volunteers after short- and long-term exposure to high altitude. *Methods Find Exp Clin Pharmacol.* 1998;20:133–137.
325. Richalet J-P, Rivera M, Bouchet P, Chirinos E, Onnen I, Petitjean O, Bienvenu A, Lasne F, Moutereau S, Leon-Velarde F. Acetazolamide: a treatment for chronic mountain sickness. *Am J Respir Crit Care Med.* 2005;172:1427–1433.
326. Jansen GF, Krins A, Basnyat B. Cerebral vasomotor reactivity at high altitude in humans. *J Appl Physiol.* 1999;86:681–686.
327. Sampson JB, Cymerman A, Burse RL, Maher JT, Rock PB. Procedures for the measurement of acute mountain sickness. *Aviat Space Environ Med.* 1983;54:1063–1073.

328. Roach RC, Bartsch P, Hackett PH, O O. The Lake Louise acute mountain sickness scoring system. Burlington: Queen City Printers; 1993.
329. Bailey DM, Roukens R, Knauth M, Kallenberg K, Christ S, Mohr A, Genius J, Storch-Hagenlocher B, Meisel F, McEneny J, Young IS, Steiner T, Hess K, Bartsch P. Free radical-mediated damage to barrier function is not associated with altered brain morphology in high-altitude headache. *J Cereb Blood Flow Metab.* 2006;26:99–111.
330. Wilson MH, Edsell MEG, Davagnanam I, Hirani SP, Martin DS, Levett DZH, Thornton JS, Golay X, Strycharczuk L, Newman SP, Montgomery HE, Grocott MPW, Imray CHE. Cerebral artery dilatation maintains cerebral oxygenation at extreme altitude and in acute hypoxia--an ultrasound and MRI study. *J Cereb Blood Flow Metab.* 2011;31:2019–2029.
331. Willie CK, Smith KJ, Day TA, Ray LA, Lewis NCS, Bakker A, Macleod DB, Ainslie PN. Regional cerebral blood flow in humans at high altitude: Gradual ascent and two weeks at 5050m. *J Appl Physiol.* 2013;
332. Lahiri S, Milledge JS. Sherpa physiology. *Nature.* 1965;207:610–612.
333. Santolaya RB, Lahiri S, Alfaro RT, Schoene RB. Respiratory adaptation in the highest inhabitants and highest Sherpa mountaineers. *Respir Physiol.* 1989;77:253–262.
334. Jansen GFA, Basnyat B. Brain blood flow in Andean and Himalayan high-altitude populations: evidence of different traits for the same environmental constraint. *J Cereb Blood Flow Metab.* 2011;31:706–714.
335. Villien M, Bouzat P, Rupp T, Robach P, Lamalle L, Tropres I, Esteve F, Krainik A, Levy P, Warnking JM, Verges S. Changes in cerebral blood flow and vasoreactivity to CO<sub>2</sub> measured by arterial spin labeling after 6days at 4350m. *Neuroimage.* 2013;72:272–279.
336. Smith ZM, Krizay E, Guo J, Shin DD, Scadeng M, Dubowitz DJ. Sustained high-altitude hypoxia increases cerebral oxygen metabolism. *J Appl Physiol.* 2013;114:11–18.
337. Celec P, Ostatnikova D, Hodosy J. On the effects of testosterone on brain behavioral functions. *Frontiers in neuroscience.* 2015;9:12.
338. Gokhale S, Caplan LR, James ML. Sex Differences in Incidence, Pathophysiology, and Outcome of Primary Intracerebral Hemorrhage. *Stroke.* 2015;46:886–892.
339. Yahagi K, Davis HR, Arbustini E, Virmani R. Sex differences in coronary artery disease: Pathological observations. *Atherosclerosis.* 2015;239:260–267.

340. Tadros R, Ton A-T, Fiset C, Nattel S. Sex differences in cardiac electrophysiology and clinical arrhythmias: epidemiology, therapeutics, and mechanisms. *Can J Cardiol.* 2014;30:783–792.
341. Panerai RB, Saeed NP, Robinson TG. Cerebrovascular effects of the thigh cuff maneuver. *Am J Physiol Heart Circ Physiol.* 2015;:ajpheart.00887.2014.
342. Chacon M, Araya C, Panerai RB. Non-linear multivariate modeling of cerebral hemodynamics with autoregressive Support Vector Machines. *Med Eng Phys.* 2011;33:180–187.
343. Chan GSH, Ainslie PN, Willie CK, Taylor CE, Atkinson G, Jones H, Lovell NH, Tzeng YC. Contribution of arterial Windkessel in low-frequency cerebral hemodynamics during transient changes in blood pressure. *J Appl Physiol.* 2011;110:917–925.
344. Tzeng YC, MacRae BA, Ainslie PN, Chan GSH. Fundamental relationships between blood pressure and cerebral blood flow in humans. *J Appl Physiol.* 2014;117:1037–1048.

## Appendix A:

### Supplementary information for high altitude study

#### A.1 Time-domain analysis of squat-stand maneuvers

##### Methods:

Time-domain analysis of the driven data were assessed by extracting 0.5-s averages during the squat-stand maneuvers. These averages were then aligned with each other with the first increase above the subjects mean blood pressure indicating the initiation of the hypertensive phase of the squat-stand maneuvers. The percent changes within the hypertensive and hypotensive phases were then recorded.

##### Results:

##### *Initial Arrival (Day 2)*

There were no significant differences in the time-domain analysis of the squat-stand induced changes in blood pressure during the hypertensive ( $20.3 \pm 10.4\%$  [SL] vs  $22.1 \pm 13.4\%$  [Day 2]) or hypotensive ( $-22.9 \pm 6.0\%$  [SL] vs  $-20.1 \pm 10.0\%$  [Day 2]) phases ( $P > 0.05$ ). Similarly, the MCAv responses were also comparable in the hypertensive ( $16.6 \pm 12.6\%$  [SL] vs  $16.9 \pm 17.4\%$  [Day 2]) and hypotensive ( $-33.2 \pm 5.9\%$  vs  $-30.9 \pm 12.0\%$ ) phase of the squat-stand intervention ( $P > 0.05$ ). Similar changes were evident in the PCAv.

### *Influence of Two-Weeks of Acclimatization (Week 2)*

There were no significant differences in the time-domain analysis of the squat-stand induced changes in blood pressure for the hypertensive ( $20.3 \pm 10.4\%$  [SL] vs  $19.7 \pm 8.0\%$  [Week 2]) or hypotensive ( $-22.9 \pm 6.0\%$  [SL] vs  $-24.3 \pm 6.9\%$  [Week 2]) phases ( $P>0.05$ ). Similarly, the MCAv responses were also comparable within the hypertensive ( $16.6 \pm 12.6\%$  vs  $15.8 \pm 9.8\%$ ) and hypotensive ( $-33.2 \pm 5.9\%$  vs  $-34.1 \pm 7.6\%$ ) phases of the squat-stand intervention ( $P>0.05$ ). The PCAv presented comparable results.

### *Comparison with high altitude natives*

There were no significant differences in the time-domain analysis of the squat-stand induced blood pressure changes within the hypertensive ( $19.7 \pm 8.0\%$  [Week 2] vs  $17.7 \pm 9.2\%$  [Sherpa]) or hypotensive ( $-24.3 \pm 6.9\%$  [Week 2] vs  $-20.5 \pm 6.6\%$  [Sherpa]) phases ( $P>0.05$ ). The MCAv responses were also comparable within the hypertensive ( $15.8 \pm 9.8\%$  [Week 2] vs  $12.4 \pm 8.1\%$  [Sherpa]) and hypotensive ( $-34.1 \pm 7.6\%$  [Week 2] vs  $-27.2 \pm 10.2\%$  [Sherpa]) phases of the squat-stand intervention ( $P>0.05$ ). The PCAv revealed similar findings.

*Effects of O<sub>2</sub> Normalization (n=8)*

There were no significant differences in the time-domain analysis of the squat-stand induced blood pressure changes within the hypertensive ( $18.2 \pm 8.7\%$  [Week 2] vs  $22.3 \pm 7.9\%$  [O<sub>2</sub>]) or hypotensive ( $-24.4 \pm 7.0\%$  [Week 2] vs  $-26.9 \pm 10.1\%$  [O<sub>2</sub>]) phases ( $P > 0.05$ ). Similarly, the findings within the MCAv were also comparable during the hypertensive ( $13.6 \pm 10.1\%$  [Week 2] vs  $15.0 \pm 7.9\%$  [O<sub>2</sub>]) and hypotensive ( $-36.9 \pm 6.6\%$  [Week 2] vs  $-35.0 \pm 10.5\%$  [O<sub>2</sub>]) phases of the squat-stand intervention ( $P > 0.05$ ). The PCAv presented similar findings.

*Returning to Sea Level (n=6)*

There were no significant differences in the time-domain analysis of the squat-stand induced blood pressure changes within the hypertensive ( $11.4 \pm 4.6\%$  [pre-] vs  $15.2 \pm 7.3\%$  [post-]) or hypotensive ( $-21.9 \pm 4.9\%$  [pre-] vs  $-28.2 \pm 8.7\%$  [post-]) phases ( $P > 0.05$ ). Similarly, the MCAv presented comparable findings within the hypertensive ( $10.7 \pm 7.9\%$  [pre-] vs  $9.4 \pm 4.9\%$  [post-]) and hypotensive ( $-36.6 \pm 2.7\%$  [pre-] vs  $-38.1 \pm 6.4\%$  [post-]) phases of the induced squat-stand intervention ( $P > 0.05$ ). The PCAv presented comparable results.

## A.2 Transcranial colour-coded duplex analysis

### Methods:

For comparisons between the lowlanders and Sherpa, the diameter and blood flow velocity in the middle cerebral artery were measured using Transcranial color-coded Duplex ultrasound (GE Vivid-E-Ultrasound; 2.5 MHz probe; GE Healthcare, United States). The middle cerebral artery was identified using color Doppler in the same plane as the mesencephalon, with flow towards the probe. Diameter (by manual calliper placement) and velocity (EchoPac, GE Healthcare, United States) was measured 1 cm distal to the internal carotid artery-middle cerebral artery-anterior cerebral artery trifurcation and were averaged over 10 cardiac cycles. Blood flow through the middle cerebral artery was calculated as the product of mean middle cerebral artery cross sectional area and mean blood velocity. One experienced sonographer collected all transcranial colour-coded duplex measures.

### Results:

#### *Comparison with HA natives*

There were no significant differences in middle cerebral artery diameter between either the partially acclimatized lowlanders ( $4.50 \pm 0.90$  mm;  $n=10$ ) or Sherpa ( $4.39 \pm 0.60$  mm;  $n=6$ ;  $P>0.05$ ). There were also no significant differences between partially acclimatized lowlanders and the Sherpa for middle cerebral artery blood flow ( $686 \pm 362$  ml/min vs.  $661 \pm 221$  ml/min;  $P>0.05$ ).